

Analysis and engineering of acetyl-CoA metabolism in *Saccharomyces cerevisiae*

van Rossum, Harmen

DOI

[10.4233/uuid:e42f9fe4-0be4-4bbd-9e67-7088b7ffceaf](https://doi.org/10.4233/uuid:e42f9fe4-0be4-4bbd-9e67-7088b7ffceaf)

Publication date

2016

Document Version

Final published version

Citation (APA)

van Rossum, H. (2016). *Analysis and engineering of acetyl-CoA metabolism in Saccharomyces cerevisiae*. [Dissertation (TU Delft), Delft University of Technology]. <https://doi.org/10.4233/uuid:e42f9fe4-0be4-4bbd-9e67-7088b7ffceaf>

Important note

To cite this publication, please use the final published version (if applicable).
Please check the document version above.

Copyright

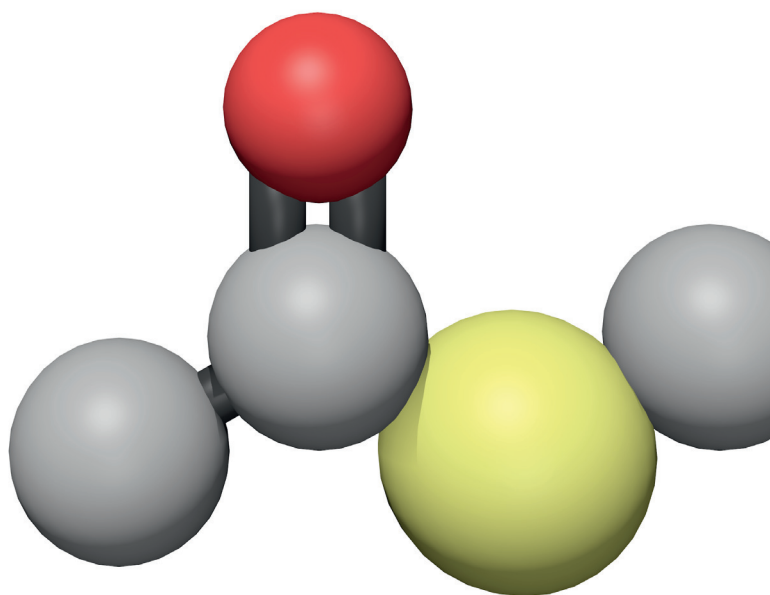
Other than for strictly personal use, it is not permitted to download, forward or distribute the text or part of it, without the consent of the author(s) and/or copyright holder(s), unless the work is under an open content license such as Creative Commons.

Takedown policy

Please contact us and provide details if you believe this document breaches copyrights.
We will remove access to the work immediately and investigate your claim.

ANALYSIS AND ENGINEERING OF ACETYL-CoA METABOLISM IN *SACCHAROMYCES CEREVISIAE*

HARMEN M. VAN ROSSUM



Analysis and engineering of acetyl-CoA metabolism in *Saccharomyces cerevisiae*

Proefschrift

ter verkrijging van de graad van doctor
aan de Technische Universiteit Delft,
op gezag van de Rector Magnificus prof. ir. K.Ch.A.M. Luyben,
voorzitter van het College voor Promoties,
in het openbaar te verdedigen op
maandag 30 mei 2016 om 10:00 uur

door

Hendrik Marinus VAN ROSSUM

Master of Science in Molecular and Cellular Life Sciences,
Universiteit Utrecht, Nederland,
geboren te Dirksland, Nederland.

Dit proefschrift is goedgekeurd door de promotor:

Prof. dr. J.T. Pronk

Copromotor:

Dr. ir. A.J.A. van Maris

Samenstelling promotiecommissie:

Rector Magnificus,	voorzitter
Prof. dr. J.T. Pronk,	TU Delft, promotor
Dr. ir. A.J.A. van Maris,	TU Delft, copromotor

Onafhankelijke leden:

Dr. J.R. Cherry	Amyris Inc, USA
Dr. R.A. Weuſthuis	Wageningen University and Research Centre
Prof. dr. J.B. Nielsen	Chalmers University of Technology, Sweden
Prof. dr. J. van der Ooſt	Wageningen University and Research Centre
Prof. dr. I.W.C.E. Arends	Technische Natuurwetenschappen, TU Delft

Reservelid:

Prof. dr. U. Hanefeld	Technische Natuurwetenschappen, TU Delft
-----------------------	--

The research presented in this thesis was performed at the Industrial Microbiology Section, Department of Biotechnology, Faculty of Applied Sciences, Delft University of Technology, The Netherlands and financed by the BE-Basic R&D Program, which in turn was granted an FES subsidy from the Dutch Ministry of Economic Affairs, Agriculture and Innovation (EL&I).

Illustrations:

Molecular model of acetyl-CoA (cover). Metabolic pathways (Page vii; Roche). Microscope pictures of CEN.PK113-7D using an Anthonie-van-Leeuwenhoek microscope (Page 1 and 5; Lesley Robertson). Photographs on page 69 and 171 are taken by Rolf van Koppen at the request of BE-Basic.

Printed by: Ipskamp Printing B.V., Enschede, The Netherlands

© 2016 by H.M. van Rossum.

ISBN 978-94-028-0122-4

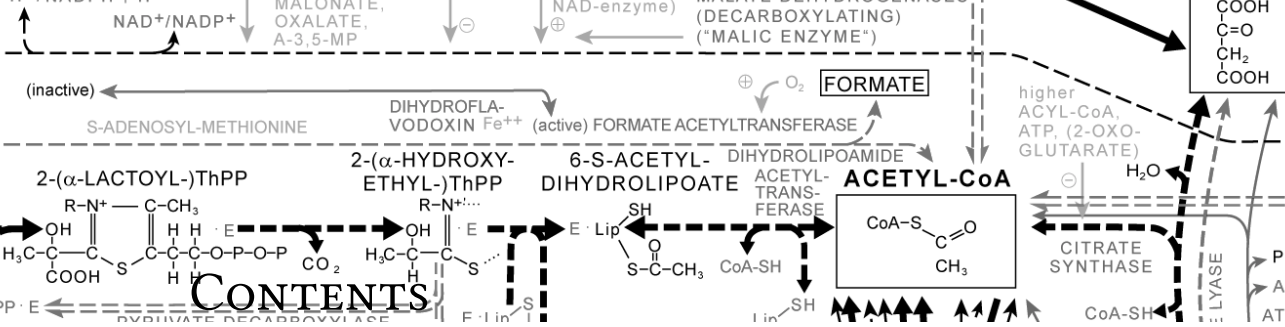
An electronic version of this dissertation is available at <http://repository.tudelft.nl/>.

Wat de wetenschap in eeuwen nog niet is gelukt, dat lukt de humor in een paar tellen.
Dus de waarheid zit in humor, niet in het serieuze.

— Herman Finkers

Maar wat is waar? Het oog ziet niet wat op het netvlies valt. Het oor hoort niet wat het trommelvlies doet trillen. Het ziet en het hoort wat in het hart ligt. En fijnzinnigheid is altijd waar. Kwetsbaarheid is ook altijd waar. Lelijkheid en lompheid zijn een dagelijkse werkelijkheid, maar: een werkelijkheid. Nóóit de waarheid. De werkelijkheid verdwijnt, de waarheid blijft.

— Herman Finkers



CONTENTS

Summary

Samenvatting

1	Engineering cytosolic acetyl-coenzyme A supply in <i>Saccharomyces cerevisiae</i> : Pathway stoichiometry, free-energy conservation and redox-cofactor balancing	1
2	CRISPR/Cas9: A molecular Swiss army knife for simultaneous introduction of multiple genetic modifications in <i>Saccharomyces cerevisiae</i>	5
3	Replacement of the <i>Saccharomyces cerevisiae</i> acetyl-CoA synthetases by alternative pathways for cytosolic acetyl-CoA synthesis	9
4	Alternative reactions at the interface of glycolysis and citric acid cycle in <i>Saccharomyces cerevisiae</i>	41
5	Requirements for carnitine-shuttle-mediated translocation of mitochondrial acetyl moieties to the yeast cytosol	69
	Bibliography	95
	Acknowledgments	117
	Curriculum vitae	143
	Publications	169
		171
		173

SUMMARY

Industrial biotechnology uses microorganisms and enzymes to produce a wide range of chemical compounds, predominantly from carbohydrate-containing agricultural feedstocks. This approach has several potential advantages over established petrochemical processes. Usage of fossil-based products releases carbon, increasing atmospheric greenhouse gases. In contrast, industrial biotechnology holds the potential of a much shorter carbon cycle and, consequently, a strongly decreased negative impact on climate and environment. Moreover, the world reserve of fossil feedstocks is limited and unequally distributed. Additionally, the mild conditions under which biotechnological processes are generally performed (ambient temperature and pressure) offer further advantages. Finally, microbial and enzyme-based catalysis offers access to an enormous range of known and yet to be discovered molecules with potential applications in the pharmaceutical, food, chemical and fuels industries.

The current low price of fossil feedstocks makes it difficult for biotechnological processes to be economically competitive with petrochemistry. Especially for high-volume products, such as commodity chemicals and transport fuels, the costs of the carbohydrate feedstock have a huge impact on overall production costs. It is therefore crucial to apply metabolic pathway engineering to improve the yield on substrate of native and heterologous products in industrial microorganisms.

Saccharomyces cerevisiae (bakers' yeast) is a highly popular industrial microorganism. A fast-growing body of knowledge on yeast biology and rapid technology developments in yeast molecular genetics, genomics and systems biology have enabled the successful introduction of a large and rapidly growing number of product pathways into *S. cerevisiae*, thereby expanding its product range.

Acetyl-coenzyme A (acetyl-CoA) is an important metabolic precursor, which participates in a wide variety of pathways. The acetyl moiety of acetyl-CoA acts as a universal C₂-building block for the synthesis of products as diverse as isoprenoids (e.g., β -carotene, farnesene and artemisinic acid), flavonoids (e.g., naringenin); *n*-butanol; (poly)hydroxybutyrate and (derivatives of) fatty acids. In *S. cerevisiae*, the native cytosolic acetyl-CoA synthesis reaction involves hydrolysis of an equivalent of two ATP to two ADP and two inorganic phosphate molecules. As a result, acetyl-CoA dependent, heterologous product pathways, which are usually expressed in the yeast cytosol, have suboptimal (theoretical) yields of product on substrate. Previous studies have already explored expression of alternative pathways for acetyl-CoA production in the yeast cytosol. **Chapter 1** reviews the literature on expression of these alternative pathways in *S. cerevisiae*, with a focus on reaction stoichiometry, redox-cofactor usage and free-energy conservation. A theoretical analysis showed that the choice of a cytosolic acetyl-CoA-production pathway strongly influences the theoretical yield of product on sugar. Different configurations of cytosolic acetyl-CoA production pathways were used to calculate theoretical yields of the model compounds *n*-butanol, citrate, palmitic acid and farnesene on glucose. This stoichiometric analysis showed that the optimal pathway configuration for cytosolic

acetyl-CoA synthesis is product dependent. Moreover, it demonstrated that, for some products, it can be advantageous to combine multiple acetyl-CoA production pathways.

To optimise a metabolic process such as cytosolic acetyl-CoA synthesis in yeast, efficient and easy-to-use genetic engineering tools are indispensable. A new, revolutionary tool that has recently become available is the CRISPR/Cas9 system. This system consists of a Cas9 nuclease and a so-called guideRNA (gRNA). The gRNA guides the nuclease to a specific, complementary, sequence of DNA, where Cas9 then introduces a double-strand break. The gRNA-dependence of the Cas9 nuclease enables its selective targeting to virtually any locus on the genome. **Chapter 2** explores and optimises the use of CRISPR/Cas9 for genetic engineering of *S. cerevisiae*. Two methods were evaluated. The first method did not require prior plasmid construction, while the second was based on a set of newly constructed plasmids capable of expressing two different gRNAs, in order to simultaneously target Cas9 to two different loci per plasmid. Using the latter approach, it was shown that open reading frames at up to six different genomic loci could be efficiently deleted in a single transformation step. The versatility of CRISPR/Cas9-based engineering ('genome editing') in yeast was further shown by the simultaneous integration of a multi-gene construct and a gene deletion and the introduction of single-nucleotide mutations at two different loci. Sets of *cas9*-bearing strains, standardised plasmids and a web-based, target-sequence identifier and primer-design tool (Yeastriction), were made available to the yeast research community to facilitate fast, standardised and efficient application of the CRISPR/Cas9 system in yeast. Genetic modification techniques, including the CRISPR/Cas9 system, were intensively applied in the following chapters to understand and engineer cytosolic acetyl-CoA production in *S. cerevisiae* (**Chapters 3, 4 and 5**).

In the cytosol of yeast, acetyl-CoA is produced via the concerted action of pyruvate decarboxylase, acetaldehyde dehydrogenase and acetyl-CoA synthetase (ACS). This reaction sequence is commonly known as the PDH (pyruvate dehydrogenase) bypass. The final reaction in the PDH bypass, the activation of acetate to acetyl-CoA, is catalysed by Acs1 or Acs2 and has a high ATP expenditure, which severely limits the maximum attainable yield of acetyl-CoA dependent products on substrate in *S. cerevisiae*. **Chapter 3** therefore explores the replacement of Acs1 and Acs2 by two ATP-independent pathways for acetyl-CoA synthesis. After evaluating the expression of different heterologous genes encoding acetylating acetaldehyde dehydrogenases (A-ALD) and pyruvate-formate lyases (PFL), *acs1Δ acs2Δ S. cerevisiae* strains were constructed, in which either A-ALD or PFL functionally replaced ACS. In A-ALD-dependent strains, aerobic specific growth rates of up to 0.27 h^{-1} were observed, while anaerobic growth of PFL-dependent *S. cerevisiae* at a specific growth rate of 0.20 h^{-1} was stoichiometrically coupled to formate production. In glucose-limited chemostat cultures, intracellular metabolite analysis did not reveal major differences between A-ALD-dependent and reference strains. However, biomass yields on glucose of A-ALD- and PFL-dependent strains were lower than those of the ACS-dependent reference strain. Transcriptome analysis suggested that these low biomass yields were caused by acetaldehyde and formate toxicity in A-ALD- and PFL-dependent strains, respectively. Transcriptome analysis also indicated that a previously proposed role of Acs2 in histone acetylation is probably linked to cytosolic acetyl-CoA levels rather than to direct involvement of Acs2 in histone acetylation. While demon-

strating that the native cytosolic acetyl-CoA synthesis pathway can be fully replaced, **Chapter 3** also revealed targets that need to be addressed to achieve optimal *in vivo* performance of the alternative reactions for supply of cytosolic acetyl-CoA.

Design and implementation of metabolic engineering strategies to improve fluxes towards precursors not only requires knowledge of flux distribution in wild-type strains, but also of compensatory 'back-up' pathways that become active when the mechanisms that carry the majority of the flux in wild-type cells are inactivated by genetic modification or by changing process conditions. **Chapter 4** therefore investigates alternative reactions at the interface of glycolysis and TCA cycle in *S. cerevisiae*. In addition to the abovementioned cytosolic PDH bypass, glucose-grown cells of this yeast harbour several other mechanisms to synthesise acetyl-CoA. Direct oxidative decarboxylation by the mitochondrial pyruvate-dehydrogenase (PDH) complex yields acetyl-CoA in the mitochondrial matrix. A second source of mitochondrial acetyl-CoA depends on activity of the mitochondrial Ach1 protein, which can transfer the CoA group from succinyl-CoA to acetate, forming acetyl-CoA and succinate. Alternatively, the PDH bypass may be connected to the TCA cycle via an extramitochondrial citrate synthase, Cit2. This enzyme catalyses the condensation of acetyl-CoA with oxaloacetate, forming citrate, which may subsequently be transported into the mitochondria and further metabolised via the TCA cycle. To assess the relative importance of different alternative reactions active at the interface of glycolysis and TCA-cycle, strains were constructed with single and combined deletions of structural genes for key enzymes in these three routes. Shake-flask studies showed that the PDH complex and Ach1 can each provide mitochondrial acetyl-CoA, although the PDH complex seems more important than Ach1 in wild-type *S. cerevisiae*. Cit2 was shown to have an important role in the synthesis of TCA-cycle intermediates in the absence of a functional mitochondrial PDH complex. Combined inactivation of the PDH complex and Ach1 had a severe effect on the physiology of the strains, resulting in a low specific growth rate (0.10 h^{-1}) in glucose synthetic medium, decreased ability to respire and a high incidence of the complete loss of respiratory competence. Together, these observations indicate a severe limitation in the availability of mitochondrial acetyl-CoA. The carnitine shuttle, whose activity in *S. cerevisiae* requires addition of L-carnitine to growth media, should in principle be able to transport acetyl moieties from the cytosol to the mitochondria. Indeed, the growth rate of strains lacking Ach1 and a functional PDH complex increased upon L-carnitine supplementation, albeit by only 30%, presumable due to repression of the carnitine shuttle during growth on glucose. Indeed, when the genes involved in the carnitine shuttle were constitutively over-expressed in this strain background, L-carnitine supplementation led to near-wild-type specific growth rates.

Mechanistically, the carnitine shuttle should also allow for export of acetyl moieties from the mitochondria to the cytosol. However, previous studies strongly suggested that such export does not occur *in vivo* in *S. cerevisiae*. To investigate the molecular mechanism that underlies this apparent unidirectionality, genes involved in the carnitine shuttle were constitutively expressed in a strain in which cytosolic acetyl-CoA provision could be simply deactivated by changing the medium composition (**Chapter 5**). Initially, no L-carnitine-dependent growth was observed, but after laboratory evolution, two strains were obtained that had both become dependent on the carnitine shuttle for

their cytosolic acetyl-CoA demand, yielding specific growth rates on glucose of 0.10 and 0.14 h⁻¹, respectively. Whole-genome sequencing of these evolved strains revealed several mutations in genes involved in the mitochondrial fatty-acid-synthesis pathway (*MCT1*), communication between nucleus and mitochondria (*RTG2*) and a proposed carnitine acetyltransferase (*YAT2*). Reverse engineering of these three mutations in the un-evolved strain showed that all mutations contributed to the acquired phenotype. These observations seem to indicate that elevated mitochondrial acetyl-CoA levels were necessary to reverse the natural direction of the carnitine shuttle. Further analysis showed that the mitochondrial PDH complex carried the majority of the flux to meet the acetyl-CoA demands of the evolved L-carnitine-dependent strains, while Ach1 did not have a significant contribution. **Chapter 5** contributed to our understanding of the *in vivo* reversibility of the carnitine shuttle and, furthermore, indicates an alternative metabolic engineering strategy to achieve cost-effective, yeast-based production of industrially relevant compounds that require cytosolic acetyl-CoA as a precursor.

This thesis illustrates how the advent of novel genetic engineering tools such as CRISPR/Cas9 accelerates and simplifies metabolic engineering of *S. cerevisiae* and allows for ever more complex interventions in the genome of this important industrial microorganism. Combination of these techniques with quantitative physiological analysis enabled a critical evaluation of strategies for optimising provision of acetyl-CoA as a precursor in yeast-based industrial processes. Moreover, it expanded our understanding of acetyl-CoA metabolism and of the carnitine shuttle in *S. cerevisiae*.

SAMENVATTING

In de industriële biotechnologie worden micro-organismen en enzymen gebruikt voor de productie van een breed scala aan chemische verbindingen, voornamelijk uit suikerhoudende agrarische grondstoffen. Deze benadering heeft een aantal potentiële voordelen ten opzichte van gevestigde petrochemische processen. Bij gebruik van fossiele producten komt koolstof vrij, hetgeen zorgt voor een toename van broeikasgassen in de atmosfeer. In de industriële biotechnologie zijn de koolstofcycli doorgaans veel korter, waardoor de negatieve invloed op klimaat en milieu beperkt wordt. Bovendien is de mondiale voorraad van fossiele grondstoffen niet onuitputtelijk en geografisch ongelijk verdeeld. De milde omstandigheden (bijv. temperatuur en druk) waaronder biotechnologische productieprocessen over het algemeen worden uitgevoerd bieden extra voordelen. Tenslotte opent katalyse door middel van microben en enzymen de toegang tot een enorme verscheidenheid aan bekende en nog te ontdekken (bio)moleculen met potentiële toepassingen in de farmaceutische -, voedingsmiddelen-, brandstoffen- en chemische industrie.

Voor producten met grote productievolumes, zoals bulkchemicaliën en transportbrandstoffen, hebben de kosten van de als substraat gebruikte suikers een enorme invloed op de totale productiekosten. De huidige lage prijs van fossiele grondstoffen bemoeilijkt de economische concurrentie van deze biotechnologische productieprocessen met petrochemische processen. Het is daarom van cruciaal belang om “metabolic pathway engineering” toe te passen op industriële micro-organismen om de opbrengst op suiker van zowel natuurlijke producten als van producten waarvan vorming door genetische modificatie mogelijk is gemaakt te verbeteren.

Saccharomyces cerevisiae (bakkersgist) is een zeer populair industrieel micro-organisme. De kennis over de biologie van deze gist neemt nog steeds in een rap tempo toe, terwijl ook snelle technologische ontwikkelingen plaatsvinden op het gebied van moleculaire genetica, genomonderzoek en systeembioogie. Dit heeft geleid tot een groot en nog steeds groeiend aantal in *S. cerevisiae* geïntroduceerde stofwisselingsroutes voor productvorming, waardoor het productspectrum van deze gist sterk is uitgebreid.

Acetyl-coenzym A (acetyl-CoA) is een belangrijke metabole bouwsteen die deelneemt aan een grote verscheidenheid van stofwisselingsroutes. De acetylgroep van acetyl-CoA fungeert als universele C₂-bouwsteen voor synthese van een grote verscheidenheid van producten, waaronder isoprenoïden (bijv. β -caroteen, farneseen en artemisinine zuur), flavonoiden (bijv. naringenine); *n*-butanol; (poly)hydroxybutyraat en (derivaten van) vetzuren. In *S. cerevisiae* gaat activering van azijnzuur tot acetyl-CoA door het cytosolische enzym acetyl-CoA synthetase (ACS) gepaard met de hydrolyse van een equivalent van twee ATP naar twee ADP en twee anorganische fosfaatmoleculen. Hierdoor hebben heterologe productieroutes in gist die cytosolisch acetyl-CoA als bouwsteen gebruiken, suboptimale (theoretisch) productopbrengsten. Verschillende eerdere studies hebben getracht om alternatieve routes voor de vorming van cytosolisch acetyl-CoA in gist te introduceren. In **Hoofdstuk 1** wordt de beschikbare literatuur over zulke alternatieve

routes in *S. cerevisiae* besproken, met een focus op reactiestoichiometrie, redoxcofactorgebruik en vrije-energieconservering. Uit een theoretische analyse werd duidelijk dat de gekozen route voor vorming van cytosolisch acetyl-CoA een sterke invloed heeft op de theoretische opbrengst van product op substraat. Daarnaast werd de impact berekend van verschillende productieroutes voor cytosolisch acetyl-CoA op de theoretisch maximale opbrengst op glucose van vier modelverbindingen: *n*-butanol, citroenzuur, palmitinezuur en farneseen. Deze stoichiometrische analyse toonde niet alleen aan dat de optimale route voor cytosolisch acetyl-CoA synthese sterk productafhankelijk is, maar ook dat het voor sommige producten voordelig kan zijn om verschillende acetyl-CoA-productieroutes te combineren.

Voor het optimaliseren van stofwisselingsroutes zoals de vorming van cytosolisch acetyl-CoA zijn efficiënte, makkelijk te gebruiken genetische technieken onontbeerlijk. Een nieuw revolutionair gereedschap dat onlangs beschikbaar kwam is het CRISPR/Cas9 systeem. Dit systeem bestaat uit de Cas9-nuclease en een zogenaamd guideRNA (gRNA) dat dit nuclease leidt naar een specifieke complementaire DNA-sequentie, waar het vervolgens een dubbelstrengsbreuk aanbrengt. Door deze gRNA-afhankelijke specificiteit kan Cas9 naar vrijwel elk locus in een genoom geleid worden. **Hoofdstuk 2** beschrijft onderzoek waarin de mogelijkheden van CRISPR/Cas9 voor genetische modificatie van *S. cerevisiae* werden uitgezocht en dit systeem verder werd geoptimaliseerd. Hierbij werden twee methoden getest. Voor de eerste methode was geen voorafgaande plasmideconstructie nodig, terwijl voor de tweede methode een set plasmiden werd geconstrueerd die het mogelijk maakte om per plasmide twee gRNAs tot expressie te brengen en daarmee Cas9 naar twee verschillende loci te leiden. Met de laatstgenoemde methode bleek het mogelijk om in één transformatiestap op zes verschillende plaatsen op het gistgenoom genen te inactiveren. De veelzijdigheid van CRISPR/Cas9 voor “genome-editing” in gist werd verder gedemonstreerd door gelijktijdige integratie van meerdere genen met een gendeletie en het aanbrengen van enkele-nucleotide mutaties op twee verschillende loci. Protocollen, stammen, plasmiden en een vrij-toegankelijk “web-based” CRISPR/Cas9 targetsequentie-zoekmachine en primer-ontwerpprogramma (Yeaststriction), werden ter beschikking gesteld voor andere gistonderzoekers voor snelle, gestandaardiseerde en efficiënte toepassing van CRISPR/Cas9. Genetische modificatietechnieken zoals het CRISPR/Cas9 systeem werden intensief gebruikt in de andere hoofdstukken om het acetyl-CoA metabolisme in *S. cerevisiae* te onderzoeken en aan te passen (**Hoofdstuk 3, 4 en 5**).

In het cytosol van wildtype bakkersgist wordt acetyl-CoA gevormd via een route die bestaat uit de reacties gekatalyseerd door de enzymen pyruvaatdecarboxylase, acetaldehyde-dehydrogenase en acetyl-CoA-synthetase. Deze reactiessequentie staat ook wel bekend als PDH (pyruvaatdehydrogenase)-bypass. De laatste reactie in de PDH-bypass, de activering van azijnzuur naar acetyl-CoA, wordt gekatalyseerd door Acs1 of Acs2 en kost veel ATP, waardoor de maximaal haalbare opbrengst van acetyl-CoA-afhankelijke producten in *S. cerevisiae* ernstig wordt beperkt. In **Hoofdstuk 3** werd daarom de ACS-reactie vervangen door twee ATP-onafhankelijke routes naar cytosolisch acetyl-CoA. Na evaluatie van verschillende heterologe genen die voor acetylerende acetaldehyde-dehydrogenases (A-ALD) en pyruvaat-formiaat lyases (PFL) coderen, werden *acs1Δ acs2Δ S. cerevisiae* stammen geconstrueerd waarin ACS func-

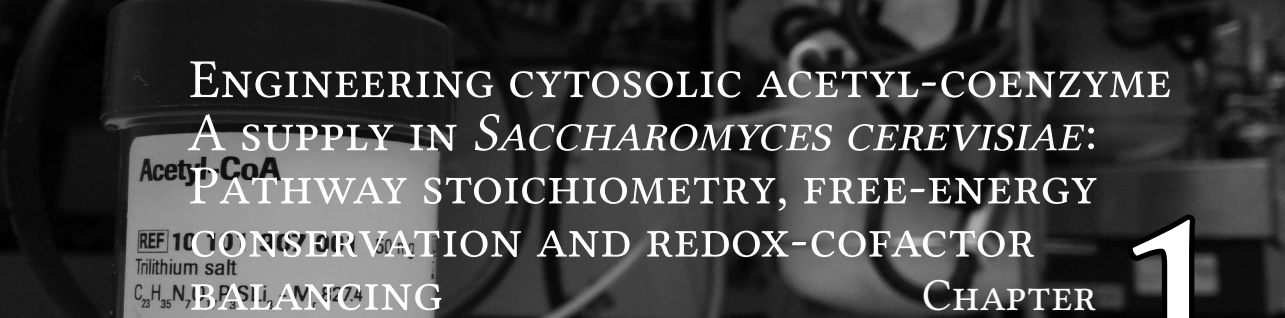
tioneel werd vervangen door A-ALD of PFL. A-ALD-afhankelijke stammen gaven onder aërobe condities specifieke groeisnelheden op glucose tot $0,27 \text{ h}^{-1}$, terwijl anaërobe groei van PFL-afhankelijke *S. cerevisiae* (met een specifieke groeisnelheid van $0,20 \text{ h}^{-1}$) stoichiometrisch gekoppeld was aan de productie van mierenzuur. In glucose-gelimiteerde chemostaatculturen waren na analyse van intracellulaire metabolieten geen grote verschillen te zien tussen de A-ALD-afhankelijke stam en de referentiestam. De biomassaopbrengsten van A-ALD- en PFL-afhankelijke stammen op glucose waren echter wel lager dan die van de ACS-afhankelijke referentiestam. Uit transcriptoomanalyse bleek dat de verminderde biomassaopbrengsten werden veroorzaakt door toxiciteit van acetaldehyde en mierenzuur in, respectievelijk, A-ALD- en PFL-afhankelijke stammen. Ook bleek dat een eerder voorgestelde rol van Acs2 in histoonacetylering vermoedelijk berustte op de rol van dit enzym in de vorming van cytosolische acetyl-CoA en niet op een directe betrokkenheid bij de acetylering van histonen. Deze studie liet voor de eerste keer zien dat de natieve route voor vorming van cytosolisch acetyl-CoA in bakkersgist volledig kan worden vervangen door heterologe routes. Daarbij werd echter ook duidelijk dat, alvorens deze heterologe routes toegepast kunnen worden voor de synthese van acetyl-CoA-afhankelijke producten, nog specifieke uitdagingen te overwinnen zijn.

Ontwerp en implementatie van “metabolic engineering”-strategieën om fluxen richting precursors te verbeteren vereist niet alleen kennis van de fluxverdeling in wildtype stammen, maar ook van compenserende “back-up” routes die actief worden wanneer mechanismen die het grootste deel van de flux in wildtype cellen dragen, worden geïnactiveerd door genetische modificatie of door veranderde procesomstandigheden. **Hoofdstuk 4** beschrijft daarom onderzoek naar de verschillende reacties die op het grensvlak van de glycolyse en de citroenzuurcyclus plaatsvinden. Naast de bovengenoemde cytosolische PDH-bypass beschikt glucose-gekte *S. cerevisiae* over verscheidene andere mechanismen om acetyl-CoA te maken. Door directe oxidatieve decarboxylering van pyrodruivenzuur via het mitochondriële pyruvaat-dehydrogenase (PDH) complex wordt acetyl-CoA gevormd in de mitochondriële matrix. Een tweede bron van mitochondrieel acetyl-CoA is afhankelijk van de activiteit van het mitochondriële eiwit Ach1. Dit enzym kan de coenzym A-groep verplaatsen van succinyl-CoA naar azijnzuur, waardoor acetyl-CoA en barnsteen zuur gevormd worden. Een ander mechanisme om de PDH-bypass te koppelen aan de citroenzuurcyclus maakt gebruik van het extramitochondriële citraatsynthase-isoenzym Cit2. Hierbij wordt citroenzuur gevormd uit de condensatie van acetyl-CoA met oxaalazijnzuur dat vervolgens naar de mitochondriën getransporteerd wordt voor verdere omzetting in de citroenzuurcyclus. Om het relatieve belang van de verschillende reacties die actief zijn op het grensvlak van de glycolyse en de citroenzuurcyclus te onderzoeken werden giststammen geconstrueerd met enkele en gecombineerde deleties van genen die coderen voor belangrijke enzymen in deze drie routes. Experimenten in schudkolven toonden aan dat zowel Ach1 als het PDH-complex belangrijk kunnen zijn voor de vorming van mitochondrieel acetyl-CoA waarbij, in wildtype gistcellen, het PDH-complex belangrijker bleek dan Ach1. In afwezigheid van een functioneel mitochondrieel PDH-complex bleek Cit2 belangrijk te zijn voor de synthese van citroenzuurcyclus-metabolieten. Gecombineerde inactivering van zowel het PDH-complex als het Ach1-enzym had een ernstige impact op de fysiologie, hetgeen tot uitdrukking kwam door lage specifieke groeisnelheden op glucose, een lagere adem-

halingscapaciteit en een hoge incidentie van het volledig verlies van ademhalingscapaciteit. Deze waarnemingen wezen op een ernstige beperking van de beschikbaarheid van mitochondrieel acetyl-CoA. De carnitine-shuttle, die in *S. cerevisiae* afhankelijk is van de toevoeging van L-carnitine aan kweekmedia, kan acetylgroepen uit het cytosol vervoeren naar de mitochondria. Toevoeging van L-carnitine aan kweekmedia bevorderde inderdaad de groei van stammen waarin Ach1 en een functioneel PDH-complex ontbraken. De toename in groeisnelheid bedroeg echter slechts 30%, vermoedelijk door glucoserepressie van de carnitine-shuttlegenen. Deze repressie kon worden vermeden door constitutieve overexpressie van de betrokken genen. Dit leidde inderdaad, in dezelfde stamachtergrond, tot specifieke groeisnelheden die bijna gelijk waren aan die van wild-type stammen.

Mechanistisch gezien zou de carnitine-shuttle ook export van acetylgroepen uit de mitochondriën naar het cytosol mogelijk moeten maken. Eerdere studies gaven echter aan dat zo'n omgekeerd mechanisme niet plaatsvindt in groeiende gistcellen. Om de moleculaire basis van deze schijnbare unidirectionaliteit van de carnitine-shuttle in gist te onderzoeken, werden de betrokken genen constitutief tot expressie gebracht in een stam waarin de vorming van cytosolisch acetyl-CoA eenvoudig kon worden voorkomen door verandering van de mediumsamenstelling (**Hoofdstuk 5**). Aanvankelijk werd geen L-carnitine-afhankelijke groei waargenomen, maar na evolutie in het laboratorium werden twee cultures verkregen waarin vorming van cytosolisch acetyl-CoA afhankelijk was van de carnitine-shuttle. Deze geëvolueerde stammen vertoonden specifieke groeisnelheden op glucose tot $0,14 \text{ h}^{-1}$. Door de DNA-volgorden van de genomen van deze geëvolueerde stammen uit te lezen, werden onder meer mutaties gevonden in genen die betrokken zijn bij de mitochondriële vetzuursynthese (*MCT1*), de communicatieroute tussen de celkern en mitochondriën (*RTG2*) en een verondersteld carnitine-acetyltransferase (*YAT2*). Deze drie mutaties werden vervolgens teruggezet in de niet-geëvolueerde stam. Uit analyse van de aldus gemaakte giststammen bleek dat alle mutaties belangrijk waren voor het verkregen fenotype. Deze waarnemingen duiden erop dat verhoogde concentraties van acetyl-CoA in de mitochondriën noodzakelijk zijn om de natuurlijke richting van de carnitineshuttle om te draaien. Verdere analyse toonde aan dat in de geëvolueerde L-carnitine-afhankelijke stammen het leeuwendeel van de benodigde flux naar mitochondrieel acetyl-CoA werd gedragen door het PDH-complex en dat Ach1 hierin geen aanzienlijke rol speelde. **Hoofdstuk 5** draagt niet alleen bij aan ons begrip van de omkeerbaarheid van de carnitine-shuttle, maar biedt bovendien een extra mogelijkheid om cytosolisch acetyl-CoA in gist te maken met een betere ATP stoichiometrie dan de PDH-bypass.

Dit proefschrift toont hoe de opkomst van nieuwe technieken voor genetische modificatie, zoals de inzet van CRISPR/Cas9, "metabolic engineering" van *S. cerevisiae* enorm kan versnellen en vereenvoudigen. Zulke ontwikkelingen zijn essentieel om steeds complexere ingrepen in het genoom van dit belangrijke industriële micro-organisme te realiseren. Door deze technieken te combineren met kwantitatieve, fysiologische analyse werd een kritische evaluatie mogelijk van diverse strategieën voor acetyl-CoA vorming in gist-gebaseerde industriële processen. Daarnaast leverde dit onderzoek nieuwe inzichten op in acetyl-CoA-metabolisme en het functioneren van de carnitine-shuttle in *S. cerevisiae*.



ENGINEERING CYTOSOLIC ACETYL-COENZYME A SUPPLY IN *SACCHAROMYCES CEREVISIAE*: PATHWAY STOICHIOMETRY, FREE-ENERGY CONSERVATION AND REDOX-COFACTOR BALANCING

CHAPTER 1

Harmen M. van Rossum, Barbara U. Kozak, Jack T. Pronk, Antonius J.A. van Maris

Abstract

Saccharomyces cerevisiae is an important industrial cell factory and an attractive experimental model for evaluating novel metabolic engineering strategies. Many current and potential products of this yeast require acetyl coenzyme A (acetyl-CoA) as a precursor and pathways towards these products are generally expressed in its cytosol. The native *S. cerevisiae* pathway for production of cytosolic acetyl-CoA consumes 2 ATP equivalents in the acetyl-CoA synthetase reaction. Catabolism of additional sugar substrate, which may be required to generate this ATP, negatively affects product yields. Here, we review alternative pathways that can be engineered into yeast to optimize supply of cytosolic acetyl-CoA as a precursor for product formation. Particular attention is paid to reaction stoichiometry, free-energy conservation and redox-cofactor balancing of alternative pathways for acetyl-CoA synthesis from glucose. A theoretical analysis of maximally attainable yields on glucose of four compounds (*n*-butanol, citric acid, palmitic acid and farnesene) showed a strong product dependency of the optimal pathway configuration for acetyl-CoA synthesis. Moreover, this analysis showed that combination of different acetyl-CoA production pathways may be required to achieve optimal product yields. This review underlines that an integral analysis of energy coupling and redox-cofactor balancing in precursor-supply and product-formation pathways is crucial for the design of efficient cell factories.

1.1 INTRODUCTION

Over the past decades, the yeast *Saccharomyces cerevisiae* has become an important, multi-purpose cell factory (219, 220). Its popularity is and continues to be stimulated by a large body of knowledge on yeast physiology and by fast developments in yeast molecular genetics, genomics and systems biology. A myriad of product pathways introduced into *S. cerevisiae* now enable the synthesis, from simple sugars, of products as diverse as benzyloquinoline alkaloids (57), C₄-alcohols (6, 22, 299), flavonoids (165), isoprenoids (10, 329), organic acids (204, 212, 240, 346) and fatty acids (46).

Acetyl coenzyme A (acetyl-CoA), an essential molecule in all known life forms (146), is a key precursor for many compounds whose production by *S. cerevisiae* has been made possible by metabolic engineering. Examples include *n*-butanol (169), (poly)hydroxybutyrate (158, 180), fatty acids and derived compounds (46), isoprenoids such as β -carotene (329), farnesene (269) and artemisinic acid (232) and flavonoids such as naringenin (165). In native yeast metabolism, acetyl-CoA is required for synthesis of amino acids (e.g. leucine, arginine, methionine and cysteine), fatty acids, sterols, glutathione, *N*-acetylglucosamine and *S*-adenosyl-methionine (146, 230). Moreover, acetyl-CoA acts as acetyl donor for protein acetylation (89, 238) and as an effector of enzymes (e.g. pyruvate carboxylase; (87, 264)).

In biotechnological processes for production of commodity chemicals from carbohydrates, costs of the feedstock may contribute up to 75% of the total costs (198). In such cases, process economy dictates that product yields on substrate should approximate the theoretical maxima defined by elemental conservation laws and thermodynamics (52). To avoid excessive biomass formation, while still fulfilling energy requirements for cellular maintenance, product formation should ideally lead to a low but positive net ATP gain. Furthermore, processes should preferably be anaerobic, to maximize product yields and eliminate costs for oxygenation of large reactors. Even when thermodynamic- or biochemical constraints demand oxygen consumption, product yields on oxygen should be maximized, for example by eliminating ATP-requiring reactions in product formation. In view of these generic optimization criteria, ATP stoichiometry, carbon conservation and redox-cofactor balancing strongly affect process economy in microbial production processes (163, 339).

The eukaryote *S. cerevisiae* uses dedicated mechanisms to meet acetyl-CoA requirements in its different subcellular compartments (170), of which the cytosolic and mi-

Abbreviations: A-ALD, acetylating acetaldehyde dehydrogenase; acetyl-CoA, acetyl coenzyme A; acetyl-P, acetyl-phosphate; Ach1, CoA-transferase; ACL, ATP-citrate lyase; ACS, acetyl-CoA synthetase; ADH, alcohol dehydrogenase; ALD, acetaldehyde dehydrogenase; CAT, carnitine acetyltransferase; CIT, citrate synthase; CoA, coenzyme A; E(erythrose-4)P, erythrose-4-phosphate; F1,6P, fructose-1,6-biphosphate; F6P, fructose-6-phosphate; FDH, formate dehydrogenase; FeS, iron-sulfur; FPR, flavodoxin-NADP⁺ reductase; fructose-6-P, fructose-6-phosphate; G(lyceraldehyde-3)P, glyceraldehyde-3-phosphate; LSC, succinyl-CoA ligase; P, phosphate; P_i, inorganic phosphate; PDC, pyruvate decarboxylase; PDH, pyruvate dehydrogenase; PDH bypass, pyruvate dehydrogenase bypass; PFL, pyruvate-formate lyase; PFO, pyruvate-ferredoxin/flavodoxin oxidoreductase; PK, phosphoketolase; POX, pyruvate oxidase; PP_i, pyrophosphate; PTA, phosphotransacetylase; R(ibose-5)-P, ribose-5-phosphate; Ribulose-5-P, ribulose-5-phosphate; S7P, sedoheptulose-7-phosphate; TCA, tricarboxylic acid; TPP, thiamine pyrophosphate; X(ylulose-5)P, xylulose-5-phosphate; γ , degree of reduction; γ_p , degree of reduction of product; γ_s , degree of reduction of substrate; ΔG_R° , the change in Gibbs free energy at pH = 7 and an ionic strength of 100 mM and 1 M concentrations of reactants;

Table 1.1. Overall stoichiometry for formation from glucose of one mole of cytosolic acetyl-CoA for the native yeast *S. cerevisiae* PDH bypass pathway and for various alternative routes based on heterologous enzyme activities. Routes with the same overall stoichiometries are presented together.

Native yeast PDH bypass (via AMP-forming acetyl-CoA synthetase)
$\frac{1}{2} \text{ glucose} + 2 \text{ NAD(P)}^+ + \text{ATP} + \text{CoA} + \text{H}_2\text{O} \longrightarrow \text{acetyl-CoA} + 2 (\text{NAD(P)H} + \text{H}^+) + \text{CO}_2 + \text{ADP} + \text{P}_i$
PDH bypass (via ADP-forming acetyl-CoA synthetase)
$\frac{1}{2} \text{ glucose} + 2 \text{ NAD(P)}^+ + \text{CoA} \longrightarrow \text{acetyl-CoA} + 2 (\text{NAD(P)H} + \text{H}^+) + \text{CO}_2$
Phosphoketolase and phosphotransacetylase
$\frac{1}{3} \text{ glucose} + \frac{1}{3} \text{ ATP} + \text{CoA} \longrightarrow \text{acetyl-CoA} + \frac{1}{3} (\text{ADP} + \text{P}_i) + \frac{2}{3} \text{ H}_2\text{O}$
ATP-independent oxidative conversion from pyruvate to acetyl-CoA (via A-ALD; PDH_{cyt}; PFL with FDH; or PDH_{mit} with carnitine shuttle)
$\frac{1}{2} \text{ glucose} + 2 \text{ NAD}^+ + \text{ADP} + \text{P}_i + \text{CoA} \longrightarrow \text{acetyl-CoA} + 2 (\text{NADH} + \text{H}^+) + \text{CO}_2 + \text{ATP} + \text{H}_2\text{O}$
Pyruvate oxidase
$\frac{1}{2} \text{ glucose} + \text{NAD}^+ + \text{ADP} + \text{P}_i + \text{CoA} + \frac{1}{2} \text{ O}_2 \longrightarrow \text{acetyl-CoA} + \text{NADH} + \text{H}^+ + \text{CO}_2 + \text{ATP} + 2 \text{ H}_2\text{O}$
Citrate-oxaloacetate shuttle with ACL; or Ach1 with succinyl-CoA ligase and ACS
$\frac{1}{2} \text{ glucose} + 2 \text{ NAD}^+ + \text{CoA} \longrightarrow \text{acetyl-CoA} + 2 (\text{NADH} + \text{H}^+) + \text{CO}_2$
Abbreviations: acetyl-CoA, acetyl coenzyme A; A-ALD, acetylating acetaldehyde dehydrogenase; Ach1, coA-transferase; ACL, ATP-citrate lyase; ACS, acetyl-CoA synthetase; ALD, acetaldehyde dehydrogenase; CoA, coenzyme A; FDH, formate dehydrogenase; PDH _{cyt} , cytosolic pyruvate dehydrogenase; PDH _{mit} , mitochondrial pyruvate dehydrogenase; PFL, pyruvate-formate lyase.

tochondrial compartments are especially relevant for industrial product formation by this yeast. Since the inner mitochondrial membrane is impermeable to acetyl-CoA, mitochondrial acetyl-CoA cannot be directly exported to the cytosol (14, 81). This compartmentation of acetyl-CoA metabolism directly affects cellular energetics since, in terms of ATP stoichiometry, the mitochondrial pyruvate-dehydrogenase (PDH) complex is superior to the PDH bypass pathway for cytosolic acetyl-CoA synthesis (Table 1.1; (245)). Directly connecting a heterologous or synthetic product pathway to the mitochondrial acetyl-CoA pool would therefore require targeting of pathway enzymes to the mitochondrial matrix. Moreover, extensive engineering would be required to enable efficient mitochondrial transport of pathway intermediates, products and/or cofactors. So far, only few studies have explored functional expression of heterologous product pathways in yeast mitochondria (6, 74). Instead, product pathways are commonly expressed in the yeast cytosol and, therefore, dependent on the cytosolic acetyl-CoA pool. Since the nuclear envelope is permeable for small molecules such as acetyl-CoA, the nucleosol, in which important histone acetylation reactions occur, is implicitly included in the cytosol throughout this review.

Recent publications have reviewed the roles of acetyl-CoA in yeast metabolism (170), yeast metabolic engineering (170, 186, 280) and yeast cellular regulation (89). The present review focuses on aspects of metabolic engineering of acetyl-CoA metabolism in *S. cerevisiae* that goes beyond the scope of these previous papers. In particular, we systematically evaluate ATP stoichiometry, carbon conservation and redox-cofactor require-

ments of different native and engineered cytosolic acetyl-CoA forming pathways and of shuttle mechanisms that may be used to transport mitochondrial acetyl-moieties to the yeast cytosol. To analyze the product dependency of optimum pathway configurations for precursor supply, the reviewed cytosolic acetyl-CoA supplying pathways are quantitatively evaluated in terms of maximally attainable yields on substrate and oxygen of four industrially relevant compounds: (i) *n*-butanol, (ii) citric acid, (iii) palmitic acid and (iv) farnesene. Additionally, thermodynamic and kinetic aspects of the alternative pathways are discussed. Although we focus on acetyl-CoA as a precursor in *S. cerevisiae*, the concepts discussed herein are also applicable to other precursors and microorganisms.

1.2 REACTION STOICHIOMETRIES OF PATHWAYS FOR CYTOSOLIC ACETYL-CoA SUPPLY

1.2.1 Native pathway in glucose-grown *S. cerevisiae*: the PDH bypass

Prokaryotes generally produce acetyl-CoA from glucose via pathways that do not involve a net hydrolysis of ATP. Instead, most eukaryotic pathways for cytosolic acetyl-CoA synthesis have a higher ATP expenditure. In *S. cerevisiae*, the native pathway for cytosolic acetyl-CoA synthesis from pyruvate consists of pyruvate decarboxylase (PDC; EC 4.1.1.1), NAD⁺- or NADP⁺-dependent acetaldehyde dehydrogenase (ALD; EC 1.2.1.3 (NAD⁺-dependent), EC 1.2.1.4 (NADP⁺-dependent)) and the ATP-requiring reaction catalyzed by acetyl-CoA synthetase (ACS; EC 6.2.1.1). These reactions are collectively referred to as the pyruvate-dehydrogenase bypass (PDH bypass; Figure 1.1A) (244). ACS catalyzes activation of acetate with the concomitant hydrolysis of ATP to AMP and PP_i:



When activation of acetate by ACS is followed by the reactions catalyzed by pyrophosphatase (EC 3.6.1.1) and adenylate kinase (EC 2.7.4.3), the overall reaction sequence involves the net hydrolysis of 2 ATP to 2 ADP and 2 P_i. Involvement of pyrophosphatase has a strong impact on the overall thermodynamics of acetate activation. Reaction 1.1 has an estimated ΔG_R° of -4.5 kJ·mol⁻¹ (79), which decreases to -20.3 kJ·mol⁻¹ (79) when the pyrophosphatase reaction is included, thus enabling this essential biosynthetic reaction to function *in vivo* at a wide range of concentrations of its substrates and products.

Stoichiometrically, formation of 1 acetyl-CoA from glucose through glycolysis and PDH bypass requires 1 ATP and results in the net formation of 2 NADH or 1 NADH and 1 NADPH (Table 1.1). ATP required for cytosolic acetyl-CoA synthesis has to be generated by dissimilation of glucose through respiratory or fermentative dissimilation of glucose. This ATP requirement for precursor supply can severely limit the maximum attainable yields on glucose of cytosolic acetyl-CoA-derived products by *S. cerevisiae*.

1.2.2 Heterologous pathways for cytosolic acetyl-CoA supply

To decrease ATP costs for cytosolic acetyl-CoA supply, alternative (heterologous) pathways that convert glucose into cytosolic acetyl-CoA can be considered for functional

replacement of the PDH bypass. For example, one might consider replacing the native *S. cerevisiae* ACS by a heterologous ADP-forming acetyl-CoA synthetase (EC 6.2.1.13), which catalyzes the conversion of acetate and ATP to acetyl-CoA and ADP:

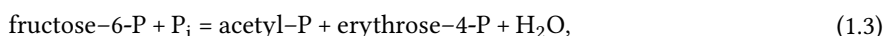


This apparently simple replacement would make formation of acetyl-CoA from glucose an ATP-neutral process, while still generating 2 moles of NAD(P)H per mole of acetyl-CoA (Table 1.1). However, with an estimated $\Delta G_R^{\circ'}$ of $+3.6 \text{ kJ}\cdot\text{mol}^{-1}$ (79), use of ADP-forming ACS as an acetyl-CoA generating reaction poses strict requirements on the concentrations of intracellular substrate and product concentrations. To our knowledge, ADP-forming acetyl-CoA synthetases have not yet been functionally expressed in yeast.

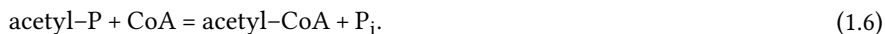
In this section, six additional heterologous acetyl-CoA supplying routes are discussed in terms of their ATP- and redox-cofactor stoichiometry and with respect to their functional expression in *S. cerevisiae*. Five of these routes, relying on phosphoketolase/transacetylase, acetylating acetaldehyde dehydrogenase, pyruvate-formate lyase, pyruvate dehydrogenase and pyruvate oxidase (Figure 1.1A and B), have already been implemented in *S. cerevisiae*. A sixth, based on pyruvate-ferredoxin/flavodoxin oxidoreductase, has not yet been expressed in yeast.

1.2.2.1 Phosphoketolase and phosphotransacetylase

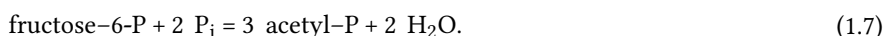
Phosphoketolase (PK; EC 4.1.2.9 and EC 4.1.2.22) and phosphotransacetylase (PTA; EC 2.3.1.8) are involved in the central carbon metabolism of heterofermentative lactic acid bacteria and in some fungi (72, 145). PK enzymes can use either fructose-6-P, xylulose-5-P or ribulose-5-P as substrates (111, 274) and differ with respect to their specificities for these three substrates (39, 111, 274). PK converts these sugar phosphates and inorganic phosphate into acetyl-P and either erythrose-4P or glyceraldehyde-3P:



The acetyl-P formed in reactions 1.3-1.5, which are all exergonic under biochemical standard conditions (estimated $\Delta G_R^{\circ'} = -49.9$ to $-63.2 \text{ kJ}\cdot\text{mol}^{-1}$; (79)), can subsequently be converted to acetyl-CoA by the reversible PTA reaction ((294); estimated $\Delta G_R^{\circ'} = -9.8 \text{ kJ}\cdot\text{mol}^{-1}$ in the acetyl-CoA forming direction; (79)):



Schramm and Racker (275) postulated that concerted action of PK, enzymes of the non-oxidative part of the pentose-phosphate pathway, glycolysis and the gluconeogenic enzyme, fructose-1,6-bisphosphatase (FBPase; EC 3.1.3.11), could catalyze conversion of 1 mole of fructose-6-P, without carbon loss, into 3 moles of acetyl-P (Figure 1.1B), according to the following net reaction:



Reaction 1.7 is strongly exergonic (estimated $\Delta G_R^\circ = -302.2 \text{ kJ}\cdot\text{mol}^{-1}$; (79)), suggesting that it should operate when the required enzymes are simultaneously present. Indeed, Schramm *et al.* (274) observed a yield of acetate on fructose-6-P in cell extracts of *Acetobacter xylinum* that was consistent with the operation of this so-called fructose-6-P shunt. Over half a century later, conversion of fructose-6-P to acetyl-P without carbon loss was ‘rediscovered’ (18), this time in a reconstituted *in vitro* enzyme system. Subsequent expression of *Bifidobacterium adolescentis* PK and overexpression of FBPase in an engineered *E. coli* strain enabled anaerobic conversion of xylose to acetate at a molar yield of $2.2 \text{ mol}\cdot\text{mol}^{-1}$. This stoichiometry is close to $2.5 \text{ mol}\cdot\text{mol}^{-1}$, the predicted yield for *in vivo* operation of the fructose-6-P shunt (18).

In theory, it should be possible to implement a full fructose-6-P shunt in *S. cerevisiae* (Figure 1.1B) by expression of heterologous PK and PTA enzymes and bypassing the glucose repression of the yeast *FBP1* gene and glucose inactivation of the encoded FBPase (90, 91). Provided that futile cycling as a result of the simultaneous presence of phosphofructokinase and FBPase (218) can be avoided, this strategy should enable formation of 1 mole of acetyl-CoA at the cost of only one-third of a mole of ATP, without involvement of redox cofactors (Table 1.1). The same stoichiometry for conversion of sugar to acetyl-CoA can be achieved in a cycle similar to the one shown in Figure 1.1B, but with xylulose-5-P as the sole substrate for PK. When subsequent formation of a product from acetyl-CoA does not yield ATP, respiratory dissimilation of acetyl-CoA via the TCA-cycle or simultaneous operation of an alternative, ATP-yielding pathway for cytosolic acetyl-CoA synthesis will be required. Similarly, when product formation from acetyl-CoA requires NAD(P)H, electrons will have to be made available elsewhere in metabolism. PK can also be combined with acetate kinase (AK; EC 2.7.2.1; acetyl-P + ADP = acetate + ATP). The thus formed acetate can be used by ACS, yielding acetyl-CoA, albeit at a decreased ATP efficacy compared to PK/PTA.

While PK activity has been reported in wild-type strains of *S. cerevisiae* (72, 291, 312), activities in cell extracts are low and the responsible gene has not been identified. Several studies have explored expression of heterologous PK and PTA or AK genes in *S. cerevisiae*. In a study on pentose fermentation, PK from *Bifidobacterium lactis* and PTA from *Bacillus subtilis* were successfully expressed in *S. cerevisiae*, as confirmed by enzyme assays (291). Later studies combined expression of a heterologous PK with either expression of an AK from *Aspergillus nidulans* or of a PTA from *B. subtilis* in order to improve production of fatty-acid ethyl esters and polyhydroxybutyrate by *S. cerevisiae* (139, 158). However, during growth on glucose, the flux through the PK pathway in these modified *S. cerevisiae* strains appeared to be low (139, 158). In patent literature, implementation of a PK/PTA pathway in yeast has been reported, combining the PK from *Leuconostoc mesenteroides* and PTA from *Clostridium kluyveri* with a route towards the isoprenoid farnesene, whose synthesis requires $9 \text{ mol}\cdot\text{mol}^{-1}$ of acetyl-CoA (94, 110).

1.2.2.2 Acetylating acetaldehyde dehydrogenase

Acetylating acetaldehyde dehydrogenase (A-ALD; EC 1.2.1.10) is involved in the C_2 metabolism of prokaryotes and catalyzes the following reversible reaction:

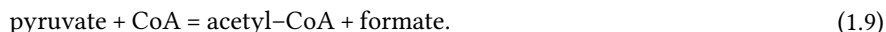


Under biochemical standard conditions, the estimated ΔG_R° of this reversible reaction is $-17 \text{ kJ}\cdot\text{mol}^{-1}$ in the acetyl-CoA forming direction (79). In contrast to NAD(P)^+ -dependent ALD and ACS (Figure 1.1A; Table 1.1), which together catalyze the conversion of acetaldehyde to acetyl-CoA in the native PDH bypass, Reaction 1.8 does not require ATP. Conversion of glucose to acetyl-CoA via glycolysis, PDC and A-ALD yields 1 mole of ATP and 2 moles of NAD(P)H per mole of acetyl-CoA (Figure 1.1A; Table 1.1). Thus, A-ALD provides metabolic engineers with an ATP-yielding option for the synthesis of cytosolic acetyl-CoA from glucose. Furthermore, in contrast to the PK/PTA pathway, this route also yields NADH.

Kozak *et al.* (166) demonstrated functional expression of five prokaryotic A-ALDs, originating from *E. coli* (mhpF and EutE), *Pseudomonas sp.* (dmpF), *Staphylococcus aureus* (adhE) and *Listeria innocua* (lin1129), in *S. cerevisiae*. Expression of A-ALD was shown to functionally complement inactivation of the native PDH bypass pathway for cytosolic acetyl-CoA synthesis (166), although biomass yields of the engineered strains were lower than expected (see below). The potential benefit of A-ALD on cellular energetics is even larger when ethanol is considered as (co-)substrate (168). Ethanol metabolism by *S. cerevisiae* is initiated by its conversion to cytosolic acetyl-CoA through the concerted activity of alcohol dehydrogenase, ALD and ACS. In a theoretical analysis, Kozak *et al.* (168) showed that replacing this native route by an engineered A-ALD-dependent route could potentially increase the biomass yield on ethanol by up to 40%. If this strategy can be functionally implemented, these ATP savings could make ethanol a much more attractive (co-)substrate for industrial production of acetyl-CoA derived molecules.

1.2.2.3 Pyruvate-formate lyase

Another reaction that yields acetyl-CoA from pyruvate is catalyzed by pyruvate-formate lyase (PFL; EC 2.3.1.54; (40)):



Reaction 1.9 has an estimated ΔG_R° of $-21.2 \text{ kJ}\cdot\text{mol}^{-1}$ (79) and plays a key role in fermentation pathways in a large number of anaerobic microorganisms (54, 295). The redox-cofactor stoichiometry of the formation of acetyl-CoA from glucose through PFL depends on the subsequent metabolic fate of formate. To obtain the highest possible electron efficacy and to avoid weak-organic-acid uncoupling by formate (95, 231), the formate produced by PFL has to be oxidized to CO_2 , a reaction catalyzed by formate dehydrogenase (FDH; EC 1.2.1.2):



Formation of acetyl-CoA from glucose through the combined action of PFL and NAD^+ -dependent FDH yields 1 ATP and 2 NADH per acetyl-CoA, which is identical to the net stoichiometry of the A-ALD route described above (Figure 1.1A; Table 1.1). Theoretically, application of PFL with or without FDH or together with a formate-hydrogen lyase (EC 1.1.99.33; (270)), creates flexibility in metabolic engineering strategies that include these enzymes. Furthermore, protein engineering has yielded FDH enzymes that

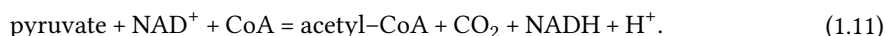
use NADP^+ instead of NAD^+ as a cofactor (120, 277). The latter option is of particular interest when product formation pathways downstream of acetyl-CoA use NADPH as the electron donor, as is for instance the case in fatty-acid synthesis. However, the biochemistry of PFL and, as will be discussed later, FDH represent significant challenges.

Catalytic activity of PFL depends on a radical residue, which is introduced by abstraction of a hydrogen atom from its active site by a specific PFL-activating enzyme (PFL-AE; EC 1.97.1.4). Activation of PFL by PFL-AE involves the flavoprotein flavodoxin (155). In *E. coli*, flavodoxin is encoded by *fldA* and its reduction depends on the flavodoxin- NADP^+ reductase, encoded by *fpr* (210). Its radical residue makes PFL highly sensitive to molecular oxygen, which causes irreversible cleavage of PFL in two inactive fragments (155). Moreover, also the essential $[4\text{Fe-4S}]$ cluster in the active site of PFL-AE is oxygen labile (173).

PFL and PFL-AE from *E. coli* were first expressed in *S. cerevisiae* by Waks and Silver (331), who demonstrated formate accumulation during anaerobic growth of the resulting yeast strains. PFL was subsequently shown to functionally replace the native PDH bypass as the sole pathway for cytosolic acetyl-CoA synthesis in anaerobic *S. cerevisiae* cultures (166). Expression of PFL and PFL-AE from either *E. coli* or *Lactobacillus plantarum* supported anaerobic specific growth rates of an Acs^- strain of up to 73% of that of the Acs^+ reference strain. It is presently unclear which *S. cerevisiae* proteins functionally replace bacterial flavodoxins in these studies (166, 331). Recently, co-expression of the flavodoxin: NADP^+ reductase system from *E. coli* was shown to enable PFL-dependent growth of engineered Pdc^- *S. cerevisiae* strains under microaerobic conditions (350).

1.2.2.4 Pyruvate dehydrogenase complex

The pyruvate dehydrogenase (PDH) complex (EC 1.2.4.1, EC 2.3.1.12, EC 1.8.1.4) catalyzes the oxidative decarboxylation of pyruvate into acetyl-CoA:



The estimated $\Delta G_{\text{R}}^{\circ}$ of the overall reaction catalyzed by this multi-enzyme complex is $-40.2 \text{ kJ} \cdot \text{mol}^{-1}$ (79). Before the recent discovery of a nuclear PDH complex in human cells (303), eukaryotic PDH complexes were assumed to be confined to mitochondria, as is also the case in *S. cerevisiae* (14). Direct conversion of pyruvate to cytosolic acetyl-CoA via Reaction 1.11 therefore either requires relocalization of the native yeast mitochondrial PDH complex to the cytosol or cytosolic expression of a heterologous PDH complex. Stoichiometrically, formation of acetyl-CoA via a cytosolic PDH complex corresponds to the A-ALD or PFL/FDH-based pathways discussed above (Table 1.1). However, in contrast to these pathways, acetyl-CoA generation by the PDH complex does not involve the potentially toxic intermediates acetaldehyde or formate (Figure 1.1A).

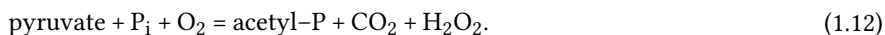
Functional expression of a heterologous PDH complex is complicated by its multi-subunit organization. The E1 subunit, in many organisms consisting of separate $\text{E1}\alpha$ and $\text{E1}\beta$ subunits, has pyruvate dehydrogenase activity (EC 1.2.4.1), E2 has dihydrolipoamide acetyltransferase activity (EC 1.2.4.1) and E3 has dihydrolipoyl dehydrogenase activity (EC 1.2.4.1) (161, 351). Multiple copies of each subunit assemble into a $\sim 10 \text{ MDa}$ complex (286), which makes the whole complex larger than a yeast ribosome (211). Furthermore,

the E2 subunit is only active when covalently linked to lipoic acid, which requires a specific lipoylation system (51). As an additional complication, the E3 subunit of many PDH complexes is strongly inhibited by high $[\text{NADH}]/[\text{NAD}^+]$ ratios. In most organisms, the PDH complex is therefore only active under aerobic conditions, when $[\text{NADH}]/[\text{NAD}^+]$ ratios are lower than under anaerobic conditions (11, 30, 286). However, the PDH complex from the Gram-positive bacterium *Enterococcus faecalis* was shown to exhibit a remarkably low sensitivity to high $[\text{NADH}]/[\text{NAD}^+]$ ratios (285), which enables it to function in its native host under anaerobic conditions (286).

Functional expression and assembly of the *E. faecalis* PDH complex in the cytosol of *S. cerevisiae* was recently demonstrated (167). *In vivo* PDH activity not only required heterologous expression of the E1 α , E1 β , E2 and E3 subunits of *E. faecalis* PDH, but also of two *E. faecalis* genes involved in lipoylation of the E2 subunit and supplementation of growth media with lipoic acid. The *in vivo* activity of the cytosolic PDH-complex was sufficient to meet the cytosolic acetyl-CoA demand for growth, as demonstrated by complementation in Acs⁻ *S. cerevisiae* strains (167). Growth of these strains was also observed under anaerobic conditions, consistent with the previously reported ability of this PDH complex to operate at elevated $[\text{NADH}]/[\text{NAD}^+]$ ratios (see above).

1.2.2.5 Pyruvate oxidase

In many prokaryotes, the flavoprotein pyruvate oxidase (POX; EC 1.2.3.3) catalyzes oxidative decarboxylation of pyruvate to acetyl-P and donates electrons to oxygen, thereby forming hydrogen peroxide (191, 313):



Following this strongly exergonic reaction (estimated $\Delta G_R^\circ = -163.8 \text{ kJ}\cdot\text{mol}^{-1}$; (79)), acetyl-CoA can be formed from acetyl-P by PTA (Reaction 1.6). Detoxification of hydrogen peroxide can, for example, occur via catalase (EC 1.11.1.6):

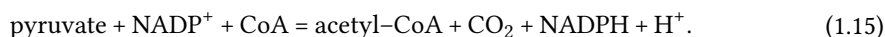
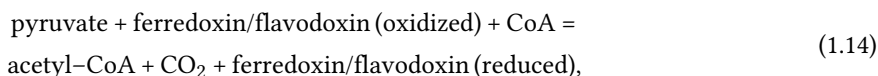


Formation of 1 acetyl-CoA from glucose via glycolysis, reactions 1.13 and PTA (Reaction 1.6) consumes $\frac{1}{2} \text{ O}_2$ and forms 1 NADH and ATP (Figure 1.1A; Table 1.1). Compared to the ATP-independent oxidative conversions of pyruvate into acetyl-CoA (by A-ALD, PFL/FDH or PDH), the POX route requires oxygen and yields fewer reducing equivalents. There is as yet no scientific literature on implementation of the POX strategy for cytosolic acetyl-CoA supply in *S. cerevisiae*. However, a recent patent application reports that combined expression of POX from *Aerococcus viridans* with a PTA increased the specific growth rate of an *S. cerevisiae* strain in which the PDH bypass was inactivated by deletion of all three pyruvate-decarboxylase genes (221).

1.2.2.6 Pyruvate-ferredoxin/flavodoxin oxidoreductase

Similar to the PDH complex, pyruvate-ferredoxin/flavodoxin oxidoreductase (PFO; EC 1.2.7.1) catalyzes oxidative decarboxylation of pyruvate to acetyl-CoA (248). However,

unlike the NADH-yielding PDH reaction, PFO transfers electrons to ferredoxin or flavodoxin. The iron-sulfur-cluster-containing PFO is oxygen sensitive, which probably restricts its applicability to anaerobic conditions. In some organisms, including *Helicobacter pylori*, an NADP⁺-flavodoxin oxidoreductase (FPR; EC 1.18.1.2) can transfer electrons from reduced flavodoxin to NADP⁺, yielding NADPH (128). Interestingly, the protist *Euglena gracilis* harbors a chimeric mitochondrial pyruvate-NADP⁺ oxidoreductase (EC 1.2.1.51) protein, which integrates PFO and FPR activity (135, 260). In these reactions, pyruvate is converted into acetyl-CoA via PFO or via PFO and FPR through, respectively, the following reactions:



Reactions 1.14 and 1.15 both have negative $\Delta G_R^{\circ'}$ values (estimated at -23.6 (with ferredoxin as redox cofactor) and -32.9 kJ·mol⁻¹, respectively; (79)). Application of PFO and/or PFR for yeast metabolic engineering would require efficient regeneration of the reduced co-factors. For optimal electron efficacy, this would require reductive reaction steps downstream of acetyl-CoA that re-oxidize either reduced ferredoxin/flavodoxin or NADPH, as has for instance been shown for the anaerobic conversion of glucose to wax esters by *E. gracilis* (134). If this requirement can be met, the overall stoichiometric impact of these enzymes on product formation would be identical to that of PDH, but would expand flexibility with respect to redox-cofactor specificity.

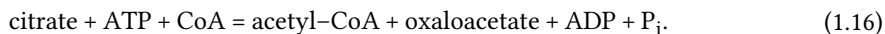
1.2.3 Export of mitochondrial acetyl moieties to the cytosol via shuttle mechanisms

The six strategies discussed above rely on direct formation of acetyl-CoA in the yeast cytosol. Alternatively, cytosolic acetyl-CoA may be provided through mitochondrial, ATP-independent formation of acetyl-CoA via the native PDH complex using shuttle mechanisms. Three such mechanisms that, by a combination of enzyme-catalyzed reactions and transport steps, enable the net export of mitochondrial acetyl moieties to the cytosol, are discussed below: the citrate-oxaloacetate shuttle, the carnitine shuttle and a shuttle mechanism that relies on mitochondrial conversion of acetyl-CoA to acetate.

1.2.3.1 Citrate-oxaloacetate shuttle

The citrate-oxaloacetate shuttle uses oxaloacetate as a carrier molecule to transfer acetyl moieties across the mitochondrial membrane. This shuttle not only occurs in many higher eukaryotes, but also in oleaginous yeasts, where it provides cytosolic acetyl-CoA for lipid synthesis (20). In the citrate-oxaloacetate shuttle, acetyl-CoA formed by the mitochondrial PDH complex first reacts with oxaloacetate in a reaction catalyzed by mitochondrial citrate synthase (EC 2.3.3.1; Figure 1.1C). Citrate generated in this reaction is then exported from the mitochondria via antiport with oxaloacetate or malate (26). The acceptor molecule in this shuttle mechanism, oxaloacetate, is then regenerated by

ATP-dependent cleavage of citrate, catalyzed by cytosolic ATP-citrate lyase (ACL; EC 2.3.3.8):



Finally, antiport of cytosolic oxaloacetate with mitochondrial citrate enables a new cycle of the shuttle (Figure 1.1C). As the ATP generated via glycolysis is hydrolyzed again in Reaction 1.16, formation of cytosolic acetyl-CoA from glucose via ACL is ATP neutral and results in formation of 1 NADH in the cytosol and 1 NADH in the mitochondria (Table 1.1). To maintain redox-cofactor balance, NADH formed in the mitochondria should either be re-oxidized via respiration or, via involvement of mitochondrial redox shuttles (7), be translocated to the cytosol to be reoxidized in a product formation pathway.

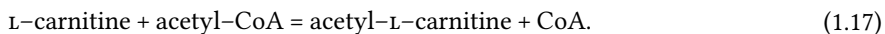
In contrast to oleaginous yeasts, *S. cerevisiae* does not contain ACL (20). However, *S. cerevisiae* mitochondria do contain a functional citrate- α -ketoglutarate antiporter, encoded by *YHM2*, which also has activity with oxaloacetate (37). Functional expression of ACL from *Arabidopsis thaliana* in *S. cerevisiae* was first demonstrated by *in vitro* enzyme assays (76). Two subsequent studies investigated the impact of the citrate-oxaloacetate shuttle on production of acetyl-CoA derived compounds by *S. cerevisiae*. Tang *et al.* (307) showed that expression of a murine ACL resulted in a 1.1 to 1.2 fold increase in fatty-acid content during stationary phase (307). Similarly, expression of ACL from *Yarrowia lipolytica* resulted in a 2.4 fold increase of the *n*-butanol yield on glucose in *S. cerevisiae* strains that co-expressed a heterologous, acetyl-CoA dependent pathway to *n*-butanol (185). In another study, expression of the ACL enzymes from *A. nidulans*, *Mus musculus*, *Y. lipolytica*, *Rhodospiridium toruloides* and *Lipomyces starkeyii* in *S. cerevisiae* demonstrated that the *A. nidulans* ACL resulted in 4.2 – 9.7 fold higher activity than the other ACLs (256). By applying a push/pull/block strategy on an *S. cerevisiae* strain expressing the *A. nidulans* ACL, acetyl-CoA-dependent production of mevalonate was improved (256).

ACL is also involved in another potentially interesting strategy for cytosolic acetyl-CoA formation. This strategy, which has hitherto only been partially successful in *E. coli*, relies on reversal of the glyoxylate cycle by introduction of several ATP-dependent steps (199). By combined expression of ATP-citrate lyase, malate thiokinase (EC 6.2.1.9; $\text{malate} + \text{CoA} + \text{ATP} = \text{malyl-CoA} + \text{ADP} + \text{P}_i$) and a malyl-CoA lyase (EC 4.1.3.24; $\text{malyl-CoA} = \text{acetyl-CoA} + \text{glyoxylate}$), this pathway should enable the *in vivo* conversion of succinate and malate to oxaloacetate and 2 acetyl-CoA (199). While further research is required before this strategy can be applied in metabolic engineering, it could enable efficient conversion of C_4 substrates to 2 acetyl-CoA, without loss of carbon in the form of CO_2 . However, this high carbon conversion will be at the expense of ATP hydrolysis.

1.2.3.2 Carnitine shuttle

The carnitine shuttle, which uses the quaternary ammonium compound L-carnitine as a carrier molecule, enables transport of acyl moieties between eukaryotic organelles (15). When acetyl-CoA is the substrate, the carnitine shuttle consists of cytosolic and mitochondrial carnitine acetyltransferases (EC 2.3.1.7), which transfer activated acetyl-CoA

to L-carnitine and vice versa (Reaction 1.17), as well as an acetyl-carnitine translocase in the inner mitochondrial membrane (Figure 1.1C).



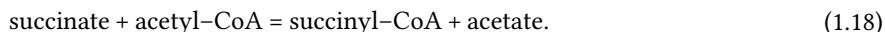
In *S. cerevisiae*, at least six proteins contribute to a functional carnitine shuttle. In contrast to many other eukaryotes, including mammals (319) and the yeast *Candida albicans* (302), *S. cerevisiae* lacks the genetic information required for L-carnitine biosynthesis (257, 305). Operation of the carnitine shuttle in *S. cerevisiae* therefore depends on availability of exogenous L-carnitine, which is imported via the Hnm1 plasma-membrane transporter (4). Expression of *HNM1* is regulated by the plasma-membrane-spanning protein Agp2 (4, 258). *S. cerevisiae* harbors three carnitine acetyltransferases (15), with different subcellular localizations: Cat2 is active in the peroxisomal and mitochondrial matrices (69), Yat1 is localized to the outer mitochondrial membrane (271) and Yat2 is a cytosolic protein (129, 159, 305). The inner mitochondrial membrane contains an acetyl-carnitine translocase, Crc1 (84, 160, 233, 258).

All components of the carnitine shuttle catalyze reversible reactions. Transport of the acetyl moiety of acetyl-CoA from the mitochondria to the cytosol via the carnitine shuttle should therefore, at least theoretically, enable the formation of acetyl-CoA from glucose with the generation of 1 ATP and the formation of 1 NADH in the mitochondria and 1 NADH in the cytosol (Table 1.1). However, in *S. cerevisiae* strains that express the genes of the carnitine shuttle from their native promoters, the shuttle does not contribute to export of mitochondrial acetyl moieties during growth on glucose (203). To circumvent the glucose repression that occurs in wild-type *S. cerevisiae* (69, 151, 271), Van Rossum *et al.* (259) recently constructed an *S. cerevisiae* strain in which all genes involved in the carnitine shuttle were constitutively expressed. Elimination of the PDH bypass in such a strain background, followed by laboratory evolution, yielded strains whose growth on glucose was dependent on L-carnitine supplementation (259). This result indicated that acquisition of specific mutations in the yeast genome indeed allows the carnitine shuttle to export mitochondrial acetyl units to the cytosol. While this study presented a first proof of concept, further research is necessary to explore the potential industrial relevance of the carnitine shuttle as an alternative mechanism for supplying acetyl-CoA in *S. cerevisiae*.

1.2.3.3 Mitochondrial conversion of acetyl-CoA to acetate through the CoA-transferase Ach1

Whereas acetyl-CoA cannot cross the mitochondrial membrane, acetate likely can (see below). Mitochondrial conversion of acetyl-CoA to acetate, followed by export of acetate from the mitochondria and its subsequent activation by cytosolic ACS, could constitute an alternative acetyl-CoA shuttle (Figure 1.1C). In *S. cerevisiae*, mitochondrial release of acetate from acetyl-CoA is catalyzed by Ach1, which was originally characterized as a mitochondrial acetyl-CoA hydrolase (EC 3.1.2.1; (28)). Subsequent *in vitro* studies with purified protein showed that Ach1 is, in fact, a CoA-transferase that can also catalyze the transfer of the CoA group between various CoA esters and short-chain organic acids

(80). When Ach1 uses succinate and acetyl-CoA as substrates, this results in the following reversible reaction:



The overall ATP cost (or yield) of formation of cytosolic acetyl-CoA through this system depends on the reactions by which acetate is formed. If acetate is formed by hydrolysis of mitochondrial acetyl-CoA, formation of cytosolic acetyl-CoA from glucose, involving the native ACS, through this route costs 1 ATP. This stoichiometry would not provide an energetic benefit over the native PDH bypass. However, if mitochondrial acetate is formed by a CoA-transfer reaction with succinate as CoA acceptor, one ATP can be recovered by subsequently regenerating succinate via succinyl-CoA ligase (EC 6.2.1.5; (247)):



In this scenario, formation of cytosolic acetyl-CoA from glucose via Ach1-catalyzed CoA-transfer is an ATP neutral process (Figure 1.1C; Table 1.1). When combined with an ADP-forming ACS (see above), formation of acetyl-CoA from glucose via this pathway could even result in a net yield of 1 mole of ATP per mole of acetyl-CoA. These three scenarios all result in the formation of 1 mole of cytosolic NADH and 1 mole of mitochondrial NADH per mole of acetyl-CoA produced from glucose.

Combination of Ach1 activity with export of acetate to the cytosol has recently been shown to enable cytosolic acetyl-CoA synthesis in *S. cerevisiae* strains in which the PDH bypass was impaired by deletion of the pyruvate decarboxylases *PDC1*, *PDC5* and *PDC6* (44). Such *Pdc*[−] strains become auxotrophic for externally added acetate (or other C₂ compounds) as substrate for the cytosolic acetyl-CoA synthase (81). After previous studies had shown that this auxotrophy can be overcome by either laboratory evolution or by introduction of a stable *MTH1* allele (202, 228), Chen *et al.* (44) showed that the acquired acetate prototrophy relies on Ach1. In these strains, Ach1 releases acetate in the mitochondria that is subsequently transported to the cytosol and activated to acetyl-CoA by cytosolic Acs1 and/or Acs2 (Reaction 1.11) (44). The *in vivo* capacity of Ach1 in glucose-grown cultures of *S. cerevisiae* is low (318) and insufficient to sustain fast growth of *Pdc*[−] strains in the absence of further modification or evolution (228). Therefore, to fully explore the potential stoichiometric benefits of this system for product formation, increasing pathway capacity should be a first priority.

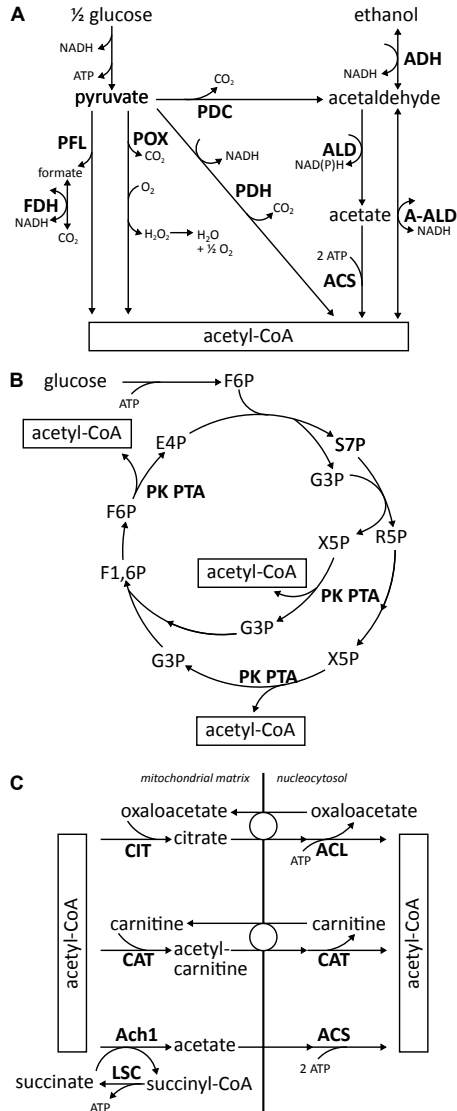


Figure 1.1. Schematic representation of alternative routes for formation of acetyl-CoA in the cytosol of *Saccharomyces cerevisiae*. **A** native PDH bypass; engineered pyruvate oxidase; pyruvate-formate lyase and formate dehydrogenase; pyruvate dehydrogenase; and acetylating acetaldehyde dehydrogenase. **B** One possible configuration of acetyl-CoA formation via phosphoketolase/-transacetylase in combination with pentose-phosphate-pathway enzymes, fructose-1,6-bisphosphatase and glycolysis (figure adapted from Bogorad *et al.* (18)). **C** Shuttle mechanisms that result in net export of acetyl moieties from the mitochondrial matrix to the cytosol: citrate-oxaloacetate shuttle; carnitine shuttle; and mitochondrial formation of acetate by Ach1 followed by export to the cytosol. Abbreviations: acetyl-CoA, acetyl coenzyme A; A-ALD, acetylating acetaldehyde dehydrogenase; Ach1, CoA-transferase; ACL, ATP-citrate lyase; ACS, acetyl-CoA synthetase; ADH, alcohol dehydrogenase; ALD, acetaldehyde dehydrogenase; CAT, carnitine acetyltransferase; CIT, citrate synthase; E4P, erythrose-4-phosphate; F1,6P, fructose-1,6-bisphosphate; F6P, fructose-6-phosphate; FDH, formate dehydrogenase; G3P, glyceraldehyde-3-phosphate; LSC, succinyl-CoA ligase; PDC, pyruvate decarboxylase; PDH, pyruvate dehydrogenase complex; PFL, pyruvate-formate lyase; PK, phosphoketolase; POX, pyruvate oxidase; PTA, phosphotransacetylase; R5P, ribose-5-phosphate; S7P, sedoheptulose-7-phosphate; X5P, xylulose-5-phosphate.

1.3 COUPLING OF CYTOSOLIC ACETYL-CoA FORMING PATHWAYS TO PRODUCT FORMATION: A STOICHIOMETRIC ANALYSIS

The cytosolic acetyl-CoA forming pathways discussed above differ with respect to their acetyl-CoA, ATP, NAD(P)H and CO₂ stoichiometries (Table 1.1). Pathways that further convert cytosolic acetyl-CoA into industrially relevant products can have different redox-cofactor and ATP requirements. Therefore, the design of metabolic engineering strategies for optimal integration of acetyl-CoA forming pathway(s) with product pathways requires *a priori* stoichiometric analysis. Important considerations for designing optimal pathway configurations include the theoretical maximum reaction stoichiometry, thermodynamic feasibility and compatibility with the native biochemistry of the (engineered) host organism.

The maximum theoretical yield (mole product per mole substrate, in the absence of growth) can be calculated without prior assumptions on pathway biochemistry and describes a situation in which all available electrons from the substrate end up in the product of interest. In this situation, which does not involve the use of external electron acceptors such as oxygen, the theoretical maximum molar reaction stoichiometry can be written as follows (52):

$$-\gamma_P/\gamma_S \text{ substrate} + n_{\text{CO}_2} \text{ CO}_2 + n_{\text{H}_2\text{O}} \text{ H}_2\text{O} + n_{\text{H}^+} \text{ H}^+ + 1 \text{ product} = 0$$

In this equation, γ_P and γ_S represent the degree of reduction (in e-mol·mol⁻¹) of the product and substrate (113). Molar stoichiometries of the other compounds (n_{CO_2} , $n_{\text{H}_2\text{O}}$ and n_{H^+}) then follow from elemental and charge balances. The degree of reduction is defined as the number of electrons that are released when a chemical compound is completely converted to its most oxidized stable reference compound(s). For carbohydrates and other C-, H- and O-containing molecules, these oxidized reference compounds are H₂O, CO₂ and H⁺ which, by convention, are assigned a γ -value of 0. This assignment results in the following γ -value for the elements and charges: H = 1; C = 4; O = -2; + = -1; - = +1. The degree of reduction of any compound can then be simply calculated from the sum of the γ -values of its elements.

A first indication of whether a reaction is thermodynamically feasible is provided by its Gibbs free energy change under biochemical standard conditions (ΔG_R°), taking into account that actual *in vivo* values of ΔG_R also depend on concentrations of substrates and products. In addition, ΔG_R° provides valuable indications on whether the Gibbs-free energy change is sufficiently negative to conserve free energy in the form of ATP for growth and cellular maintenance and to provide the thermodynamic driving force required for high reaction rates (52). When experimental data on the free energy of formation ($\Delta_f G^\circ$) of relevant compounds are not available, ΔG_R° estimations can instead be based on group contribution methods (79, 224). If the theoretical maximum stoichiometry calculated via the degree-of-reduction approach is thermodynamically feasible, it represents the ultimate benchmark for assessment of alternative pathway configurations during the design phase of metabolic engineering projects.

Challenges in experimentally approaching maximum theoretical product yields by metabolic engineering are to a large extent caused by constraints that are imposed by the native biochemistry of microbial production hosts and/or by its (in)compatibility with relevant heterologous and/or synthetic pathways for precursor supply and prod-

uct formation. For example, involvement of ATP-requiring reactions or non-matching redox-cofactor specificities of oxidative and reductive reactions in a pathway can constrain the experimentally attainable product yield. Optimally choosing or (re)designing pathway configurations in (central) metabolism is therefore crucial for systematically approaching the theoretical production yield.

To evaluate product dependency of the optimal reconfiguration of cytosolic acetyl-CoA provision in yeast, we evaluate the alternative pathways discussed above for the production of four model compounds: *n*-butanol, citric acid, palmitic acid and farnesene. This analysis is based on a compartmentalized model of central metabolism described by Carlson *et al.* (32), supplemented with (heterologous) reactions for acetyl-CoA formation, the lumped reaction pathways from acetyl-CoA to the four products, as well as some additional modifications (Box 1.1).

Box 1.1 – Modifications to the *Saccharomyces cerevisiae* stoichiometric model of Carlson *et al.* (32), introduced to enable stoichiometric comparison of different cytosolic acetyl-CoA forming pathways in the context of the production of *n*-butanol, citric acid, palmitic acid or farnesene (for complete model in MetaTool format (144), see Supplementary data 1.1).

- Based on experimental data (203, 259), transport of mitochondrial acetyl-CoA to the cytosol was removed from the model,
- Introduction of reactions for formation of *n*-butanol, citric acid, palmitic acid or farnesene from cytosolic acetyl-CoA. Lumped stoichiometries are given by reactions 1.20 – 1.23.
- Introduction of NAD⁺-dependent acetaldehyde dehydrogenase, in addition to the NADP⁺-dependent reaction present in the original model, thereby introducing redox cofactor flexibility in the PDH bypass.
- Introduction of ATP-citrate lyase to enable the citrate-oxaloacetate shuttle.
- Introduction of independent phosphoketolase activities with fructose-6-phosphate and xylulose-5-phosphate as the substrate; introduction of phosphotransacetylase.
- Introduction of NAD⁺-dependent acetylating acetaldehyde dehydrogenase. The following three oxidative, ATP-independent options from pyruvate to acetyl-CoA (Table 1.1) have the same overall stoichiometry as the acetylating acetaldehyde dehydrogenase-based pathway and are therefore not individually modelled: cytosolic PDH complex, pyruvate-formate lyase with formate dehydrogenase and export of mitochondrial acetyl moieties to the cytosol via the carnitine shuttle.
- To facilitate NADH generation via the TCA-cycle for products with a degree of reduction that is higher than that of glucose, the succinate dehydrogenase reaction was modified to use NAD⁺ instead of FAD⁺. In practice, this could for instance be achieved by overexpressing an NADH-dependent fumarate reductase (266, 343).

1.3.1 *n*-Butanol

n-Butanol, a linear 4-carbon alcohol, is a promising renewable transport fuel as well as an industrial solvent and precursor for chemical synthesis (206), with a maximum theo-

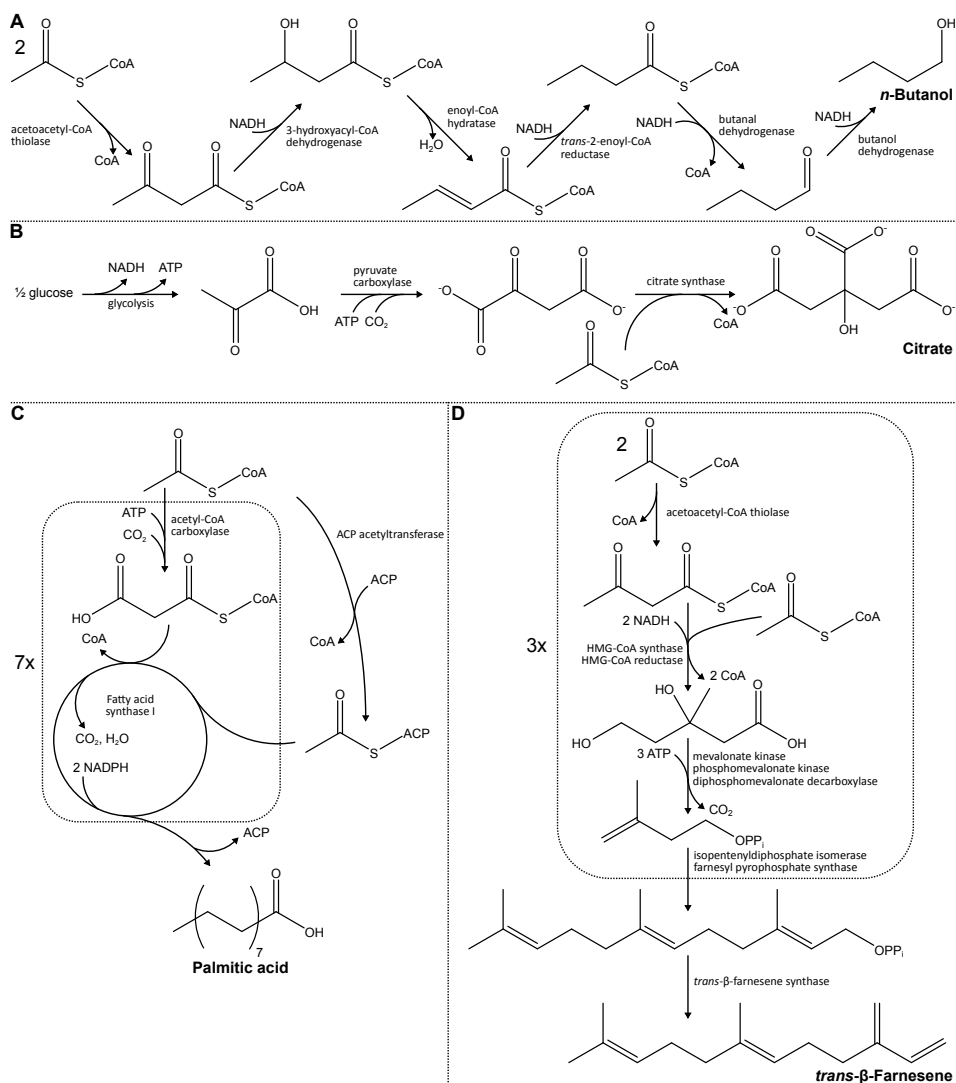


Figure 1.2. Pathways for synthesis of four model compounds starting from cytosolic acetyl-CoA as the (main) precursor: **A** *n*-butanol, **B** citrate, **C** palmitic acid and **D** *trans*- β -farnesene. Pathways are adapted and based on MetaCyc pathways (36) PWY-6883, PWY-5750, PWY-922, PWY-5123 and PWY-5725 and on the review by Tehlivets *et al.* (308).

retical yield on glucose of 1 mol·mol⁻¹ (Table 1.2). While various pathways to *n*-butanol have been expressed in *S. cerevisiae* (22, 185, 299, 304), only the *Clostridium* pathway has acetyl-CoA as a precursor and is therefore considered in this review (Figure 1.2A). This pathway has the following reaction stoichiometry:

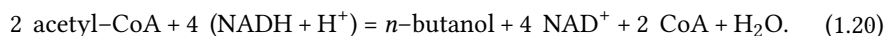


Table 1.2. Overall stoichiometry for the formation of 1 mole of *n*-butanol with glucose as the sole source of electrons ($C_4H_{10}O$; $\gamma = 24 \text{ e-mol-mol}^{-1}$). The Gibbs free energy change under biochemical standard conditions (ΔG_R°) for the theoretical maximum reaction stoichiometry is estimated at $-265.9 \pm 12.6 \text{ kJ-mol}^{-1}$ (79). Overall reaction stoichiometries are obtained using MetaTool 5.1 (144), based on an adapted version of the stoichiometric model of central carbon metabolism of *S. cerevisiae* by Carlson *et al.* (32). The listed reaction stoichiometry for each pathway represents the flux solution with the highest product yield on substrate. Any ATP requirement was preferentially met by reoxidation of surplus NADH. If additional ATP was required, additional glucose was used for complete respiratory dissimilation to generate the remaining ATP (P/O ratio assumed to be 1 (327)). Surplus NADH not required for ATP generation and/or ATP generated from the product formation pathways are indicated in the stoichiometry. For simplicity, the reactants NAD^+ , ADP, P_i and H^+ are not shown.

Pathway	Reaction stoichiometry	Yield (mol _p /mol _s)
Theoretical maximum	glucose \longrightarrow <i>n</i> -butanol + 2 CO ₂ + H ₂ O	1
PDH bypass	$1\frac{1}{8} \text{ glucose} + \frac{3}{4} \text{ O}_2 \longrightarrow \textit{n}\text{-butanol} + 2\frac{3}{4} \text{ CO}_2 + 1\frac{3}{4} \text{ H}_2\text{O}$	0.889
Citrate-oxaloacetate shuttle with ACL	glucose \longrightarrow <i>n</i> -butanol + 2 CO ₂ + H ₂ O	1
Phosphoketolase/-transacetylase	glucose \longrightarrow <i>n</i> -butanol + 2 CO ₂ + H ₂ O + ATP	1
ATP-independent pyruvate to acetyl-CoA routes*	glucose \longrightarrow <i>n</i> -butanol + 2 CO ₂ + H ₂ O + 2 ATP	1

* These pathway use either A-ALD, PDH_{cyt}, PDH_{mit} with the carnitine shuttle or, when conditions are anaerobic, PFL with FDH

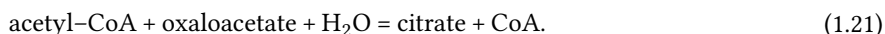
All four pathways for acetyl-CoA production can result in redox-cofactor balanced formation of butanol from glucose (Table 1.2). For the three routes that produce acetyl-CoA from glucose via pyruvate, the 4 NADH required for synthesis of 1 *n*-butanol are produced by glycolysis and by the subsequent oxidative conversion of pyruvate to acetyl-CoA. In the PK/PTA pathway, non-oxidative conversion of $\frac{2}{3}$ glucose to 2 acetyl-CoA requires, in parallel, the oxidation of $\frac{1}{3}$ glucose via glycolysis and TCA cycle to generate these 4 NADH. Deriving NADH from the TCA cycle will require additional metabolic engineering to overcome the subcellular compartmentation of NADH metabolism in *S. cerevisiae* (7) and the down-regulation of TCA-cycle enzymes in anaerobic *S. cerevisiae* cultures (77, 92).

Comparison of *n*-butanol formation from glucose via the four different pathways for acetyl-CoA formation clearly demonstrates their impact on product yield. The ATP cost of the ACS reaction in the PDH bypass necessitates respiratory dissimilation of glucose, constraining the maximum attainable yield of *n*-butanol to $0.889 \text{ mol} \cdot (\text{mol glucose})^{-1}$. This pathway configuration therefore precludes anaerobic, fermentative *n*-butanol production (Table 1.2). Production of *n*-butanol from glucose is ATP neutral when acetyl-CoA is formed via the citrate-oxaloacetate shuttle. This configuration, however, still requires another dissimilatory pathway to provide ATP for growth and cellular maintenance. The remaining two pathways for acetyl-CoA formation enable production of *n*-butanol at the maximum theoretical yield of $1 \text{ mol} \cdot (\text{mol glucose})^{-1}$ and with a positive ATP yield, thereby potentially allowing for an anaerobic, fermentative process. Use of the PK/PTA route partially bypasses the substrate phosphorylation steps of glycolysis and therefore yields only 1 mole of ATP per mole of *n*-butanol. ATP-independent, oxidative conversion of pyruvate to acetyl-CoA (A-ALD, PDH_{cyt} and PFL/FDH) enables the

formation of 2 moles of ATP per mole of *n*-butanol, which is identical to the ATP yield from classical alcoholic fermentation of glucose by *S. cerevisiae*.

1.3.2 Citric acid

Citric acid, a six-carbon tricarboxylic acid, is currently produced on an industrial scale using *A. niger* and can, alternatively, be produced with the yeast *Y. lipolytica* (209). Since citric acid is more oxidized than glucose (degrees of reduction 18 and 24, respectively), it represents an interesting model product to theoretically explore how redox-cofactor balancing of precursor supply and product pathways can affect product yield. The key enzyme in citric acid production (Figure 1.2B), citrate synthase, uses acetyl-CoA and oxaloacetate as substrates:



In *A. niger*, and likely also in *Y. lipolytica*, citrate synthase is localized in the mitochondrial matrix (263). However, for this theoretical assessment of the impact of the different cytosolic acetyl-CoA formation pathways on product yield, we will assume a cytosolic localization. Formation of oxaloacetate from glucose via the ATP-dependent carboxylation of pyruvate (EC 6.4.1.1; $\text{pyruvate} + \text{CO}_2 + \text{ATP} + \text{H}_2\text{O} = \text{oxaloacetate} + \text{ADP} + \text{P}_i$) results in the formation of 1 NADH. Additionally, all oxidative routes for acetyl-CoA formation result in the formation of an additional 2 NADH per citric acid. This ‘excess’ NADH can be reoxidized by mitochondrial respiration, thus providing ATP for growth, maintenance, product export and, in some pathway configurations, for acetyl-CoA formation (Table 1.3). Oxidative formation of acetyl-CoA from pyruvate limits the maximum attainable yield of citric acid to 1 mole per mole glucose (Table 1.3), which is substantially lower than the theoretical maximum yield of citric acid on glucose ($1.33 \text{ mol} \cdot \text{mol}^{-1}$; Table 1.3). As described above, conversion of glucose to acetyl-CoA via the PK/PTA pathway does not result in NADH formation and even enables net incorporation of CO_2 into the product. Use of PK/PTA for acetyl-CoA synthesis should therefore enable a higher maximum attainable citrate yield on glucose of $1.2 \text{ mol} \cdot \text{mol}^{-1}$ (Table 1.3), which corresponds to 90% of the maximum theoretical yield (Table 1.3). Engineering acetyl-CoA formation via the PK/PTA route into *Y. lipolytica* and *A. niger* might therefore be an interesting approach to increase citric acid yield on glucose. Interestingly, both microorganisms already harbor a cytosolic PK and, thereby, only seems to lack a functional PTA (65, 235, 249). This strategy does not only have the potential to increase the citric acid yield on glucose, but also to increase the product yield on oxygen. The lower ATP yield from citric acid formation via a PK/PTA pathway can be beneficial for minimizing growth, although ATP availability will be required for cellular maintenance, especially at the low pH values that are typical for these processes.

1.3.3 Palmitic acid

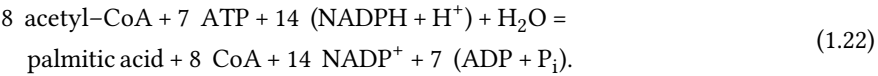
Microbial production of lipids, whose applications range from biofuels to cosmetics, is intensively investigated (261, 280). As a model compound, we consider palmitic acid, a sat-

Table 1.3. Overall stoichiometry for the formation of 1 mole of citric acid with glucose as the sole source of electrons ($C_6H_8O_7$; $\gamma = 18 \text{ e-mol-mol}^{-1}$). The Gibbs free energy change under biochemical standard conditions (ΔG_R°) for the theoretical maximum reaction stoichiometry is estimated at $-143.5 \pm 9.1 \text{ kJ-mol}^{-1}$ (79). Overall reaction stoichiometries are obtained using MetaTool 5.1 (144), based on an adapted version of the stoichiometric model of central carbon metabolism of *S. cerevisiae* by Carlson *et al.* (32). The listed reaction stoichiometry for each pathway represents the flux solution with the highest product yield on substrate. Any ATP requirement was preferentially met by reoxidation of surplus NADH. If additional ATP was required, additional glucose was used for complete respiratory dissimilation to generate the remaining ATP (P/O ratio assumed to be 1 (327)). Surplus NADH not required for ATP generation and/or ATP generated from the product formation pathways are indicated in the stoichiometry. For simplicity, the reactants NAD^+ , ADP, P_i and H^+ are not shown.

Pathway	Reaction stoichiometry	Yield (mol _p /mol _s)
Theoretical maximum	$\frac{3}{4} \text{ glucose} + 1\frac{1}{2} \text{ CO}_2 \longrightarrow \text{citrate} + \frac{1}{2} \text{ H}_2\text{O}$	1.333
PDH bypass	$\text{glucose} + \frac{1}{2} \text{ O}_2 \longrightarrow \text{citrate} + 2 \text{ NADH}$	1
Citrate-oxaloacetate shuttle with ACL	N.A.	N.A.
Phosphoketolase/-transacetylase	$\frac{5}{6} \text{ glucose} + \text{CO}_2 \longrightarrow \text{citrate} + \text{NADH}$	1.2
ATP-independent pyruvate to acetyl-CoA routes*	$\text{glucose} \longrightarrow \text{citrate} + 3 \text{ NADH} + \text{ATP}$	1

* These pathway use either A-ALD, PDH_{cyt} , PDH_{mit} with the carnitine shuttle or, when conditions are anaerobic, PFL with FDH

urated C_{16} fatty acid that is considerably more reduced than glucose ($5\frac{3}{4} \text{ e-mol-C-mol}^{-1}$ and $4 \text{ e-mol-C-mol}^{-1}$, respectively). Its theoretical maximum yield on glucose is $0.261 \text{ mol-mol}^{-1}$. In the yeast cytosol, palmitic acid is synthesized by a type-I fatty acid synthase (308). Synthesis of palmitic acid starts with an acetyl moiety, originating from cytosolic acetyl-CoA, as a primer. The following 7 cycles of elongation use malonyl-CoA, which is also produced from cytosolic acetyl-CoA, as acetyl donor and involve the use of 2 NADPH for each elongation step (Figure 1.2C). When synthesis of malonyl-CoA from cytosolic acetyl-CoA by acetyl-CoA carboxylase (EC 6.4.1.2), which requires 1 ATP per malonyl-CoA, is included, the net reaction for formation of palmitic acid from acetyl-CoA (Figure 1.2C) is:



Stoichiometric analysis reveals the impact of redox-cofactor balancing on the palmitic acid yield on glucose (Table 1.4). NADPH is the preferred electron donor in fatty acid synthesis pathways, while NADH is formed in most pathways that convert glucose into acetyl-CoA (Table 1.4). Combining these precursor supply and product pathways therefore not only requires a large additional flux through the oxidative pentose-phosphate pathway to generate NADPH, but also generates a large amount of NADH. When palmitic acid production uses cytosolic acetyl-CoA generated by the NAD^+ -dependent PDH bypass route, all NADH generated in precursor supply has to be reoxidized to NAD^+ to provide ATP required for the ACS reaction. Use of the citrate-oxaloacetate shuttle, which has a lower ATP requirement for acetyl-CoA synthesis, leaves a larger fraction of the NADH from palmitic acid production unused (Table 1.4). This fraction increases even further when any of the ATP-independent pathways towards cytosolic

Table 1.4. Overall stoichiometry for the formation of 1 mole of palmitic acid with glucose as the sole source of electrons ($C_{16}H_{32}O_2$; $\gamma = 92 \text{ e-mol}^{-1}$). The Gibbs free energy change under biochemical standard conditions (ΔG_R°) for the theoretical maximum reaction stoichiometry is estimated at $-1161.2 \pm 42.2 \text{ kJ} \cdot \text{mol}^{-1}$ (79). Overall reaction stoichiometries are obtained using MetaTool 5.1 (144), based on an adapted version of the stoichiometric model of central carbon metabolism of *S. cerevisiae* by Carlson *et al.* (32). The listed reaction stoichiometry for each pathway represents the flux solution with the highest product yield on substrate. Any ATP requirement was preferentially met by reoxidation of surplus NADH. If additional ATP was required, additional glucose was used for complete respiratory dissimilation to generate the remaining ATP (P/O ratio assumed to be 1 (327)). Surplus NADH not required for ATP generation and/or ATP generated from the product formation pathways are indicated in the stoichiometry. For simplicity, the reactants NAD^+ , ADP, P_i and H^+ are not shown.

Pathway	Reaction stoichiometry	Yield ($\text{mol}_p/\text{mol}_s$)
Theoretical maximum	$35/6 \text{ glucose} \longrightarrow \text{palmitic acid} + 7 \text{ CO}_2 + 7 \text{ H}_2\text{O}$	0.261
PDH bypass	$41\frac{1}{12} \text{ glucose} + 6\frac{1}{2} \text{ O}_2 \longrightarrow \text{palmitic acid} + 13\frac{1}{2} \text{ CO}_2 + 13\frac{1}{2} \text{ H}_2\text{O}$	0.203
Citrate-oxaloacetate shuttle with ACL	$5\frac{1}{6} \text{ glucose} + 3\frac{1}{2} \text{ O}_2 \longrightarrow \text{palmitic acid} + 15 \text{ CO}_2 + 6 \text{ H}_2\text{O} + 9 \text{ NADH}$	0.194
Phosphoketolase/-transacetylase	$43/7 \text{ glucose} + 34/7 \text{ O}_2 \longrightarrow \text{palmitic acid} + 104/7 \text{ CO}_2 + 104/7 \text{ H}_2\text{O}$	0.226
ATP-independent pyruvate to acetyl-CoA routes*	$5\frac{1}{6} \text{ glucose} \longrightarrow \text{palmitic acid} + 15 \text{ CO}_2 + 16 \text{ NADH} + \text{ATP}$	0.194
Optimal combinatorial configuration**	$43/10 \text{ glucose} + 28/10 \text{ O}_2 \longrightarrow \text{palmitic acid} + 94/5 \text{ CO}_2 + 94/5 \text{ H}_2\text{O}$	0.232

* These pathway use either A-ALD, PDH_{cyt} , PDH_{mit} with the carnitine shuttle or, when conditions are anaerobic, PFL with FDH

** 65% via phosphoketolase/-transacetylase and 35% via an ATP-independent pyruvate to acetyl-CoA route

acetyl-CoA are used (Table 1.4). Respiratory reoxidation of this ‘excess’ NADH respiration generates ATP, which enables extensive diversion of glucose to biomass formation, thereby decreasing product yields. As a result of this imbalance between NADH production and NADPH consumption, the citrate-oxaloacetate shuttle and the ATP-independent acetyl-CoA formation routes result in the lowest attainable palmitic acid yields ($0.194 \text{ mol} \cdot \text{mol}^{-1}$; Table 1.4).

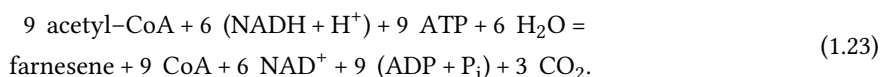
The two remaining pathways for cytosolic acetyl-CoA formation are intrinsically more flexible in balancing NADH and NADPH generation with cellular requirements. In the PDH bypass, involvement of $NADP^+$ -dependent acetaldehyde dehydrogenase can provide part of the NADPH required in reaction 1.22, whilst simultaneously decreasing the formation of excess NADH. In contrast to the other pathways for cytosolic acetyl-CoA production from glucose, the PK/PTA pathway does not result in NADH formation (Figure 1.1B). This property is highly advantageous for palmitic acid production and enables a maximum attainable yield of palmitic acid to glucose that corresponds to 87% of the maximum theoretical yield when NADPH formation occurs via the oxidative pentose-phosphate pathway (Table 1.4). An even higher maximum attainable yield can be obtained by combining the PK/PTA pathway with an ATP-independent route from pyruvate to acetyl-CoA. In an optimal scenario, 65% of the acetyl-CoA should then be derived

from the PK/PTA pathway, enabling a maximum attainable yield that corresponds to 89% of the theoretical maximum.

Regardless of the acetyl-CoA synthesis route, the dependence of the discussed pathways on respiration to produce ATP and/or to regenerate NAD^+ precludes the synthesis of palmitic acid a sole catabolic pathway under anaerobic conditions. Interestingly, some organisms do rely on fatty-acid synthesis as a catabolic, ATP generating pathway. For example, *Euglena gracilis* ferments sugars, via fatty acids, to wax esters, which can constitute up to 60% of its dry mass (315). In this organism, pyruvate is converted to acetyl-CoA via the chimeric PFO/PFR system discussed above (135, 136). Moreover, fatty acid synthesis in *E. gracilis* does not rely on a malonyl-CoA-dependent fatty acid synthase pathway, but on a reversed β -oxidation pathway, which does not involve ATP hydrolysis (149).

1.3.4 Farnesene

The sesquiterpene *trans*- β -farnesene is a C_{15} branched, unsaturated hydrocarbon, which can be used for production of diesel fuel, polymers and cosmetics (261). Farnesene can be produced from 3 molecules of mevalonate, generated in the eukaryotic isoprenoid biosynthesis pathway. The mevalonate pathway not only requires large amounts of ATP (see Reaction 1.23), but also combines all previously mentioned challenges in balancing NADH, NADPH and ATP conversions. *S. cerevisiae*, which does not naturally synthesize *trans*- β -farnesene, has been genetically modified to produce this compound at high titers and yields (269). One of the mevalonate pathway enzymes, HMG-CoA reductase, uses NADPH. To reduce the need for extensive glucose oxidation via the oxidative pentose phosphate pathway, this enzyme has been successfully replaced by an NADH-dependent HMG-CoA reductase (94), thus enabling the following reaction stoichiometry for formation of farnesene from acetyl-CoA (Figure 1.2D):



The maximum theoretical yield of farnesene on glucose is $0.286 \text{ mol} \cdot \text{mol}^{-1}$ (Table 1.5). When using the native PDH bypass for cytosolic acetyl-CoA formation, the high ATP cost for acetyl-CoA synthesis via ACS necessitates respiratory dissimilation of over one mole of glucose per mole of farnesene. This ATP requirement limits the maximum attainable yield of farnesene on glucose to only $0.205 \text{ mol} \cdot \text{mol}^{-1}$. The more ATP-efficient routes for acetyl-CoA synthesis via the citrate-oxaloacetate shuttle and the ATP-independent routes from pyruvate to acetyl-CoA enable significantly higher maximum attainable yields of $0.222 \text{ mol} \cdot (\text{mol glucose})^{-1}$. In both routes, 18 NADH is formed per 9 acetyl-CoA, while only 6 NADH is consumed in the synthesis of farnesene from acetyl-CoA (Reaction 1.23). When using the citrate-oxaloacetate shuttle, 9 of the remaining 12 NADH need to be oxidized to provide ATP for farnesene synthesis. In the absence of other catabolic pathways, this would only leave 3 NADH to provide ATP for growth and cellular maintenance via oxidative phosphorylation. Conversely, when ATP-independent routes for acetyl-CoA synthesis are used, all 12 moles NADH generated per mole of farnesene are

Table 1.5. Overall stoichiometry for the formation of 1 mole of *trans*- β -farnesene with glucose as the sole source of electrons ($C_{15}H_{24}$; $\gamma = 84 \text{ e-mol}^{-1}$). The Gibbs free energy change under biochemical standard conditions (ΔG_R°) for the theoretical maximum reaction stoichiometry is estimated at $-870.1 \pm 39.3 \text{ kJ} \cdot \text{mol}^{-1}$ (79). Overall reaction stoichiometries are obtained using MetaTool 5.1 (144), based on an adapted version of the stoichiometric model of central carbon metabolism of *S. cerevisiae* by Carlson *et al.* (32). The listed reaction stoichiometry for each pathway represents the flux solution with the highest product yield on substrate. Any ATP requirement was preferentially met by reoxidation of surplus NADH. If additional ATP was required, additional glucose was used for complete respiratory dissimilation to generate the remaining ATP (P/O ratio assumed to be 1 (327)). Surplus NADH not required for ATP generation and/or ATP generated from the product formation pathways are indicated in the stoichiometry. For simplicity, the reactants NAD^+ , ADP, P_i and H^+ are not shown.

Pathway	Reaction stoichiometry	Yield (mol _p /mol _s)
Theoretical maximum	$3\frac{1}{2} \text{ glucose} \longrightarrow \text{farnesene} + 6 \text{ CO}_2 + 9 \text{ H}_2\text{O}$	0.286
PDH bypass	$4\frac{7}{8} \text{ glucose} + 8\frac{1}{4} \text{ O}_2 \longrightarrow \text{farnesene} + 14\frac{1}{4} \text{ CO}_2 + 17\frac{1}{4} \text{ H}_2\text{O}$	0.205
Citrate-oxaloacetate shuttle with ACL	$4\frac{1}{2} \text{ glucose} + 4\frac{1}{2} \text{ O}_2 \longrightarrow \text{farnesene} + 12 \text{ CO}_2 + 12 \text{ H}_2\text{O} + 3 \text{ NADH}$	0.222
Phosphoketolase/-transacetylase	$4\frac{1}{17} \text{ glucose} + 3\frac{6}{17} \text{ O}_2 \longrightarrow \text{farnesene} + 9\frac{6}{17} \text{ CO}_2 + 12\frac{6}{17} \text{ H}_2\text{O}$	0.246
ATP-independent pyruvate to acetyl-CoA routes*	$4\frac{1}{2} \text{ glucose} \longrightarrow \text{farnesene} + 12 \text{ CO}_2 + 3 \text{ H}_2\text{O} + 12 \text{ NADH}$	0.222
Combinatorial configuration**	$3\frac{5}{6} \text{ glucose} + 2 \text{ O}_2 \longrightarrow \text{farnesene} + 8 \text{ CO}_2 + 11 \text{ H}_2\text{O}$	0.261

* These pathway use either A-ALD, PDH_{cyt} , PDH_{mit} with the carnitine shuttle or, when conditions are anaerobic, PFL with FDH

**44% via phosphoketolase/-transacetylase and 56% via an ATP-independent pyruvate to acetyl-CoA route

available for ATP production to sustain growth and maintenance. The absence of NADH generation makes the PK/PTA pathway the most attractive of the four individual routes, with a maximum attainable yield of $0.246 \text{ mol} \cdot (\text{mol glucose})^{-1}$, which corresponds 86% of the maximum theoretical yield. The deviation of this maximum attainable yield from the theoretical yield is caused by the need for respiratory dissimilation of part of the glucose to provide the required ATP. In theory, the maximum attainable yield of farnesene on glucose can be further improved by combining the PK/PTA pathway with any of the ATP-independent pyruvate-to-acetyl-CoA pathways, resulting in a maximum attainable yield of farnesene on glucose of up to 91% of the theoretical maximum. This requires a pathway configuration in which, for each mole of farnesene, 4 moles of acetyl-CoA are produced via the PK/PTA pathway and 5 moles of acetyl-CoA via an ATP-independent route from pyruvate to acetyl-CoA. In this scenario, oxygen is still required to provide ATP, but this requirement is reduced to 2 mole of oxygen per mole of farnesene. In industrial practice, additional oxygen may, however, be required to provide ATP for growth and cellular maintenance.

1.4 KINETICS AND THERMODYNAMICS

Stoichiometric analysis of metabolic pathways provides valuable insights to shape metabolic engineering strategies. However, implementation of a (heterologous) route in an industrial strain not only demands high product yields, but also high productivities. Therefore, not only the stoichiometry, but also the thermodynamic driving force (ΔG_R), the ensuing intracellular concentrations of metabolites and the enzyme kinetics of the enzymes (V_{\max} , K_M) have to be considered. Below, we briefly discuss observations on engineering of cytosolic acetyl-CoA synthesis that affect the delicate balance between kinetics and stoichiometry.

The biosynthetic and regulatory requirements for acetyl-CoA in the cytosol and nucleus of wild-type *S. cerevisiae* require only relatively low fluxes through the PDH bypass (166). Shiba *et al.* (281) engineered the native *S. cerevisiae* PDH bypass pathway (Figure 1.1A) for cytosolic acetyl-CoA synthesis by overexpression of the responsible enzymes (281). ALD and ACS activities were increased by overexpressing the native cytosolic NADP⁺-dependent acetaldehyde dehydrogenase Ald6 and a heterologous ACS from *Salmonella enterica*, respectively. Since high intracellular acetyl-CoA levels can inhibit ACS enzymes by acetylation of a lysine residue, the *S. enterica* ACS was engineered to prevent acetylation through an L641P amino acid substitution. These modifications substantially increased *in vitro* ALD and ACS activities and, importantly, improved the *in vivo* synthesis rate of amorphaadiene, a product derived from cytosolic acetyl-CoA via the mevalonate pathway, by 1.8 fold. This result shows that the PDH bypass can be engineered to sustain higher *in vivo* fluxes towards industrially relevant compounds.

While alternative acetyl-CoA-forming pathways are stoichiometrically superior to the PDH bypass, their expression in *S. cerevisiae* has revealed some interesting challenges related to *in vivo* kinetics. As discussed above, the PFL pathway theoretically enables ATP-efficient production of acetyl-CoA under anaerobic conditions. Additionally, the turnover number of PFL enzymes is generally high $\sim 10^3 \text{ s}^{-1}$ (154). However, efficient use of this pathway requires that formic acid, which is co-produced with acetyl-CoA, is re-oxidized to CO₂ by NAD⁺-dependent formate dehydrogenase (FDH). Achieving high *in vivo* FDH activities in *S. cerevisiae* is a highly non-trivial challenge because of the low turnover numbers ($\sim 10 \text{ s}^{-1}$) of currently characterized NAD⁺-dependent FDH enzymes (39). In chemostat cultures of an *S. cerevisiae* Acs⁻ strain expressing *E. coli* PFL (166), accumulation of formate showed that native FDH activity was insufficient to oxidize excess formate. Previous attempts to increase *in vivo* FDH activity in anaerobic cultures of *S. cerevisiae* by overexpression of its *FDH1* gene were not only complicated by the low turnover number of its gene product, but also by the negative impact of high NADH/NAD⁺ ratios on its enzyme activity (95). Increasing the *in vivo* capacity and activity of FDH is therefore a priority target for successful implementation of the PFL pathway for acetyl-CoA synthesis in *S. cerevisiae*.

In a recent study, co-expression of the *Clostridium n*-butanol pathway with four different cytosolic acetyl-CoA forming pathways in *S. cerevisiae* resulted in only small increases of an already low butanol yield (185). These studies indicate that optimization of the flux through these heterologous acetyl-CoA and product-forming pathways is often required. Ideally, experiments for assessing the kinetics of alternative precursor supply

pathways should be performed in strain backgrounds with a high overcapacity of all reactions downstream of the precursor.

Compatibility of a heterologous enzyme with a metabolic engineering strategy may not only be determined by its *in vivo* capacity (V_{\max}) in the host organism, but also by its affinity ($\frac{V_{\max}}{K_M}$), which dictates the intracellular concentration of its substrate that is required to achieve a target flux. Affinity is especially important when the substrate of an enzyme is toxic, as is the case for A-ALD (Reaction 1.8), which shows a much lower affinity for acetaldehyde than the native yeast acetaldehyde dehydrogenase isoenzymes (166). Consistent with this observation, yeast strains in which the native yeast ALDs were replaced by heterologous A-ALDs showed elevated intracellular acetaldehyde levels. Acetaldehyde toxicity was implicated in the lower than expected biomass yields of these engineered strains.

The elevated acetaldehyde concentrations in A-ALD dependent strains may not solely reflect a kinetic requirement. Although, as mentioned above, $\Delta G_R'$ of the A-ALD reaction (Reaction 1.8) is negative, biochemical standard conditions are unlikely to reflect the thermodynamics of this reaction in the yeast cytosol. Assuming an $[NADH]/[NAD^+]$ ratio of 0.01 (30), the $\Delta G_R'$ of the reaction at the acetaldehyde levels that were measured in wild-type *S. cerevisiae* was estimated to be $+7.2 \text{ kJ}\cdot\text{mol}^{-1}$ (166), which would render use of the A-ALD pathway for acetyl-CoA synthesis thermodynamically impossible. The observed increased acetaldehyde concentrations in an A-ALD-dependent strain increased the estimated $\Delta G_R'$ of the reaction close to zero ($+0.7 \text{ kJ}\cdot\text{mol}^{-1}$) (166). This observation suggests that toxic levels of acetaldehyde may have been a thermodynamic prerequisite to allow the A-ALD reaction to proceed in the oxidative reactions in the yeast cytosol.

As described above, in their metabolic engineering strategy for farnesene production, Gardner *et al.* (94) replaced the native *S. cerevisiae* HMG-CoA reductase, which is NADPH dependent, for an NADH-dependent enzyme. Interestingly, strains with an NADH-dependent HMG-CoA reductase exhibited approximately 4-fold lower intracellular mevalonate levels than strains expressing the NADPH-dependent enzyme (94). The $[NADPH]/[NADP^+]$ ratio in the yeast cytosol is generally much higher than the $[NADH]/[NAD^+]$ (under aerobic conditions: 15.6 – 22.0 as compared to 0.01, respectively; (30, 349)). When these different ‘redox charges’ of the two cofactor couples are taken into account, the thermodynamic driving force for the NADH-dependent reaction is much less favorable (difference in $\Delta G_R' \sim 40 \text{ kJ}\cdot\text{mol}^{-1}$) than for the NADPH-dependent reaction. This difference in $\Delta G_R'$ offers a plausible explanation for the kinetically superior performance of the NADPH-dependent native HMG-CoA reductase. Consistent with this interpretation, deletion of the gene encoding the Adh2 alcohol dehydrogenase, which was anticipated to lead to higher cytosolic $[NADH]/[NAD^+]$ ratios, indeed led to increased mevalonate levels (94). These examples illustrate how not only stoichiometry, but also kinetics and thermodynamics need to be considered when designing metabolic engineering strategies to optimize acetyl-CoA provision.

1.5 DISCUSSION AND OUTLOOK

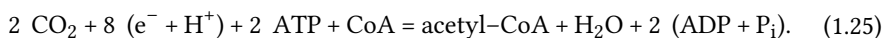
This review focused on reaction stoichiometry, kinetics and thermodynamics of alternative pathways for providing acetyl-CoA, a key precursor for the formation of many industrially relevant compounds, in the yeast cytosol. Several of the acetyl-CoA-producing pathways discussed here have recently been successfully expressed in *S. cerevisiae*, thereby providing metabolic engineers with new options to optimally align and integrate precursor supply with product pathways downstream of acetyl-CoA (219). The stoichiometric analyses discussed above show how the optimal pathway configuration for the synthesis of a single metabolic precursor, cytosolic acetyl-CoA, is strongly product dependent. This observation underlines the importance of evaluating multiple pathways for precursor supply at the outset of metabolic engineering projects.

In general terms, the PK/PTA provides the highest possible carbon conversion of the routes discussed in this paper, while the acetyl-CoA forming routes via A-ALD, PDH or PFL/FDH enable the net formation of ATP. In addition to ATP formation, cofactor balancing is another key factor in defining the optimal precursor supply strategy. Stoichiometric evaluation of individual acetyl-CoA forming routes for a given product pathway already provide valuable leads for improving product yield on substrate. However, as illustrated by the examples of palmitic acid production and farnesene production (Table 1.4 and Table 1.5), combinations of different precursor supply routes can lead to even higher maximum product yields. To achieve the stoichiometric potential of combined routes requires that the relative *in vivo* activities of the contributing precursor supply pathways can be accurately controlled, even under dynamic industrial conditions. Achieving such accurately tunable *in vivo* flux distributions and, consequently, optimal product yields, represents a highly relevant challenge for metabolic engineers.

In this review, we limited our discussion of cytosolic acetyl-CoA supply in yeast to pathways that naturally occur in heterotrophic organisms. Implementation of autotrophic acetyl-CoA forming pathways in *S. cerevisiae* provides additional highly interesting scientific challenges and possibilities. For example, the Wood-Ljungdahl pathway, or reductive acetyl-CoA pathway, is used by acetogens to conserve free energy and to generate acetyl-CoA for growth (194). In an otherwise heterotrophic cell factory, this system could be useful to donate excess electrons to CO₂ for the synthesis of additional acetyl-CoA, according to the overall stoichiometry:



Functional expression of the enzymes of this system in *S. cerevisiae* itself already present a formidable challenge, while complexity is further increased by the use of different redox cofactors: H₂, reduced ferredoxin and/or NAD(P)H (276). Several other autotrophs use a reductive TCA cycle to produce acetyl-CoA from CO₂, with the following overall reaction stoichiometry (27):



An important difference with the conventional oxidative TCA cycle is the involvement of an α -ketoglutarate ferredoxin oxidoreductase (EC 1.2.7.3), which enables the *in*

in vivo carboxylation of succinyl-CoA to α -ketoglutarate, and of ATP-citrate lyase (ACL), which cleaves citrate into oxaloacetate and acetyl-CoA. Although the ATP stoichiometry of this pathway is less favourable than that of the Wood-Ljungdahl pathway, two aspects might make it (slightly) less challenging to functionally express this system in *S. cerevisiae*. Firstly, while reduced ferredoxin as an electron donor is required for the α -ketoglutarate dehydrogenase reaction, the remaining redox reactions in the reductive TCA cycle use NADH as cofactor. Secondly, the enzymes involved in the reductive TCA cycle are generally less complex and some, such as ACL, have already been successfully expressed in yeast (see above).

Producing industrially relevant compounds of interest at near-theoretical yields requires that, if thermodynamically possible, all electrons from the substrate end up in the product. Instead, in many of the scenarios analyzed in this review, precursor formation resulted in formation of excess NADH (Table 1.2-1.5). In other cases, NADH was required to enable ATP formation via oxidative phosphorylation, to provide the free-energy for product formation and cellular maintenance. Only in the case of *n*-butanol formation via the A-ALD, PDH or PFL/FDH pathway, a redox-neutral, ATP-yielding pathway could be assembled, which should theoretically allow for the maximum theoretical yield in non-growing cultures. For the pathway combinations that yielded excess ATP and/or NADH, implementation of autotrophic acetyl-CoA yielding pathways, or alternatively the expression of the Calvin-cycle enzymes phosphoribulokinase and RuBisCO (105), might further increase the yields of the products of interest. Another recent development that may ultimately contribute to the production of fatty acids as catabolic, anaerobic products in *S. cerevisiae*, is the recent expression of a reverse β -oxidation cycle in the yeast cytosol (187). This pathway for fatty acid synthesis is ATP-independent and, instead of NADPH, has NADH as the redox cofactor. Combining this system with the PK/PTA pathway and an ATP-independent route from pyruvate to acetyl-CoA can, at least theoretically, result in a redox-neutral and ATP yielding pathway.

In addition to quantitative insight into pathway stoichiometry, knowledge about the thermodynamics and kinetics of individual reactions and about the biochemical context in which the corresponding enzymes have to operate, is of crucial importance for evaluating alternative metabolic engineering strategies and to find targets for further optimization. Powerful algorithms for metabolic network evaluation that include thermodynamic and kinetic analyses are among the valuable new tools to find engineering targets and rank alternative strategies (38, 115, 267, 287).

1.6 ACKNOWLEDGEMENTS

This work was carried out within the BE-Basic R&D Program, which was granted an FES subsidy from the Dutch Ministry of Economic Affairs, Agriculture and Innovation (EL&I). We thank DSM (The Netherlands) and Amyris (USA) for funding. Liang Wu (DSM) and Kirsten Benjamin (Amyris) are gratefully acknowledged for a fruitful collaboration and many constructive discussions.

1.7 SCOPE AND OUTLINE OF THIS THESIS

In wild-type *Saccharomyces cerevisiae* strains, the cytosolic acetyl-CoA synthesis reaction requires hydrolysis of ATP. This ATP requirement limits the theoretical yield of acetyl-CoA-derived (heterologous) products that are synthesised in the yeast cytosol. Therefore, improving the ATP stoichiometry of this precursor pathway has a huge impact on the theoretical yield on substrate of products that have acetyl-CoA as a precursor.

Chapter 1 reviews strategies that have been proposed and evaluated for functionally replacing the native cytosolic yeast acetyl-CoA synthesis pathway. As these strategies involve multiple pathways that differ in terms of redox cofactor usage, ATP stoichiometry and carbon conservation, the optimal solution is product specific. In some cases, a combination of different acetyl-CoA synthesis pathways is required to achieve optimal theoretical yields of product on substrate.

The genetic accessibility of *S. cerevisiae* continues to be key to its popularity as a eukaryotic laboratory model and industrial ‘work horse’. Studying and modifying acetyl-CoA metabolism relies heavily on fast and efficient techniques for genetic engineering. During the course of this PhD project, a new genetic engineering tool became available, the CRISPR/Cas9 system. **Chapter 2** explores the use of this system to genetically engineer *S. cerevisiae*. A number of case studies described in this chapter demonstrate the versatility and efficiency of the CRISPR/Cas9 system in (multiplexed) strain engineering strategies. Another goal of this study was to design a set of plasmids and a software tool for efficient genetic modification of *S. cerevisiae* with the CRISPR/Cas9 system and to make these available to the scientific community.

In **Chapter 3**, two alternative cytosolic acetyl-CoA synthesis pathways, involving acetylating acetaldehyde dehydrogenase and pyruvate-formate lyase as key enzymes, were expressed in *S. cerevisiae*. As cytosolic acetyl-CoA provision is essential for growth, the functionality of these pathways was evaluated by investigating their ability to support growth in strains in which the genes encoding the enzymes involved in the native cytosolic acetyl-CoA synthesis pathway were deleted. The impact of these alternative routes on yeast physiology was further evaluated in batch and chemostat cultures of engineered strains using transcriptome, metabolome and flux analysis.

In yeast, several mechanisms link glycolysis, a cytosolic pathway, to the mitochondrial acetyl-CoA pool and to the citric-acid cycle. In **Chapter 4**, the importance of the mitochondrial pyruvate-dehydrogenase complex, the mitochondrial CoA-transferase Ach1 and the extramitochondrial citrate synthase Cit2 in linking glycolysis to the citric-acid cycle was evaluated during growth on glucose of a set of mutant yeast strains. A fourth system, the carnitine shuttle, is also able to translocate cytosolic acetyl moieties to the mitochondria. As transcription of the genes involved in this shuttle are repressed by glucose, the impact of constitutively expressing all carnitine-shuttle genes was evaluated in strains with impaired mitochondrial acetyl-CoA synthesis.

Mechanistically, the carnitine shuttle has the potential to export mitochondrial acetyl moieties to the cytosol. However, previous studies showed that in the presence of carnitine, such carnitine-shuttle mediated export does not occur at a significant rate in *S. cerevisiae*. In **Chapter 5**, the reversibility of the yeast mitochondrial carnitine shuttle was investigated by constitutively overexpressing the carnitine-shuttle genes in an es-

pecially designed *S. cerevisiae* strain in which the native cytosolic acetyl-CoA production pathway could be completely inactivated by changing the medium composition. As, initially, constitutive expression of the carnitine shuttle did not support carnitine-dependent growth, laboratory evolution was applied. Mutations that contributed to the acquired phenotype of evolved strains were studied by whole-genome sequencing and by reverse engineering in a naïve genetic background.

SUPPLEMENTARY MATERIALS

Supplementary data 1.1: Model of yeast metabolism (MetaTool format)

The model used for the stoichiometric analyses described in this paper was based on the model described by Carlson *et al.* (32), with the following modifications. The exchange reaction of acetyl-CoA between the mitochondria and cytosol was removed (R45r) and the cytosolic alcohol dehydrogenase reaction was changed to be reversible (R65r). The cytosolic acetaldehyde dehydrogenase reaction was changed to accept not only NADP⁺, but also NAD⁺ as redox cofactor (R66b). The succinate dehydrogenase reaction was modified to accept only NAD⁺ as a cofactor instead of FADH (R25r and R75). Oxidative phosphorylation reactions were changed to have NADH as the sole electron donor and O₂ as the electron acceptor (R28, R29 and resp). The four stoichiometrically different acetyl-CoA formation routes were added: (i) the PDH bypass (the ACS reaction was changed to be irreversible (R68)), (ii) the citrate-oxaloacetate shuttle with ATP-citrate lyase (ACL), (iii) the phosphoketolase/-transacetylase route (PK_1, PK_2 and PTAr) and (iv) the oxidative, ATP-independent routes from pyruvate to acetyl-CoA, which are all stoichiometrically identical (AALD; acetylating acetaldehyde dehydrogenase, cytosolic PDH complex, pyruvate-formate lyase with formate dehydrogenase and export of mitochondrial acetyl moieties to the cytosol via the carnitine shuttle). The product pathways from acetyl-CoA to (i) palmitic acid (PA_1 and PA_2), (ii) farnesene (F_1) (iii) *n*-butanol (BOH_1 and BOH_2) and (iv) citric acid were added (CIT_1).

-ENZREV

R3r R5r R6r R7r R10r R11r R12r R13r R14r R22r R25r R26r R27r R41r
R43r R60r R63r R64r R65r R67r R69r R72r R80r AALD PTAr BOH_1

-ENZIRREV

R1 R2 R4 RR4 R8 R9 R20 R21 R23 R24 R28 R30 R31 R40 R42 R44 R45r R46
R47 R48 R49 R50 R61 R62 R66 R70 R71 R73 R74 R75 R76 R77 R78 R79 R81
resp R66b NADH_base NADH_base_2 NADPH_base R68 PA_1 PA_2 ACL PK_1
PK_2 BOH_2 CIT_1 F_1

-METINT

GLU_cyt ATP_cyt ADP_cyt P_cyt GLU_6_P FRU_6_P FRU_BIS_P DHAP
GA_3P NAD_cyt NADH_cyt NADPH NADP RIBULOSE_5_P XYL_5_P RIBOSE_5_P
SED_7_P ERYTH_4_P PYR_cyt MALATE_cyt CITRATE_cyt OXALO_cyt CoASH_cyt
ACETYL_CoA_cyt GLYCEROL_P PEP AKG_cyt ISOCIT_cyt PYR_mit CITRATE_mit
OXALO_mit MALATE_mit CoASH_mit ACETYL_CoA_mit ATP_mit ADP_mit P_mit
NADH_mit NAD_mit AKG_mit ISOCIT_mit ETOH_cyt ACEADH_cyt ACETATE_cyt
GLYCEROL_cyt SUCC_mit GLYOX_cyt ETOH_mit FUMARATE_mit SUCC_cyt FU-
MARATE_cyt NADP_mit NADPH_mit MALONYL_CoA_cyt ACETOACETYL_CoA_cyt
ACETYL_P_cyt

-METEXT

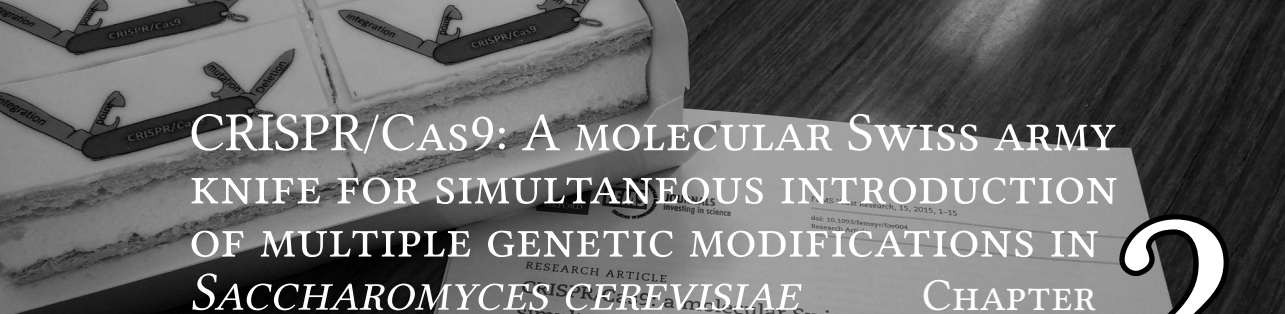
ATP_base ACETATE_ext O2 CO2 SUCC_ext ETOH_ext GLYCEROL_ext GLU_ext
NADH_base NADPH_base PALMITIC_ACID BUTANOL CITRATE FARNESENE

-CAT

R1 : GLU_ext = GLU_cyt .

R2 : $\text{GLU_cyt} + \text{ATP_cyt} = \text{GLU_6_P} + \text{ADP_cyt}$.
 R3r : $\text{GLU_6_P} = \text{FRU_6_P}$.
 R4 : $\text{FRU_6_P} + \text{ATP_cyt} = \text{FRU_BIS_P} + \text{ADP_cyt}$.
 RR4 : $\text{FRU_BIS_P} = \text{FRU_6_P} + \text{P_cyt}$.
 R5r : $\text{FRU_BIS_P} = \text{DHAP} + \text{GA_3P}$.
 R6r : $\text{GA_3P} = \text{DHAP}$.
 R7r : $\text{GA_3P} + \text{ADP_cyt} + \text{P_cyt} + \text{NAD_cyt} = \text{PEP} + \text{ATP_cyt} + \text{NADH_cyt}$.
 R8 : $\text{PEP} + \text{ADP_cyt} = \text{PYR_cyt} + \text{ATP_cyt}$.
 R9 : $\text{GLU_6_P} + 2 \text{ NADP} = \text{RIBULOSE_5_P} + 2 \text{ NADPH} + \text{CO}_2$.
 R10r : $\text{RIBULOSE_5_P} = \text{XYL_5_P}$.
 R11r : $\text{RIBULOSE_5_P} = \text{RIBOSE_5_P}$.
 R12r : $\text{RIBOSE_5_P} + \text{XYL_5_P} = \text{SED_7_P} + \text{GA_3P}$.
 R13r : $\text{GA_3P} + \text{SED_7_P} = \text{ERYTH_4_P} + \text{FRU_6_P}$.
 R14r : $\text{ERYTH_4_P} + \text{XYL_5_P} = \text{GA_3P} + \text{FRU_6_P}$.
 R20 : $\text{PYR_mit} + \text{CoASH_mit} + \text{NAD_mit} = \text{ACETYL_CoA_mit} + \text{NADH_mit} + \text{CO}_2$.
 R21 : $\text{OXALO_mit} + \text{ACETYL_CoA_mit} = \text{CITRATE_mit} + \text{CoASH_mit}$.
 R22r : $\text{CITRATE_mit} = \text{ISOCIT_mit}$.
 R23 : $\text{ISOCIT_mit} + \text{NAD_mit} = \text{AKG_mit} + \text{NADH_mit} + \text{CO}_2$.
 R24 : $\text{AKG_mit} + \text{NAD_mit} + \text{ADP_mit} + \text{P_mit} = \text{NADH_mit} + \text{ATP_mit} + \text{SUCC_mit} + \text{CO}_2$.
 R25r : $\text{SUCC_mit} + \text{NAD_mit} = \text{FUMARATE_mit} + \text{NADH_mit}$.
 R26r : $\text{FUMARATE_mit} = \text{MALATE_mit}$.
 R27r : $\text{MALATE_mit} + \text{NAD_mit} = \text{OXALO_mit} + \text{NADH_mit}$.
 R28 : $\text{NADH_mit} + \text{ADP_mit} + \text{P_mit} + 0.5 \text{ O}_2 = \text{NAD_mit} + \text{ATP_mit}$.
~~R29 : $\text{FADH_mit} + \text{ADP_mit} + \text{P_mit} = \text{FAD_mit} + \text{ATP_mit}$.~~
 R30 : $\text{ETOH_mit} + \text{CoASH_mit} + 2 \text{ ATP_mit} + 2 \text{ NAD_mit} = \text{ACETYL_CoA_mit} + 2 \text{ ADP_mit} + 2 \text{ P_mit} + 2 \text{ NADH_mit}$.
 R31 : $\text{MALATE_mit} + \text{NADP_mit} = \text{PYR_mit} + \text{NADPH_mit} + \text{CO}_2$.
 R40 : $\text{ADP_cyt} + \text{ATP_mit} = \text{ADP_mit} + \text{ATP_cyt}$.
 R41r : $\text{P_cyt} = \text{P_mit}$.
 R42 : $\text{PYR_cyt} = \text{PYR_mit}$.
 R43r : $\text{ETOH_cyt} = \text{ETOH_mit}$.
 R44 : $\text{MALATE_mit} + \text{P_cyt} = \text{MALATE_cyt} + \text{P_mit}$.
 R46 : $\text{FUMARATE_mit} + \text{SUCC_cyt} = \text{FUMARATE_cyt} + \text{SUCC_mit}$.
 R47 : $\text{CITRATE_mit} + \text{MALATE_cyt} = \text{CITRATE_cyt} + \text{MALATE_mit}$.
 R48 : $\text{SUCC_cyt} + \text{P_mit} = \text{SUCC_mit} + \text{P_cyt}$.
 R49 : $\text{AKG_cyt} + \text{MALATE_mit} = \text{AKG_mit} + \text{MALATE_cyt}$.
 R50 : $\text{OXALO_cyt} = \text{OXALO_mit}$.
 R60r : $\text{GLYCEROL_cyt} = \text{GLYCEROL_ext}$.
 R61 : $\text{GLYCEROL_cyt} + \text{ATP_cyt} = \text{GLYCEROL_P} + \text{ADP_cyt}$.
 R62 : $\text{GLYCEROL_P} = \text{GLYCEROL_cyt} + \text{P_cyt}$.
 R63r : $\text{DHAP} + \text{NADH_cyt} = \text{GLYCEROL_P} + \text{NAD_cyt}$.
 R64r : $\text{ETOH_cyt} = \text{ETOH_ext}$.
 R65r : $\text{ACEADH_cyt} + \text{NADH_cyt} = \text{ETOH_cyt} + \text{NAD_cyt}$.

R66 : ACEADH_cyt + NADP = ACETATE_cyt + NADPH .
 R66b : ACEADH_cyt + NAD_cyt = ACETATE_cyt + NADH_cyt .
 R67r : ACETATE_cyt = ACETATE_ext .
 R68 : ACETATE_cyt + CoASH_cyt + 2 ATP_cyt = ACETYL_CoA_cyt + 2 ADP_cyt + 2 P_cyt .
 R69r : CITRATE_cyt = ISOCIT_cyt .
 R70 : ISOCIT_cyt = GLYOX_cyt + SUCC_cyt .
 R71 : GLYOX_cyt + ACETYL_CoA_cyt = MALATE_cyt + CoASH_cyt .
 R72r : OXALO_cyt + NADH_cyt = MALATE_cyt + NAD_cyt .
 R73 : OXALO_cyt + ACETYL_CoA_cyt = CITRATE_cyt + CoASH_cyt .
 R74 : ISOCIT_cyt + NADP = AKG_cyt + NADPH + CO2 .
 R75 : FUMARATE_cyt + NADH_cyt = SUCC_cyt + NAD_cyt .
 R76 : OXALO_cyt + ATP_cyt = PEP + ADP_cyt + CO2 .
 R77 : PYR_cyt + ATP_cyt + CO2 = ADP_cyt + P_cyt + OXALO_cyt .
 R78 : PYR_cyt = ACEADH_cyt + CO2 .
 R79 : ATP_cyt = ADP_cyt + P_cyt + ATP_base .
 R80r : MALATE_cyt = FUMARATE_cyt .
 R81 : SUCC_cyt = SUCC_ext .
 resp : NADH_cyt + ADP_cyt + P_cyt + 0.5 O2 = NAD_cyt + ATP_cyt .
 NADH_base : NADH_cyt = NADH_base + NAD_cyt .
 NADH_base_2 : NADH_mit = NADH_base + NAD_mit .
 NADPH_base : NADPH = NADPH_base + NADP .
 PK_1 : XYL_5_P + P_cyt = GA_3P + ACETYL_P_cyt .
 PK_2 : FRU_6_P + P_cyt = ERYTH_4_P + ACETYL_P_cyt .
 PTAr : ACETYL_P_cyt + CoASH_cyt = P_cyt + ACETYL_CoA_cyt .
 AALD : ACEADH_cyt + NAD_cyt + CoASH_cyt = ACETYL_CoA_cyt + NADH_cyt .
 ACL : CITRATE_cyt + ATP_cyt + CoASH_cyt = ACETYL_CoA_cyt + OXALO_cyt + ADP_cyt + P_cyt .
 PA_1 : ACETYL_CoA_cyt + CO2 + ATP_cyt = MALONYL_CoA_cyt + ADP_cyt + P_cyt .
 PA_2 : ACETYL_CoA_cyt + 7 MALONYL_CoA_cyt + 14 NADPH = PALMITIC_ACID + 8 CoASH_cyt + 14 NADP + 7 CO2 .
 F_1 : 9 ACETYL_CoA_cyt + 6 NADH_cyt + 9 ATP_cyt = FARNESENE + 9 CoASH_cyt + 6 NAD_cyt + 9 ADP_cyt + 9 P_cyt + 3 CO2 .
 BOH_1 : 2 ACETYL_CoA_cyt = ACETOACETYL_CoA_cyt + CoASH_cyt .
 BOH_2 : ACETOACETYL_CoA_cyt + 4 NADH_cyt = BUTANOL + 4 NAD_cyt + CoASH_cyt .
 CIT_1 : CITRATE_cyt = CITRATE .



CRISPR/Cas9: A MOLECULAR SWISS ARMY KNIFE FOR SIMULTANEOUS INTRODUCTION OF MULTIPLE GENETIC MODIFICATIONS IN *SACCHAROMYCES CEREVISIAE*

CHAPTER 2

Robert Mans¹, Harmen M. van Rossum¹, Melanie Wijsman, Antoon Backx, Niels G.A. Kuijpers, Marcel van den Broek, Pascale Daran-Lapujade, Jack T. Pronk, Antonius J.A. van Maris and Jean-Marc G. Daran

Abstract

A variety of techniques for strain engineering in *Saccharomyces cerevisiae* have recently been developed. However, especially when multiple genetic manipulations are required, strain construction is still a time-consuming process. This study describes new CRISPR/Cas9-based approaches for easy, fast strain construction in yeast and explores their potential for simultaneous introduction of multiple genetic modifications. An open-source tool (<http://yeastriction.tnw.tudelft.nl>) is presented for identification of suitable Cas9 target sites in *S. cerevisiae* strains. A transformation strategy, using *in vivo* assembly of a guideRNA plasmid and subsequent genetic modification, was successfully implemented with high accuracies. An alternative strategy, using *in vitro* assembled plasmids containing 2 gRNAs was used to simultaneously introduce up to 6 genetic modifications in a single transformation step with high efficiencies. Where previous studies mainly focused on the use of CRISPR/Cas9 for gene inactivation, we demonstrate the versatility of CRISPR/Cas9-based engineering of yeast by achieving simultaneous integration of a multi-gene construct combined with gene deletion and the simultaneous introduction of 2 single-nucleotide mutations at different loci. Sets of standardized plasmids, as well as the web-based Yeastriction target-sequence identifier and primer-design tool, are made available to the yeast research community to facilitate fast, standardized and efficient application of the CRISPR/Cas9 system.

2.1 INTRODUCTION

For decades, *Saccharomyces cerevisiae* has been successfully used as a model organism to decipher biological processes in higher eukaryotes (19) and as a popular metabolic engineering platform (220). Expression and optimization of heterologous product pathways in *S. cerevisiae* (see e.g. (10, 232)), requires introduction of multiple (successive) genetic modifications, including integration of product pathway genes at multiple genetic loci and rewiring central metabolism by modifying properties of specific metabolic reactions (e.g. via gene deletion, changing regulatory properties or replacement of native genes by heterologous counterparts) (254, 340). Introduction of the required genetic modifications has so far remained a time-consuming and labour-intensive process, as each individual alteration requires a cycle of transformation, selection and confirmation. Furthermore, since each modification is accompanied by the integration of a selection marker gene, the maximum number of sequential modifications may be limited by selection marker availability. This limitation stimulated extensive research into the identification of novel genetic markers for *S. cerevisiae* (41, 282, 288). Additionally, multiple strategies for the recycling of genetic markers have been developed, such as homologous-recombination-mediated counter selection (gene “loop-out”) and use of recombinases such as the Cre/*loxP* or 2 μ m-plasmid-based Flp/FRT methods (108, 112, 300). These recombinase-based methods leave a copy of a repeat sequence (e.g. *loxP* or FRT site) in the genome, which leads to genome instability after multiple, repeated rounds of marker recovery (56, 289). ‘Scarless’ removal of counter-selectable markers has been made possible via the *delitto perfetto* method (301), while a recently reported marker-recovery method based on generation of I-SceI-induced double-stranded breaks even allows simultaneous, seamless removal of multiple markers (290). While these methods largely eliminate limitations by marker-gene availability, substitution of target genes by marker cassettes remained a time-consuming process, due to the absence of robust methods for simultaneous introduction of multiple genetic modifications in a single transformation step. Alternative methods such as meganucleases, zinc finger nucleases (ZFNs) (33, 317) and transcription activator-like effector nucleases (TALENs) (47, 213, 215) utilize double-stranded DNA breaks (DSBs) for site-directed genome editing. Due to the lethal nature of DSBs in yeast, these methods could theoretically be used for marker-free modifications. However, for each genetic modification a new ZFN or TALEN protein has to be designed and generated.

Bacteria have developed several systems to degrade foreign DNA. Very quickly after their discovery, restriction enzymes became the “workhorses of molecular biology” (reviewed by Roberts (255)). Another prokaryotic immune mechanism, consisting of Clustered Regularly Interspaced Short Palindromic Repeats (CRISPR) and CRISPR-associated (Cas) systems was discovered in 2007 (9, 25, 205). To function *in vivo*, the type-II bacterial CRISPR system of *Streptococcus pyogenes* requires the Cas9 nuclease and the RNA complex that guides it to a specific sequence of the (foreign) DNA. This RNA complex generally consists of two RNA molecules; the CRISPR RNA (crRNA) and the trans-activating CRISPR RNA (tracrRNA). The crRNA contains the 20-30 bp target sequence and a sequence that binds to the tracrRNA, resulting in a duplex RNA complex, recognized by the Cas9 nuclease. When directly after the target sequence, a proper protospacer adja-

cent motif (PAM) is present (in case of the *S. pyogenes* Cas9 this sequence is NGG), Cas9 will bind to and restrict the target sequence of the (invading) DNA (58). A unique feature of this system is the RNA-dependence for targeting of the nuclease Cas9, which makes selective targeting of any locus for the introduction of DSBs possible. Since its discovery, Cas9 based systems have been used for the construction of (multiplexed) genetic modifications in a variety of organisms, including human pluripotent stem cells (99), zebrafish (130), plants (78), fly (101) and mice (333) (for a more extensive list see (125)).

In 2013, DiCarlo and coworkers employed the CRISPR/Cas9 system for the introduction of DSBs in *S. cerevisiae* (61). In a strain expressing a plasmid-borne *cas9* gene from *S. pyogenes*, a second plasmid was introduced, containing the *SNR52* promoter followed by a sequence encoding for a chimeric crRNA-tracrRNA, or guide-RNA (gRNA) with a 20 bp targeting sequence for *CAN1*. The gRNA was recognized by the Cas9 protein, resulting in a double-strand break at the *CAN1* locus. Subsequently, this otherwise lethal break was repaired by the yeast homologous-recombination machinery, using a co-transformed repair fragment that bridged the flanking regions of the break. Since the repair fragment was designed to introduce a premature stop-codon, introduction and repair of a DSB resulted in colonies that were resistant to canavanine. It has recently been shown that the CRISPR/Cas9 system can be used for making up to three simultaneous gene deletions in yeast (8).

The goal of the present study is to explore the use of CRISPR/Cas9 for, standardized (multiplexed) construction of gene deletions, multi-pathway integrations and site-directed single-nucleotide mutagenesis. To this end, we present a web-based CRISPR tool to facilitate selection of suitable targets and to design the primers necessary for construction of plasmids that express specific gRNAs. Furthermore, we report on the construction of standardized plasmids for expression of one or two gRNAs and explore their use for multiplexed gene deletions, both alone and in combination with multigene chromosomal integrations and/or with the introduction of single-nucleotide changes.

2.2 METHODS

STRAINS AND MAINTENANCE

The *S. cerevisiae* strains used in this study (Table 2.1) share the CEN.PK genetic background (71, 222). Shake flask cultures were grown at 30 °C in 500 mL flasks containing 100 mL synthetic medium (SM) (326) with 20 g·L⁻¹ glucose in an Innova incubator shaker (New Brunswick Scientific, Edison, NJ) set at 200 rpm. When required, auxotrophic requirements were complemented via addition of 150 mg·L⁻¹ uracil, 100 mg·L⁻¹ histidine, 500 mg·L⁻¹ leucine, 75 mg·L⁻¹ tryptophan (246) or by growth in YP medium (demineralized water, 10 g·L⁻¹ Bacto yeast extract, 20 g·L⁻¹ Bacto peptone). As a carbon source, 20 g·L⁻¹ glucose was used. Frozen stocks were prepared by addition of glycerol (30% v/v) to exponentially growing shake-flask cultures of *S. cerevisiae* and overnight cultures of *E. coli* and stored aseptically in 1 mL aliquots at -80 °C.

PLASMID CONSTRUCTION

Construction of the single gRNA plasmid series (pMEL10 – pMEL17) The single gRNA plasmids (pMEL10 – pMEL17) were constructed via Gibson assembly (New England Biolabs, Beverly, MA) of a marker cassette with one fragment containing both the gRNA *CAN1.Y* (61) and the 2µm replication sequence. This fragment was obtained by PCR from plasmid p426-

Table 2.1. *Saccharomyces cerevisiae* strains used in this study

Name (Accession no.)*	Relevant genotype	Parental strain	Origin
CEN.PK113-7D	<i>MATa URA3 TRP1 LEU2 HIS3</i>		P. Kötter
CEN.PK113-5D	<i>MATa ura3-52 TRP1 LEU2 HIS3</i>		P. Kötter
CEN.PK122	<i>MATa/MATα URA3/URA3 TRP1/TRP1 LEU2/LEU2 HIS3/HIS3</i>		P. Kötter
CEN.PK2-1C	<i>MATa ura3-52 trp1-289 leu2-3,112 his3Δ</i>		P. Kötter
CEN.PK115	<i>MATa/MATα ura3-52/ura3-52 TRP1/TRP1 LEU2/LEU2 HIS3/HIS3</i>		P. Kötter
IMX585 (Y40592)	<i>MATa can1Δ::cas9-natNT2 URA3 TRP1 LEU2 HIS3</i>	CEN.PK113-7D	This study
IMX581 (Y40593)	<i>MATa ura3-52 can1Δ::cas9-natNT2 TRP1 LEU2 HIS3</i>	CEN.PK113-5D	This study
IMX664 (Y40594)	<i>MATa/MATα CAN1/can1Δ::cas9-natNT2 URA3/URA3 TRP1/TRP1 LEU2/LEU2 HIS3/HIS3</i>	CEN.PK122	This study
IMX672 (Y40595)	<i>MATa ura3-52 trp1-289 leu2-3,112 his3Δ can1Δ::cas9-natNT2</i>	CEN.PK2-1C	This study
IMX673 (Y40596)	<i>MATa/MATα ura3-52/ura3-52 CAN1/can1Δ::cas9-natNT2 TRP1/TRP1 LEU2/LEU2 HIS3/HIS3</i>	CEN.PK115	This study
IMX711	<i>MATa ura3-52 trp1-289 leu2-3,112 his3Δ can1Δ::cas9-natNT2 mch1Δ pMEL10-gRNA-MCH1</i>	IMX672	This study
IMX712	<i>MATa ura3-52 trp1-289 leu2-3,112 his3Δ can1Δ::cas9-natNT2 mch2Δ pMEL10-gRNA-MCH2</i>	IMX672	This study
IMX713	<i>MATa ura3-52 trp1-289 leu2-3,112 his3Δ can1Δ::cas9-natNT2 mch5Δ pMEL10-gRNA-MCH5</i>	IMX672	This study
IMX714	<i>MATa ura3-52 trp1-289 leu2-3,112 his3Δ can1Δ::cas9-natNT2 mch1Δ mch5Δ pMEL10-gRNA-MCH1 pMEL10-gRNA-MCH5</i>	IMX672	This study
IMX715	<i>MATa ura3-52 trp1-289 leu2-3,112 his3Δ can1Δ::cas9-natNT2 itr1Δ pdr12Δ pUDR005</i>	IMX672	This study
IMX716	<i>MATa ura3-52 trp1-289 leu2-3,112 his3Δ can1Δ::cas9-natNT2 mch1Δ mch2Δ itr1Δ pdr12Δ pUDR002 pUDR005</i>	IMX672	This study
IMX717	<i>MATa ura3-52 trp1-289 leu2-3,112 his3Δ can1Δ::cas9-natNT2 mch1Δ mch2Δ mch5Δ aqy1Δ itr1Δ pdr12Δ pUDR002 pUDR004 pUDR005</i>	IMX672	This study
IMX718	<i>MATa ura3-52 trp1-289 leu2-3,112 his3Δ can1Δ::cas9-natNT2 GET4^{G315C} NAT1^{C1139G} pUDR020</i>	IMX672	This study
IMX719	<i>MATa can1Δ::cas9-natNT2 URA3 TRP1 LEU2 HIS3 acs1Δ acs2Δ::(pADH1-aceF-tPGI1 pPGI1-lplA2-tPYK1 pPGK1-lplA-tPMA1 pTDH3-pdhB-tCYC1 pTEF1-lpd-tADH1 pTPI1-pdhA-tTEF1)</i>	IMX585	This study

* Strains with an accession number have been deposited at EUROSCARF.

SNR52p-gRNA.CAN1.Y-SUP4t, using primers 6845 & 6846 (Table S2.1). The various marker cassettes were PCR amplified from plasmid templates pUG72, pUG-amdSYM, pUG-hphNT1, pUG6, pUG73 and pUG-natNT2 with primers 3093 & 3096 resulting in the *KIURA3*, *amdSYM*, *hphNT1*, *kanMX*, *KILEU2* and *natNT2* cassettes, respectively. The *HIS3* and *TRP1* cassettes were obtained by PCR with primers 6847 & 6848 on plasmid templates pRS423 and pRS424. Assembly of the single gRNA plasmids was done by combining the appropriate marker cassette with the backbone containing the gRNA *CAN1.Y* and 2μm sequences in a Gibson assembly reaction, following the manufacturer's recommendations. For each single gRNA plasmid (pMEL10 – pMEL17), an *E. coli*

Table 2.2. Plasmids used in this study

Name (Accession no.)*	Relevant characteristics	Origin
pUG6	Template for A- <i>kanMX</i> -B ¹ cassette	(107)
pUG72	Template for A- <i>KIURA3</i> -B cassette	(107)
pUG73	Template for A- <i>KILEU2</i> -B cassette	(107)
pUG-hphNT1	Template for A- <i>hphNT1</i> -B cassette	(162)
pUG-natNT2	Template for A- <i>natNT2</i> -B cassette	(164)
pUG-amdSYM	Template for A- <i>amdSYM</i> -B cassette	(288)
pRS423	Template for A- <i>ScHIS3</i> -B cassette	(48)
pRS424	Template for A- <i>ScTRP1</i> -B cassette	(48)
p414-TEF1p-Cas9-CYC1t	<i>CEN6/ARS4</i> ampR <i>TRP1 pTEF1-cas9-tCYC1</i>	(61)
p426-SNR52p-gRNA.CAN1.Y-SUP4t	2μm ampR <i>URA3</i> gRNA- <i>CAN1.Y</i>	(61)
pUD192	pUC57 + <i>ScURA3</i>	(167)
pUD194	pUC57 + 2μm	(167)
pUD195	pUC57 + pMB1 + ampR	(167)
pUD301	pUC57 + <i>pTP1-pdhA E. faecalis-tTEF1</i>	(167)
pUD302	pUC57 + <i>pTDH3-pdhB E. faecalis-tCYC1</i>	(167)
pUD303	pUC57 + <i>pADH1-aceF E. faecalis-tPGI1</i>	(167)
pUD304	pUC57 + <i>pTEF1-lpd E. faecalis-tADH1</i>	(167)
pUD305	pUC57 + <i>pPGK1-lplA E. faecalis-tPMA1</i>	(167)
pUD306	pUC57 + <i>pPGI1-lplA2 E. faecalis-tPYK1</i>	(167)
pUDE330	2μm ampR <i>ScURA3</i> gRNA- <i>CAN1.Y</i> [2x]	This study
pMEL10 (P30779)	2μm ampR <i>KURA3</i> gRNA- <i>CAN1.Y</i>	This study
pMEL11 (P30780)	2μm ampR <i>amdSYM</i> gRNA- <i>CAN1.Y</i>	This study
pMEL12 (P30781)	2μm ampR <i>hphNT1</i> gRNA- <i>CAN1.Y</i>	This study
pMEL13 (P30782)	2μm ampR <i>kanMX</i> gRNA- <i>CAN1.Y</i>	This study
pMEL14 (P30783)	2μm ampR <i>KILEU2</i> gRNA- <i>CAN1.Y</i>	This study
pMEL15 (P30784)	2μm ampR <i>natNT2</i> gRNA- <i>CAN1.Y</i>	This study
pMEL16 (P30785)	2μm ampR <i>HIS3</i> gRNA- <i>CAN1.Y</i>	This study
pMEL17 (P30786)	2μm ampR <i>TRP1</i> gRNA- <i>CAN1.Y</i>	This study
pROS10 (P30787)	2μm ampR <i>ScURA3</i> gRNA- <i>CAN1.Y</i> gRNA- <i>ADE2.Y</i>	This study
pROS11 (P30788)	2μm ampR <i>amdSYM</i> gRNA- <i>CAN1.Y</i> gRNA- <i>ADE2.Y</i>	This study
pROS12 (P30789)	2μm ampR <i>hphNT1</i> gRNA- <i>CAN1.Y</i> gRNA- <i>ADE2.Y</i>	This study
pROS13 (P30790)	2μm ampR <i>kanMX</i> gRNA- <i>CAN1.Y</i> gRNA- <i>ADE2.Y</i>	This study
pROS14 (P30791)	2μm ampR <i>KILEU2</i> gRNA- <i>CAN1.Y</i> gRNA- <i>ADE2.Y</i>	This study
pROS15 (P30792)	2μm ampR <i>natNT2</i> gRNA- <i>CAN1.Y</i> gRNA- <i>ADE2.Y</i>	This study
pROS16 (P30793)	2μm ampR <i>HIS3</i> gRNA- <i>CAN1.Y</i> gRNA- <i>ADE2.Y</i>	This study
pROS17 (P30794)	2μm ampR <i>TRP1</i> gRNA- <i>CAN1.Y</i> gRNA- <i>ADE2.Y</i>	This study
pUDR002	2μm ampR <i>TRP1</i> gRNA- <i>MCH1</i> gRNA- <i>MCH2</i>	This study
pUDR004	2μm ampR <i>HIS3</i> gRNA- <i>MCH5</i> gRNA- <i>AQY1</i>	This study
pUDR005	2μm ampR <i>ScURA3</i> gRNA- <i>ITR1</i> gRNA- <i>PDR12</i>	This study
pUDR020	2μm ampR <i>ScURA3</i> gRNA- <i>NAT1</i> gRNA- <i>GET4</i>	This study
pUDR022	2μm ampR <i>kanMX</i> gRNA- <i>ACS1</i> gRNA- <i>ACS2</i>	This study

¹ A and B refer to 60 bp tags that are incorporated via PCR, enabling homologous recombination.

* Plasmids with an accession number have been deposited at EUROSCARF.

clone containing the correctly assembled plasmid (confirmed by restriction analysis) was selected, stocked and deposited at EUROSCARF (<http://web.uni-frankfurt.de/fb15/mikro/euroscarf/>).

Construction of the double gRNA plasmid series (pROS10 – pROS17) To construct the double gRNA plasmids (pROS10 – pROS17), an intermediate plasmid was first constructed, carrying two gRNA cassettes that both targeted *CAN1.Y* (61). This intermediate plasmid was assembled out of four different overlapping fragments: the two gRNA cassettes overlapping with each other in the 2μm replicon, one *ScURA3* marker cassette and a cassette containing all sequences for amplification in *E. coli*. The gRNA cassettes were obtained in a two-step PCR approach. First a 2μm fragment was obtained from pUD194 (Table 2.2) with primers 3289 & 4692 and two different gRNA cassettes

were PCR amplified from p426-SNR52p-gRNA.CAN1.Y-SUP4t with primers 5972 & 5976 for the first cassette and 5977 & 5973 for the second cassette. Each gRNA cassette was separately pooled with the 2 μ m fragment and in a second PCR reaction the gRNA cassettes were extended with either the 5' or 3' half of the 2 μ m fragment, resulting in two different gRNA cassettes, overlapping in the 2 μ m sequence, by using primer pair 5975 & 4068 for the first and 5974 & 3841 for the second fragment. The marker fragment containing *ScURA3* was obtained from pUD192 with primers 3847 & 3276 (Table 2.2) and the fragment containing all sequences for amplification in *E. coli* was PCR amplified from pUD195 (Table 2.2) with primers 3274 & 3275. Using Gibson assembly, the four overlapping fragments were assembled into the intermediate plasmid pUDE330. To obtain pROS10, pUDE330 was linearized by PCR-amplification of the backbone, excluding the gRNA fragments, and co-transformed with two gRNA cassettes for *in vivo* assembly by homologous recombination in yeast (172). For linearizing the backbone, a single primer was used (5793) and the gRNA fragments were obtained by PCR from pUDE330 with primers 6008 & 5975 and 6007 & 5974. The plasmid was extracted from yeast and transformed into *E. coli* for storage and plasmid propagation. The other double gRNA plasmids were assembled by the Gibson assembly method with a marker cassette and the pROS10 plasmid backbone fragment. This backbone fragment was obtained by linearization of pROS10 with restriction enzymes PvuII and NotI. The various marker cassettes were PCR amplified from plasmid templates pUG-*amdSYM*, pUG-*hphNT1*, pUG6, pUG73 and pUG-*natNT2* with primers 3093 & 3096 resulting in the *amdSYM*, *hphNT1*, *kanMX*, *KILEU2* and *natNT2* cassettes, respectively. The *HIS3* and *TRP1* cassettes were obtained by PCR with primers 6847 & 6848 on plasmid templates pRS423 and pRS424. Combining the appropriate marker cassette with the pROS10 backbone fragment in a Gibson assembly reaction, following the manufacturer's recommendations, resulted in pROS11 – pROS17. For each of these double gRNA plasmids, an *E. coli* clone containing the correctly assembled plasmid was selected, stocked and deposited at EUROSCARF (<http://web.uni-frankfurt.de/fb15/mikro/euroscarf/>).

STRAIN CONSTRUCTION

S. cerevisiae strains were transformed according to Gietz and Woods (97). Mutants were selected on solid YP medium (demineralized water, 10 g·L⁻¹ Ba ϕ to yeast extract, 20 g·L⁻¹ Ba ϕ to peptone, 2% (w/v) agar), supplemented with 200 mg·L⁻¹ G418, 200 mg·L⁻¹ hygromycin B or 100 mg·L⁻¹ nourseothricin (for dominant markers) or on synthetic medium supplemented with appropriate auxotrophic requirements (326). In all cases, gene deletions and integrations were confirmed by colony PCR on randomly picked colonies, using the diagnostic primers listed in Table S2.1. Integration of *cas9* into the genome was achieved via assembly and integration of two cassettes containing *cas9* and the *natNT2* marker into the *CAN1* locus. The *cas9* cassette was obtained by PCR from p414-TEF1p-*cas9*-CYC1t (61), using primers 2873 & 4653. The *natNT2* cassette was PCR amplified from pUG-*natNT2* with primers 3093 & 5542. 2.5 μ g *cas9* and 800 ng *natNT2* cassette were pooled and used for each transformation. Correct integration was verified by colony PCR (Supplemental information) using the primers given in Table S2.1, the resulting strains have been deposited at EUROSCARF. IMX719 was constructed by co-transformation of pUDR022 (see below) with genes required for functional *Enterococcus faecalis* PDH expression (167). The gene cassettes were obtained by PCR using plasmids pUD301 – pUD306 as template (Table 2.2) with the primers indicated in Table S2.1 and the *ACS1* dsDNA repair fragment, obtained by annealing two complementary single stranded oligos (6422 & 6423). After confirmation of the relevant genotype (Figure 2.4B), the pUDR022 plasmid was removed as explained in Supplemental information.

SINGLE GRNA METHOD (CLONING FREE)

The yeast homologous recombination (HR) machinery was used to assemble plasmids with specific gRNA sequences out of two different fragments: a plasmid backbone and a gRNA target sequence. Depending on the preferred selectable marker, the linearized plasmid backbone was obtained via

PCR using the appropriate single gRNA plasmid (pMEL10 – pMEL17) as a template, with primers 6005 & 6006. To obtain the double stranded gRNA cassettes (the target sequences are listed in Table 2.3), two complementary single stranded oligos (Table S2.1) were mixed in a 1:1 molar ratio, heated to 95 °C and then cooled down to room temperature. The resulting gRNA fragments contained the 20 bp gRNA recognition sequences, flanked by 50 bp overlaps with the linearized plasmid backbone. The 120 bp repair fragments were obtained by following the same procedure and were identical to the up- and downstream regions of the DSB break, allowing for effective repair by the HR-machinery. For each transformation, a linearized plasmid backbone, a double stranded cassette containing the gRNA sequence of choice and the double stranded DNA cassette for repair of the DSB were pooled and co-transformed to the appropriate strain.

DOUBLE GRNA METHOD

Plasmids with two gRNAs were assembled *in vitro*, using Gibson assembly of a 2µm fragment containing the two gRNA sequences and a double gRNA (pROS10 – pROS17) plasmid backbone. The 2µm fragment was obtained via PCR, using pROS10 as a template with two primers containing the 20 bp gRNA recognition sequences and a 50 bp sequence, homologous to the linearized plasmid backbone (Table S2.1). The linearized plasmid backbone was obtained via PCR using one of the double gRNA plasmids (pROS10 – pROS17, depending on the preferred selective marker) as a template with a single primer (6005), binding at each of the two *SNR52* promoters (Supplemental information). The two fragments were combined using Gibson assembly, followed by transformation to *E. coli* for storage and plasmid propagation. Since both of the gRNA containing primers could bind on either side of the 2µm fragment, it was important to check that the final plasmid contained one copy of each gRNA (theoretically this would be the case in 50% of the *E. coli* transformants). To simplify this confirmation step, the gRNA target sequences were selected for the presence of a restriction site. Alternatively, diagnostic primers specific for the introduced 20 bp recognition sequences were used for the identification of correctly assembled gRNA plasmids using PCR (see Protocol in Supplemental information).

To construct the plasmid pUDR002 (targeting *MCH1&MCH2*, *TRP1* marker), the 2µm fragment was amplified using DreamTaq (Fisher Scientific) from pROS10 using primers 6835 & 6837 (Supplemental information). The backbone of pROS17 was amplified using the Phusion polymerase (Fisher Scientific) with a single primer 6005 (Supplemental information). The two fragments were assembled using Gibson assembly and confirmed via restriction analysis. Similarly, the following plasmids were constructed: pUDR004 (targeting *MCH5&AQY1*, *HIS3* marker), pUDR005 (targeting *ITR1&PDR12*, *KIURA3* marker), pUDR020 (targeting *NAT1&GET4*, *URA3* marker), pUDR022 (targeting *ACS1&ACS2*, *kanMX* marker). Transformations using the double gRNA method required co-transformation of 2 µg of (each) pUDR plasmid together with 1 µg of (each) corresponding double stranded DNA cassette for DSB repair.

MOLECULAR BIOLOGY TECHNIQUES

PCR amplification with Phusion® Hot Start II High Fidelity Polymerase (Thermo Fisher Scientific) was performed according to the manufacturer's instructions using PAGE-purified oligonucleotide primers (Sigma-Aldrich, St. Louis, MO). Diagnostic PCR was done via colony PCR on randomly picked yeast colonies, using DreamTaq (Thermo Fisher Scientific) and desalted primers (Sigma-Aldrich). The primers used to confirm successful deletions by one of the two described methods can be found in Table S2.1. DNA fragments obtained by PCR were separated by gel electrophoresis on 1% (w/v) agarose gels (Thermo Fisher Scientific) in TAE buffer (Thermo Fisher Scientific) at 100V for 30 minutes. Fragments were excised from gel and purified by gel purification (Zymoclean™, D2004, Zymo Research, Irvine, CA). Plasmids were isolated from *E. coli* with Sigma GenElute Plasmid kit (Sigma-Aldrich) according to the supplier's manual. Yeast plasmids were isolated with Zymoprep Yeast Plasmid Miniprep II Kit (Zymo Research). *E. coli* DH5α (18258-012,

Life Technologies) was used for chemical transformation (T3001, Zymo Research) or for electroporation. Chemical transformation was done according to the supplier's instructions. Electrocompetent DH5 α cells were prepared according to Bio-Rad's protocol, with the exception that the cells were grown in LB medium without NaCl. Electroporation was done in a 2 mm cuvette (165-2086, BioRad, Hercules, CA) using a Gene PulserXcell Electroporation System (BioRad), following the manufacturer's protocol.

YEASTRICTION WEBTOOL

The tool is written in Javascript and based on the MEAN.io stack (MongoDB, Express, AngularJS and Node.js). The source code is available at <https://github.com/hillstuf/YeaStriction>. Genome and ORF sequences were downloaded from SGD (<http://www.yeastgenome.org>) in GFF and FASTA file format, respectively. ORFs, including their 1kb up- and downstream sequences were extracted and imported into YeaStriction, with the aid of an in-house script. YeaStriction extracts all possible Cas9 target sequences (20 basepairs followed by NGG) from a specified ORF and from its complementary strand. Subsequently, sequences containing 6 or more Ts are discarded as this can terminate transcription (21, 334). Target sequences are then tested for off-targets (an off-target is defined as a sequence with either the NGG or NAG PAM sequence and 17 or more nucleotides identical to the original 20 bp target sequence (126)) by matching the sequences against the reference genome using Bowtie (version 1) (179). If any off-target is found the original target sequence is discarded. In a next step, the AT content is calculated for the target sequence. Using the RNAfold library (essentially with the parameters `-MEA -noLP -temp=30.`) (196) the maximum expected accuracy structure of each RNA molecule is calculated. The target sequence is also searched for the presence of restriction sites based on a default list or a user-defined list. The targets can be ranked based on presence of restriction sites (1 for containing and 0 for lacking a restriction site), AT content (1 having the highest AT-content and 0 for the lowest AT-content) and secondary structure (1 having the lowest amount of pairing nucleotides and 0 for the highest number of nucleotides involved in secondary structures (indicated by brackets)). The range for every parameter is determined per locus and used to normalize the values. Subsequently, the target sequences are ranked by summation of the score for each parameter. These ranking scores should only be used to order the targets from a single locus and not to compare targets for different loci. The application can be accessed at the following URL: <http://yeastriction.tnw.tudelft.nl/>.

2.3 RESULTS AND DISCUSSION

2.3.1 *YeaStriction: a CRISPR design tool*

To streamline design and construction of CRISPR/Cas9 gRNA plasmids for introduction of (multiple) genetic modifications, the YeaStriction webtool (<http://yeastriction.tnw.tudelft.nl>) was developed. This webtool was designed to be compatible with the single and double gRNA plasmid series (pMEL10 – pMEL17 and pROS10 – pROS17, respectively), as described below. Because the CRISPR/Cas9 system can be highly sequence specific, it is crucially important to select target sequences based on correct reference genome sequence information. A difference of a single nucleotide in the gRNA, as compared to the genomic target sequence, can already completely abolish Cas9 nuclease activity (126). To make YeaStriction useful for the entire yeast community, a set of 33 *S. cerevisiae* genomes (www.yeastgenome.org) was implemented. In the first step, the user can select the desired reference genome and enter (multiple) systematic names

(e.g. *YDL054C*, *YKL221W*) or gene names (e.g. *MCH1*, *MCH2*). For each entered gene, the tool matches every potential target sequence to the selected reference genome. If there are potential off-targets (other sequences present in the same genome with either NAG or NGG as PAM sequence and with a 0 – 3 nucleotide difference in the 20 bp target sequence (126)) the target sequence is discarded. Sequences that contain 6 or more consecutive Ts are also discarded as they may cause transcript termination (21, 334). A recent report indicates that the AT content of Cas9 target sequences should preferably be above 65% (190). Furthermore, there are indications that target sequences without obvious nucleotide interactions in secondary structures are more efficient (347). The presence of unique restriction sites within the target sequence simplifies verification of correct plasmid assembly. Yeastriction therefore ranks potential Cas9 target sequences according to AT-content, secondary structures and the presence of restriction sites. To increase flexibility, the user can also choose to leave out one of the parameters in the final ranking. For the top-ranked target sequence, the tool automatically designs the oligonucleotide primers required for plasmid construction and the oligonucleotides (which can be ordered as primers) needed to form the repair fragment when a gene deletion is desired. To increase flexibility, the user can also choose another target site than the top-ranked sequence (Supplemental information).

2.3.2 Construction of a set of plasmids for transformation with one or two gRNAs

DiCarlo and co-workers (61) described construction of plasmid p426-SNR52p-gRNA.CAN1.Y-SUP4t (Addgene www.addgene.org/43803/) for expression of a single gRNA in yeast, using the *SNR52* promoter and *SUP4* terminator. We hypothesized that the gRNA could be easily changed by *in vivo* homologous recombination via co-transformation of the linearized p426-SNR52p-gRNA.CAN1.Y-SUP4t backbone (from which the 20 bp recognition sequence “CAN1.Y” was omitted) together with a new 20 bp gRNA fragment, flanked by 50 bp overlaps with the plasmid backbone. In order to further increase the flexibility of this system, and to allow its use with genetic markers other than *URA3*, a standardized set of plasmids was constructed (Figure 2.1B). To this end, a linearized plasmid backbone of the p426-SNR52p-gRNA.CAN1.Y-SUP4t plasmid that excluded the *URA3* marker gene, was obtained by PCR. Subsequently, eight different genetic markers (*KIURA3*, *amdSYM*, *hphNT1*, *kanMX*, *KILEU2*, *natNT2*, *HIS3* and *TRP1*) were PCR amplified and (re-)introduced in this backbone using Gibson assembly. The resulting plasmids were named pMEL10 to pMEL17 (Figure 2.1B, Table 2.2).

Use of *in vivo* recombination enabled the introduction of one gRNA sequence per single gRNA plasmid backbone (pMEL10 – pMEL17), without the need of prior cloning. When multiple genetic modifications are required, marker availability might become a limitation. In this case, plasmids containing multiple gRNA sequences would be preferred as this allows introduction of more genetic modifications before plasmid removal is required. For this purpose, a second set of plasmids was constructed that contained 2 gRNA sequences, between separate promoters and terminators.

First pROS10 was constructed (Figure 2.1C), containing the *ScURA3* marker, *ampR* for selection in *E. coli* and a 2µm fragment flanked by two pSNR52-gRNA-tSUP4 cassettes in

(a) Primer design + synthesis

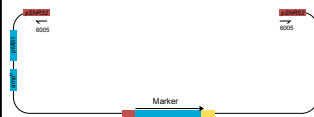
yeastriction.tnw.tudelft.nl



5 minutes + 3 days

PCR backbone

double gRNA method



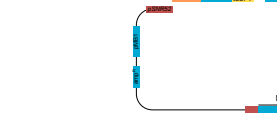
single gRNA method



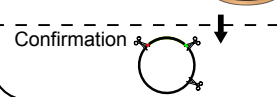
Plasmid construction

PCR 2 μ m fragment

Gibson Assembly

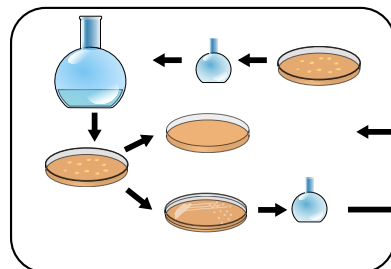


E. coli transformation



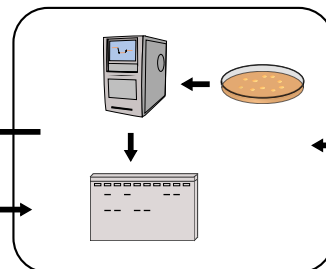
48 - 72h

Plasmid removal



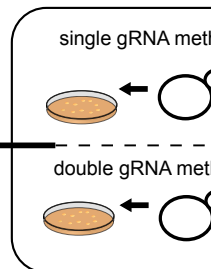
6 days

Confirmation



4h

Transformation



3 days

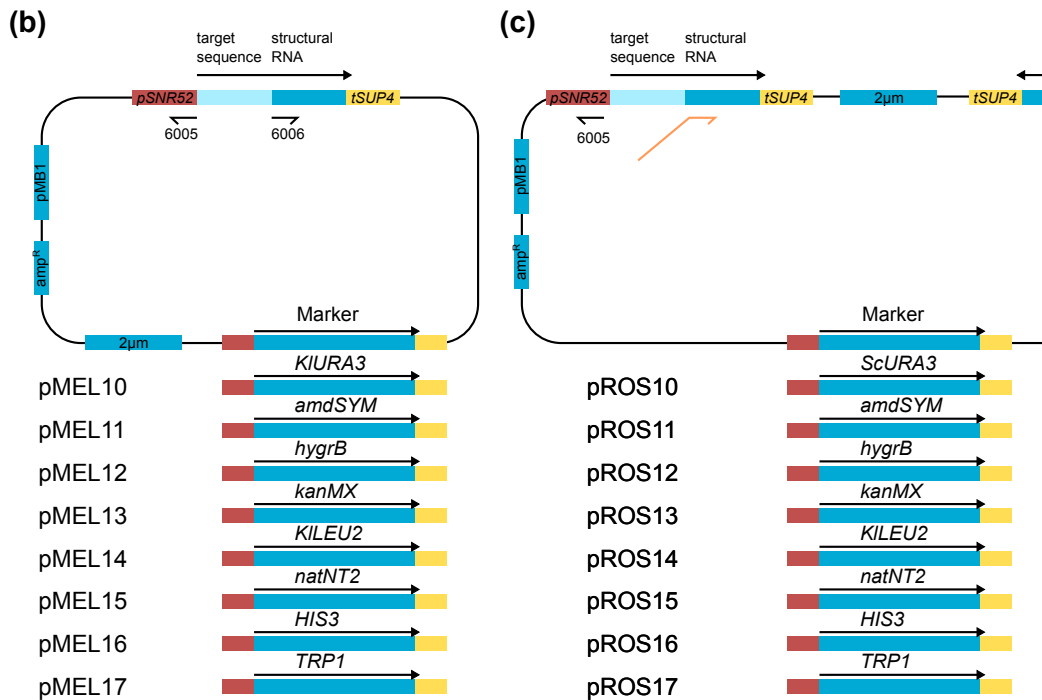


Figure 2.1. Workflow for CRISPR/Cas9 modification of *S. cerevisiae* genome using single and double gRNA plasmid series (pMEL10 to pMEL17). **(a)** All oligonucleotides, required for targeting the gene(s) of interest (GOI), can be automatically designed with YeaStriction (single gRNA method, the tool designs complementary oligonucleotides that can be annealed to form (i) a double stranded repair fragment which contains the target sequence for the GOI. For expression of the gRNA, a plasmid backbone containing the genetic marker of interest (pMEL10 – pMEL17). Gene deletion is achieved via co-transformation of the plasmid backbone, the dsDNA insert and the repair fragment. In the double gRNA method, YeaStriction designs two sets of oligonucleotides, the first oligonucleotide binds to the 2μm fragment and has a tail containing the GOI and a sequence identical to both sides of a linearized double gRNA plasmid backbone (pROS10 - pROS17), the second set of oligonucleotides binds to the target sequence. The target sequence is integrated into the genome, replacing a marker gene.

Figure 2.1 (continued from previous page) . To construct a gRNA plasmid with two target sequences, a double gRNA plasmid backbone with the appropriate marker (pROS10 – pROS17) is amplified by PCR, excluding the 2 μ m fragment. The 2 μ m fragment is amplified using the primers harbouring the targets for the GOIs and sequences identical to the plasmid backbone. The final plasmid is then constructed *in vitro* using the plasmid backbone and the 2 μ m fragment, e.g. with Gibson assembly. After confirmation of correct plasmid assembly using restriction analysis or PCR, the resulting plasmid is transformed to yeast, together with the appropriate 120 bp dsDNA repair fragment(s). After transformation the desired genetic modification(s) are checked by PCR, Southern blot analysis or sequencing. Subsequently, the strain can be modified again in a new round of transformation. Before physiological analysis, the gRNA plasmid(s) are preferably removed. This can be done by growing the strains in liquid media without selection pressure or, if possible, by counter-selection pressure (with 5-fluoroorotic acid, fluoroacetamide or 5-fluoroanthranilic acid for pMEL10+pROS10 plasmids, pMEL11+pROS11 plasmids and pMEL17+pROS17 plasmids, respectively). After confirming plasmid removal by restreaking the same colony on selective and non-selective medium and/or PCR analysis, the resulting strain is re-grown in liquid medium and stored at -80 °C. **(b)** Architecture of the single gRNA plasmid series (pMEL10 – pMEL17). The primers used for PCR amplification of the plasmid backbone are indicated by black arrows. **(c)** Architecture of the double gRNA plasmid series (pROS10 – pROS17) with two gRNA cassettes. The plasmid backbone can be PCR amplified with a single primer (indicated with a black arrow). The 2 μ m fragment is amplified with primers designed using Yeastriktion (indicated in orange and light green coloured arrows).

opposite directions, with one of these cassettes containing the target sequence *CAN1.Y* and the other *ADE2.Y* (61). This design enables construction of plasmids that target other loci, by first PCR-amplifying the 2 μ m fragment, using primers that incorporate the new target sites, followed by assembly into a linearized backbone that contains the desired marker gene via an *in vitro* method such as Gibson assembly. To generate plasmids with marker genes other than *URA3*, the backbone of pROS10 was first digested with restriction enzymes to remove the *ScURA3* marker. Subsequently, other markers were PCR amplified and inserted using Gibson assembly. This yielded plasmids pROS11 to pROS17 (Figure 2.1C, Table 2.2), which contained the marker genes *amdSYM*, *hphNT1*, *kanMX*, *KILEU2*, *natNT2*, *HIS3* and *TRP1*, respectively. Both plasmid series (pMEL10 – pMEL17 and pROS10 – pROS17) have been made available through EUROSCARF.

2.3.3 Construction of various *cas9* expressing CEN.PK strains

In the *cas9* bearing strains described by DiCarlo and co-workers (61), a centromeric plasmid was used to express *cas9*, either from a variant of the inducible *GAL1* promoter or from the constitutive *TEF1* promoter. When multiple rounds of transformation and gRNA plasmid removal are desired, a stable integrated copy of *cas9* is preferred, since this allows growth of strains on complex medium, which enables faster growth and efficient plasmid recycling. To this end, a *cas9* gene under the control of the *TEF1* promoter was integrated into the *CAN1* locus together with the *natNT2* marker. In order to increase the flexibility of the CRISPR/Cas9 system, *cas9* was integrated in the haploid strains CEN.PK113-7D and CEN.PK113-5D (Ura⁻) and the diploid strains CEN.PK122 and CEN.PK115 (Ura⁻). Additionally, *cas9* was integrated in the quadruple auxotrophic strain CEN.PK2-1C (Ura⁻, Leu⁻, Trp⁻, His⁻), resulting in strain IMX672, which was used to test the efficiencies of the gRNA plasmids developed in this study. All these strains are deposited at EUROSCARF. Constitutive expression of *cas9* in CEN.PK113-7D (IMX585)

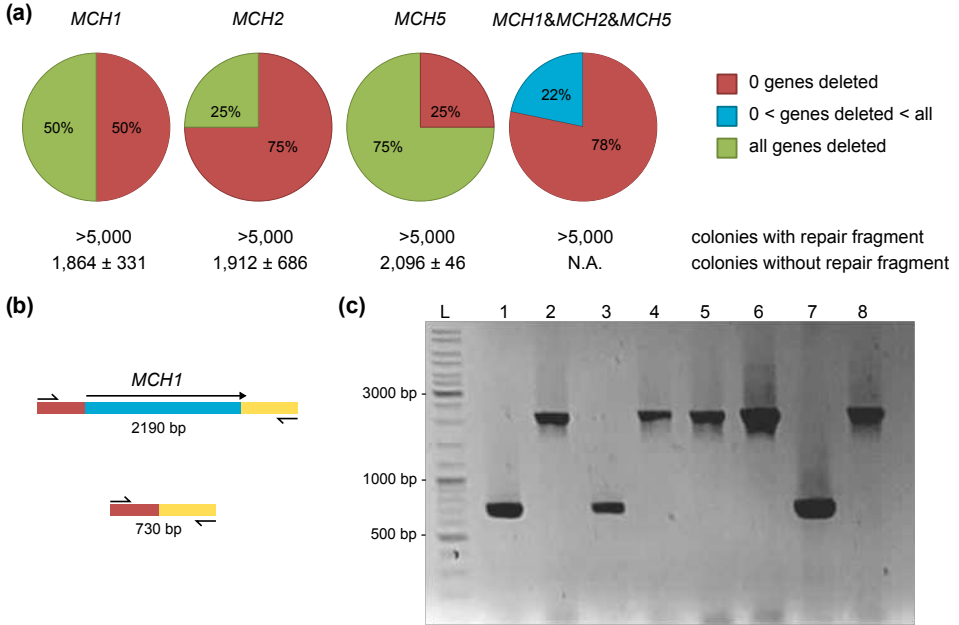


Figure 2.2. Efficiency of gene deletion obtained after transformation with a single gRNA plasmid. **(a)** Quantification of the number of colonies and corresponding gene deletion efficiencies, obtained after transformation of *S. cerevisiae* IMX672 (*ura3-52 trp1-289 leu2-3,112 his3Δ, can1Δ::cas9*) with 100 ng pMEL10 backbone, 300 ng of gRNA insert DNA and 2 μg of the corresponding 120 bp dsDNA repair fragment. The transformation targeting *MCH1*, *MCH2* and *MCH5* simultaneously was performed using 300 ng of each insert and 2 μg of each repair fragment. For the transformations with repair fragments, the exact number of transformants could not be determined, but exceeded 5,000 colonies per plate. The data represent average and standard deviation of transformants of three independent transformation experiments. The estimated total number of colonies carrying gene deletions was based on colony PCR results of 24 randomly picked colonies. In red: percentage of colonies without gene deletions, in blue: percentage of colonies containing one or two but not all deletions, green: percentage of colonies containing all desired gene deletions. No transformants with all three genes deleted were identified. **(b)** Diagnostic primers were designed outside of the target ORFs to differentiate between successful and non-successful colonies via PCR. In this colony PCR example, primers 6862 & 6863 were used to amplify the *MCH1* locus. **(c)** Example of a diagnostic gel from the transformation targeting the *MCH1* locus. The first lane (L) contains the GeneRuler DNA Ladder Mix. Lane 1 to 8 show the PCR results of 8 randomly picked colonies. Successful deletion of *MCH1* results in a PCR fragment with a length of 729 bp (lane 1, 3 and 7), when *MCH1* is still present a band is observed at 2190 bp (lane 2, 4, 5, 6 and 8).

did not significantly affect the maximum specific growth rate. IMX585 grew at $0.37 \pm 0.003 \text{ h}^{-1}$ (value and mean deviation are based on two independent experiments) on glucose synthetic medium in shake-flask cultures while the growth rate of the reference CEN.PK113-7D was of $0.39 \pm 0.01 \text{ h}^{-1}$.

2.3.4 Seamless and markerless gene deletion using in vivo assembled plasmids containing single gRNAs

The first plasmid series, pMEL10 – pMEL17, was designed to perform gene deletions from plasmids assembled *in vivo*, harnessing the high frequency and fidelity of homolo-

gous recombination in *S. cerevisiae* (172, 175, 226, 227) and obviating the need for prior cloning of the gRNA sequence. To test whether *in vivo* assembly of a plasmid carrying the gRNA sequence could be combined with CRISPR-mediated genetic modification, a plasmid backbone and insert containing the gRNA of choice were co-transformed with a 120 bp “repair fragment” for markerless and scarless gene deletion. The gRNA sequence targeting the gene *MCH1* (Table 2.3) was selected based on a high score (AT content 0.65, RNA score 0.50) in YeaStriction and contained 50 bp overlaps to each side of the linearized plasmid backbone with the *KIURA3* marker, facilitating homologous recombination. Transformation of IMX672 (*ura3-52 trp1-289 leu2-3,112 his3Δ can1Δ::cas9*) resulted in >5,000 colonies per plate and colony PCR was performed to confirm successful gene deletion. Out of 24 randomly tested colonies, 12 (50%) showed the intended single gene deletion of *MCH1* (Figure 2.2). The colonies that did not show the intended deletion could be caused by misassembly of the plasmid, as omitting either the insert or the repair fragment from the transformation mixture yielded ~2,000 colonies. To test whether these results could be reproduced when different loci were targeted, the same strategy was employed to target *MCH2* and *MCH5*. A gRNA recognition sequence was selected for each gene using YeaStriction, based on a low score for *MCH2* (AT content 0.45, RNA score 0.30) and a high score for *MCH5* (AT content 0.65, RNA score 0.50) targeting sequence respectively. Transformation with gRNA inserts targeting either of these loci and the corresponding repair fragments resulted in similar colony counts as observed for *MCH1*. Furthermore, colony PCR determined successful deletions for both loci at varying efficiencies, 25% and 75% for *MCH2* and *MCH5* respectively (Figure 2.2). This observed difference in deletion efficiency was in line with the targeted site quality scores predicted by YeaStriction for *MCH2* and *MCH5* selected gRNAs. This cloning-free approach might be extended to enable co-transformation of multiple gRNA inserts and their corresponding repair fragments. By assembly of multiple plasmids bearing different gRNA sequences in a single cell, this might facilitate the simultaneous introduction of multiple gene deletions. To test this possibility, the same plasmid backbone, containing the *KIURA3* marker, was co-transformed with three different gRNA fragments (*MCH1*, *MCH2* & *MCH5*) and their corresponding repair fragments. Over 5,000 colonies were obtained after transformation and 24 randomly picked colonies were tested via colony PCR. Transformation with three inserts led to the identification of 4 mutants containing a single and 1 mutant containing a double deletion (24 colonies tested, Figure 2.2A) but none with three deletions. Only one of the 6 identified deletions was found in the *MCH1* locus (targeted by a gRNA with a low YeaStriction score, Table 2.3), while three and two deletions corresponded to ORFs of *MCH1* and *MCH5* respectively. These results indicated that mutants containing multiple gene deletions could be obtained via combined *in vivo* recombination and gene disruption, although at low (~4%) efficiencies. This low efficiency of multiple gene disruption might have several reasons (i) it can be the result of misassembly of the plasmid, as transformation of the backbone without insert or repair oligo already resulted in ~2,000 colonies when making single deletions (ii) a cell does not need to assemble all three plasmids, as one plasmid is enough to restore prototrophy and (iii) errors present in the gRNA inserts affecting its targeting efficiency. Indeed, sequencing of *in vivo* assembled plasmids of three false positive colonies, showed that the gRNA sequence contained nucleotidic insertions and deletions, impairing Cas9

Table 2.3. Target sequences used in this study

Locus	Sequence (including PAM)	Restriction site	AT score	RNA score
<i>MCH1</i>	TATTGGCAATAAACATCTCGAGG		0.65	0.55
<i>MCH2</i>	ATCTCGATCGAGGTGCCTGATGG	PvuI	0.45	0.30
<i>MCH5</i>	ACTCTTCGGTTTTAGATATCTGG	EcoRV	0.65	0.60
<i>AQY1</i>	ACCATCGCTTTAAATCTCTAGG	DraI	0.65	0.50
<i>ITR1</i>	ATACATCAACGAATTCCAACCGG	EcoRI	0.65	0.60
<i>PDR12</i>	GCATTTTCGGTACCTAACTCCGG	KpnI	0.55	0.60
<i>NAT1</i>	AAAGGAATTGGATCCTGCGTAGG	BamHI	0.55	0.60
<i>GET4</i>	GGGCTCGCTAGGATCCAATTCGG	BamHI	0.45	0.50
<i>ACS1</i>	TTCTTCACAGCTGGAGACATTGG	PvuII	0.55	0.45
<i>ACS2</i>	TCCTTGCCGTAAATCACCATGG		0.55	0.80

restriction in the target ORF. These mutations of the gRNA sequence likely derived from imperfect annealing of the two complementary oligonucleotide used to form the *in vivo* assembled gRNA fragment.

All collectively these results showed that single gene deletions could be easily performed by this method, however when more than one locus has to be altered a more effective strategy is needed as is detailed in the next section.

2.3.5 Multiplexing seamless gene deletions using *in vitro* assembled plasmids containing two gRNAs

While *in vivo* assembly of the gRNA plasmid and CRISPR-assisted genetic modification can be combined in a single transformation, the relatively high incidence of false positive colonies limits use of this system for simultaneous introduction of multiple chromosomal modifications. Since some of the false positives could be the result of misassembly of the gRNA containing plasmid, it was expected that pre-assembly of the plasmid using *in vitro* Gibson assembly would result in a lower number of false positives. Therefore, a double gRNA plasmid was constructed, expressing guideRNAs designed to target *ITR1* and *PDR12*. First, the pROS10 backbone and the 2 μ m fragment flanked by the gRNAs containing the target sequences for *ITR1* and *PDR12* were amplified using PCR (Figure 2.1). The resulting DNA fragments were assembled and the plasmid (pUDR005) was verified by digestion with restriction enzymes specifically targeting the *ITR1* and *PDR12* target sequences (Table 2.3). Co-transformation of the resulting plasmid with the corresponding repair fragments into the *cas9* expressing strain IMX672 yielded 900 colonies per plate. In contrast, a single transformation in which repair fragments were omitted yielded only two colonies. 24 Colonies were randomly picked and PCR verification determined that all of these contained both gene disruptions (IMX715, Figure 2.3). The transformation of an already assembled plasmid might enable immediate transcription of the gRNA, while the other method required assembly of a correct plasmid prior to transcription of the gRNA. This might explain the significantly higher observed efficiency of this approach compared to the method using *in vivo* assembled plasmids. Most likely, pre-assembly and confirmation of the plasmid containing two gRNAs greatly reduces the number of false positives.

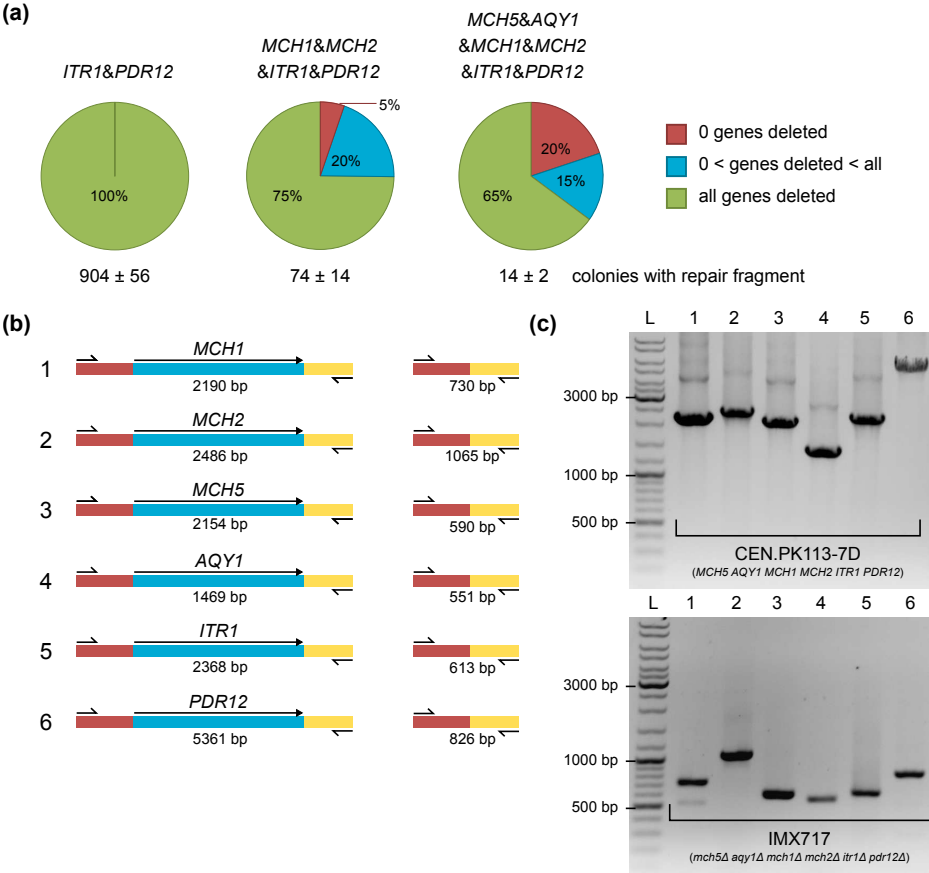


Figure 2.3. Efficiency of gene deletion obtained after transformation with double gRNA plasmids. **(a)** Quantification of the number of colonies and corresponding gene deletion efficiencies after transformation of *S. cerevisiae* IMX672 (*ura3-52 trp1-289 leu2-3,112 his3Δ, can1Δ::cas9*) with 2 μg of various double gRNA plasmids with 1 μg of the appropriate repair fragment(s). When multiple plasmids were transformed simultaneously, 2 μg of each plasmid was added. The data represent average and standard deviation of transformants of three independent transformation experiments. In red: percentage of colonies containing no gene deletions, in blue: percentage of colonies containing some but not all targeted gene deletions (1, 1-3 and 1-5 respectively), in green: percentage of colonies containing all targeted simultaneous gene deletions (2, 4 and 6 respectively). **(b)** Diagnostic primers were designed outside of the target ORFs to differentiate between successful and non-successful colonies via PCR. In this colony PCR example, primers 6862 & 6863, 6864 & 6865, 6866 & 6867, 6868 & 6870, 6869 & 6870 and 253 & 3998, were used to amplify the *MCH1*, *MCH2*, *MCH5*, *AQY1*, *ITR1* and *PDR12* loci respectively. The expected sizes of the PCR products obtained when the gene is present (left) or deleted (right) are indicated. **(c)** Example of a diagnostic gel from the transformation introducing 6 simultaneous gene deletions, resulting in IMX717. The first lane (L) contains the GeneRuler DNA Ladder Mix. Lane 1 to 6 show the PCR results of the reference strain CEN.PK113-7D (top) and a randomly picked colony of IMX717 (bottom) with primers 6862 & 6863 for *MCH1* (lane 1), 6864 & 6865 for *MCH2* (lane 2), 6866 & 6867 for *MCH5* (lane 3), 6868 & 5593 for *AQY1* (lane 4), 6869 & 6870 *ITR1* (lane 5) and 253 & 3998 for *PDR12* (lane 6).

Encouraged by these extremely high efficiencies, transformations were performed using multiple plasmids that carried different genetic markers. To this end, two new plasmids were constructed, each targeting two different genetic loci (*MCH1/MCH2* (pUDR002) and *MCH5/AQY1* (pUDR004)). Two and three plasmids were co-transformed, containing either the *KIURA3* and *TRP1* or the *KIURA3*, *TRP1* and *HIS3* selectable markers. In contrast to the transformations with a single plasmid, which yielded over 900 colonies, only 74 colonies and 14 colonies were obtained when transforming two and three plasmids, respectively. These lower numbers of colonies might reflect the decreasing probability that a single cell successfully takes up multiple plasmids and, subsequently, performs the corresponding gene deletions. The characterization of the colonies from the transformation with two plasmids revealed that out of the 20 tested clones, 14 (70%) harboured all 4 deletions (IMX716). Similarly, out of 20 randomly tested colonies obtained from the transformation with 3 plasmids, 13 (65%) clones contained all 6 deletions (IMX717, Figure 2.3).

These results unequivocally demonstrate the efficiency of CRISPR/Cas9 mediated genetic modification of yeast in simultaneously generating multiple deletions in a single transformation step. Recently, CRISPR/Cas9 was successfully applied to simultaneously disrupt all homozygous alleles in the polyploid ATCC4124 strain. In four transformation iterations a quadruple *ura3 trp1 leu2 his3* auxotrophic strain was constructed (348). A design similar to the native polycistronic CRISPR array consisting of a tracrRNA and crRNA instead of the chimeric gRNA was used to achieve three concurrent deletions using a single crRNA array (8). To the best of our knowledge, the present study is the first to demonstrate generation of a sextuple deletion strain of *S. cerevisiae* in a single transformation event.

2.3.6 Multiplexing deletion, multi-gene integration and introduction of single nucleotide mutations

Hitherto, reported applications of CRISPR/Cas9 in *S. cerevisiae* focused on gene inactivation. I-SceI-mediated introduction of double-stranded breaks has previously been shown to facilitate simultaneous integration of several gene expression cassettes at chromosomal loci (171). To explore the potential of CRISPR to combine gene deletion with the simultaneous *in vivo* assembly and chromosomal integration of multiple DNA fragments, we attempted to construct an *S. cerevisiae* strain with a double *ACS1 ACS2* deletion that also overexpresses the *Enterococcus faecalis* pyruvate dehydrogenase (PDH) complex (167) in a single transformation. To this end, IMX585 was transformed with a plasmid expressing the gRNAs targeting the ACS genes (pUDR022). A 120 bp repair fragment was co-transformed for the deletion of *ACS1* and the ORF of *ACS2* was replaced via integration of six gene cassettes expressing the genes of the E1 α , E1 β , E2 and E3 subunits of *Enterococcus faecalis* PDH encoded by *pdhA*, *pdhB*, *aceF*, and *lpd*, as well as the *lplA* and *lplA2* genes required for PDH lipoylation (167) (Figure 2.4A). Cytosolic acetyl-CoA is essential and a double *acs1 Δ acs2 Δ* mutant is not viable (13) unless acetyl-CoA is provided by an alternative route (166, 167). The transformation targeting the two ACS genes yielded 11 colonies, with 10 out of 10 picked colonies showing the desired

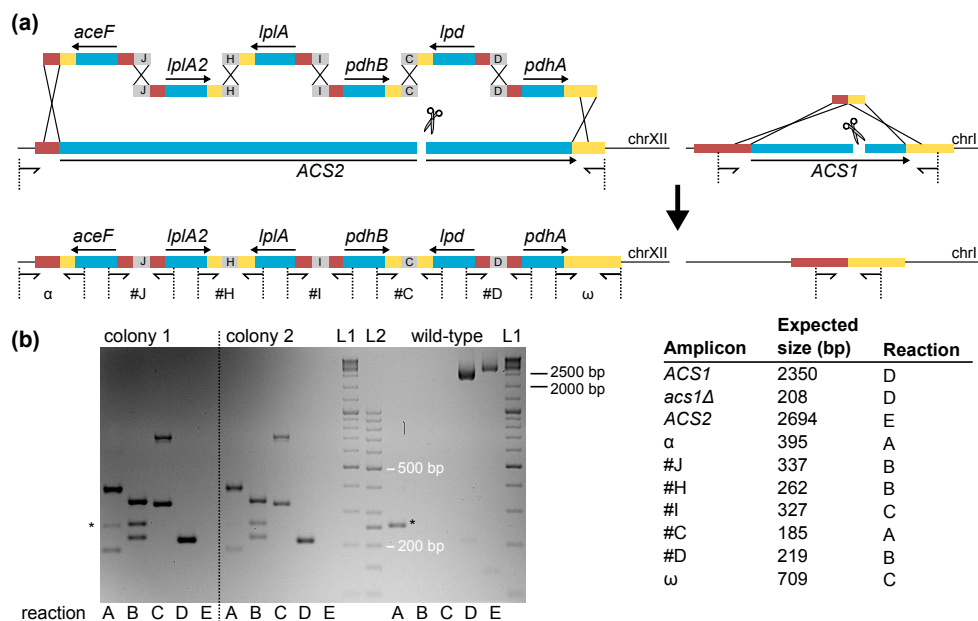


Figure 2.4. Multiplexing CRISPR/Cas9 in *S. cerevisiae*. (a) Chromosomal integration of the six genes required for expression of a functional *Enterococcus faecalis* pyruvate dehydrogenase complex in the yeast cytosol. All six genes are flanked by 60 bp sequences enabling homologous recombination (indicated with black crosses). The first and the last fragments are homologous to 60 bp just up- and downstream of the *ACS2* ORF, respectively, thus enabling repair of the Cas9-induced double strand break by homologous recombination (left panel). Deletion of *ACS1* using a 120 bp dsDNA repair fragment is shown in the right panel. (b) Multiplex colony PCR was performed on ten transformants to check their genotypes. Results are shown for two representative colonies, confirming the intended genotype. The PCR on the wild-type strain shows the predicted bands for the presence of the wild-type *ACS1* and *ACS2* alleles. Two DNA ladders were used; L1 refers to the GeneRuler DNA ladder (Thermo Scientific) and L2 to the GeneRuler 50 bp DNA ladder (Thermo Scientific). (The bands indicated with an asterisk reflect aspecific PCR products)

genotype (Figure 2.4B). From one colony, the gRNA plasmid was removed by growing on non-selective YP medium, yielding strain IMX719. This strain showed only growth on synthetic medium with 2% glucose and lipoate and failed to grow on synthetic medium with 2% glucose and on YP with 2% ethanol. This phenotype is entirely consistent with the phenotype reported by Kozak *et al.* (167) for an *acs1 acs2* strain of *S. cerevisiae* that expresses the *E. faecalis* PDH subunits and lipoylation genes, thereby further confirming the genotype of the strain IMX719.

To explore the potential of CRISPR/Cas9 to introduce specific single-nucleotide mutations in genomic DNA, a plasmid was constructed with gRNAs targeting the *GET4* and *NAT1* loci (pUDR020). Both of the target sequences contained a BamHI (G|GATCC) restriction site. The corresponding repair oligonucleotides were designed to introduce a single-nucleotide change in the genomic target sequence, which at both sites resulted in the introduction of a restriction site for EcoRI (G|AATTC) and simultaneously disrupted the BamHI restriction site (Figure 2.5A). Transformation of the *cas9* bearing strain IMX672 with pUDR020 (*NAT1* and *GET4* gRNA, *KIURA3*) and the corresponding repair

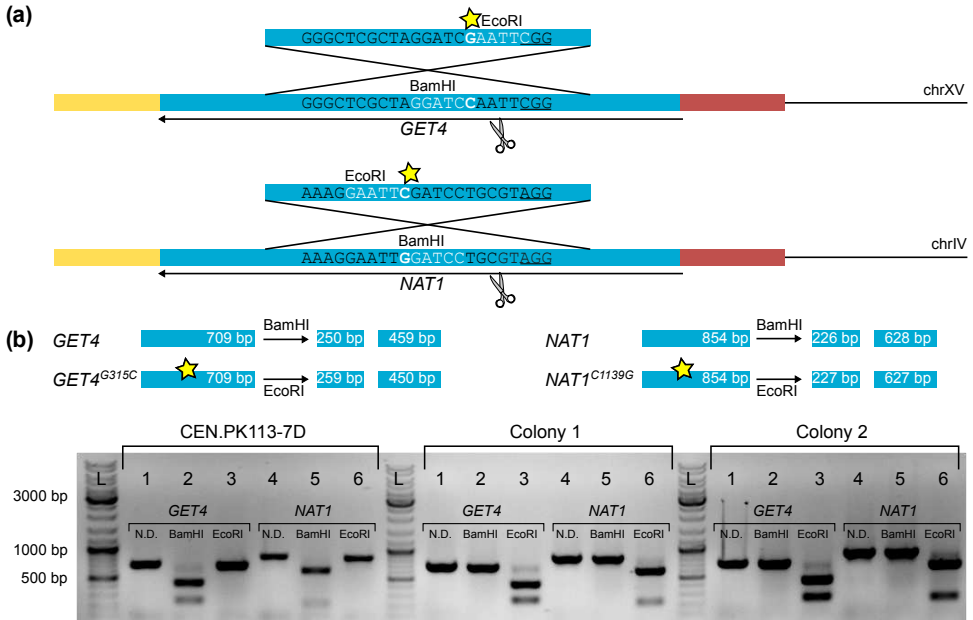


Figure 2.5. Simultaneous introduction of different single-nucleotide mutations in *S. cerevisiae*. **(a)** Transformation of IMX581 (*ura3-52, can1Δ::CAS9*) was performed with pUDR020, resulting in the introduction of two mutations in *NAT1* and *GET4*. Underlined: the protospacer adjacent motif (PAM) sequences associated with the gRNA targets. In white: restriction sites present in the original gRNA targeting sequence (BamHI) and in the repair fragment used to correct the double strand break (EcoRI). **(b)** Introduction of the double strand break and subsequent repair using the mutagenic repair fragment resulted in a change of restriction site from BamHI to EcoRI. In this colony PCR example, primers 7030 & 7031 and 7036 & 7037 were used to amplify a part of the *GET4* and *NAT1* locus (lane 1 and 4 respectively) from CEN.PK113-7D and two colonies of IMX581, transformed with pUDR020 and mutagenic repair fragments. In lanes labelled 2 and 5: digestion of the PCR fragments with BamHI, which only results in digestion fragments of sizes 250 bp + 459 bp and 226 bp and 628 bp when the original restriction sites in *GET4* and *NAT1* are still present (CEN.PK113-7D). In lanes labelled 3 and 6: digestion of the PCR fragments with EcoRI, which only results in digestion fragments of sizes 259 bp + 450 bp and 227 bp and 627 bp when this new restriction site has been introduced via the mutagenic repair fragment (Colony 1 and 2).

fragments resulted in ~1,500 colonies, while omitting both repair fragments did not result in any colonies. Eight colonies were randomly picked and a part of the ORF containing the target sequence was PCR amplified for both *GET4* and *NAT1*. Digestion of the amplified PCR product with BamHI and EcoRI, followed by gel electrophoresis showed that four of the eight colonies contained both mutations after transformation (Figure 2.5B). To confirm whether these four colonies indeed contained the desired mutations, a fragment of 120 bp around the target site was sequenced. All colonies contained the desired mutations, although two of the four colonies also showed additional, undesired, mutations at the *GET4* locus (Table S2.2 and S2.3, colony 2 and 4). Although these results show that one mutation can already abolish restriction, Cas9 induced DSBs might still occur, as long as the gRNA cassette is expressed. We therefore advise to (re)sequence mutated sites after gRNA plasmid removal and/or use the two step strategy discussed below.

The ease with which specific single-nucleotide mutations can be simultaneously introduced, makes the CRISPR/Cas9 system a highly valuable tool for analysing the biological significance of mutations identified by whole genome resequencing of strains obtained by mutagenesis (e.g. UV, X-rays) (143) or evolutionary engineering (35, 100, 124, 229). Reverse engineering of such mutations essentially encompasses restoration of the reference nucleotide in the mutant strain and/or introduction of the mutated nucleotide position in a naïve (non-mutated or non-evolved) genetic background. Even laboratory evolution experiments performed in the absence of mutagenesis typically yield multiple mutations, not all of which contribute to the phenotype of interest (see e.g. (100, 164)). Therefore availability of methods that enabled reintroduction of multiple point mutations at various genomic loci is invaluable for rapid identification of relevant mutations. Similar to the YOG (Yeast Oligo-Mediated Genome Engineering) method (60), the CRISPR approach enables multiplexing and offers flexibility. In contrast to the YOG method, which requires a specific background (*mlh1Δ msh2Δ RAD51^{K342E}↑ RAD54↑*) (60), the CRISPR approach should be applicable to any *S. cerevisiae* strain background that expresses a functional *cas9* gene. The two examples used in this study (*GET4* and *NAT1*) were designed for easy verification. If the desired point mutation is not present in a suitable target sequence, it may be possible to introduce (multiple) Single Nucleotide Variation(s) (SNV) in two rounds of CRISPR/Cas9 mediated genome modification. In the first round, a larger part surrounding one or several SNVs could be deleted while repairing the DSBs with repair fragments that contain a generic synthetic target sequence. In a second round, these generic target sequences can then be cut by Cas9, combined with the repair of the DSBs with 120 bp sequences that contain the desired SNVs.

2.4 OUTLOOK

The use of homologous recombination for the assembly of multi-gene constructs (96, 279) had a tremendous impact on genetic engineering strategies (3, 34). Even before the advent of CRISPR/Cas9 these developments have immensely decreased strain construction time in our group and enabled us to express complicated multi-step pathways and multi-component enzymes (10, 105, 165, 167, 171). Until recently the deletion of multiple genes and insertions at multiple loci remained a cumbersome and time-intensive process. Here, building on the pioneering conceptual proof of CRISPR functionality in lower eukaryotes (61), we show that CRISPR/Cas9 will further improve and accelerate yeast strain construction, not only by allowing multiplexing gene deletions (61, 348) but also by allowing simultaneous introduction of gene deletions, chromosomal integration of multi-gene constructs and the introduction of specific mutations. Although it is difficult to quantify the impact on the overall time requirements for complex pathway engineering, the examples presented here suggest that a three to four-fold acceleration is unlikely to be exaggerated.

This paper focuses on *S. cerevisiae*, a microbial species that is already known for its easy genetic accessibility. Therefore, it is logical to speculate that this methodology should have an even higher impact on species of yeasts and filamentous fungi that are notoriously more difficult to alter genetically. Indeed, a very recent example described the

benefit of the introduction of CRISPR/Cas9 in *Schizosaccharomyces pombe* (137). While the methodology reported in this study streamlines the use of CRISPR in *S. cerevisiae*, the method can be further improved. The RNA polymerase III dependent promoter *SNR52* is not a broadly recognized promoter (265). Recently, it has been shown that guideRNAs, flanked by the hammerhead and hepatitis delta virus ribozymes, can be expressed using polymerase II promoters (93). A promising promoter would then be the *TEF1* promoter from *Blasotobotrys adenivorans* (309) as this is a strong, constitutive promoter, recognized in different species, like *S. cerevisiae*, *Hansenula polymorpha* and *Pichia pastoris*.

We hope that by providing the easy-to-use Yeastriction design tool, two versatile plasmid series for gRNA expression, a set of *S. cerevisiae* CEN.PK strains harbouring the *cas9* expression cassette and standardized protocols (Supplemental information), this paper will help colleagues to facilitate and accelerate yeast strain engineering.

2.5 ACKNOWLEDGEMENTS

We thank James Dykstra for the construction of IMX719 and Arthur Dobbe for sharing the growth rates of IMX585. PDL and NK were financially supported by the Technology Foundation STW (Vidi Grant 10776). HMvR, RM, AJAvM, JTP and JMD were supported by the BE-Basic R&D Program, which was granted an FES subsidy from the Dutch Ministry of Economic Affairs, Agriculture and Innovation (EL&I).

SUPPLEMENTARY MATERIALS

Note

2

For the protocols and Yeaststriction tutorial see <http://femsyr.oxfordjournals.org/content/-suppl/2015/03/04/fov004.DC1>

Table S2.1. Primers used in this study.

Number	Name	Sequence 5' → 3'
cas9 integration		
2873	CAN1DelcassFW	TCAGACTTCTTAACCTCCTGTAAAAACAAAAAAAAA AAAAGGCATAGCAATAAGCTGGAGCTCATAGCTTC
3093	tagA-pUG	ACTATATGTGAAGGCATGGCTATGGCACGGCAGAC ATTCCGCCAGATCATCAATAGGCACCTTCGTACGC TGCAGGTCGAC
4653	A-CYC1t-rv	GTGCCTATTGATGATCTGGCGGAATGTCTGCCGTG CCATAGCCATGCCTTCACATATAGTCCGCAAATTA AAGCCTTCGAG
5542	CAN1 KO rv	CTATGCTACAACATTCCAAAATTTGTCCCAAAAAG TCTTTGGTTCATGATCTTCCCATACGCATAGGCCA CTAGTGGATCTG
cas9 integration confirmation		
5829	CAN1 cut rv	AGAAGAGTGGTTGCGAACAGAG
2673	m-PCR-HR4-RV	TGAAGTGGTACGGCGATGC
2668	m-PCR-HR2-FW	ACGCGTGACGCATGTAAC
9	KanA	CGCACGTCAAGACTGTCAAG
2620	Nat Ctrl Fw	GCCGAGCAAATGCCTGCAAATC
2615	Can1RV	GAAATGGCGTGGGAATGTGA
Construction pMEL series		
3093	tagA-pUG	ACTATATGTGAAGGCATGGCTATGGCACGGCAGAC ATTCCGCCAGATCATCAATAGGCACCTTCGTACGC TGCAGGTCGAC
3096	tagB-pUG	GTTGAACATTCTTAGGCTGGTCTGAATCATTTAGAC ACGGGCATCGTCCTCTCGAAAGGTGGCATAGGCCA CTAGTGGATCTG
6845	p426 cRNA-rv A	GTGCCTATTGATGATCTGGCGGAATGTCTGCCGTG CCATAGCCATGCCTTCACATATAGTACAGGCAACA CGCAGATATAGG
6846	p426 cRNA-fw B	CACCTTTCGAGAGGACGATGCCCGTGTCTAAATGA TTCGACCAGCCTAAGAATGTTCAACGGCCCACTAC GTGAACCATC
6847	pRS Marker fw A	ACTATATGTGAAGGCATGGCTATGGCACGGCAGAC ATTCCGCCAGATCATCAATAGGCACTGCGGCATCA GAGCAGATTG
6848	pRS Marker rv B	GTTGAACATTCTTAGGCTGGTCTGAATCATTTAGAC ACGGGCATCGTCCTCTCGAAAGGTGCATCTGTGCG GTATTTACACC

Number	Name	Sequence 5' → 3'
Construction pROS series		
5972	tSUP4 rv ol 2mu-5*	GTTCTACAAAATGAAGCACAGATGCTTCGTTGGAG GGCGTGAACGTAAG
5974	2mu inside fw	TACTTTTGAGCAATGTTTGTGGA
5975	2mu inside rv	AACGAGCTACTAAAAATTGCGAA
6007	struct-guideRNA ADE2.y (ol pSNR52)	GTGCGCATGTTTCGGCGTTCGAACTTCTCCGCAG TGAAAGATAAATGATCACTTGAAGATTCTTTAGTG TGTTTTAGAGCTAGAAATAGCAAGTTAAAATAAG
6008	struct-guideRNA CAN1.y (ol pSNR52)	GTGCGCATGTTTCGGCGTTCGAACTTCTCCGCAG TGAAAGATAAATGATCGATACGTTCTCTATGGAGG AGTTTTAGAGCTAGAAATAGCAAGTTAAAATAAG
3289	Fus Tag F fw	CATACGTTGAAACTACGGCAAAGG
4692	Fus Tag G rv	AAGGGCCATGACCACCTG
5976	pSNR52 fw ol tag I-2	GCCTACGGTTCGCCAAGTATGCTGCTGATGTCTGG CTATACCTATCCGTCTACGTGAATACCCTCACTAA AGGGAACAAAAAG
5977	pSNR52 fw ol tag B	CACCTTTCGAGAGGACGATGCCCGTGTCTAAATGA TTCGACCAGCCTAAGAAATGTTCAACCCCTCACTAA AGGGAACAAAAAG
5973	tSUP4 rv ol 2mu 3*	GGCATAGTGC GTGTTTATGCTTAAATGCGTGGAGG GCGTGAACGTAAG
5975	2mu inside rv	AACGAGCTACTAAAAATTGCGAA
4068	Nic1 amp Fwd	GCCTACGGTTCGCCAAGTATGC
5974	2mu inside fw	TACTTTTGAGCAATGTTTGTGGA
3841	for f3h	CACCTTTCGAGAGGACGATG
3847	FUS Tag A fw	ACTATATGTGAAGGCATGGCTATGG
3276	Fus Tag B-rv	GTTGAACATTCTTAGGCTGGTCAATC
3274	Fus Tag I-fw	TATTCACGTAGACGGATAGGTATAGC
3275	Fus Tag A-rv	GTGCCTATTGATGATCTGGCGGAATG
5793	pCAS9 rv	GATCATTTATCTTTCACTGCGGAG
Construction PDH cassettes		
5654	D_FW_E1a	GAATTCACGCATCTACGACTG
7426	tTEF1_yeast ol tACS2	GAAAAATAGAAAACAGAAAAGGAGCGAAAATTTTATC TCATTACGAAAATTTTCTCATTTAAGGAGGCACTA TTACTGATGTGATTTT
3277	Fus Tag C rv	CTAGCGTGTCTCGCATAGTTCTTAGATTG
7338	pTDH3 fw ol tag I	TATTCACGTAGACGGATAGGTATAGCCAGACATCA GCAGCATACTTCGGGAACCGTAGGCATAAAAAACA CGCTTTTTTCAGTTTCG
3284	Fus Tag J rv	CGACGAGATGCTCAGACTATGTGTTC
7356	tPGI1 ol pACS2	GGTTAGTGATTGTTATACAAACAGAAATACAGGA AAGTAAATCAATACAATAATAAAATTAATTTTTTAA AATTTTTACTTTTCGCGAC
5653	D_RV_E3	AAGCTTAATCACTCTCCATACAGGG
3283	Fus Tag C fw	ACGTCTCACGGATCGTATATGC
5661	I_RV_LLLA1	TCTAGAGCCTACGGTTCCCGA
5663	H_FW_LA1	TCTAGAAGATTACTTAACGCCTCAGC

Number	Name	Sequence 5' → 3'
2686	Tag H fusion reverse	GTCACGGGTTCTCAGCAATTCG
3285	Fus Tag J fw	GGCCGTCATATACGCGAAGATGTC
gRNA cassette construction		
6835	CrRNA insert MCH1 XhoI FW	TGCGCATGTTTCGGCGTTCGAAACTTCTCCGCAGT GAAAGATAAATGATCTATTGGCAATAAACATCTCG GTTTTAGAGCTAGAAATAGCAAGTTAAAATAAGGC TAGTCCGTTATCAAC
6836	CrRNA insert MCH1 XhoI RV	GTTGATAACGGACTAGCCTTATTTAACTTGCTAT TTCTAGCTCTAAAACCGAGATGTTTATTGCCAATA GATCATTATCTTTCACTGCGGAGAAGTTTCGAAC GCCGAAACATGCGCA
6837	CrRNA insert MCH2 PvuI FW	TGCGCATGTTTCGGCGTTCGAAACTTCTCCGCAGT GAAAGATAAATGATCATCTCGATCGAGGTGCCTGA GTTTTAGAGCTAGAAATAGCAAGTTAAAATAAGGC TAGTCCGTTATCAAC
6838	CrRNA insert MCH2 PvuI RV	GTTGATAACGGACTAGCCTTATTTAACTTGCTAT TTCTAGCTCTAAAACCTCAGGCACCTCGATCGAGAT GATCATTATCTTTCACTGCGGAGAAGTTTCGAAC GCCGAAACATGCGCA
6839	CrRNA insert MCH5 EcoRV FW	TGCGCATGTTTCGGCGTTCGAAACTTCTCCGCAGT GAAAGATAAATGATCACTCTTCCGTTTTAGATATC GTTTTAGAGCTAGAAATAGCAAGTTAAAATAAGGC TAGTCCGTTATCAAC
6840	CrRNA insert MCH5 EcoRV RV	GTTGATAACGGACTAGCCTTATTTAACTTGCTAT TTCTAGCTCTAAAACGATATCTAAAACGGAAGAGT GATCATTATCTTTCACTGCGGAGAAGTTTCGAAC GCCGAAACATGCGCA
6841	CrRNA insert AQY1 DraI FW	TGCGCATGTTTCGGCGTTCGAAACTTCTCCGCAGT GAAAGATAAATGATCACCATCGCTTTAAATCTCT GTTTTAGAGCTAGAAATAGCAAGTTAAAATAAGGC TAGTCCGTTATCAAC
6842	CrRNA insert AQY1 DraI RV	GTTGATAACGGACTAGCCTTATTTAACTTGCTAT TTCTAGCTCTAAAACAGAGATTTTAAAGCGATGGT GATCATTATCTTTCACTGCGGAGAAGTTTCGAAC GCCGAAACATGCGCA
6843	CrRNA insert ITRI EcoRI FW	TGCGCATGTTTCGGCGTTCGAAACTTCTCCGCAGT GAAAGATAAATGATCATAATCAACGAATTCCAAC GTTTTAGAGCTAGAAATAGCAAGTTAAAATAAGGC TAGTCCGTTATCAAC
6844	CrRNA insert ITRI EcoRI RV	GTTGATAACGGACTAGCCTTATTTAACTTGCTAT TTCTAGCTCTAAAACGTTGGAATTCGTTGATGTAT GATCATTATCTTTCACTGCGGAGAAGTTTCGAAC GCCGAAACATGCGCA
7040	CrRNA insert PDR12 KpnI FW	TGCGCATGTTTCGGCGTTCGAAACTTCTCCGCAGT GAAAGATAAATGATCGCATTTTCGGTACCTAACTC GTTTTAGAGCTAGAAATAGCAAGTTAAAATAAGGC TAGTCCGTTATCAAC

Number	Name	Sequence 5' → 3'
7041	CrRNA insert PDR12 KpnI RV	GTTGATAACGGACTAGCCTTATTTTAACTTGCTAT TTCTAGCTCTAAAACGAGTTAGGTACCGAAAATGC GATCATTTTATCTTTCAGTGGGAGAAGTTTCGAAC GCCGAAACATGCGCA
7348	ACS2_targetRNA FW	TGCGCATGTTTCGGCGTTCGAAACTTCTCCGCAGT GAAAGATAAATGATCTCCTTGCCGTTAAATCACCA GTTTTAGAGCTAGAAATAGCAAGTTAAAATAAGGC TAGTCCGTTATCAAC
6414	ACS1 gRNA	GTGCGCATGTTTCGGCGTTCGAAACTTCTCCGCAG TGAAAGATAAATGATCTCTTCACAGCTGGAGACA TGTTTTAGAGCTAGAAATAGCAAGTTAAAATAAG
7026	GET4_targetRNA FW BamHI, DpnI	TGCGCATGTTTCGGCGTTCGAAACTTCTCCGCAGT GAAAGATAAATGATCGGGCTCGCTAGGATCCAATT GTTTTAGAGCTAGAAATAGCAAGTTAAAATAAGGC TAGTCCGTTATCAAC
7032	NAT1_targetRNA FW BamHI, DpnI	TGCGCATGTTTCGGCGTTCGAAACTTCTCCGCAGT GAAAGATAAATGATCAAAGGAATTGGATCCTGCGT GTTTTAGAGCTAGAAATAGCAAGTTAAAATAAGGC TAGTCCGTTATCAAC
Repair oligos		
6849	MCH1 Repair Oligo FW	GGTGTCATTTATATAAGCTATGAATTTTAAAAAAA ATAAATGTAGCAGTTTCTTTTTGTGATTTGCACT TGAAAAATGGTTATTGCTATAAAATGATATGAAAG GAACTAGTCTCGAT
6850	MCH1 Repair Oligo RV	ATCGAGACTAGTTTCCTTTCATATCATTTTATAGC AATAACCATTTTCCAAGTGCAATCACAAAAAAGA AACTGCTACATTTATTTTAAAAATTCATAGCT TATATAAATGACACC
6851	MCH2 Repair Oligo FW	TATAGAACTATATAACTGATACTAGAATATACTAA TTCGTGCACTATTAACCGTTTGCGAGGTCACTTT TATTTACACTGTAGATAAGAAGGGATAGAGTTG CCAGAAAATTTTTTG
6852	MCH2 Repair Oligo RV	CAAAAAATTTTCTGGCAACTCTATCCCCCTTCTTAT CTACAGTGTGAAATAAAAGTGACCTCGCCAAACGG TTAATAGTGCACGAATTAGTATATTCTAGTATCAG TTATATAGTTCTATA
6853	MCH5 Repair Oligo FW	TAAAAGAAAATATTATTGCATTACTTTTTGAAGA TCTATAAAGGCACTGTCTACTTTTATTTTCTT TTAATCTATAGTAAAATCAGAGCTTTTAATCGA TAGTATGCCCCGTG
6854	MCH5 Repair Oligo RV	CACGGGGGCATACTATCGATTAAAAAGCTCTGATT TACTATAGATTAAAAAGAAAATAAAAGTAAGAC AGTGCCCTTTATAGATCTTCAAAAAAGTAATGCAA TAATATTTTCTTTTA

Number	Name	Sequence 5' → 3'
6855	AQY1 Repair Oligo FW	CTTTGTATTTGGTGTCTGTGTC AATACGGCACAT AAAGTAACATGTAATTA ACTATAACTTTTTCCCTC CTTTTCTTTATTTCTCGCTCACTAGCACTTAATGT TATAATACTCGGCAA
6856	AQY1 Repair Oligo RV	TTGCCGAGTATTATAACATTAAGTGCTAGTGAGCG AGAAATAAAGAAAAGGAGGGAAAAAGTTATAGTTA ATTACATGTTACTTTATGTGCCGTATTGACAGACA GCACCAAATACAAAG
6857	ITR1 Repair Oligo FW	ATTTTCTACTATGTATTTGAATATTCAATTGCGTC TCCTTCCTTTTACCTCGTGAAAGGATTTAACACCC ACTGCAGAAACAAAGAAAATGAAAGAGATGTATAC AGTAGGACGACCAAT
6858	ITR1 Repair Oligo RV	ATTGGTCGTCCTACTGTATACATCTCTTTCATTTT CTTTGTTTCTGCAGTGGGTGTTAAATCCTTTTCACG AGGTAAAAGGAAGGAGACGCAATTGAATATTCAAA TACATAGTAGAAAAAT
7042	PDR12 Repair Oligo FW	AAAATTGAAAATAAAAAATTGTGTGTTAAACCACGA AATACAAATATATTTGCTTGCTTGTTTTTTTATTA ATAAGAACAATAACAATAAATCTGTAAACCTTTTT TTTAAGTGA AAAATTA
7043	PDR12 Repair Oligo RV	TAATTTTCACTTAAAAAAAAGGTTTACAGATTTAT TGTTATTGTTCTTATTAATAAAAAACAAGCAAGC AAATATATTTGTATTTCGTGGTTAACACACAATT TTTATTTTCAATTTT
6422	ACS1 repair fw	CTATCTATAAGCAAAACCAACATATCAAAACTAC TAGAAAGACATTGCCCCACTGTGTTTGATGATTTT TTTCCTTTTTATATTGACGACTTTTTTTTTTCGTGT GTTTTTGTTCTCTTA
6423	ACS1 repair rv	TAAGAGAACA AAAACACACGAAAAAAAAGTCGTC AATATAAAAAGGAAAGAAATCATCAAACACAGTGG GGCAATGTCCTTCTAGTAGTTTGTATGTTTGGT TTTGCTTATAGATAG
7028	GET4_repair oligo fw	GGAAGTTAAAGTTGATGACATCTCAGTTGCTAGAT TGGTTAGATTAATAGCCGAATTCGATCCTAGCGAG CCCAATTTAAAGGACGTTATTACTGGTATGAACAA TTGGTCTATCAAATT
7029	GET4_repair oligo rv	AATTTGATAGACCAATTGTTTCATACCAGTAATAAC GTCCTTTAAATTGGGCTCGCTAGGATCGAATTCGG CTATTAATCTAACCAATCTAGCAACTGAGATGTCA TCAACTTTAACTTCC
7034	NAT1_repair oligo fw	GTTTCACCACTATTGGAGAAAATTGTCCTTGATTA TTTGTCCGGATTAGATCCTACGCAGGATCGAATTC CTTTTATTTGGACCAATTATTACTTGTCTCAACAT TTCCTTTTCCTTAAG

Number	Name	Sequence 5' → 3'
7035	NAT1_repair oligo rv	CTTAAGGAAAAAGGAAATGTTGAGACAAGTAATAAT TGGTCCAAATAAAAAGGAATTCGATCTGCGTAGGA TCTAATCCGGACAAATAATCAAGGACAATTTTCTC CAATAGTGGTGAAAC
Diagnostic primers for confirming correct double gRNA plasmid assembly		
	Primer A	CACCTTTCGAGAGGACGATG
	Primer B	GCTGGCCTTTTGCTCACATG
7351	GET4 dg fw-2	AATTGGATCCTAGCGAGCCC
7352	NAT1 dg fw-2	ACGAGGATCCAATTCCTTTG
Diagnostic primers for seamless deletion confirmation		
6862	MCH1 check FW	GTCCAGGATTCTCCGAAGAACTC
6863	MCH1 check RV	ACGGCTGTTGTCCGATATTGC
6864	MCH2 check FW	GCACGACTTTCAGGCTTTC
6865	MCH2 check RV	CACCGAACCAACATTAGGTAGC
6866	MCH5 check FW	GAAGACTGACGGGCACTTTG
6867	MCH5 check RV	GCCCTAGGCGGTATTGTATGAG
6868	AQY1 check FW	GATGTCCTTCCACCCTCTTACAC
5593	42 - CBS1483_Sc16_Scf39 _HPA2-Rv	CGTGTATTGGTGACGGATGAGTC
6869	ITR1 check FW	AGGTCTTCAATGCCGGGTTAG
6870	ITR1 check RV	GTATCAGCCGTCAGTAGTATCCAG
253	PDR12 - CTRL FW	CGGTATCACATTTTCTCGACGG
3998	PDR12 KO rv	CGCGACAGACATTGTTGG
Diagnostic primers for GET4 and NAT1 mutation confirmation		
7030	GET4_dg fw	TGTTTCGTTTGTGCTCTTTCG
7031	GET4_dg rv	AACTCAGCCACCGTGCTATC
7036	NAT1_dg fw	TATCCAAGATGCGAACCACCC
7037	NAT1_dg rv	AGATAGGCTCTTGCGGTACC
Diagnostic primers for confirming strain IMX719		
2619	acs2 KO Ctrl Rv	CCGATATTCGGTAGCCGATTCC
2430	Tag C-reverse short	GCGTCCAAGTAACTACATTATGTG
2668	m-PCR-HR2-FW	ACGCGTGACGCATGTAAC
7330	NATDiagfw	CGAGCAAATGCCTGCAAATC
5044	ADH1 Flank right FW	CTAGCGGTTATGCGGCTCTCAC
2913	G_RV_2 (PDH construct ctrl)	AATAGCCGCCAGGAAATGCC
2914	J_FW (PDH construct ctrl)	GTCGTCATAACGATGAGGTGTTGC
2915	J_RV (PDH construct ctrl)	GGAGCCAACAAGAATAAGCCGC
2908	D_FW (PDH construct ctrl)	GGATTGGGTGTGATGTAAGGATTCCG
2909	D_RV (PDH construct ctrl)	CCCGCTCACACTAACGTAGG
2916	I_FW (PDH construct ctrl)	GCAGGTATGCGATAGTTCCTCAC

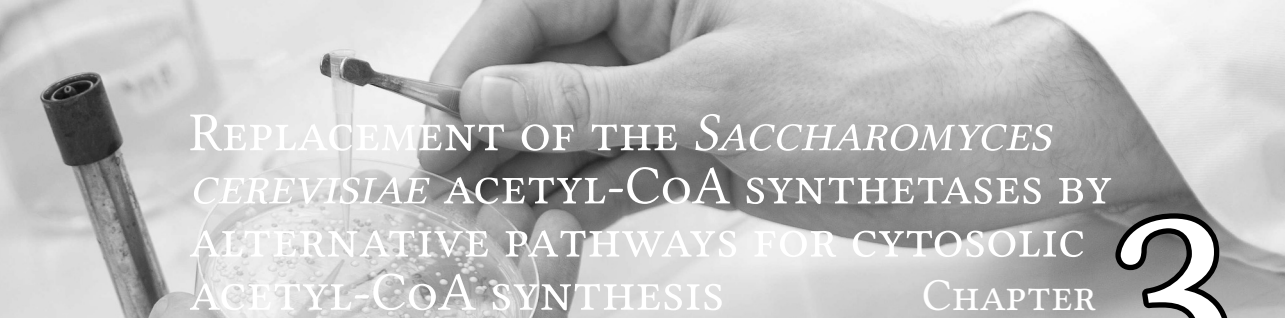
Number	Name	Sequence 5' → 3'
2905	B_RV (PDH construct ctrl)	TGGCAGTATTGATAATGATAAACTCG
5641	F_FW_EF	CCATTGCTGAAGCTGACAAG
2618	acs2 Ctrl Fw	TACCCTATCCCGGGCGAAGAAC
2927	ACS1 KO ctrl FW	AAACTGGGCGGCTATTCTAAGC
2928	ACS1 KO ctrl RV	AGCAGCTCGGTTATAAGAGAAC

Table S2.2. Alignment of 120 bp surrounding the target site at the mutated *GET4* locus of the four sequenced colonies (the target site is underlined, in lowercase the intended mutation, in gray additional, undesired mutations).

Reference	258	GGAAGTTAAAGTTGATGACATCTCAGTTGCTAGATTGGTTAGATTAATAGCCGAATTGGA
Colony #1		GGAAGTTAAAGTTGATGACATCTCAGTTGCTAGATTGGTTAGATTAATAGCCGAATTcGA
Colony #2		GGAAGTTAAAGTTGATGACATCTCAGTTGCTAGATTGGTTAGATTAATAGCCGAATTcGA
Colony #4		GGAAGTTAAAGTTGATGACATCTCAGTTGCTAGATTGGTTAGATTAATAGCCGAATTcGA
Colony #6		GGAAGTTAAAGTTGATGACATCTCAGTTGCTAGATTGGTTAGATTAATAGCCGAATTcGA
Reference	318	TCCTAGCGAGCCCAATTTAAAGGACGTTATTACTGGTATGAACAATTGGTCTATCAAATT
Colony #1		TCCTAGCGAGCCCAATTTAAAGGACGTTATTACTGGTATGAACAATTGGTCTATCAAATT
Colony #2		TCCTAGCGAGCCCAATTTAAAG-----TTACTGGTATGAACAATTGGTCTATCAAATT
Colony #4		TCTAGCGAGCCCAATTTAAAGGACGTTATTATTGGTATGAACAATTGGTCTATCAAATT
Colony #6		TCCTAGCGAGCCCAATTTAAAGGACGTTATTACTGGTATGAACAATTGGTCTATCAAATT

Table S2.3. Alignment of 120 bp surrounding the target site at the mutated *NAT1* locus of the four sequenced colonies (the target site is underlined, in lowercase the intended mutation).

Reference	1075	GTTTCACCACTATTGGAGAAAATTGTCCTTGATTATTTGTCCGGATTAGATCCTACGCAG
Colony #1		GTTTCACCACTATTGGAGAAAATTGTCCTTGATTATTTGTCCGGATTAGATCCTACGCAG
Colony #2		GTTTCACCACTATTGGAGAAAATTGTCCTTGATTATTTGTCCGGATTAGATCCTACGCAG
Colony #4		GTTTCACCACTATTGGAGAAAATTGTCCTTGATTATTTGTCCGGATTAGATCCTACGCAG
Colony #6		GTTTCACCACTATTGGAGAAAATTGTCCTTGATTATTTGTCCGGATTAGATCCTACGCAG
Reference	1135	GATCCAATTCCCTTTTATTGGACCAATTATTACTTGTCTCAACATTTCCCTTTTCCTTAAG
Colony #1		GATCgAATTCCTTTTATTGGACCAATTATTACTTGTCTCAACATTTCCCTTTTCCTTAAG
Colony #2		GATCgAATTCCTTTTATTGGACCAATTATTACTTGTCTCAACATTTCCCTTTTCCTTAAG
Colony #4		GATCgAATTCCTTTTATTGGACCAATTATTACTTGTCTCAACATTTCCCTTTTCCTTAAG
Colony #6		GATCgAATTCCTTTTATTGGACCAATTATTACTTGTCTCAACATTTCCCTTTTCCTTAAG



REPLACEMENT OF THE *SACCHAROMYCES CEREVISIAE* ACETYL-CoA SYNTHETASES BY ALTERNATIVE PATHWAYS FOR CYTOSOLIC ACETYL-CoA SYNTHESIS

CHAPTER

3

Barbara U. Kozak¹, Harmen M. van Rossum¹, Kirsten R. Benjamin, Liang Wu, Jean-Marc G. Daran, Jack T. Pronk and Antonius J.A. van Maris

Abstract

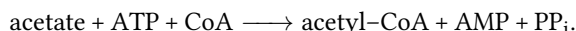
Cytosolic acetyl-coenzyme A is a precursor for many biotechnologically relevant compounds produced by *Saccharomyces cerevisiae*. In this yeast, cytosolic acetyl-CoA synthesis and growth strictly depend on expression of either the Acs1 or Acs2 isoenzyme of acetyl-CoA synthetase (ACS). Since hydrolysis of ATP to AMP and pyrophosphate in the ACS reaction constrains maximum yields of acetyl-CoA-derived products, this study explores replacement of ACS by two ATP-independent pathways for acetyl-CoA synthesis. After evaluating expression of different genes encoding acetylating acetaldehyde dehydrogenase (A-ALD) and pyruvate-formate lyase (PFL), *acs1Δ acs2Δ S. cerevisiae* strains were constructed in which A-ALD or PFL successfully replaced ACS. In A-ALD-dependent strains, aerobic growth rates of up to 0.27 h^{-1} were observed, while anaerobic growth rates of PFL-dependent *S. cerevisiae* (0.20 h^{-1}) were stoichiometrically coupled to formate production. In glucose-limited chemostat cultures, intracellular metabolite analysis did not reveal major differences between A-ALD-dependent and reference strains. However, biomass yields on glucose of A-ALD- and PFL-dependent strains were lower than those of the reference strain. Transcriptome analysis suggested that reduced biomass yields were caused by acetaldehyde and formate in A-ALD- and PFL-dependent strains, respectively. Transcript profiles also indicated that a previously proposed role of Acs2 in histone acetylation is probably linked to cytosolic acetyl-CoA levels rather than to direct involvement of Acs2 in histone acetylation. While demonstrating that yeast ACS can be fully replaced, this study demonstrates that further modifications are needed to achieve optimal *in vivo* performance of the alternative reactions for supply of cytosolic acetyl-CoA as a product precursor.

3.1 INTRODUCTION

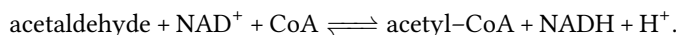
The robustness of *Saccharomyces cerevisiae* in industrial fermentation processes, combined with fast developments in yeast synthetic biology and systems biology, have made this microorganism a popular platform for metabolic engineering (123). Many natural and heterologous compounds whose production from sugars is under investigation or already implemented in industry require acetyl-coenzyme A (acetyl-CoA) as a key precursor. Examples of such products include *n*-butanol, isoprenoids, lipids and flavonoids (67, 165, 281, 299, 320).

Acetyl-CoA metabolism in *S. cerevisiae* is compartmented (244, 257). During respiratory growth on sugars, a substantial flux through acetyl-CoA occurs via the mitochondrial pyruvate dehydrogenase complex (245). However, mutant analysis has shown that mitochondrial acetyl-CoA cannot meet the extramitochondrial requirement for acetyl-CoA in the yeast cytosol, which includes, for example, its use as a precursor for synthesis of lipids and lysine (14, 81). In this respect, it is relevant to note that *S. cerevisiae* does not contain ATP-citrate lyase, an enzyme that plays a major role in translocation of acetyl-CoA across the mitochondrial membrane in mammalian cells and in several non-*Saccharomyces* yeasts (20). When sugars are used as the carbon source, cytosolic acetyl-CoA synthesis in *S. cerevisiae* occurs via the concerted action of pyruvate decarboxylase (Pdc1, 5 and 6), acetaldehyde dehydrogenase (Ald2, 3, 4, 5 and 6) and acetyl-CoA synthetase (Acs1 and 2) (244). Heterologous, acetyl-CoA-dependent product pathways expressed in the *S. cerevisiae* cytosol exclusively depend on this 'pyruvate dehydrogenase bypass' for provision of acetyl-CoA. Indeed, overexpression of acetyl-CoA synthetase (ACS) from *Salmonella enterica* has been shown to lead to increased productivities of the isoprenoid amorphadiene by engineered *S. cerevisiae* strains (281).

The ACS reaction involves the hydrolysis of ATP to AMP and pyrophosphate (PP_i):



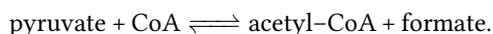
Together with the subsequent hydrolysis of PP_i to inorganic phosphate (P_i), this ATP consumption is equivalent to the hydrolysis of 2 ATP to 2 ADP and 2 P_i. The resulting ATP expenditure for acetate activation can have a huge impact on the maximum theoretical yields of acetyl-CoA derived products. For example, the production of a C₁₆ lipid from sugars requires 8 acetyl-CoA, whose synthesis via ACS requires 16 ATP. At an effective P/O ratio of respiration in *S. cerevisiae* of 1 (323), this ATP requirement for acetyl-CoA synthesis corresponds to 1 mole of glucose that needs to be respired for the synthesis of 1 mole of product. In addition to the pyruvate-dehydrogenase complex, other reactions have been described in nature that enable the ATP-independent conversion of pyruvate into acetyl-CoA (242, 262, 284). Many prokaryotes contain an acetylating acetaldehyde dehydrogenase (A-ALD; EC 1.2.1.10) which catalyses the reversible reaction:



Although functional expression of bacterial genes encoding A-ALD in *S. cerevisiae* has been described in the literature, these studies focused on reductive conversion of acetyl-CoA to ethanol as part of a phosphoketolase pathway for pentose fermentation (291) or

as part of a metabolic engineering strategy to convert acetic acid to ethanol (104). Complete replacement of the native acetaldehyde dehydrogenases and/or ACS of *S. cerevisiae* by A-ALD, thereby bypassing ATP hydrolysis in the ACS reaction, has not been demonstrated.

In many anaerobic bacteria and some eukaryotes (295), pyruvate can be converted into acetyl-CoA and formate in the non-oxidative, ATP-independent reaction catalysed by pyruvate-formate lyase (PFL; EC 2.3.1.54):



PFL and PFL-activating enzyme (PFL-AE; EC 1.97.1.4) from *Escherichia coli* have previously been expressed in *S. cerevisiae* (331). Although formate production by this oxygen-sensitive enzyme system was demonstrated in anaerobic yeast cultures, its impact on cytosolic acetyl-CoA metabolism has not been investigated.

To gain the full potential benefit of ATP-independent cytosolic acetyl-CoA synthesis, the implemented heterologous pathways expressed in *S. cerevisiae* should, ideally, completely replace the ACS reaction. In wild-type strain backgrounds, deletion of both *ACS1* and *ACS2* is lethal (14) and, during batch cultivation on glucose, presence of a functional *ACS2* gene is essential (14) because *ACS1* is subject to glucose repression (13) and its product is inactivated in the presence of glucose (141). Moreover, it has been proposed that *Acs2*, which was demonstrated to be partially localized in the yeast nucleus, is involved in histone acetylation (306). Involvement of *Acs* isoenzymes in the acetylation of histones and/or other proteins might present an additional challenge in replacing them with heterologous reactions, if this includes another mechanism than merely the provision of extramitochondrial acetyl-CoA.

The goal of this study is to investigate whether the heterologous ATP-independent A-ALD and PFL pathways can support the growth of *acs1 acs2* mutants of *S. cerevisiae* by providing extramitochondrial acetyl-CoA and to study the impact of such an intervention on growth, energetics and cellular regulation. To this end, several heterologous genes encoding A-ALD and PFL were screened by expression in appropriate yeast genetic backgrounds, followed by detailed analysis of *S. cerevisiae* strains in which both *ACS1* and *ACS2* were replaced by either of the alternative reactions. The resulting strains were studied in batch and chemostat cultures. Furthermore, genome-wide transcriptional responses to these modifications were studied by chemostat-based transcriptome analysis of engineered and reference strains.

3.2 METHODS

STRAINS AND MAINTENANCE

The *S. cerevisiae* strains used in this study (Table 3.1) share the CEN.PK genetic background (71, 222). Stock cultures were grown aerobically in synthetic medium (326). When required, auxotrophic requirements were complemented with synthetic yeast drop-out medium supplements (Sigma-Aldrich, St. Louis, MO, USA) or by growth in YP medium (demineralized water, 10 g·L⁻¹ Ba₅to yeast extract, 20 g·L⁻¹ Ba₅to peptone). Carbon sources were either 20 g·L⁻¹ glucose, 2% (v/v) ethanol and/or 11.3 g·L⁻¹ sodium acetate trihydrate. Stock cultures of *S. cerevisiae* strains IMZ383 and IMZ384 were grown anaerobically and supplemented with Tween-80 (420 mg·L⁻¹) and ergosterol (10 mg·L⁻¹) added to the medium. Frozen stocks of *S. cerevisiae* and *E. coli* were prepared by

Table 3.1. *Saccharomyces cerevisiae* strains used in this study

Name	Relevant genotype	Origin
CEN.PK113-7D	<i>MATa MAL2-8^C SUC2</i>	P. Kötter
CEN.PK113-5D	<i>MATa MAL2-8^C SUC2 ura3-53</i>	P. Kötter
CEN.PK102-12A	<i>MATa MAL2-8^C SUC2 ura3-53 leu2-3,112 his3-Δ1</i>	P. Kötter
IMK337	CEN.PK102-12 <i>ald2-ald3Δ::loxP-LEU2-loxP</i>	This study
IMK342	IMK337 <i>ald4Δ::loxP-HIS3-loxP</i>	This study
IMK346	IMK342 <i>ald5Δ::loxP-KanMX4-loxP</i>	This study
IMK354	IMK346 <i>ald6Δ::loxP-hphNT1-loxP</i>	This study
IMZ281	IMK354 p426GPD	This study
IMZ284	IMK354 pUDE047 (<i>URA3, dmpF Pseudomons sp.</i>)	This study
IMZ286	IMK354 pUD043 (<i>URA3, mhpF E. coli</i> (not codon-optimized))	This study
IMZ289	IMK354 pUDE150 (<i>URA3, adhE S. aureus</i>)	This study
IMZ290	IMK354 pUDE151(<i>URA3, eutE E. coli</i>)	This study
IMZ291	IMK354 pUDE152 (<i>URA3, lin1129 L. innocua</i>)	This study
IME140	CEN.PK113-5D p426GPD	This study
IMZ304	IMZ290 <i>acs2Δ::loxP-natNT2-loxP</i>	This study
IMZ305	IMZ304 <i>acs1Δ::AmdS</i>	This study
IMK427	CEN.PK102-12A <i>acs2Δ::loxP-HIS3-loxP</i>	This study
IMZ374	IMK427 pRS426 (<i>URA3</i>)	This study
IMZ369	IMK427 pUDE201 (<i>URA3, PFL, PFL-AE Thalassiosira pseudonana</i>)	This study
IMZ370	IMK427 pUDE202 (<i>URA3, pfl, pflA Chlamydomonas reinhardtii</i>)	This study
IMZ371	IMK427 pUDE204 (<i>URA3, pflB, pflA Escherichia coli</i>)	This study
IMZ372	IMK427 pUDE214 (<i>URA3, pflB, pflA Lactobacillus plantarum</i>)	This study
IMZ373	IMK427 pUDE215 (<i>URA3, PFL, PFL-AE Neocallimastix frontalis</i>)	This study
IMZ383	IMZ371 <i>acs1Δ::loxP-LEU2-loxP</i>	This study
IMZ384	IMZ372 <i>acs1Δ::loxP-LEU2-loxP</i>	This study

the addition of glycerol (30% v/v) to the growing shake-flask cultures and aseptically storing 1 mL aliquots at -80 °C.

PLASMID CONSTRUCTION

Coding sequences of *Staphylococcus aureus adhE* (NP_370672.1), *Escherichia coli eutE* (YP_001459232.1) and *Listeria innocua lin1129* (NP_470466) were codon-optimized for *S. cerevisiae* with the JCat algorithm (102). Custom-synthesized coding sequences cloned in the pMA vector (Table 3.2) were provided by GeneArt GmbH (Regensburg, Germany). Gateway Cloning technology (Invitrogen, Carlsbad, A) was used to insert these coding sequences in the intermediate vector pDONR221 (BP reaction) and subsequently into pAG426-pGPD (2) (LR reaction). The resulting plasmids pUDE150 to pUDE152 were transformed into *E. coli* and their sequences checked by Sanger sequencing (BaseClear BV, Leiden, The Netherlands).

PFL- and PFL-AE-encoding sequences from *Thalassiosira pseudonana* (Genbank accession no. XM_002296598.1 and XM_002296597.1), *Chlamydomonas reinhardtii* (AJ620191.1 and AY831434.1), *E. coli* (X08035.1), *Lactobacillus plantarum* (YP_003064242.1 and YP_003064243.1) and *Neocallimastix frontalis* (AY500825.1 and AY500826.1) were codon-optimized for expression in *S. cerevisiae* and signal sequences, predicted by TargetP, were removed (70). Expression cassettes in which these coding sequences were flanked by the *TPI1* promoter and *GND2* terminator (PFL) or *FBA1* promoter and *PMA1* terminator (PFL-AE), were synthesized by GeneArt GmbH. PFL and PFL-AE expression cassettes were PCR amplified with primer combinations 3384 & 3385 and 3386 & 3387, respectively (Supplementary Table 3.1). Overlaps between the fragments were obtained using the primers, enabling homologous recombination. After linearization with SpeI and XhoI, the pRS426 backbone was assembled with the PFL and PFL-AE fragments via *in vivo* homologous recombination in *S. cerevisiae* CEN.PK113-5D (172). Assembled plasmids were purified from uracil prototrophic transformants and transformed into *E. coli*. Sequences of the resulting plas-

Table 3.2. Plasmids used in this study

Name	Characteristics	Origin
pMA	Delivery vectors	GeneArt, Germany
pENTR221	Gateway entry clone	Invitrogen, USA
pUG6	Template for <i>loxP-KanMX-loxP</i> cassette	(107)
pUG27	Template for <i>loxP-HIS5 (Schizosaccharomyces pombe)-loxP</i> cassette	(107)
pUG72	Template for <i>loxP-URA3 (Kluyveromyces lactis)-loxP</i> cassette	(107)
pUG73	Template for <i>loxP-LEU2 (K. lactis)-loxP</i> cassette	(107)
pUG-hphNT1	Template for <i>loxP-hphNT1-loxP</i> cassette	(162)
pUG-natNT2	Template for <i>loxP-natNT2-loxP</i> cassette	(164)
pUDE158	Template for <i>AmdS</i> cassette	(288)
p426GPD	2 μ m ori, <i>URA3</i> , <i>pTDH3-tCYC1</i>	(214)
pAG426GPD	2 μ m ori, <i>URA3</i> , <i>pTDH3-ccdB-tCYC1</i>	(2)
pRS424	2 μ m ori, <i>TRP1</i>	(48)
pRS426	2 μ m ori, <i>URA3</i>	(48)
pUDE043	2 μ m ori, <i>URA3</i> , <i>pTDH3-mhpF (E. coli)</i> (not codon-optimized)- <i>tCYC1</i>	(104)
pUDE047	2 μ m ori, <i>URA3</i> , <i>pTDH3-dmpF (Pseudomonas sp.)-tCYC1</i>	(243)
pUDE150	2 μ m ori, <i>URA3</i> , <i>pTDH3-adhE (S. aureus)-tCYC1</i>	This study
pUDE151	2 μ m ori, <i>URA3</i> , <i>pTDH3-eutE (E. coli)-tCYC1</i>	This study
pUDE152	2 μ m ori, <i>URA3</i> , <i>pTDH3-lin1129 (L. innocua)-tCYC1</i>	This study
pUDE201	2 μ m ori, <i>URA3</i> , <i>pTPI1-PFL (T. pseudomonana)-tGND2</i> , <i>pFBA1-PFL-AE (T. pseudomonas)-tPMA1</i>	This study
pUDE202	2 μ m ori, <i>URA3</i> , <i>pTPI1-pfl (C. reinhardtii)-tGND2</i> , <i>pFBA1-pflA (C. reinhardtii)-tPMA1</i>	This study
pUDE204	2 μ m ori, <i>URA3</i> , <i>pTPI1-pflB (E. coli)-tGND2</i> , <i>pFBA1-pflA (E. coli)-tPMA1</i>	This study
pUDE214	2 μ m ori, <i>URA3</i> , <i>pTPI1-pflB (L. plantarum)-tGND2</i> , <i>pFBA1-pflA (L. plantarum)-tPMA1</i>	This study
pUDE215	2 μ m ori, <i>URA3</i> , <i>pTPI1-PFL (N. frontalis)-tGND2</i> , <i>pFBA1-PFL-AE (N. frontalis)-tPMA1</i>	This study

mids pUDE201 to pUDE215 (Table 3.2) were checked by sequencing (Illumina HiSeq2000, Base-Clear BV, Leiden, The Netherlands), assembled as described previously (172). All plasmid sequences were deposited at GenBank under accession numbers KF170375 (pUDE215), KF170376 (pUDE150), KF170377 (pUDE151), KF170378 (pUDE152), KF170379 (pUDE201), KF170380 (pUDE202), KF170381 (pUDE204) and KF170382 (pUDE214).

STRAIN CONSTRUCTION

S. cerevisiae strains were transformed according to Gietz and Woods (97). Knockout cassettes were obtained by PCR using primers listed in Supplementary Table S3.1 with the templates pUG6, pUG27, pUG72, pUG73 (107), pUG-amdS (288), pUG-hphNT1 (162) and pUG-natNT2. Mutants were selected on solid medium (2% (w/v) agar) with 200 mg·L⁻¹ G418, 200 mg·L⁻¹ hygromycin B or 100 mg·L⁻¹ nourseothricin (for dominant markers) or on drop-out (Sigma-Aldrich) or synthetic medium from which the appropriate auxotrophic requirements had been omitted. The Ald⁻ strain IMK354 was obtained by the consecutive deletion of *ALD2-ALD3*, *ALD4*, *ALD5* and *ALD6* in strain CEN.PK102-12A. During strain construction, the Ald⁻ strains were grown on acetate as a carbon source. IMK354 was transformed with the plasmids p426GPD (214), pUDE043, pUDE047, pUDE150, pUDE151 and pUDE152. In one of the resulting strains, IMZ290, *ACS2* and *ACS1* were subsequently deleted, yielding IMZ305. IMK427 was constructed by deletion of *ACS2* in strain CEN.PK102-12A. The *acs2Δ* strain was grown on ethanol as a carbon source. Transformation of strain IMK427 with plasmids pUDE201, pUDE202, pUDE204, pUDE214 and pUDE215 yielded strains IMZ369 – IMZ373, respectively (Table 3.1). In two strains, IMZ371 and IMZ372, *ACS1* was deleted. In all cases gene

deletions and plasmid presence were confirmed by PCR using the diagnostic primers listed in Supplementary Table S3.1.

MOLECULAR BIOLOGY TECHNIQUES

PCR amplification with Phusion® Hot Start II High Fidelity Polymerase (Thermo Scientific, Waltham, MA) was performed according to the manufacturer's manual using HPLC- or PAGE-purified, custom-synthesized oligonucleotide primers (Sigma-Aldrich). Diagnostic PCR was done with DreamTaq (Thermo Scientific) and desalted primers (Sigma-Aldrich). DNA fragments obtained by PCR were loaded on gels containing 1% or 2% (w/v) agarose (Thermo Scientific) and 1xTAE buffer (Thermo Scientific), excised and purified (Zymoclean™, D2004, Zymo Research, Irvine, CA). Alternatively, fragments were purified using the GenElute™ PCR Clean-Up Kit (Sigma-Aldrich). Plasmids were isolated from *E. coli* with Sigma GenElute Plasmid kit (Sigma-Aldrich) according to the supplier's manual. Yeast plasmids were isolated according to (172). Yeast genomic DNA was isolated using a YeaStar Genomic DNA kit (Zymo Research). *E. coli* DH5α (18258-012, Invitrogen) was transformed chemically (T3001, Zymo Research) or by electroporation. Chemical transformation was done according to supplier's instructions. Electroporation was done in a 2 mm cuvette (165-2086, BioRad, Hercules, CA) using a Gene PulserXcell Electroporation System (BioRad), following the manufacturer's protocol.

MEDIA AND CULTIVATION

Shake flask cultures were grown at 30 °C in 500 mL flasks containing 100 mL synthetic medium (326) with 20 g·L⁻¹ glucose in an Innova incubator shaker (New Brunswick Scientific, Edison, NJ) set at 200 rpm. Anaerobic cultures were grown in 100 mL shake flasks on the same medium, supplemented with the anaerobic growth factors ergosterol (10 mg·L⁻¹) and Tween-80 (420 mg·L⁻¹) according to (325) and incubated on a Unimax1010 shaker (Heidolph, Kelheim, Germany) set at 200 rpm, placed in a Baçtron anaerobic chamber (Sheldon MFG Inc., Cornelius, OR, USA) with a gas mixture of 5% H₂, 6% CO₂, and 89% N₂. Optical density at 660 nm was measured in regular time intervals with a Libra S11 spectrophotometer (Biochrom, Cambridge, UK). Controlled batch and chemostat cultivation was carried out at 30 °C in 2-L laboratory bioreactors (Applikon, Schiedam, The Netherlands) with working volumes of 1 L. Chemostat cultivation was preceded by a batch phase under the same conditions. When a rapid decrease in CO₂ production indicated glucose depletion in the batch cultures, continuous cultivation at a dilution rate of 0.10 h⁻¹ was initiated. Synthetic medium (326) supplemented with 7.5 g·L⁻¹ or 20 g·L⁻¹ glucose was used in aerobic and anaerobic chemostat cultures, respectively. Culture pH was maintained at 5.0 by automatic addition of 2 M KOH. In aerobic cultures, antifoam Pluronic PE 6100 (BASF, Ludwigshafen, Germany) was used. The antifoam was autoclaved (110 °C) separately from the other medium ingredients and added as a 15% (w/v) stock solution to a final concentration of 0.15 g·L⁻¹. Aerobic bioreactors were sparged with 500 mL·min⁻¹ air and stirred at 800 rpm to ensure fully aerobic conditions. Anaerobic bioreactors were stirred at 800 rpm and sparged with 500 mL·min⁻¹ nitrogen (< 10 ppm oxygen). Anaerobic growth media were supplemented with the anaerobic growth factors ergosterol (10 mg·L⁻¹) and Tween-80 (420 mg·L⁻¹). Antifoam C Emulsion (Sigma-Aldrich) was autoclaved separately (120 °C) as a 20 % (w/v) solution and added to a final concentration of 0.2 g·L⁻¹. In anaerobic bioreactor batch cultures, the medium contained 25 g·L⁻¹ glucose. To minimize diffusion of oxygen, the bioreactors were equipped with Norprene tubing and Viton O-rings and medium reservoirs were continuously flushed with nitrogen. Specific growth rates were calculated from biomass dry weight determinations.

ANALYTICAL METHODS

Chemostat cultures were assumed to be in steady state when, after at least five volume changes, the carbon dioxide production rates changed by less than by 4% over 2 volume changes. Steady state

samples were taken between 10 and 15 volume changes after inoculation. Dry weight measurements, HPLC analysis of the supernatant and off-gas analysis were performed as described previously (162). Ethanol concentrations were corrected for evaporation as described by Guadalupe Medina *et al.* (104). Samples for formate, glycerol and residual glucose determination were taken with the stainless steel bead method for rapid quenching of metabolites (207).

ENZYMATIC DETERMINATION OF METABOLITES

Extracellular formate, glycerol and residual glucose were measured using the Formic Acid Determination Kit (10979732035, R-Biopharm AG, Zaandijk, The Netherlands), Glycerol Enzymatic Determination Kit (10148270035, R-Biopharm AG) and EnzyPlus D-Glucose kit (EZX781, BioControl Systems Inc., Bellevue, WA, USA), respectively. Measurements were done according to manufacturer's instructions, except that the volume of the assays was proportionally downscaled. Absorbance was measured using cuvettes (final volume 1 mL, with at least two replicates) on a LibraS11 spectrophotometer or using 96-well plates (final volume 0.3 mL, with at least three replicates) on a Tecan GENios Pro (Tecan, Giessen, Netherlands).

INTRACELLULAR METABOLITES DETERMINATION

Culture samples for intracellular metabolite analysis were taken from bioreactors with a cold methanol rapid quenching method using a specially designed rapid sampling setup (178). 1.2 mL of broth was withdrawn into 5 mL of 80% aqueous methanol (v/v) solution pre-cooled to -40 °C. Samples subsequently were washed with cold methanol and extracted with boiling ethanol as described in (31). The concentrations of glucose, glucose-6-phosphate, fructose-6-phosphate, 2-phosphoglycerate, 3-phosphoglycerate, glyceraldehyde phosphate, dihydroxyacetone phosphate, 6-phosphogluconate, erythrose-4-phosphate, ribose-5-phosphate, ribulose-5-phosphate, xylulose-5-phosphate, sedoheptulose-7-phosphate, citrate, fumarate, malate, α -ketoglutarate and trehalose were determined as methoxime-trimethylsilyl derivatives by GC-MS (50). The concentrations of succinate, fructose-1,6-bisphosphate, trehalose-6-phosphate, glucose-1-phosphate, glycerol-3-phosphate, phosphoenolpyruvate, UDP-glucose and mannitol-1-phosphate were determined by anion-exchange LC-MS/MS (53). Concentrations of 20 amino acids and of pyruvate were determined by GC-MS (140). Concentrations of AMP, ADP, ATP, NAD⁺, NADH, NADP⁺, NADPH, CoA, acetyl-CoA and FAD were determined by ultra high performance liquid chromatography hyphenated with tandem mass spectrometry, UPLC-MS/MS. All measurements were carried out on an AcQuity™ UPLC system (Waters, Milford, MA, USA) coupled to a Waters Quattro Premier XE mass spectrometer, (Micromass MS Technologies-Waters) equipped with an electrospray ion source. The MS was operated in negative ion mode. Metabolite detection was performed in multiple reaction monitoring mode (MRM). The MRM transitions and corresponding instrument settings yielding the highest S/N, were separately found for each individual metabolite by direct infusion into the MS. The chromatographic separation of coenzymes in cell extracts was based on ion pair liquid chromatography on a reverse phase column AcQuity™ UPLC® BEH C18 (1.7 μ m, 100 \times 2.1 mm i.d., waters, Ireland). A linear gradient of mobile phase A (2 mM dibutylammonium acetate, DBAA, and 5% (v/v) acetonitrile) and mobile phase B (2 mM DBAA and 84% (v/v) acetonitrile) was used to separate the coenzymes. For both analytical platforms, uniformly ¹³C-labelled cell extracts were used as internal standards (341).

ACETALDEHYDE DETERMINATION

Culture samples for acetaldehyde analysis were obtained with the rapid sampling setup used for intracellular metabolites analysis (178). The acetaldehyde determination was performed as described previously (11). Approximately 1.2 mL of broth was withdrawn into 6 mL of pre-cooled (-40 °C) quenching and derivatization solution containing 0.9 g·L⁻¹ 2,4-dinitrophenylhydrazine and 1% (v/v) phosphoric acid in acetonitrile. After mixing and incubation for 2 hours on a Nutating Mixer

(VWR International, Leuven, Belgium) at 4 °C, samples were stored at -40 °C. Before analysis 1 mL of defrosted and well mixed sample was centrifuged (15,000 g, 3 min). The supernatant was analysed via HPLC using a WATERS WAT086344 silica-based, reverse phase C18 column operated at room temperature with a gradient of acetonitrile as a mobile phase. A linear gradient was generated from eluent A – 30 % (v/v) aqueous acetonitrile solution and eluent B – 80% (v/v) aqueous acetonitrile solution. The mobile phase composition was changing from 0% to 100% of eluent B in 20 min, at a flow rate of 1 mL·min⁻¹. A calibration curve was prepared with standard solution of 50.9 g·L⁻¹ acetaldehyde-2,4-dinitrophenylhydrazine in acetonitrile.

3

MICROARRAYS ASSAY AND ANALYSIS

Sampling for transcriptome analysis from chemostat cultures and total RNA extraction was performed as described previously (237). Processing of total RNA was performed according to Affymetrix instructions. RNA target preparation for microarray expression analysis was done with the Gene 3' IVT Express Kit (Affymetrix, Santa Clara, CA) using 200 ng of total RNA. The manufacturer's protocol was carried out with minor modifications, i.e the Affymetrix polyA RNA controls were excluded from the aRNA amplification protocol and the IVT reactions were incubated for 16 h at 40 °C. Quality of total RNA, cDNA, aRNA and fragmented aRNA was checked with an Agilent Bioanalyzer 2100 (Agilent Technologies, Amstelveen, The Netherlands). Hybridization, washing and scanning of Affymetrix chips were done according to manufacturer's instructions. For each strain analysed, microarrays were run on three independent cultures. Processing of expression data (normalization, expression cut-off, etc.) was performed as described previously (17). The Significance Analysis of Microarrays (SAM, version 3.0) (316) add-in to Microsoft Excel was used for comparison of replicate array experiments using a minimal fold change of two and false discovery rate of 1%. Overrepresentation of functional categories in sets of differentially expressed genes was analysed according to (156). Transcript data are available at the Genome Expression Omnibus database (<http://www.ncbi.nlm.nih.gov/geo>) under accession number GSE47983.

A set of acetaldehyde-responsive genes (5) used as a reference is accessible from www.uv.es/~arandaa. Statistical significance of the over-representation of these genes in subsets of yeast genes was computed as described in (156), replacing functional categories by reference set of acetaldehyde-responsive genes.

A-ALD ACTIVITY ASSAY

For preparation of cell extracts, culture samples (corresponding to ca. 62.5 mg dry weight) were harvested from exponentially growing shake flasks cultures on 20 g·L⁻¹ glucose, washed, stored and prepared for sonication as described previously (241). Cell extracts were prepared by sonication (4 bursts of 30 s with 30 s intervals and at 0 °C) with an amplitude setting of 7 – 8 µm on a Soniprep 150 sonicator (Beun de Ronde BV, Abcoude, The Netherlands). After removal of cells and debris by centrifugation (4 °C, 20 min at 48,000 g), the supernatant was used for enzyme assays. Protein concentrations in cell extracts were estimated with the Lowry method (197). A-ALD activity was measured at 30 °C on a Hitachi model 100-60 spectrophotometer by monitoring the reduction of NAD⁺ at 340 nm in a 1 mL reaction mixture containing 0.1 mM Coenzyme A, 50 mM CHES buffer pH 9.5, 0.8 mM NAD⁺, 0.2 mM DTT and 20 – 100 µL of cell extract. The reaction was started by adding 100 µL of freshly prepared 100 mM acetaldehyde solution. A-ALD activity in the reverse reaction was assayed as described previously (104). Enzyme activities are expressed as µmol substrate converted per min per mg protein (U·mg protein⁻¹). Reaction rates were proportional to the amounts of cell extract added.

VIABILITY STAINING

The staining procedure was performed as described previously (16), using the FungaLight™ CFDA, AM / Propidium Iodide Yeast Vitality Kit (Invitrogen, Carlsbad, CA). When membrane integrity is

Table 3.3. Aerobic maximum specific growth rates on glucose and acetylating acetaldehyde dehydrogenases activities with acetaldehyde or acetyl-CoA as a substrate of *Saccharomyces cerevisiae* strains carrying different acetylating acetaldehyde dehydrogenases. Averages and mean deviations were obtained from duplicate experiments. The detection limit of the enzyme assays was 2 nmol·min⁻¹·(mg protein)⁻¹.

Strain	Relevant genotype	Growth (h ⁻¹)	Enzyme activity (μmol·mg protein ⁻¹ ·min ⁻¹)	
			Acetaldehyde	Acetyl-CoA
IME140	<i>ALD2 ALD3 ALD4 ALD5 ALD6</i>	0.33 ± 0.004	N.D.*	N. D.
IMZ282	<i>aldΔ</i>	0.03 ± 0.001	N.D.	N.D.
IMZ284	<i>aldΔ dmpF</i>	0.21 ± 0.001	0.31 ± 0.06	0.04 ± 0.01
IMZ286	<i>aldΔ mhpF</i>	0.23 ± 0.004	0.19 ± 0.01	0.02 ± 0.001
IMZ289	<i>aldΔ adhE</i>	0.22 ± 0.001	0.18 ± 0.04	0.06 ± 0.02
IMZ290	<i>aldΔ eutE</i>	0.27 ± 0.001	7.95 ± 0.33	2.01 ± 0.04
IMZ291	<i>aldΔ lin1129</i>	0.25 ± 0.002	6.57 ± 0.61	1.15 ± 0.13

*N.D. = not detected

compromised, propidium iodide can diffuse into the cell and intercalate with DNA, yielding a red fluorescence. The acetoxymethyl ester of 5-carboxyfluorescein diacetate (CFDA, AM in DMSO) can permeate through intact membranes. In metabolically active cells, diacetate- and lipophilic blocking-groups are cleaved off by cytosolic non-specific esterases, yielding a charged, green fluorescent product. The pictures were taken with a fluorescent microscope (Imager-D1, Carl-Zeiss, Oberkochen, Germany) equipped with Filter Set 09 (FITC LP Ex. BP 450-490 Beamso. FT 510 Em. LP 515, Carl-Zeiss).

CHITINASE DIGESTION

100 μL of chemoostat culture was spun down and resuspended in 100 μL potassium phosphate buffer (50 mM, pH 6.10) or potassium phosphate buffer (50 mM, pH 6.10) with 1 mg·mL⁻¹ of chitinase (Chitinase from *Trichoderma viride*, >600 units·mg⁻¹, Sigma-Aldrich). The reaction mixture was incubated for 3 h at 30 °C.

3.3 RESULTS

3.3.1 Heterologous genes encoding A-ALD and PFL restore fast growth on glucose of *Ald*⁻ and *acs2Δ* mutants

To enable analysis of the functional expression of heterologous A-ALD genes, the five genes encoding acetaldehyde dehydrogenases (*ALD2*, *ALD3*, *ALD4*, *ALD5* and *ALD6*; (217)) in *S. cerevisiae* were deleted. In cell extracts of the resulting strain IMK354, NAD- and NADP-dependent acetaldehyde dehydrogenase activities measured according to (241) were below the detection limit of the assay of 2 nmol·min⁻¹·mg protein⁻¹. Subsequently, four different genes encoding A-ALD, (*dmpF* from *Pseudomonas sp.*, *adhE* from *Staphylococcus aureus*, *eutE* from *E. coli* and *lin1129* from *Listeria innocua*) were codon-optimised for expression in *S. cerevisiae* and individually introduced in strain IMK354 under the control of the constitutive *TDH3* promoter (Table 3.2). A non-codon-optimised version of *E. coli mhpF* was also tested. Expression of all tested A-ALD variants enabled fast growth of *Ald*⁻ *S. cerevisiae* on synthetic medium agar plates containing 20 g·L⁻¹

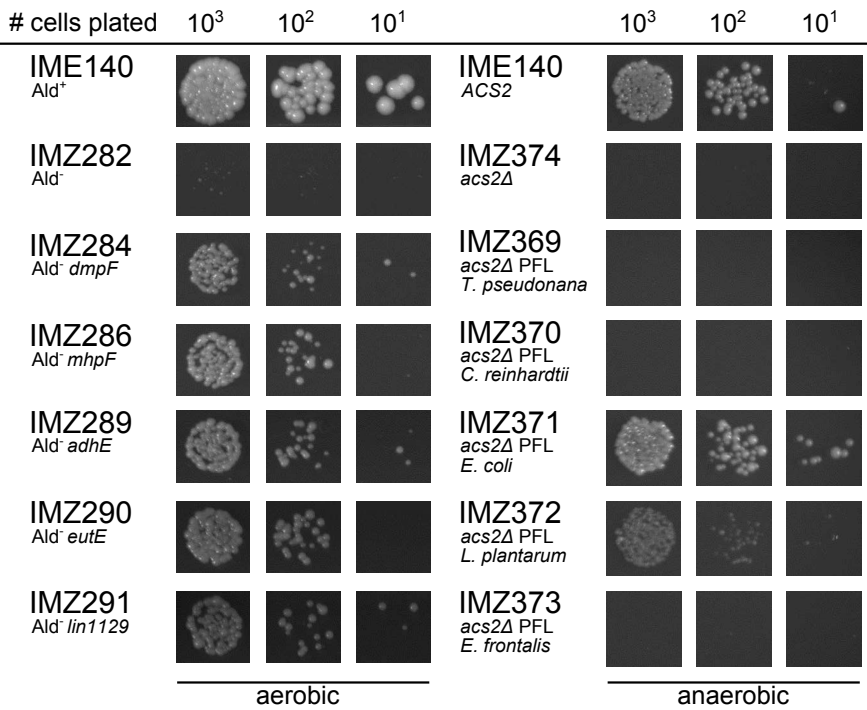


Figure 3.1. Growth of the Ald[−] strains expressing A-ALDs (IMZ284 – IMZ291), the *acs2Δ* PFL and PFL-AE expressing strains (IMZ369 – IMZ373), the Ald[−] reference strain IMZ282, the *acs2Δ* reference strain IMZ374 and Ald⁺ ACS2 reference strain IME140 on synthetic medium agar plates with 20 g·L^{−1} glucose. Plates containing A-ALD strains were incubated aerobically for 48 h. Plates containing PFL strains were incubated anaerobically for 90 h.

glucose (Figure 3.1, left panel). In shake-flask cultures grown on glucose as sole carbon source, the specific growth rate of the reference strain IMZ282 (Ald[−], empty expression vector) was 0.03 h^{−1}, which is less than 10 % of the growth rate of the Ald⁺ strain IME140 (empty vector reference, Table 3.1) under the same conditions. Of the Ald[−] strains expressing heterologous A-ALD genes, strains IMZ290 (expressing *E. coli eutE*) and IMZ291 (expressing *L. innocua lin1129*) showed the highest maximum specific growth rates (0.27 h^{−1} and 0.25 h^{−1}, respectively). These growth rates were over 75% of that of the Ald⁺ reference strain IME140. The high growth rates of these strains coincided with high activities of A-ALD in cell extracts (Table 3.3). Based on these results, strain IMZ290, which expresses *E. coli eutE*, was selected for further studies.

To investigate functional expression of the PFL and PFL-AE genes (those two genes are further referred to as PFL, unless otherwise stated) in *S. cerevisiae*, the *acs2Δ* strain IMK427 was used as a screening platform. As reported previously, deletion of ACS2 completely abolished growth on glucose plates due to repression and glucose catabolite inactivation of ACS1 and its gene product (13, 141) (Figure 3.1). Genes encoding PFL and PFL-AE from five different organisms (*Thalassiosira pseudonana*, *Chlamydomonas reinhardtii*, *E. coli*, *Lactobacillus plantarum* and *Neocallimastix frontalis*) were codon-optimized and

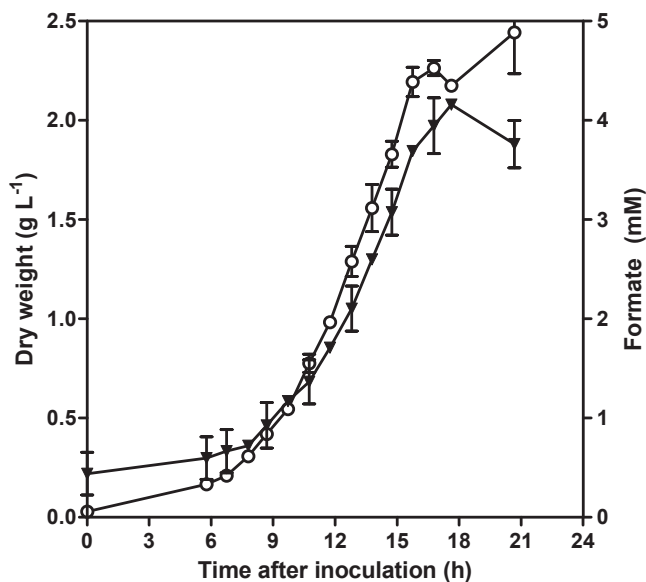


Figure 3.2. Growth of IMZ383 (Acs^- expressing *E. coli* PFL) in an anaerobic bioreactor on synthetic medium with an initial glucose concentrations of $25 \text{ g} \cdot \text{L}^{-1}$. The indicated averages and mean deviations are from a single batch experiment that is qualitatively representative of duplicate batch experiments. Symbols: extracellular formate (○) and dryweight (▼).

expressed in strain IMK427 under the control of the constitutive *TPI1* and *FBA1* promoters, respectively. To prevent oxygen inactivation of PFL (155), growth was compared on anaerobic plates with glucose as sole carbon source. Under these conditions, growth was only observed for strains IMZ371 and IMZ372, which expressed PFL from *E. coli* and *L. plantarum*, respectively (Figure 3.1). These strains were therefore used for further physiological analysis.

3.3.2 Complementation of *acs1 acs2* double mutants by A-ALD or PFL

Viable *S. cerevisiae* strains in which both *ACS1* and *ACS2* have been inactivated have not been described in the literature. We therefore investigated whether replacement of the role of acetyl-CoA synthetase in cytosolic acetyl-CoA synthesis by A-ALD or PFL is sufficient to enable growth of *acs1Δ acs2Δ* mutants.

Deletion of both ACS genes in strain IMZ290 (Ald^- expressing *E. coli eutE*) yielded strain IMZ305, which, in glucose-grown shake-flask cultures, showed a specific growth rate of $0.26 \pm 0.01 \text{ h}^{-1}$ (79% of the $Ald^+ Acs^+$ reference strain IME140). Similarly, deletion of *ACS1* in strains IMZ371 and IMZ372 (*acs2Δ* expressing PFL and PFL-AE from *E. coli* and *L. plantarum*, respectively) resulted in two strains (IMZ383 and IMZ384) that were able to grow anaerobically on glucose. Consistent with an essential role of oxygen-sensitive PFL in acetyl-CoA synthesis, these strains did not grow on glucose aerobically. Specific growth rates on glucose of the Acs^- PFL-expressing strains IMZ383 and IMZ384 in anaerobic shake-flask cultures were $0.20 \pm 0.00 \text{ h}^{-1}$ (73% of the Acs^+ reference strain

IME140) and $0.14 \pm 0.00 \text{ h}^{-1}$ (53%), respectively (average values and mean deviations are from at least two independent experiments). Growth and product formation of strain IMZ383 on glucose was further studied in anaerobic bioreactors (Figure 3.2), in which its specific growth rate ($0.20 \pm 0.00 \text{ h}^{-1}$) was the same as observed in anaerobic shake flasks. In contrast to the Acs^+ reference strain CEN.PK113-7D (data not shown), strain IMZ383 produced formate throughout exponential growth, with a stoichiometry of $2.5 \pm 0.1 \text{ mmol formate per gram biomass dry weight}$.

Because, in an Acs^- PFL-expressing yeast strain, production of acetyl-CoA and formate via PFL is stoichiometrically coupled, the turnover of cytosolic acetyl-CoA should at least equal the specific rate of formate production. In *S. cerevisiae*, cytosolic acetyl-CoA is required for synthesis of lipids, lysine, methionine, sterols and N-acetylglucosamine as well as for protein acetylation. Since the synthesis of unsaturated fatty acids and sterols requires molecular oxygen, these compounds are routinely included in anaerobic growth media. The cytosolic acetyl-CoA requirement for lipid and lysine synthesis in aerobic cultures has earlier been estimated at $1.04 \text{ mmol acetyl-CoA per gram dry biomass}$ (81). Based on published pathways and biomass compositions of *S. cerevisiae* (230), cytosolic acetyl-CoA requirements of methionine and cysteine for protein biosynthesis can be estimated at a combined $0.05 \text{ mmol per gram dry biomass}$. Additional $0.05 \text{ mmol acetyl-CoA per gram dry biomass}$ is required for the synthesis of glutathione (59) and chitin synthetis requires another $0.02 \text{ mmol N-acetylglucosamine per gram dry biomass}$ (182). Approximately one sixth of the proteins in the yeast proteome is estimated to be lysine acetylated (114). Even if all those proteins are simultaneously acetylated this would only correspond to an additional acetyl-CoA requirement of circa $2.5 \cdot 10^{-3} \text{ mmol per gram dry biomass}$ (including also poly-acetylation), assuming a protein content of 39% (230) and an average protein molecular weight of 56 kDa. The combined cytosolic acetyl-CoA requirement is therefore estimated at $1.16 \text{ mmol per gram dry biomass}$. Hence, the observed formate production in the anaerobic cultures of *acs1Δ acs2Δ* PFL-expressing *S. cerevisiae* is sufficient to account for the major ‘sinks’ of cytosolic acetyl-CoA in biosynthetic pathways.

3.3.3 Chemostat-based characterization of an Acs^- PFL-expressing *S. cerevisiae* strain

To analyze the physiological impact of replacing *ACS1* and *ACS2* by PFL, the reference strain CEN.PK113-7D (Acs^+) and strain IMZ383 (Acs^- expressing *E. coli* PFL) were grown in anaerobic, glucose-limited chemostats at a dilution rate of 0.10 h^{-1} (Table 3.4). Strain IMZ383 showed a 15% lower biomass yield on glucose as well as a proportionally increased ethanol production rate and reduced glycerol production rate relative to the reference strain. Conversely, acetate production by the PFL-expressing strain was five-fold higher than in the reference strain (Table 3.4). Formate, which was not detectable in cultures of the reference strain, was produced by the PFL-expressing strain at a rate of $0.18 \text{ mmol} \cdot \text{g biomass}^{-1} \cdot \text{h}^{-1}$. Acetate and formate have previously been shown to cause a reduction of biomass yields in cultures of *S. cerevisiae* by uncoupling the plasma membrane pH gradient (1, 231, 324). In anaerobic chemostat cultures, this uncoupling causes a concomitant increase of the ethanol production rate (1, 231, 324). Production of acetate and formate therefore offers a plausible explanation for the reduced biomass yield of the PFL-expressing strain.

Table 3.4. Physiology of the wild-type strain CEN.PK113-7D and the *E. coli* PFL expressing strain IMZ383 in anaerobic chemostat cultures with 25 g·L⁻¹ glucose, pH 5.0 and a dilution rate of 0.1 h⁻¹. Values and standard deviations shown are from three replicates.

	Units	CEN.PK113-7D	IMZ383
Relevant genotype		Ald ⁺ Acs ⁺	Ald ⁺ Acs ⁻ PFL
Dilution rate	(h ⁻¹)	0.099 ± 0.004	0.102 ± 0.004
Biomass yield	(g biomass·g glucose ⁻¹)	0.096 ± 0.002	0.082 ± 0.002
q _{glucose}	(mmol·g biomass ⁻¹ ·h ⁻¹)	-5.76 ± 0.15	-6.94 ± 0.31
q _{ethanol}	(mmol·g biomass ⁻¹ ·h ⁻¹)	9.51 ± 0.43	11.38 ± 0.49
q _{CO₂}	(mmol·g biomass ⁻¹ ·h ⁻¹)	9.93 ± 0.12	12.01 ± 0.37
q _{glycerol}	(mmol·g biomass ⁻¹ ·h ⁻¹)	0.82 ± 0.06	0.70 ± 0.03
q _{lactate}	(mmol·g biomass ⁻¹ ·h ⁻¹)	0.06 ± 0.004	0.04 ± 0.002
q _{pyruvate}	(mmol·g biomass ⁻¹ ·h ⁻¹)	0.01 ± 0.004	0.03 ± 0.001
q _{acetate}	(mmol·g biomass ⁻¹ ·h ⁻¹)	0.02 ± 0.003	0.11 ± 0.02
q _{formate}	(mmol·g biomass ⁻¹ ·h ⁻¹)	N.D.*	0.18 ± 0.01
Residual glucose	(g·L ⁻¹)	0.05 ± 0.002	0.15 ± 0.01
Carbon recovery	(%)	104 ± 2	100 ± 1

*N.D. = not detected

Table 3.5. MIPS and GO categories overrepresented in the genes that were significantly differential expressed (0.5 >= fold change (FC) or FC >= 2, false discovery rate <= 1%) in glucose-limited chemostat cultures of IMZ305 (Ald⁻ Acs⁻, expressing *E. coli* *eutE*, aerobic) and IMZ383 (Acs⁻ expressing *E. coli* PFL, anaerobic) compared to the reference strain CEN.PK113-7D (Ald⁺ Acs⁺) grown under the same conditions.

	Term id	Description	k ^a	n ^b	p-value
IMZ305 up (148 genes)					
MIPS	01.06.06	isoprenoid metabolism	7	41	3.96·10 ⁻⁵
	01.06.06.11	tetracyclic and pentacyclic triterpenes (cholesterin, steroids and hopanoids) metabolism	7	36	1.62·10 ⁻⁵
	32	CELL RESCUE, DEFENSE AND VIRULENCE	28	558	8.28·10 ⁻⁵
GO	I ^c GO:0006950	response to stress	13	161	9.46·10 ⁻⁵
	c ^d GO:0016125	sterol metabolic process	7	44	6.36·10 ⁻⁵
IMZ305 down (212 genes)					
MIPS	1	METABOLISM	80	1530	3.75·10 ⁻⁶
	01.05	C-compound and carbohydrate metabolism	37	510	3.76·10 ⁻⁶
	01.06.05	fatty acid metabolism	8	25	8.62·10 ⁻⁷
	2	ENERGY	34	360	2.00·10 ⁻⁸
	02.19	metabolism of energy reserves (e.g. glycogen, trehalose)	11	53	9.36·10 ⁻⁷
GO	I GO:0008152	metabolic process	36	389	1.23·10 ⁻⁸
	GO:0006635	fatty acid beta-oxidation	5	9	4.36·10 ⁻⁶
	GO:0055114	oxidation reduction	23	270	2.67·10 ⁻⁵
	c GO:0032787	monocarboxylic acid metabolic process	18	155	3.13·10 ⁻⁶

			Term id	Description	k	n	p-value
			GO:0006635	fatty acid beta-oxidation	5	9	4.36·10 ⁻⁶
			GO:0009062	fatty acid catabolic process	5	10	8.48·10 ⁻⁶
			GO:0019395	fatty acid oxidation	5	10	8.48·10 ⁻⁶
			GO:0034440	lipid oxidation	5	10	8.48·10 ⁻⁶
			GO:0016042	lipid catabolic process	9	43	8.76·10 ⁻⁶
			GO:0005975	carbohydrate metabolic process	28	361	1.97·10 ⁻⁵
			GO:0044242	cellular lipid catabolic process	7	27	2.03·10 ⁻⁵
			GO:0044262	cellular carbohydrate metabolic process	26	323	2.11·10 ⁻⁵
			GO:0055114	oxidation reduction	25	305	2.26·10 ⁻⁵
			GO:0044281	small molecule metabolic process	52	916	4.47·10 ⁻⁵
			GO:0009056	catabolic process	42	683	4.77·10 ⁻⁵
			GO:0006631	fatty acid metabolic process	10	65	4.78·10 ⁻⁵
			GO:0016054	organic acid catabolic process	9	53	5.16·10 ⁻⁵
			GO:0046395	carboxylic acid catabolic process	9	53	5.16·10 ⁻⁵
			GO:0015980	energy derivation by oxidation of organic compounds	16	161	7.88·10 ⁻⁵
IMZ383 up (71 genes)							
MIPS		20.01	transported compounds (substrates)	19	585	1.30·10 ⁻⁵	
		32	CELL RESCUE, DEFENSE AND VIRULENCE	20	558	1.56·10 ⁻⁶	
GO	l c	GO:0006811	ion transport	12	176	4.12·10 ⁻⁷	
		GO:0051186	cofactor metabolic process	10	192	4.49·10 ⁻⁵	
		GO:0006879	cellular iron ion homeostasis	5	41	8.11·10 ⁻⁵	
		GO:0055072	iron ion homeostasis	5	41	8.11·10 ⁻⁵	
		GO:0006811	ion transport	8	108	2.28·10 ⁻⁵	
IMZ383 down (29 genes)							
MIPS		1	METABOLISM	20	1530	3.58·10 ⁻⁷	
		01.01	amino acid metabolism	7	243	8.09·10 ⁻⁵	
		01.01.09.01	metabolism of glycine	4	8	2.38·10 ⁻⁸	
		01.01.09.01.02	degradation of glycine	4	6	5.12·10 ⁻⁹	
		01.05	C-compound and carbohydrate metabolism	13	510	9.58·10 ⁻⁸	
GO		01.05.05	C-1 compound metabolism	4	8	2.38·10 ⁻⁸	
		01.05.05.07	C-1 compound catabolism	3	5	8.38·10 ⁻⁷	
		02.16	fermentation	4	48	5.83·10 ⁻⁵	
		GO:0006730	one-carbon metabolic process	6	16	3.94·10 ⁻¹¹	
		GO:0055114	oxidation reduction	8	270	1.83·10 ⁻⁵	
		GO:0006082	organic acid metabolic process	13	397	4.68·10 ⁻⁹	
		GO:0019752	carboxylic acid metabolic process	13	397	4.68·10 ⁻⁹	
		GO:0043436	oxoacid metabolic process	13	397	4.68·10 ⁻⁹	
		GO:0042180	cellular ketone metabolic process	13	410	6.93·10 ⁻⁹	
		GO:0044281	small molecule metabolic process	17	916	3.82·10 ⁻⁸	
		GO:0006544	glycine metabolic process	4	9	4.26·10 ⁻⁸	

	Term id	Description	k	n	p-value
	GO:0009071	serine family amino acid catabolic process	3	5	$8.38 \cdot 10^{-7}$
	GO:0006730	one-carbon metabolic process	6	76	$8.92 \cdot 10^{-7}$
	GO:0032787	monocarboxylic acid metabolic process	7	155	$4.33 \cdot 10^{-6}$
	GO:0009069	serine family amino acid metabolic process	4	34	$1.45 \cdot 10^{-5}$
	GO:0055114	oxidation reduction	8	305	$4.41 \cdot 10^{-5}$
	GO:0016054	organic acid catabolic process	4	53	$8.63 \cdot 10^{-5}$
	GO:0046395	carboxylic acid catabolic process	4	53	$8.63 \cdot 10^{-5}$
IMZ305 up \cap IMZ383 up (8 genes)					
MIPS	20.01.01.01.01.01	siderophore-iron transport	2	12	$9.02 \cdot 10^{-5}$
GO	c GO:0006879	cellular iron ion homeostasis	3	41	$1.35 \cdot 10^{-5}$
	GO:0055072	iron ion homeostasis	3	41	$1.35 \cdot 10^{-5}$
	GO:0034755	iron ion transmembrane transport	2	5	$1.37 \cdot 10^{-5}$
	GO:0034220	ion transmembrane transport	3	48	$2.18 \cdot 10^{-5}$
	GO:0033212	iron assimilation	2	8	$3.83 \cdot 10^{-5}$
	GO:0030005	cellular di-, tri-valent inorganic cation homeostasis	3	72	$7.40 \cdot 10^{-5}$
	GO:0055066	di-, tri-valent inorganic cation homeostasis	3	72	$7.40 \cdot 10^{-5}$
IMZ305 down \cap IMZ383 down (8 genes)					
MIPS	02.25	oxidation of fatty acids	2	9	$4.93 \cdot 10^{-5}$
IMZ305 down \cap IMZ383 up (10 genes)					
no enrichment					
IMZ305 up \cap IMZ383 down (0 genes)					
empty set					

^a The number of genes differentially expressed present in the set

^b The number of genes of the set present in the whole genome.

GO categories are divided between ^c the GO leaf categories and ^d the GO complete categories.

Transcriptome analysis on anaerobic glucose-limited chemostat cultures yielded 71 genes whose transcript levels were higher, and 29 genes whose transcript levels were lower in IMZ383 (excluding *URA3*, *ACS1* and *ACS2*) than in the reference strain. The set of up-regulated genes showed an overrepresentation of the GO categories ion transport, cellular iron ion homeostasis and cofactor metabolic process. The transcriptional responses of genes involved in iron homeostasis may be related to the assembly in yeast of PFL-AE, which contains an oxygen-sensitive [4Fe-4S] cluster required for activation of PFL (173). Additionally, transcript levels of the formate dehydrogenase genes *FDH1* and *FDH2* were over 25-fold higher in the PFL-expressing strain. Among the genes that showed lower transcript levels in IMZ383 (Table 3.5), the GO category ‘glycine metabolic process’ was overrepresented. The four down-regulated genes in this category, *GCV1*,

Table 3.6. Physiology of *S. cerevisiae* strains CEN.PK113-7D (Ald⁺ Acs⁺) and IMZ305 (Ald⁻ Acs⁻ expressing *E. coli eutE*) in aerobic glucose-limited chemo \hat{s} tat cultures at a dilution rate of 0.1 h⁻¹. Averages and standard deviations were obtained from three replicates.

	Units	CEN.PK113-7D	IMZ305
Relevant genotype		Ald ⁺ Acs ⁺	Ald ⁻ Acs ⁻ <i>eutE</i>
Dilution rate	(h ⁻¹)	0.100 \pm 0.001	0.098 \pm 0.001
Biomass yield	(g biomass·g glucose ⁻¹)	0.501 \pm 0.002	0.429 \pm 0.009
q _{glucose}	(mmol·g biomass ⁻¹ ·h ⁻¹)	-1.10 \pm 0.01	-1.27 \pm 0.02
q _{ethanol}	(mmol·g biomass ⁻¹ ·h ⁻¹)	0.00 \pm 0.00	0.00 \pm 0.00
q _{CO₂}	(mmol·g biomass ⁻¹ ·h ⁻¹)	2.78 \pm 0.09	3.52 \pm 0.04
q _{O₂}	(mmol·g biomass ⁻¹ ·h ⁻¹)	-2.61 \pm 0.14	-3.36 \pm 0.02
q _{pyruvate}	(mmol·g biomass ⁻¹ ·h ⁻¹)	N.D.*	N.D.
q _{glycerol}	(mmol·g biomass ⁻¹ ·h ⁻¹)	N.D.	N.D.
q _{acetate}	(mmol·g biomass ⁻¹ ·h ⁻¹)	N.D.	N.D.
Residual glucose	(g·L ⁻¹)	0.03 \pm 0.01	0.04 \pm 0.02
Carbon recovery	(%)	102 \pm 1	98 \pm 2

* N.D. = not detected

GCV2, GCV3 and SHM2 encode proteins that, together with Lpd1, form the glycine cleavage system, which contributes to the synthesis of the C₁-donor 5,10-methylene tetrahydrofolate (5,10-MTHF) in *S. cerevisiae* (216). The observed down-regulation suggests that conversion of formate, produced by PFL, to 5,10-MTHF via Mis1 or Ade3 (278, 293) reduces the requirement for synthesis of C₁-donor compounds via the glycine cleavage pathway.

3.3.4 Characterization of an Ald⁻ Acs⁻ A-ALD expressing *S. cerevisiae* strain in chemo \hat{s} tats

The physiology of strain IMZ305 (Ald⁻ Acs⁻ expressing *E. coli eutE*) was studied in aerobic glucose-limited chemo \hat{s} tats at a dilution rate of 0.10 h⁻¹ and compared to that of the reference strain CEN.PK113-7D (Ald⁺ Acs⁺). Under fully aerobic conditions, the low residual glucose concentration in glucose-limited chemo \hat{s} tat cultures at low dilution rates (< ca. 0.25 h⁻¹), enables a fully respiratory sugar metabolism in wild-type *S. cerevisiae* strains (241, 328). Although the sugar metabolism of both strains was indeed completely respiratory (Table 3.6), the biomass yield on glucose of strain IMZ305 was 14% lower than that of the reference strain. The lower biomass yield was in agreement with higher rates of oxygen consumption and CO₂ production (Table 3.6). This lower biomass yield of strain IMZ305 was unexpected in view of the improved ATP-stoichiometry for producing cytosolic acetyl-CoA via A-ALD.

Chemo \hat{s} tat-based transcriptome analysis yielded 362 genes whose expression levels were different in strains CEN.PK113-7D (Ald⁺ Acs⁺) and IMZ305 (Ald⁻ Acs⁻ expressing *E. coli eutE*) based on the statistical criteria applied in this study. *URA3*, *ALD2*, *ALD3*, *ALD4*, *ALD5*, *ALD6*, *ACS1* and *ACS2* were not included in this comparison. Fisher's exact test analysis indicated the overrepresentation of several functional categories, involved in energy, metabolism (isoprenoids, triterpenes, fatty acids, sterol, lipids, monocarboxylic acids, carbohydrates and energy reserves), response to stress and cell res-

Table 3.7. Steady-state intracellular metabolites concentrations ($\mu\text{mol}\cdot\text{g dry weight}^{-1}$) and acetaldehyde concentration in the broth (mM) in *S. cerevisiae* cultures of CEN.PK113-7D ($\text{Ald}^+ \text{Acs}^+$) and IMZ305 ($\text{Ald}^- \text{Acs}^-$) expressing *E. coli eutE* in aerobic glucose-limited chemostat cultures at a dilution rate of 0.1 h^{-1} . Averages and mean deviations were obtained from two replicates.

Metabolite	CEN.PK113-7D	IMZ305
Glycolysis		
Fructose-1,6-bisphosphate	0.30 ± 0.02	1.96 ± 0.12
Dihydroxyacetone phosphate	0.19 ± 0.02	0.53 ± 0.05
2-Phosphoglycerate	0.42 ± 0.05	0.16 ± 0.02
3-Phosphoglycerate	4.41 ± 0.62	2.06 ± 0.27
Phosphoenolpyruvate	1.71 ± 0.37	0.29 ± 0.06
Pentose phosphate pathway		
Ribulose-5-phosphate	0.11 ± 0.03	0.23 ± 0.03
Xylulose-5-phosphate	0.26 ± 0.06	0.54 ± 0.08
Sedoheptulose-7-phosphate	2.60 ± 0.46	5.93 ± 0.68
Erythrose-4-phosphate	0.00 ± 0.00	0.01 ± 0.00
Amino acids		
Alanine	2.04 ± 0.05	5.24 ± 1.29
Isoleucine	0.27 ± 0.10	0.66 ± 0.11
Histidine	1.79 ± 0.20	4.65 ± 0.63
Lysine	3.30 ± 0.50	9.60 ± 1.72
Proline	0.25 ± 0.10	0.64 ± 0.16
Threonine	0.55 ± 0.10	1.28 ± 0.24
Tyrosine	0.37 ± 0.10	0.93 ± 0.13
Coenzymes and cofactors		
AMP	0.32 ± 0.02	0.72 ± 0.16
NAD^+	2.65 ± 0.18	3.04 ± 0.32
NADH	0.15 ± 0.04	0.05 ± 0.01
NADP^+	0.57 ± 0.08	0.78 ± 0.07
NADPH	2.70 ± 0.62	2.10 ± 0.72
Other		
Glycerol-3-phosphate	0.03 ± 0.02	0.10 ± 0.01
Intra- + extracellular		
Acetaldehyde	0.002 ± 0.000	0.028 ± 0.003

cue, defence and virulence (Table 3.5). To investigate the impact of possible changes in the levels of acetaldehyde, which is a substrate of both the A-ALD and ALD reactions, the transcriptome data were compared to those from a previous study on the transcriptional response of *S. cerevisiae* to acetaldehyde (5). Of a set of 1196 genes that showed an over 2-fold increase in transcript level upon exposure to acetaldehyde in the study of Aranda and Del Olmo (5), 56 were also up-regulated in strain IMZ305 relative to the reference strain. This overlap of the two gene sets was statistically highly significant (p -value $4.54 \cdot 10^{-8}$) and showed an overrepresentation of the GO category ‘response to stress’ (p -value $1 \cdot 10^{-5}$). Other genes that were previously reported to be up-regulated in response to acetaldehyde (e.g. *MET8*, *TPO2* and *MUP1* (5)) similarly showed elevated expression levels in IMZ305. Analysis of combined intracellular and extracellular concentrations of acetaldehyde in chemostat cultures, using a fast sampling and derivatization protocol, showed that acetaldehyde concentrations in cultures of strain IMZ305 were 12-fold higher than in cultures of the reference strain CEN.PK113-7D (Table 3.7).

Microscopic analysis of cultures of strain IMZ305 (Ald⁻ Acs⁻ expressing *E. coli eutE*) showed that this strain formed multicellular aggregates. The same atypical morphology was observed in shake-flask and chemostat cultures of IMZ290 (Ald⁻ expressing *E. coli eutE*) and IMZ291 (Ald⁻ expressing *L. innocua lin1129*) which indicates that it is not caused by deletion of *ACS1* and *ACS2* and is not dependent on the type of acetylating acetaldehyde dehydrogenase. The multicellular aggregates could not be disrupted by sonication, but were resolved into single cells by incubation with chitinase (data not shown). Multicellular aggregates were not observed in cultures of strain IMZ383 (Acs⁻ expressing *E. coli* PFL and PFL-AE), further indicating that they were specifically linked to the expression of A-ALD and/or ALD deletion. Viability staining of chemostat cultures of strain IMZ305 (Ald⁻ Acs⁻ expressing *E. coli eutE*) indicated that integrity of the plasma membrane was compromised in a significant fraction of the cells in the multicellular aggregates (Figure 3.3).

Cytosolic acetyl-CoA is a key precursor in yeast metabolism as well as a regulator of several important metabolic enzymes. To investigate whether replacing Acs1 and Acs2 by A-ALD affected concentrations of key compounds in central carbon metabolism, intracellular metabolite analysis was performed on aerobic, glucose-limited chemostat cultures of strain IMZ305 (Ald⁻ Acs⁻ expressing *E. coli eutE*) and on the reference strain CEN.PK113-7D (Ald⁺ Acs⁺). The compounds analysed included acetyl-CoA, intermediates of glycolysis, pentose phosphate pathway (PPP) and tricarboxylic acid cycle (TCA), amino acids, nucleotides, coenzymes and trehalose. A full list of analysed compounds and measured levels is presented in supplementary materials (Table S3.1). Intracellular concentrations of most of the compounds, including acetyl-CoA and CoA, were not significantly different in the two strains, suggesting that replacing ACS by A-ALD as main source of cytosolic acetyl-CoA did not cause major changes in the central metabolic pathways. However, for a few metabolites a fold-change of at least two was observed (Table 3.7). Lysine, whose synthesis requires cytosolic acetyl-CoA, was among six amino acids whose intracellular concentrations were higher in strain IMZ305. Intracellular levels of glycerol-3-phosphate, which forms the backbone of glycerolipids and is thereby linked to lipid synthesis, another important biosynthetic sink of cytosolic acetyl-CoA, were also higher in this strain. Further changes in IMZ305 included higher concentrations of four intermediates of the non-oxidative part of the pentose phosphate pathway and changes in the levels of several glycolytic intermediates (Table 3.7).

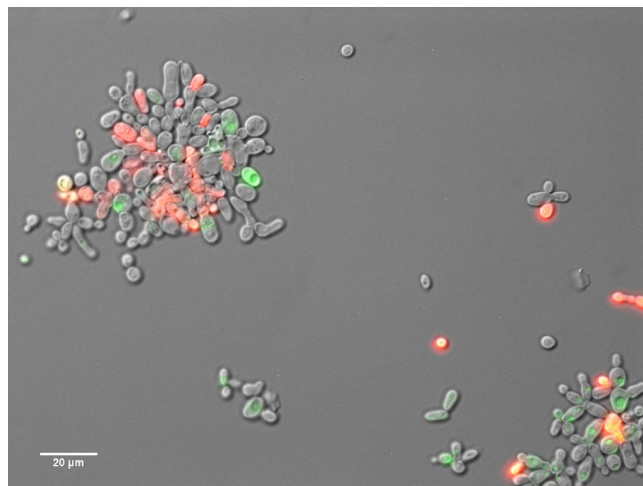


Figure 3.3. Fluorescent micrographs of double stained cells aggregates formed in chemo $\hat{\text{stat}}$ cultures of IMZ305 strain (Ald $^-$ Acs $^-$ expressing *E. coli eutE*). Cells were stained with acetoxymethyl ester of 5-carboxyfluorescein diacetate (CFDA, AM in DMSO, green) and propidium iodide (PI, red) to indicate metabolically active cells and cells with compromised integrity of the membrane, respectively. The bar corresponds to 20 μm .

3.4 DISCUSSION

Previous studies have demonstrated that increasing the availability of cytosolic acetyl-CoA improved rates of product formation in *S. cerevisiae* strains engineered for production of isoprenoids, fatty acids and polyhydroxybutyrate. Some of these studies were based on the overexpression of an acetyl-CoA synthetase that was insensitive to inhibition by acetylation, either alone or in combination with acetaldehyde dehydrogenase (43, 281). In other studies, availability of acetyl-CoA was boosted by expression of murine ATP-citrate lyase (307) or of a fungal phosphoketolase pathway that generates acetate (158). These previously studied heterologous pathways still require ATP for synthesis of cytosolic acetyl-CoA and, moreover, the native pathway via acetyl-CoA synthetase was still active in the engineered strains. The present study demonstrates, for the first time, that the native pathway for cytosolic acetyl-CoA biosynthesis in *S. cerevisiae* can be entirely replaced by heterologous pathways that, at least in terms of pathway stoichiometry, do not involve a net investment of ATP.

In wild-type *S. cerevisiae* genetic backgrounds, deletion of the two genes encoding isoenzymes of acetyl-CoA synthetase (*ACS1* and *ACS2*) resulted in a complete loss of viability, which was originally entirely attributed to a key role of acetyl-CoA synthetase in cytosolic acetyl-CoA synthesis (14, 245). Later studies investigated the role of *Acs2*, which has a dual cytosolic and nuclear localization, in histone acetylation (73, 306). Using a temperature-sensitive allele of *ACS2*, Takahashi *et al.* (306) showed that, in glucose-grown cultures, inactivation of *ACS2* caused global histone deacetylation and massive changes in gene expression, affecting over half of the yeast transcriptome. Using a similar approach Galdieri and Vancura (88) proposed that reduced nucleocytosolic acetyl-CoA concentrations primarily affect cell physiology via histone deacetylation rather than

via biosynthetic constraints. The limited and different transcriptome changes in strains IMZ305 (Ald⁻ Acs⁻ expressing *E. coli eutE*) and IMZ383 (Acs⁻ expressing *E. coli* PFL and PFL-AE) relative to an Acs⁺ reference strain indicated that, in these strains, activities of A-ALD and PFL, respectively, were sufficient to cover acetyl-CoA requirements for histone acetylation. These results also support the conclusion of Takahashi *et al.* (306) that Acs2 affects histone acetylation via provision of acetyl-CoA rather than via a direct catalytic or regulatory function in the acetylation process.

In addition to a possible effect on histone acetylation, changes in cytosolic acetyl-CoA biosynthesis might affect central metabolism via acetylation of non-histone proteins (106, 292, 298) and via its direct participation in key reactions. The fast growth of the engineered strains IMZ305 and IMZ383 suggest that there were no major kinetic limitations in acetyl-CoA provision. This conclusion was further substantiated by the minor differences in intracellular metabolite levels of strain IMZ305 relative to a reference strain. Intracellular acetyl-CoA concentrations in the two strains, which reflect the combination of mitochondrial and nucleocytosolic pools, were not significantly different. This observation is consistent with the conclusion of Cai *et al.* (29) that intracellular acetyl-CoA concentrations are subject to strong homeostatic regulation. However, the higher intracellular lysine concentrations in strain IMZ305 might be indicative for increased availability of cytosolic acetyl-CoA in this A-ALD-expressing strain. Despite the stoichiometric advantage of the A-ALD pathway with respect to ATP costs for acetyl-CoA synthesis, the biomass yield on glucose of strain IMZ305 was lower than that of the Ald⁺ Acs⁺ reference strain. Moreover, strain IMZ305 exhibited a reduced viability and formation of multicellular aggregates. Transcriptome analysis (Table 3.5) and direct measurements of acetaldehyde (Table 3.7) strongly suggested that these phenomena were due to acetaldehyde toxicity. Similar multicellular aggregates observed in *S. cerevisiae* cultures exposed to boric acid stress were attributed to activation of cell wall repair and overproduction of chitin, thereby disturbing cell division (272). Although whole-broth concentrations of acetaldehyde in cultures of strain IMZ305 were previously not reported to be toxic to *S. cerevisiae* (296), accumulation of acetaldehyde inside cells (297) may have led to underestimation of intracellular concentrations in our experiments. Matsufuji *et al.* (208) recently showed that reaction with glutathione contributes to acetaldehyde tolerance. Although the metabolic fate of the resulting acetaldehyde–glutathione adducts is unclear regeneration of free glutathione from these adducts may well require metabolic energy and/or reducing equivalents.

The increased acetaldehyde level in strain IMZ305 could be the result of the lower affinity for acetaldehyde of A-ALD in comparison to the native non-acetylating acetaldehyde dehydrogenases (Table 3.8) (335). Literature data on acetylating acetaldehyde dehydrogenases from other organisms suggest that a high K_M for acetaldehyde is a common characteristic of these enzymes (268, 284). The standard free energy change (ΔG° , pH 7, ionic strength of 0.2 M) of the A-ALD reaction is $-13.7 \text{ kJ}\cdot\text{mol}^{-1}$ (79). If measured intracellular metabolite concentrations (this study) and a cytosolic NAD⁺/NADH ratio of 100 (30) are assumed, $\Delta G'$ would be positive at the acetaldehyde concentrations measured in the reference strain ($+7.2 \text{ kJ}\cdot\text{mol}^{-1}$), while it would be close to zero ($+0.7 \text{ kJ}\cdot\text{mol}^{-1}$) at the higher acetaldehyde concentration measured in strain IMZ305. Increased intracellular levels of acetaldehyde may therefore not only be a consequence of a low affinity of

Table 3.8. Kinetic parameters of the acetylating acetaldehyde dehydrogenases EutE from *E. coli* and Lin1129 from *L. innocua* and of three out of five acetaldehyde dehydrogenases from *S. cerevisiae* (Ald2, Ald5 and Ald6). Activities were assayed as the oxidation of acetaldehyde to acetyl-CoA or acetate, respectively. Data for EutE and Lin1129 are the average of triplicate measurements on cell extracts from two independent shake-flask cultures.

Enzyme	K_m for acetaldehyde ($\mu\text{mol}\cdot\text{L}^{-1}$)	V_{\max} ($\mu\text{mol}\cdot\text{mg}$ $\text{protein}^{-1}\cdot\text{min}^{-1}$)	V_{\max}/K_m	References
EutE	$1.5\cdot 10^3$	9.4 ± 0.4	0.006	This study
Lin1129	$3.9\cdot 10^3$	9.2 ± 1.3	0.002	This study
Ald2	10	5.2	0.52	(335)
Ald5	58	1.1	0.019	(335)
Ald6	24	24	1	(335)

A-ALD for acetaldehyde, but also be thermodynamically required for acetyl-CoA synthesis via A-ALD. If this interpretation is correct, applicability of this reaction for product formation in engineered yeast strains will either require improved tolerance to acetaldehyde or further changes in the cytosolic concentrations of acetyl-CoA, NADH and/or NAD^+ .

Also the biomass yield on glucose of strain IMZ383 (Acs^- expressing *E. coli* PFL) in anaerobic cultures was lower than that of an Acs^+ reference strain. Weak-acid uncoupling by formate, the formation of which was stoichiometrically coupled to growth of this strain, offers a plausible explanation for this reduced biomass yield (231). To prevent accumulation and possible toxicity, the formate formed in the PFL reaction should preferably be oxidized to CO_2 via formate dehydrogenase. Depending on the product of interest, this conversion by formate dehydrogenase may also be required for redox balancing of product formation in engineered pathways. Although *FDH1* and *FDH2*, encoding the two NAD^+ -dependent formate dehydrogenase isoenzymes in *S. cerevisiae*, were transcriptionally strongly up-regulated in strain IMZ383, *in vivo* formate dehydrogenase activity was apparently not sufficient to oxidize all formate produced. Under standard conditions, formate oxidation ($\text{formate} + \text{NAD}^+ \rightleftharpoons \text{CO}_2 + \text{NADH} + \text{H}^+$) is thermodynamically feasible ($\Delta G^\circ = -13.9 \text{ kJ}\cdot\text{mol}^{-1}$, pH 7, ionic strength of 0.2 M (79)) and calculations showed that $\Delta G'$ is also negative under industrially relevant conditions (data not shown). Inefficient anaerobic oxidation of formate upon overexpression of *FDH1* was previously attributed to the sequential bi-bi two-substrate kinetics of formate dehydrogenase, which leads to a strongly decreased affinity for formate at low NAD^+ concentrations (95).

In *S. cerevisiae*, several metabolic reactions as well as protein deacetylation, yield free acetate. Nevertheless, no increased acetate concentrations were observed in cultures of strain IMZ305 ($\text{Ald}^- \text{Acs}^-$ *E. coli* *eutE*). This observation suggests that small amounts of acetate can be activated to acetyl-CoA via an Acs -independent pathway. A mitochondrial CoA transferase encoded by *ACH1* may, in theory, be responsible for acetate activation, using succinyl-CoA as CoA donor (80). However, *ACH1* was not up-regulated, neither in strain IMZ305 nor in strain IMZ383 (Acs^- expressing *E. coli* PFL). The latter strain did show increased production of acetate in comparison with Acs^+ reference strain, probably via pyruvate decarboxylase and acetaldehyde dehydrogenase, which were still present

in this strain. This observation suggests that a possible ACS-independent pathway for acetate activation in anaerobic *S. cerevisiae* cultures only has a very low capacity.

3.5 OUTLOOK

This study demonstrates that it is possible to entirely replace the ATP-intensive native pathway of cytosolic acetyl-CoA formation in *S. cerevisiae* by two different ATP-independent routes. Although these metabolic engineering strategies are stoichiometrically sound, our results show how their application can be kinetically and/or thermodynamically challenging. Before the full potential of the A-ALD and PFL strategies for generating cytosolic acetyl-CoA for industrial product formation can be realized, problems related to acetaldehyde toxicity and formate reoxidation, respectively, will need to be addressed. Availability of strains in which A-ALD and/or PFL are the only source of cytosolic acetyl-CoA will be of great value for their further optimization, either by targeted genetic modification or by evolutionary approaches. Alternatively, the native yeast pathway might be replaced by other mechanisms for cytosolic acetyl-CoA synthesis with an improved ATP stoichiometry, such as ATP-citrate lyase (which requires an input of one ATP for each pyruvate converted to cytosolic acetyl-CoA) or the combination of phosphoketolase and phosphotransacetylase. Even before the remaining challenges are solved, A-ALD and PFL can provide increased fluxes towards products that require cytosolic acetyl-CoA. For some products, this may ultimately even contribute to the replacement of expensive aerobic processes by cost-effective anaerobic conversions.

3.6 ACKNOWLEDGEMENTS

This work was carried out within the BE-Basic R&D Program, which was granted an FES subsidy from the Dutch Ministry of Economic affairs, agriculture and innovation (EL&I). We thank our colleagues Reza Maleki Seifar, Feibai Zhu, Marinka Almering, Marijke Luttik, Erik de Hulster, Marcel van den Broek and Nakul Barfa for technical support.

SUPPLEMENTARY MATERIALS

Table S3.1. Primers used in this study.

Number	Name	Sequence 5' → 3'
Primers for knockout cassettes		
1749	ALD2,3 KO Fw	GGATGCAATCTTGTCTGACACTCACTGATCATATCC CGAATTTTGTCTCAAGCACCAGAGCCGAGGATTCAT CAGCTGAAGCTTCGTACGC
1750	ALD2,3 KO Rv	ACATGGACTGATTTTATTTGTAAATAGTTATCAAC GCCGGTGTCTGCTGAGAGATAGCTCGAATCAGTCC GCATAGGCCACTAGTGGATCTG
1769	ALD4 KO Fw	ATGTTTCAGTAGATCTACGCTCTGCTTAAAGACGTC TGCATCCTCCATTGGTCTCTGCACGGATGCGTAGT CAGCTGAAGCTTCGTACGC
1770	ALD4 KO Rv	CACCAGGCTTATTGATGACCTTACTCGTCCAATTT GGCACGGACCGCTTTGGATCATAGTCATGCAGTTG GCATAGGCCACTAGTGGATCTG
1773	ALD5 KO Fw	CAAACGTGGTTAAGACAGAAAACCTTCTTCACAACA TTAACAAAAAGCCAAACATGAGCCATAAGTGTCTC CAGCTGAAGCTTCGTACGC
1774	ALD5 KO Rv	TGTTTATCATACATACCTTCAATGAGCAGTCAACT CGGGCCTGAGTTACTCGCGCTTATGCGATATAGTT GCATAGGCCACTAGTGGATCTG
1777	ALD6 KO Fw	ACTATCAGAATACAATGACTAAGCTACACTTTGAC ACTGCTGAACCAGTCTCTAAGCCGACAGGAGTCTC CAGCTGAAGCTTCGTACGC
1778	ALD6 KO Rv	TATGACGGAAAGAAATGCAGGTTGGTACATTACAA CTTAATTCTGACAGCTACCGAGTCAAGCAGTTTCAAG GCATAGGCCACTAGTGGATCTG
2616	ACS2-natNT2 KO Fw	ACAGAAAAGGAGCGAAATTTTATCTCATTACGAAA TTTTTCTCATTTAAGCCAGCTGAAGCTTCGTACGC
2617	ACS2-natNT2 KO Rv	TGTTATACACAAACAGAATACAGGAAAGTAAATCA ATACAATAATAAAATCGCATAGGCCACTAGTGGAT C
2622	ACS1-AmdS KO Fw	TTACAACCTTGACCGAATCAATTAGATGTCTAACAA TGCCAGGGTTTGACAGCGCAATTAACCCTCACTAA AG
2623	ACS1-AmdS KO Rv	TGCTATGTCTGCCCTCTGCCGTACAATCATCAAAAC TAGAAGAACAGTCAACTATAGGGCGAATTGGGTAC CG
2687	ACS2-HIS3 KO Fw	ACAGAAAAGGAGCGAAATTTTATCTCATTACGAAA TTTTTCTCATTTAAGCAGCTGAAGCTTCGTACGC
2688	ACS2-HIS3 KO Rv	TGTTATACACAAACAGAATACAGGAAAGTAAATCA ATACAATAATAAAATGCATAGGCCACTAGTGGATC TG


Number	Name	Sequence 5' → 3'
2929	ACS1-LEU2 KO Fw	AGCAAAACCAAACATATCAAACTACTAGAAAGAC ATTGCCCACTGTGCTCAGCTGAAGCTTCGTACGC
2930	ACS2-LEU2 KO Rv	AACACACGAAAAAAAAAAGTCGTCAATATAAAAA GGAAAGAAATCATCAGCATAGGCCACTAGTGGATC TG
Primers for verification of knockouts		
9	KanA	CGCACGTCAAGACTGTCAAG
10	Kan B	TCGTATGTGAATGCTGGTCTG
1076	LEU2_prom5'.K.laëtis	CACGTGACTGCGTGAATTG
1077	LEU2_3'.K.laëtis	AGCTTCCTACCTGACACTAAC
1751	LEU2_Ctrl_Fw	AACGCCCTATGATGTTCCCCG
1752	LEU2_Ctrl_Rv	ACACGGAACAGGGATGCTTG
1771	ald4 Ctrl Fw	GCGGGTGTAGGTAAGCAGAA
1772	ald4 Ctrl Rv	ACGGTAAGGTCTTGCCATCT
1775	ald5 Ctrl Fw	CGCGGAGCCTTTAGAATACC
1776	ald5 Ctrl Rv	GTACAGTCCCATAATGGCA
1779	ald6 Ctrl Fw	AAGCCTGGCGTGTTAACAA
1780	ald6 Ctrl Rv	GAAGGCACAAGCCTGTTCTC
1781	hph NT1 Fw / 2	TACTCGCCGATAGTGGAAC
1782	hph NT1 Rv / 2	CAGAACTTCTCGACAGACG
2618	acs2 CtrlFw	TACCCTATCCCGGGCGAAGAAC
2619	acs2 KO Ctr lRv	CCGATATTCGGTAGCCGATTCC
2620	Nat Ctrl Fw	GCCGAGCAAATGCCTGCATAATC
2621	Nat Ctrl Rv	GGTATTCTGGGCCCTCCATGTGC
2624	acs1 Ctrl Fw	ATCATTACAACCTGACCGAATC
2625	acs1 Ctrl Rv	CCTCGGTGGCAAATAGTTCTCC
2626	AmdS Ctrl Fw	TGGCTATCGCTGAAGAAGTTGG
2627	AmdS Ctrl Rv	CTTCCCAAGATTGTGGCATGTC
2927	ACS1 KO ctrl Fw	AAACTGGGCGGCTATTCTAAGC
2928	ACS1 KO ctrl Rv	AGCAGCTCGGTTATAAGAGAAC
Primers for verification of plasmid presence		
586	p426GPD Fw	CATTCAAGGCTGCGCAACTG
1153	GPDp Fw	GACCCACGCATGTATCTATCTC
1368	mhpF Fw	GGGGACAAGTTTGTACAAAAAAGCAGGCTATGAGT AAGCGTAAAGTCGCCATTATCGG
1369	mhpF Rv	GGGGACCACTTTGTACAAGAAAGCTGGGTGTTTCAT GCCGCTTCTCCTGCCTTGC
1372	dmpF Fw	CATTGATTGCGCCATACG
1373	dmpF Rv	CCGTAATATCGGAACAGAC
2038	adhE S. aureus Fw	TATCGGTGACATGTACAAC
2039	adhE S. aureus Rv	TTGCTTGTAAGTCGTAAGAAG
2040	EutE E.coli Fw	GAACCAACAAGACATCGAAC
2041	EutE E.coli Rv	ACGATTCTGAAAGCGTCAAC
2042	Lin1129 Fw	GGAACAATTGGTTAAGAAGG
2043	Lin1129 Rv	ATAGAGAAACCGTCAGTCAA
1642	pRS426 Fw	TTTCCCAAGTCACGACGTTG
2675	pTPI1 Rv	CCGCACTTTCTCCATGAGG

Number	Name	Sequence 5' → 3'
2677	pRS426 Rv	CTTCCGGCTCCTATGTTGTG
Primers for cloning		
3384	pTPI1 Fw (pRS424)	ACGGCCAGTGAGCGCGTAATACGACTCACTATA GGGCGAATTGGGTACCGGGCCCCCTCGAGAAGG ATGAGCCAAGAATAAG
3385	tGND2 Rv	GAATTCCGTTTAGTGCAATATATTGGAGTTC
3386	pFBA1 Fw (tGND2)	AAATCGAGTAGAATCTAGCCATAGTCTTTC
3387	tPMA1 Rv(pRS424)	CCTCACTAAAGGGAACAAAAGCTGGAGCTCCACCG CGGTGGCGCGCTCTAGAACTAGTGGATCCAAAC GTGTGTGTGC

Table S3.2. Full list of measured steady-state intracellular metabolites concentrations ($\mu\text{mol} \cdot (\text{g dry weight})^{-1}$) in *S. cerevisiae* cultures of CEN.PK113-7D (Ald⁺ Acs⁺) and IMZ305 (Ald⁻ Acs⁻ expressing *E. coli eutE*) in aerobic glucose-limited chemostat cultures at a dilution rate of 0.10 h^{-1} . Averages and mean deviations were obtained from two replicates.

Metabolite	CEN.PK113-7D	IMZ305
Glycolysis		
2-Phosphoglycerate	0.42 ± 0.05	0.16 ± 0.02
3-Phosphoglycerate	4.41 ± 0.62	2.06 ± 0.27
Dihydroxyacetone phosphate	0.19 ± 0.02	0.53 ± 0.05
Fructose-6-phosphate	0.73 ± 0.17	0.84 ± 0.17
Fructose-1,6-bisphosphate	0.30 ± 0.03	1.96 ± 0.11
Glucose	0.84 ± 0.03	1.14 ± 0.11
Glucose-6-phosphate	3.16 ± 0.54	3.62 ± 0.62
Glyceraldehyde phosphate	0.03 ± 0.00	0.05 ± 0.01
Phosphoenolpyruvate	1.71 ± 0.37	0.29 ± 0.06
Pyruvate	0.29 ± 0.06	0.40 ± 0.04
Tricarboxylic acid cycle		
α -Ketoglutarate	0.29 ± 0.08	0.40 ± 0.08
Citrate	6.87 ± 0.56	10.57 ± 0.53
Fumarate	0.10 ± 0.02	0.16 ± 0.03
Isocitrate	0.17 ± 0.04	0.30 ± 0.04
Malate	0.63 ± 0.14	1.05 ± 0.10
Succinate	0.15 ± 0.10	0.21 ± 0.08
Pentose phosphate pathway		
6-Phosphogluconate	0.65 ± 0.05	0.95 ± 0.10
Erythrose-4-phosphate	0.00 ± 0.00	0.01 ± 0.00
Ribose-5-phosphate	0.28 ± 0.03	0.41 ± 0.06
Ribulose-5-phosphate	0.11 ± 0.03	0.23 ± 0.03
Sedoheptulose-7-phosphate	2.60 ± 0.46	5.93 ± 0.68
Xylulose-5-phosphate	0.26 ± 0.06	0.54 ± 0.08
Amino acids		
Alanine	2.04 ± 0.48	5.24 ± 1.29
Asparagine	1.26 ± 0.27	1.32 ± 0.15
Aspartate	4.05 ± 1.04	4.38 ± 0.35

Metabolite	CEN.PK113-7D	IMZ305
Cysteine	0.08 ± 0.01	0.15 ± 0.01
Glutamate	34.49 ± 7.26	44.95 ± 8.97
Glutamine	9.53 ± 2.08	10.63 ± 2.17
Glycine	0.28 ± 0.05	0.47 ± 0.06
Histidine	1.79 ± 0.25	4.65 ± 0.63
Isoleucine	0.27 ± 0.07	0.66 ± 0.11
Leucine	0.17 ± 0.04	0.26 ± 0.05
Lysine	3.30 ± 0.50	9.60 ± 1.72
Methionine	0.03 ± 0.01	0.03 ± 0.00
Ornithine	4.03 ± 0.41	5.12 ± 0.56
Phenylalanine	0.19 ± 0.05	0.36 ± 0.03
Proline	0.25 ± 0.06	0.64 ± 0.16
Serine	0.56 ± 0.12	0.86 ± 0.12
Threonine	0.55 ± 0.14	1.28 ± 0.24
Tryptophane	0.11 ± 0.02	0.16 ± 0.03
Tyrosine	0.37 ± 0.07	0.93 ± 0.13
Valine	1.12 ± 0.29	2.02 ± 0.49
Coenzymes and cofactors		
Acetyl-CoA	0.17 ± 0.03	0.21 ± 0.04
ADP	1.57 ± 0.08	2.19 ± 0.21
AMP	0.32 ± 0.02	0.72 ± 0.16
ATP	7.80 ± 0.41	9.07 ± 0.97
CoA	0.19 ± 0.08	0.23 ± 0.02
FAD	0.09 ± 0.00	0.12 ± 0.01
NAD ⁺	2.65 ± 0.18	3.04 ± 0.32
NADH	0.15 ± 0.04	0.05 ± 0.01
NADP ⁺	0.57 ± 0.08	0.78 ± 0.07
NADPH	2.70 ± 0.62	2.10 ± 0.72
Other		
Glucose-1-phosphate	0.15 ± 0.03	0.18 ± 0.03
Glycerol-3-phosphate	0.03 ± 0.02	0.10 ± 0.01
Trehalose	93.56 ± 6.79	50.33 ± 4.71
Trehalose-6-phosphate	0.23 ± 0.03	0.42 ± 0.02
UDP-Glucose	2.62 ± 0.29	2.78 ± 0.16



ALTERNATIVE REACTIONS AT THE INTERFACE OF GLYCOLYSIS AND CITRIC ACID CYCLE IN *SACCHAROMYCES* *CEREVISIAE*

CHAPTER

4

Harmen M. van Rossum, Barbara U. Kozak, Matthijs S. Niemeijer, Hendrik J. Duine, Marijke A.H. Luttik, Viktor M. Boer, Peter Kötter, Jean-Marc G. Daran, Antonius J.A. van Maris and Jack T. Pronk

Abstract

Pyruvate and acetyl-coenzyme A, located at the interface between glycolysis and TCA cycle, are important intermediates in yeast metabolism and key precursors for industrially relevant products. Rational engineering of their supply requires knowledge of compensatory reactions that replace predominant pathways when these are inactivated. This study investigates effects of individual and combined mutations that inactivate the mitochondrial pyruvate-dehydrogenase (PDH) complex, extramitochondrial citrate synthase (Cit2) and mitochondrial CoA-transferase (Ach1) in *Saccharomyces cerevisiae*. Additionally, strains with a constitutively expressed carnitine shuttle were constructed and analyzed. A predominant role of the PDH complex in linking glycolysis and TCA cycle in glucose-grown batch cultures could be functionally replaced by the combined activity of the cytosolic PDH bypass and Cit2. Strongly impaired growth and a high incidence of respiratory deficiency in *pda1Δ ach1Δ* strains showed that synthesis of intramitochondrial acetyl-CoA as a metabolic precursor requires activity of either the PDH complex or Ach1. Constitutive overexpression of *AGP2*, *HNMI*, *YAT2*, *YAT1*, *CRC1* and *CAT2* enabled the carnitine shuttle to efficiently link glycolysis and TCA cycle in L-carnitine-supplemented, glucose-grown batch cultures. Strains in which all known reactions at the glycolysis-TCA cycle interface were inactivated still grew slowly on glucose, indicating additional flexibility at this key metabolic junction.

4.1 INTRODUCTION

In many organisms, the Embden-Meyerhof variant of glycolysis catalyzes oxidation of glucose to pyruvate. The subsequent oxidative decarboxylation of pyruvate yields acetyl coenzyme A (acetyl-CoA), which can be fully oxidized to carbon dioxide in the tricarboxylic acid (TCA) cycle. In addition to their roles as dissimilatory pathways, glycolysis and TCA cycle provide key biosynthetic precursors. Both of these ‘textbook’ pathways have been intensively studied but, even in the intensively studied eukaryotic model organism *Saccharomyces cerevisiae*, their interface is less well understood.

Cytosolic pyruvate can be imported into the mitochondrial matrix via the transporters Mpc1, 2 and/or 3 (23, 116). Direct oxidative decarboxylation by the mitochondrial pyruvate-dehydrogenase (PDH) complex yields acetyl-CoA in the mitochondrial matrix (pyruvate + NAD⁺ + CoA → acetyl-CoA_{mit} + NADH + H⁺ + CO₂). Null mutants in *PDA1*, which encodes the essential E1α subunit of the PDH complex, show a reduced growth rate in aerobic batch cultures on glucose synthetic media (338). Moreover, they exhibit an increased frequency of respiratory-deficient mutants and loss of mitochondrial DNA (338). Alternatively, acetyl-CoA can be formed in the cytosol of *S. cerevisiae* via a reaction sequence known as the PDH bypass (122, 244), consisting of pyruvate decarboxylase (pyruvate → acetaldehyde + CO₂), acetaldehyde dehydrogenase (acetaldehyde + NAD⁺ + H₂O → acetate + NADH + H⁺) and acetyl-CoA synthetase (acetate + ATP + CoA ⇌ acetyl-CoA_{cyt} + AMP + PP_i). Glucose-grown cultures of *S. cerevisiae*, which unlike many other eukaryotes does not contain ATP-citrate lyase (20), depend on this route for synthesis of acetyl-CoA in the nucleocytoplasmic compartment, where it acts as a precursor for synthesis of lipids, *N*-acetylglucosamine, sterols and lysine (81, 82, 230) and as acetyl donor for protein acetylation (114, 306). An observed 13% reduction of the biomass yield on glucose of *pda1Δ* mutants in aerobic, glucose-limited chemostat cultures was quantitatively consistent with rerouting of respiratory pyruvate metabolism via the cytosolic, ATP-consuming PDH bypass (245). The nucleocytoplasmic localization of acetyl-CoA synthetase in *S. cerevisiae* (14, 142, 244, 306) implies that the PDH bypass cannot directly generate intramitochondrial acetyl-CoA. Two mechanisms might link glycolysis and the TCA cycle in PDH-negative *S. cerevisiae* mutants (Figure 4.1). Firstly, cytosolic acetyl-CoA might first be converted to citrate via the extramitochondrial citrate synthase isoenzyme Cit2 (Figure 4.1) (152, 321), followed by uptake of citrate via the mitochondrial transporter Ctp1 (147). Alternatively, a transport or shuttle mechanism might catalyze translocation of cytosolic acetyl-CoA into the mitochondria.

In many eukaryotes, the carnitine shuttle is responsible for translocation of acetyl moieties across organellar membranes. The carnitine shuttle involves cytosolic and organellar acetyl-CoA:carnitine *O*-acetyltransferases (acetyl-CoA + L-carnitine ⇌ acetyl-L-carnitine + CoA) (15). In *S. cerevisiae*, acetyl-L-carnitine can be transported across the mitochondrial membrane by the mitochondrial acetyl-carnitine translocase Crc1 (84, 160, 233, 258). The three acetyl-carnitine transferases in *S. cerevisiae* have different subcellular localizations: Cat2 is peroxisomal and mitochondrial (69), Yat1 is localised to the outer mitochondrial membrane (271) and Yat2 is reported to be cytosolic (129, 159, 305). Since *S. cerevisiae* cannot synthesize L-carnitine *de novo*, activity of the

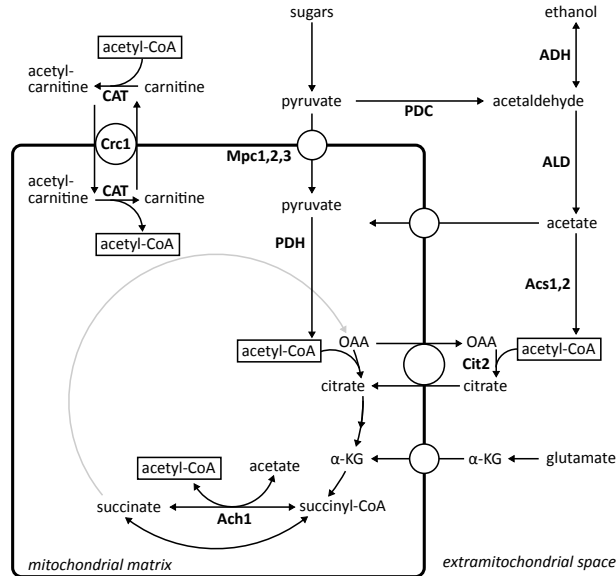


Figure 4.1. Mechanisms important for the provision of acetyl moieties in *Saccharomyces cerevisiae* mitochondria. In glycolysis glucose is converted to pyruvate, which can be transported into the mitochondria via the mitochondrial pyruvate carriers Mpc1, Mpc2 and Mpc3, followed by its conversion to acetyl-CoA via the pyruvate dehydrogenase (PDH) complex. Alternatively, pyruvate can be converted to cytosolic acetyl-CoA via the pyruvate dehydrogenase bypass. Cytosolic acetyl-CoA can be condensed with oxaloacetate via Cit2 to form citrate, which can be exchanged with, for example, mitochondrial oxaloacetate, and hence fuel the TCA cycle. Acetate from the cytosol can also be activated to mitochondrial acetyl-CoA via Ach1 by transfer of the CoA group from succinyl-CoA to acetate. Only when cells are supplemented with L-carnitine, the carnitine shuttle can transport cytosolic acetyl units into the mitochondria. Abbreviations: α -KG, α -ketoglutarate; Acs1, Acs2, acetyl-CoA synthetase; Ach1, CoA transferase; ADH, alcohol dehydrogenase; ALD, acetaldehyde dehydrogenase; CAT, carnitine acetyltransferase; Cit2, citrate synthase; Crc1, acetyl-carnitine translocase; Mpc1, Mpc2, Mpc3, mitochondrial pyruvate carrier; OAA, oxaloacetate; PDC, pyruvate decarboxylase; PDH, pyruvate dehydrogenase complex.

carnitine shuttle is strictly dependent on uptake of exogenous carnitine via the Hnm1 transporter, whose expression is regulated by Agp2 (4, 257, 258, 305). Strong transcriptional repression of the carnitine shuttle structural genes by glucose (69, 151, 271) would seem to prevent an important contribution in glucose-grown batch cultures, even when carnitine is present.

At least two metabolic processes in *S. cerevisiae* are strictly dependent on intramitochondrial acetyl-CoA. Although the bulk of lipid synthesis in *S. cerevisiae* occurs in the cytosol, long-chain fatty acids needed for lipoic acid biosynthesis are exclusively synthesized in the mitochondrial matrix (24). Additionally, arginine biosynthesis requires catalytic amounts of intramitochondrial acetyl-CoA (138). The ability of *pda1* Δ mutants to grow on glucose in synthetic media lacking L-carnitine indicates that, in addition to the PDH complex, *S. cerevisiae* must contain at least one other mechanism for mitochondrial acetyl-CoA provision. Ach1, a key candidate for this role, was first described as an acetyl-CoA hydrolase (28, 181). Later, it was demonstrated to have in fact a much higher *in vitro* activity for the transfer of the CoA group from various

acyl-CoA substrates to other organic acids (80). One such reaction involves the transfer of the CoA-group from succinyl-CoA to acetate, forming acetyl-CoA (succinyl-CoA + acetate \rightleftharpoons acetyl-CoA + succinate). This Ach1 catalyzed reaction could generate mitochondrial acetyl-CoA from acetate, derived from the PDH bypass, and mitochondrial succinyl-CoA, derived from the TCA cycle (via the α -ketoglutarate dehydrogenase complex) or via ATP-dependent activation of succinate by succinyl-CoA ligase (succinate + ATP + CoA \rightleftharpoons succinyl-CoA + ADP + Pi). Although a role of Ach1 in mitochondrial acetyl-CoA synthesis has been shown before (68, 80, 225), its significance in glucose-grown batch cultures of wild-type and mutant *S. cerevisiae* strains remains to be elucidated.

The aim of the present study is to assess the relative importance of different alternative reactions active at the interface of glycolysis and TCA cycle in *S. cerevisiae* strains that lack a functional PDH complex. To this end, we reinvestigated growth of *pda1Δ S. cerevisiae* on glucose in synthetic medium and analysed the effects of additional null mutations in *ACH1* and *CIT2* on growth rate, respiratory competence and metabolite formation. Moreover, we investigate whether constitutive expression of carnitine-shuttle genes enables the carnitine shuttle to function as an effective link between glycolysis and TCA cycle in glucose-grown batch cultures supplemented with L-carnitine.

4.2 MATERIALS AND METHODS

GROWTH MEDIA

Yeast-extract/peptone (YP) medium was prepared with demineralized water, 10 g·L⁻¹ Bacto yeast extract (BD, Franklin Lakes, NJ, USA) and 20 g·L⁻¹ Bacto peptone (BD). Synthetic medium with ammonium as nitrogen source (SM-ammonium) was prepared according to Verduyn *et al.* (326). Synthetic medium with other nitrogen sources was prepared similarly, but with 38 mM K₂SO₄ instead of (NH₄)₂SO₄ and with 38 mM urea (SM-urea), 76 mM L-glutamate (SM-glutamate). These modifications were made to maintain equivalent concentrations of nitrogen and sulfate relative to the original medium description. Media with these alternative nitrogen sources were sterilized with 0.2 μm bottle-top filters (Thermo Fisher Scientific, Waltham, MA, USA). Solid media were prepared by addition of 20 g·L⁻¹ agar (BD) prior to heat sterilization of the medium for 20 min at 121 °C.

STRAINS, GROWTH CONDITIONS AND STORAGE

The *S. cerevisiae* strains used in this study (Table 4.1) share the CEN.PK genetic background (71, 222). Shake-flask cultures were grown at 30 °C in 500 mL flasks containing 100 mL SM-ammonium with 20 g·L⁻¹ glucose, in an Innova incubator shaker (New Brunswick Scientific, Edison, NJ, USA) set at 200 rpm. Stock cultures were grown in YP medium with 20 g·L⁻¹ glucose. For strains IMK640, IMK641, IMX710 and IMX744, 2% (v/v) ethanol was used as carbon source to prevent loss of respiratory competence. Frozen stocks were prepared by adding 30% (v/v) glycerol to exponentially growing cultures and stored in 1 mL aliquots at -80 °C. To induce sporulation, strains were pre-grown in YP medium with 10 g·L⁻¹ potassium acetate, followed by incubation in sporulation medium (demineralized water, 20 g·L⁻¹ potassium acetate, pH 7.0) (75).

STRAIN AND PLASMID CONSTRUCTION

S. cerevisiae strains were transformed according to Gietz and Woods (97). Mutants were selected on solid YP medium, supplemented with 20 g·L⁻¹ glucose and the appropriate antibiotic, 200 mg·L⁻¹ G418 (InvivoGen, San Diego, CA, USA) or 100 mg·L⁻¹ nourseothricin (Jena Bioscience,

Table 4.1. *Saccharomyces cerevisiae* strains used in this study and their relevant genotypes.

Name	Relevant genotype	Parental strain(s)	Origin
CEN.PK113-7D	<i>MATa</i>		P. Kötter
IMK439	<i>MATa ura3Δ::loxP-kanMX-loxP</i>	CEN.PK113-1A	(100)
IMX585	<i>MATa can1Δ::cas9-natNT2</i>	CEN.PK113-7D	(200)
CEN.PK541-1A	<i>MATa pda1Δ::loxP-kanMX-loxP</i>		This study
CEN.PK542-1A	<i>MATa cit2Δ::loxP-kanMX-loxP</i>		This study
CEN.PK544-4D	<i>MATa pda1Δ::loxP-kanMX-loxP</i> <i>cit2Δ::loxP-kanMX-loxP</i>		This study
IMK627	<i>MATa ach1Δ::loxP-natNT2-loxP</i>	CEN.PK113-7D	This study
IMK629	<i>MATa cit2Δ::loxP-kanMX-loxP</i> <i>ach1Δ::loxP-natNT2-loxP</i>	CEN.PK542-1A	This study
IMK640	<i>MATa pda1Δ::loxP-kanMX-loxP</i> <i>ach1Δ::loxP-natNT2-loxP</i>	CEN.PK541-1A	This study
IMK641	<i>MATa pda1Δ::loxP-kanMX-loxP</i> <i>cit2Δ::loxP-kanMX-loxP</i> <i>ach1Δ::loxP-natNT2-loxP</i>	CEN.PK544-4D	This study
IMX710	<i>MATa can1Δ::cas9-natNT2 pda1Δ ach1Δ</i>	IMX585	This study
IMX744	<i>MATa can1Δ::cas9-natNT2 pda1Δ ach1Δ</i> <i>sga1Δ::[CARN]*</i>	IMX710	This study
IMD015	<i>MATa ura3Δ::loxP-kanMX-loxP × MATa URA3</i> <i>can1Δ::cas9-natNT2 pda1Δ ach1Δ</i> <i>sga1Δ::[CARN]</i>	IMK439 × IMX744	This study
IMX868	<i>MATa can1Δ::cas9-natNT2 URA3 PDA1 ACH1</i> <i>sga1Δ::[CARN]</i>	IMD015	This study

*[CARN], *pTDH3-AGP2-tAGP2 pPGK1-HNM1-tHNM1 pADH1-YAT2-tYAT2 pPGI1-YAT1-tYAT1 pTPI1-CRC1-tCRC1 pTEF1-CAT2-tCAT2*

Jena, Germany). SM containing 10 mM acetamide as the sole nitrogen source (SM-acetamide) was used for selection of the *amdSYM* marker (288). Deletion cassettes for *PDA1* and *CIT2* were constructed with a PCR-based method using pUG6 as template (108), using primer pairs 9087 & 9088 and 9089 & 9090, respectively. Thus amplified *kanMX* cassettes were used to replace the target genes in the prototrophic diploid strain CEN.PK122 (*MATa/MATa*). Transformants were verified for correct gene replacement by diagnostic PCR (Table S4.2). After sporulation and tetrad dissection, the haploid deletion strains CEN.PK541-1A (*MATa pda1Δ*) and CEN.PK542-1A (*MATa cit2Δ*) were obtained. To obtain a strain with both *CIT2* and *PDA1* deleted, strains CEN.PK541-1A and CEN.PK542-1A were crossed. After tetrad dissection, spores showing the non-parental ditype for the *kanMX* marker were analysed by diagnostic PCR to confirm correct deletion of both genes, resulting in strain CEN.PK544-4D (*MATa pda1Δ cit2Δ*). Deletion of *ACH1* in strains CEN.PK113-7D, CEN.PK542-1A, CEN.PK541-1A and CEN.PK544-4D was achieved by integration of the *natNT2* marker into its locus. The *natNT2* cassette was PCR amplified from pUG-natNT2 (164) with primer pair 3636 & 3637. Correct deletion was verified by colony PCR (195) using the primers shown in Table S4.2, resulting in strains IMK627, IMK629, IMK640 and IMK641, respectively.

IMX710 was constructed by removing *PDA1* and *ACH1* in strain IMX585 using the CRISPR/-Cas9 system, by introduction of a plasmid containing two guideRNA (gRNA) cassettes, targeting *PDA1* and *ACH1*. The plasmid was constructed as described before (200), with primers 5794 & 6159 to incorporate the appropriate target sites and with pROS13 as a backbone, resulting in plasmid pUDE340. Strain IMX585 was transformed with plasmid pUDE340 together with the repair fragments that were obtained by annealing primers 6157 & 6158 (*PDA1* deletion) and 6160 & 6161 (*ACH1* deletion). After confirmation of the gene deletions using diagnostic PCR (Table S4.2), plasmid pUDE340 was removed as described before (200), resulting in strain IMX710.

Strain IMX744 was obtained by placing the genes encoding the carnitine shuttle proteins (*HNM1*, *AGP2*, *CRC1*, *YAT1*, *YAT2* and *CAT2*), under control of strong constitutive promoters and integrat-

ing them into the *SGA1* locus. *SGA1* encodes a glucoamylase that is not expressed during vegetative growth of *S. cerevisiae* (342). Its inactivation was therefore considered to be neutral under the conditions employed in this study. For this purpose, the constitutive promoters *pTPI1*, *pTDH3*, *pADH1*, *pTEF1*, *pPGK1* and *pPGI1* were amplified by PCR from plasmids pUD301 – pUD306 (167) (Table S4.1 and S4.3). The ORFs of the six genes involved in the carnitine shuttle, together with their terminator sequences, were amplified from the CEN.PK113-7D genome and fused to the constitutive promoters with fusion PCR (344) (See Table S4.3 for primers and templates). Gene cassettes were ligated in pJET1.2 (Life Technologies, Carlsbad, CA, USA) and the resulting plasmids (pUD366 – pUD371; Table 4.1) were verified by Sanger sequencing (BaseClear BV, Leiden, The Netherlands). The plasmid with the gRNA cassette targeting *SGA1* (pUDR119) was constructed by Gibson Assembly of the pMEL11 backbone (200), obtained by PCR with pMEL11 as a template and using primers 5792 & 5980, and the gRNA cassette, obtained by PCR with primers 5979 & 7023 using the same template. Strain IMX710 was transformed with plasmid pUDR119 and the six gene cassettes, amplified from plasmids pUD366 – pUDE371 with PCR using primers as indicated in Table S4.3. The six gene cassettes were concatenated via *in vivo* homologous recombination, mediated by 60 bp overlapping sequences, and after a Cas9 induced double-strand break, integrated into the *SGA1* locus. After confirmation of correct integration by diagnostic PCR (for primers see Table, pUDR119 was removed as described before (200), resulting in strain IMX744 (*MATa can1Δ::cas9-natNT2 pda1Δ ach1Δ sga1Δ::pTDH3-AGP2-tAGP2 pPGK1-HNM1-tHNM1 pADH1-YAT2-tYAT2 pPGI1-YAT1-tYAT1 pTPI1-CRC1-tCRC1 pTEF1-CAT2-tCAT2*). The set of genes that are involved in the carnitine shuttle and introduced in the *SGA1* locus are further referred to as {CARN}. IMX868 was obtained by crossing, sporulation and spore dissection. Strain IMX744 (*MATa*) was crossed with IMK439 (*MATα*) by selecting for diploids on YP medium with 20 g·L⁻¹ glucose, G418 and nourseothricin. The resulting diploid IMD015 was sporulated and the asci were dissected on YP with 20 g·L⁻¹ glucose using a micromanipulator (Singer Instruments, Watchet, UK). One spore with the desired genotype (*PDA1 ACH1 URA3 sga1Δ::{CARN}*) was stocked as IMX868.

MOLECULAR BIOLOGY TECHNIQUES

PCR amplification with Phusion® Hot Start II High Fidelity Polymerase (Thermo Fisher Scientific) was performed according to the manufacturer's instructions using HPLC- or PAGE-purified oligonucleotide primers (Sigma-Aldrich). Diagnostic PCR was done via colony PCR on randomly picked yeast colonies, using DreamTaq (Thermo Fisher Scientific) and desalted primers (Sigma-Aldrich). DNA fragments obtained by PCR were separated by gel electrophoresis on 1% (w/v) agarose gels (Thermo Fisher Scientific) in TAE buffer (Thermo Fisher Scientific) at 100 V for 30 min. Alternatively, fragments were purified using the GenElute™ PCR Clean-Up Kit (Sigma-Aldrich). Plasmids were isolated from *Escherichia coli* with Sigma GenElute™ Plasmid kit (Sigma-Aldrich) according to the supplier's manual. Yeast genomic DNA was isolated using a YeaStar Genomic DNA kit (Zymo Research) or using an SDS/LiAc-based lysis protocol (195). *E. coli* DH5α (18258–012, Life Technologies) was used for chemical transformation or for electroporation. Chemical transformation was done according to Inoue *et al.* (133). Electrocompetent DH5α cells were prepared according to Bio-Rad's protocol, with the exception that during the preparation of competent cells, *E. coli* was grown in LB medium without NaCl. Electroporation was done in a 2 mm cuvette (165–2086, Bio-Rad, Hercules, CA, USA) using a Gene Pulser Xcell Electroporation System (Bio-Rad), following the manufacturer's protocol.

GROWTH STUDIES ON UREA AND L-GLUTAMATE AS NITROGEN SOURCE

Growth studies were conducted at 30 °C in 500-mL flasks. To prevent nutrient carry over from stock cultures, strains were pre-grown in two sequential shake flasks in which biomass formation was not limited by the amount of carbon source but by the nitrogen source. To this end, 200-μL cell suspension from frozen stocks were inoculated in 100 mL SM-glutamate with a decreased initial

L-glutamate concentration of 1.5 mM and with 20 g·L⁻¹ glucose. After reaching stationary phase, biomass was centrifuged (4 °C, 5 min at 3,000 g). The pellet was washed twice with demineralised water, resuspended in demineralised water and used to inoculate a second shake flask with the same medium. After reaching stationary phase, the same procedure was performed and a final set of shake flasks, containing either 100 mL SM-urea or SM-glutamate and 20 g·L⁻¹ glucose, was inoculated for growth rate determination. Where indicated, L-carnitine (Sigma-Aldrich) was added at a final concentration of 0.4 g·L⁻¹. Optical density at 660 nm was measured at regular time intervals with a Libra S11 spectrophotometer (Biochrom, Cambridge, UK).

BATCH AND CHEMOSTAT CULTURES IN BIOREACTORS

Controlled batch and chemostat cultures were grown at 30 °C in 2-L bioreactors (Applikon, Schiedam, The Netherlands) with working volumes of 1 L. Pre-cultures for batch cultivation were grown in shake flasks containing 100 mL SM-urea and 20 g·L⁻¹ glucose. Pre-cultures for chemostat experiments were grown in shake flasks with 100 mL SM-glutamate and 20 g·L⁻¹ glucose. Before inoculation of the bioreactors, pre-cultures were washed once with demineralised water. During the batch phase in bioreactors, cells were grown in SM-ammonium (326) with 20 g·L⁻¹ glucose and 0.3 g·L⁻¹ antifoam Pluronic PE 6100 (BASF, Ludwigshafen, Germany). When a rapid decrease in CO₂ production indicated glucose depletion, continuous cultivation was initiated at a dilution rate of 0.05 h⁻¹. During this chemostat phase, cells were grown on SM-ammonium with 7.5 g·L⁻¹ glucose and 0.15 g·L⁻¹ antifoam Pluronic PE 6100. Culture pH was maintained at 5.0 by automatic addition of 2 M KOH. Where indicated, 0.04 g·L⁻¹ L-carnitine was added to a sterilized bioreactor or medium vessel from a filter-sterilized stock of 40 g·L⁻¹. To ensure fully aerobic conditions, the bioreactors were sparged with 500 mL·min⁻¹ air and stirred at 800 rpm.

ANALYTICAL METHODS AND CALCULATIONS

Chemostat steady-state samples were taken between 7 and 12 volume changes after inoculation. Chemostats with CEN.PK113-7D were assumed to be in steady state when, after at least five volume changes, carbon dioxide production rates changed by less than by 4% over 2 volume changes. Due to selective pressure in the chemostats, IMK640 did not reach this requirement and was sampled after 7-12 volume changes. Dry weight measurements, HPLC analysis of supernatants and off-gas analysis were performed as described previously (162). Biomass-specific production rates of ethanol were corrected for evaporation as described previously (104). Samples for analysis of extracellular metabolite concentrations (e.g. residual glucose) were taken with the stainless-steel-bead rapid-quenching method (207). HPLC quantification of acetaldehyde measurements were performed as described previously (11) with some modifications (166). For aerobic batch cultures, maximum specific growth rates (μ_{\max}) in the glucose phase were calculated via linear regression of the natural logarithm of at least five OD₆₆₀ measurements. Biomass yield on substrate ($Y_{x/s}$ in g dry weight·(mmol glucose)⁻¹) and product yields on substrate ($Y_{i/s}$ in mol·(mol glucose)⁻¹) were calculated via linear regression on at least three experimental data points, with an interval of at least 2 h. Maximum biomass-specific glucose consumption rates ($q_{s,\max}$) were calculated by dividing μ_{\max} by $Y_{x/s}$ and maximum biomass specific production rates were calculated by multiplying the ratio of produced compound over produced biomass by μ_{\max} , based on the assumption that growth stoichiometries remained constant during the exponential growth phase.

DETERMINATION OF ACCUMULATION OF RESPIRATORY DEFICIENT MUTANTS

Shake flasks with YP and 2% (v/v) ethanol were inoculated from frozen stocks. Stationary-phase cultures were used to inoculate new 100-mL shake flasks, with 20 mL SM-glutamate and 20 g·L⁻¹ glucose at an estimated initial OD₆₆₀ of 0.001. After 12 generations (based on OD₆₆₀ measurements), ~100 cells per plate were applied on solid YP medium containing 20 g·L⁻¹ glucose. Colonies were replica plated on YP with 2% ethanol and YP with 20 g·L⁻¹ glucose. The number of colonies on

each medium was counted and the fraction of respiratory-deficient mutants was estimated from the fraction of the colonies that grew on YP-glucose medium but not on YP-ethanol medium. Two independent plating experiments were performed for each strain, with 10 plates per experiment.

CARNITINE ACETYLTRANSFERASE ENZYME ASSAY

Culture samples (corresponding to ca. 62.5 mg dry weight), harvested from exponentially growing shake flask cultures on SM-ammonium with 20 g·L⁻¹ glucose, were washed, stored and prepared as described previously (241). Cell extracts were prepared with a FastPrep-24 machine (M.P. Biomedicals, Irvine, CA, USA) using 4 bursts of 20 s at a speed of 6.0 m·s⁻¹ with 30 s cooling intervals at 0 °C as described before (162). After removal of cells and debris by centrifugation (4 °C, 20 min at 48,000 g), the supernatant was used for enzyme assays. Carnitine acetyl-transferase activity was measured at 30 °C on a Hitachi model U-3010 spectrophotometer (Sysmex, Norderstedt, Germany) by monitoring absorbance at 412 nm, which is proportional to the amount of free CoA (85). The reaction mixture, with a final volume of 1 mL, contained 100 mM Tris-HCl (pH 8), 0.5 mM acetyl-CoA, 0.1 mM DTNB and cell extract. The reaction was started by adding 40 µL of 1 M L-carnitine solution, to a final concentration of 40 mM. Enzyme activities were calculated using Beer's law with an extinction coefficient (ϵ) for TNB²⁻ of 14.15 mM⁻¹·cm⁻¹ (252). To determine the quality of the cell extracts, and thereby to eliminate poor extract quality as the cause of the absence of carnitine acetyltransferase activity in some cultures, activity of glucose-6-phosphate dehydrogenase was determined as described previously (241). Reaction rates were proportional to the amounts of cell extract added. Enzyme activities were measured in cell extracts from two independently grown shake flask cultures. Protein concentrations in cell extracts were determined with the Lowry method (197).

4.3 RESULTS

4.3.1 Determination of the specific growth rates of *pda1Δ*, *cit2Δ* and *ach1Δ* mutants

Studying the interface between glycolysis and the TCA cycle in *S. cerevisiae* is complicated by the different possible fates of mitochondrial acetyl-CoA: direct use for synthesis of arginine, leucine and lipoate; complete dissimilation via the TCA cycle; and generation of TCA-cycle intermediates as biosynthetic precursors. Only the first of these fates is strictly dependent on availability of intramitochondrial acetyl-CoA. To assess the relevance of the PDH complex, Cit2 and Ach1 (Figure 4.1) for the three processes indicated above, specific growth rates of deletion mutants were determined in glucose synthetic medium with either urea or glutamate as the nitrogen source. Of these two nitrogen sources, only glutamate can yield α -ketoglutarate and, thereby, provide an alternative source of TCA-cycle intermediates as biosynthetic precursors.

In glucose-grown cultures with glutamate as the nitrogen source, only strains IMK640 (*pda1Δ ach1Δ*) and IMK641 (*pda1Δ cit2Δ ach1Δ*) showed substantially lower specific growth rates than the reference strain CEN.PK113-7D, while single deletions of *PDA1*, *CIT2* or *ACH1* did not affect growth (Table 4.2). In *S. cerevisiae*, activity of either the PDH complex or Ach1 therefore appears to be enough to provide sufficient intramitochondrial acetyl-CoA for synthesis of arginine, leucine and lipoate. Consistent with the hypothesis that mitochondrial acetyl-CoA availability is limiting growth, addition of L-carnitine, which enables supply of intramitochondrial acetyl-CoA via the carnitine shuttle, led to a

Table 4.2. Effect of removing key reactions at the interface between glycolysis and TCA cycle interface on the specific growth rate on glucose. Strains were grown in shake flask cultures on synthetic medium with 20 g·L⁻¹ glucose with either 38 mM urea or 76 mM glutamate as the sole nitrogen source. Where indicated, L-carnitine was added at a final concentration of 400 mg·L⁻¹. The data represent averages of at least two independent experiments. In all cases the mean deviation was ≤ 0.01 h⁻¹. Background bars represent growth rates relative to the highest observed value (0.38 h⁻¹).

Strain	Relevant genotype	Specific growth rate (h ⁻¹)			
		N-source			
		urea w/o L-carnitine	glutamate w/o L-carnitine	urea w/ L-carnitine	glutamate w/ L-carnitine
CEN.PK113-7D	<i>PDA1 CIT2 ACH1</i>	0.35	0.37	0.35	0.38
CEN.PK541-1A	<i>pda1Δ CIT2 ACH1</i>	0.19	0.34	0.19	0.33
CEN.PK542-1A	<i>PDA1 cit2Δ ACH1</i>	0.34	0.36		
IMK627	<i>PDA1 CIT2 ach1Δ</i>	0.34	0.36		
IMK629	<i>PDA1 cit2Δ ach1Δ</i>	0.34	0.36		
IMK640	<i>pda1Δ CIT2 ach1Δ</i>	0.10	0.09	0.13	0.16
CEN.PK544-4D	<i>pda1Δ cit2Δ ACH1</i>	0.05	0.33	0.09	0.33
IMK641	<i>pda1Δ cit2Δ ach1Δ</i>	0.04	0.09	0.09	0.17

67 – 94% increase of the specific growth rates of the *pda1Δ ach1Δ* and *pda1Δ cit2Δ ach1Δ* mutants (Table 4.2).

With urea as a nitrogen source, CEN.PK541-1A (*pda1Δ*) showed a 45% lower specific growth rate than the reference strain, while IMK627 (*ach1Δ*) showed near wild-type growth rates. This result is consistent with an earlier report, based on glucose-limited chemostat cultures, that the PDH complex is the predominant link between glycolysis and TCA cycle in *S. cerevisiae* (245). Similar specific growth rates of the IMK640 (*pda1Δ ach1Δ*) strain on urea and glutamate media suggested that the observed reduction in those growth rates in comparison to the reference strain was not caused by a shortage of TCA-cycle intermediates. Additional disruption of *CIT2* (strain IMK641, *pda1Δ cit2Δ ach1Δ*) led to even slower growth on urea, while the growth rate on glutamate medium was the same as that of the *pda1Δ ach1Δ* strain. This observation indicates that Cit2 is involved in funnelling TCA-cycle intermediates into the mitochondria in the *pda1Δ ach1Δ* strain during growth on urea medium. Additionally, strain CEN.PK544-4D (*pda1Δ cit2Δ*) showed strongly impaired growth on urea media (0.05 h⁻¹), but near wild-type rates on glutamate (0.34 h⁻¹). Together with the observation that with glutamate as a nitrogen source, CEN.PK544-4D (*pda1Δ cit2Δ ACH1*) shows much faster growth than IMK641 (*pda1Δ cit2Δ ach1Δ*), these growth experiments support the conclusion that Ach1 is sufficiently active to cover the major requirement for intramitochondrial acetyl-CoA as a precursor of arginine, leucine and lipoate biosynthesis. However, Ach1 cannot meet the entire demand of acetyl-CoA for dissimilation via the TCA cycle and for the generation of TCA-cycle intermediates and intramitochondrial acetyl-CoA as metabolic precursors. The residual growth of strain IMK641 (*pda1Δ cit2Δ ach1Δ*, 0.04 h⁻¹ on urea medium) indicates that, in *S. cerevisiae*, at least one other mechanism can generate intramitochondrial acetyl-CoA.

Table 4.3. Effect of removing key reactions at the glycolysis-TCA cycle interface on loss of respiratory competence in *S. cerevisiae*. After initial growth in YP with 2% (v/v) ethanol, cells were transferred to SM with 20 g·L⁻¹ glucose and 76 mM glutamate as nitrogen source. After 12 generations, the cultures were plated on YP with 20 g·L⁻¹ glucose. After colonies were observed, the plates were replica plated on YP with 2% (v/v) ethanol and YP with 20 g·L⁻¹ glucose. Percentages of cells unable to grow on YP with 2% (v/v) ethanol are based on independent duplicate experiments, with 10 plates per strain per experiment and ~100 cells per plate. Standard deviations are based on 20 plates per strain.

Strain	Relevant genotype	Respiratory deficient cells (%)
CEN.PK113-7D	<i>PDA1 CIT2 ACH1</i>	0.00% ± 0.00%
CEN.PK541-1A	<i>pda1Δ CIT2 ACH1</i>	0.12% ± 0.31%
CEN.PK542-1A	<i>PDA1 cit2Δ ACH1</i>	0.15% ± 0.37%
IMK627	<i>PDA1 CIT2 ach1Δ</i>	0.16% ± 0.40%
IMK629	<i>PDA1 cit2Δ ach1Δ</i>	0.14% ± 0.45%
IMK640	<i>pda1Δ CIT2 ach1Δ</i>	93.88% ± 4.29%
CEN.PK544-4D	<i>pda1Δ cit2Δ ACH1</i>	0.07% ± 0.21%
IMK641	<i>pda1Δ cit2Δ ach1Δ</i>	92.13% ± 1.85%

4.3.2 Strains with decreased availability of mitochondrial acetyl-CoA show increased loss of respiration

An increased incidence of respiratory deficient mutants, often associated with loss of mitochondrial DNA (ρ^- *petites*) has been observed for several mutants in genes encoding components of the mitochondrial fatty-acid synthase system (109, 117, 314). Moreover, strains with reduced mitochondrial malonyl-CoA synthesis due to absence of the mitochondrial acetyl-CoA carboxylase Hfa1 exhibit a decreased lipoate content and loss of respiratory competence (121). An increased incidence of ρ^0 *petites* has also been observed in Pdh^- strains (338). To investigate the impacts of deleting *PDA1*, *CIT2* and/or *ACH1* on respiratory competence, we analysed loss of the ability to grow on the non-fermentable carbon source ethanol, after 12 generations of growth on synthetic medium with 20 g·L⁻¹ glucose and glutamate. Most strains showed a low incidence of respiratory-deficient cells (Table 4.3). However, the two strains in which both routes of mitochondrial acetyl-CoA provision were disrupted, IMK640 (*pda1Δ ach1Δ*) and IMK641 (*pda1Δ cit2Δ ach1Δ*), displayed a spectacularly high incidence of respiratory deficient cells (94% and 92%, respectively). This result strengthened the conclusion that presence of either an active PDH complex or of Ach1 is essential for sufficient supply of intramitochondrial acetyl-CoA and that the role of Cit2 in *pda1Δ* mutants (Table 4.2) is limited to the provision of TCA-cycle intermediates.

4.3.3 L-Carnitine supplementation enables respiratory growth in glucose-limited cultures of a *pda1Δ ach1Δ* strain

As the *pda1Δ ach1Δ* genotype stimulates loss of respiratory competence, IMK640 (*pda1Δ ach1Δ*) was further characterized in aerobic, glucose-limited chemostat cultures at a dilution rate of 0.05 h⁻¹. Under these conditions, sugar dissimilation of wild-type *S. cerevisiae* strains is fully respiratory (63, 119). Conversely, strain IMK640 (*pda1Δ ach1Δ*) showed respirofermentative sugar metabolism under these conditions, as evident from the pro-

Table 4.4. Physiology of the *S. cerevisiae* reference strain CEN.PK113-7D and IMK640 (*pda1Δ ach1Δ*) in aerobic glucose-limited chemostat cultures with or without 40 mg·L⁻¹ L-carnitine at a dilution rate of 0.05 h⁻¹. Averages and mean deviations from CEN.PK113-7D and IMK640 were obtained from respectively two and four replicates. The respiratory quotient is the absolute value of $q_{\text{CO}_2}/q_{\text{O}_2}$. Biomass specific consumption (q_{glucose}) and production rates (q_{product}) are expressed in mmol·g_{DW}⁻¹·h⁻¹ and the biomass yield on glucose ($Y_{x/s}$) in g·g⁻¹.

	Units	CEN.PK113-7D (<i>PDA1 ACH1</i>)	IMK640 (<i>pda1Δ ach1Δ</i>)	
		w/o L-carnitine	w/o L-carnitine	w/ L-carnitine
Biomass dry weight	g·L ⁻¹	3.46 ± 0.12	1.07 ± 0.08	2.72 ± 0.04
$Y_{x/s}$	g·g ⁻¹	0.49 ± 0.01	0.15 ± 0.01	0.37 ± 0.01
Respiratory quotient		1.06 ± 0.02	1.64 ± 0.13	0.97 ± 0.08
q_{glucose}	mmol·g ⁻¹ ·h ⁻¹	-0.57 ± 0.01	-1.87 ± 0.11	-0.74 ± 0.03
q_{O_2}	mmol·g ⁻¹ ·h ⁻¹	-1.49 ± 0.05	-2.55 ± 0.19	-2.24 ± 0.33
q_{ethanol}	mmol·g ⁻¹ ·h ⁻¹	0.00 ± 0.00	1.26 ± 0.16	0.03 ± 0.04
q_{CO_2}	mmol·g ⁻¹ ·h ⁻¹	1.57 ± 0.03	4.17 ± 0.18	2.13 ± 0.10
q_{pyruvate}	mmol·g ⁻¹ ·h ⁻¹	0.00 ± 0.00	0.03 ± 0.01	0.00 ± 0.00
q_{glycerol}	mmol·g ⁻¹ ·h ⁻¹	0.00 ± 0.00	0.03 ± 0.01	0.00 ± 0.00
q_{acetate}	mmol·g ⁻¹ ·h ⁻¹	0.00 ± 0.00	0.15 ± 0.02	0.00 ± 0.00
$q_{\text{succinate}}$	mmol·g ⁻¹ ·h ⁻¹	0.00 ± 0.00	0.10 ± 0.05	0.02 ± 0.00
q_{citrate}	mmol·g ⁻¹ ·h ⁻¹	0.00 ± 0.00	0.07 ± 0.01	0.00 ± 0.00
$q_{\text{acetaldehyde}}$	mmol·g ⁻¹ ·h ⁻¹	N.D.*	0.13 ± 0.01 ¹	0.00 ± 0.00 ²
Residual glucose	mmol·L ⁻¹	0.13 ± 0.06	0.49 ± 0.02	0.18 ± 0.06

*N.D., not determined.

¹Average from three replicates.

²Average from two replicates.

duction of ethanol and a 69% lower biomass yield on glucose compared to the reference strain (Table 4.4).

In aerobic, glucose-limited chemostat cultures, the genes encoding the multiple components of the carnitine shuttle are derepressed (Figure S4.1). When such cultures of strain IMK640 (*pda1Δ ach1Δ*) were supplemented with L-carnitine, their physiology became fully respiratory, indicated by the absence of ethanol production, a decreased respiratory quotient and an increased biomass yield on glucose (Table 4.4). The 24% lower biomass yield of strain IMK640 relative to the *PDA1 ACH1* reference strain (Table 4.4) is consistent with increased ATP consumption as a result of redirection of respiratory pyruvate dissimilation via the PDH bypass (245).

4.3.4 Constitutive expression of the carnitine shuttle enables fast growth of a *pda1Δ ach1Δ* strain on glucose

Under glucose-limited conditions, strain IMK640 (*pda1Δ ach1Δ*) does not show a mitochondrial acetyl-CoA deficiency when L-carnitine is added to the medium (Table 4.4). However, in glucose-grown batch cultures of this strain, L-carnitine addition did not support wild-type growth rates (Table 4.2), suggesting that the flux through the carnitine shuttle was limiting mitochondrial acetyl-CoA provision and thereby growth under these conditions. To test this hypothesis, expression cassettes were constructed with each of the components of the carnitine shuttle (*HNM1*, *AGP2*, *CRC1*, *YAT1*, *YAT2* and

Table 4.5. Effect of the constitutive expression of carnitine shuttle genes on growth of *pda1Δ ach1Δ S. cerevisiae*. Strains were grown in shake flasks with synthetic medium and 20 g·L⁻¹ glucose. As a nitrogen source, either 38 mM urea or 76 mM glutamate was used. Where indicated, L-carnitine was added at a final concentration of 400 mg·L⁻¹. The data represent averages of at least two independent experiments. In all cases the mean deviation was ≤ 0.01 h⁻¹. Background bars represent growth rates relative to the highest observed value (0.37 h⁻¹).

Strain	Relevant genotype	Specific growth rate (h ⁻¹)			
		N-source			
		urea w/o L-carnitine	glutamate w/o L-carnitine	urea w/ L-carnitine	glutamate w/ L-carnitine
IMX585	<i>PDA1 ACH1</i>	0.35	0.37	0.34	0.37
IMX710	<i>pda1Δ ach1Δ</i>	0.10	0.10	0.13	0.13
IMX744	<i>pda1Δ ach1Δ</i> Carnitine shuttle↑	0.08	0.09	0.27	0.25

CAT2) placed under the control of a strong, constitutive promoter. The resulting six cassettes were integrated into the *SGA1* locus of strain IMX710 (*pda1Δ ach1Δ*) resulting in strain IMX744 (*pda1Δ ach1Δ sga1Δ::[CARN]*). Enzyme assays showed a high activity of carnitine acetyltransferase activity in cell extracts of glucose-grown batch cultures of the constitutively expressing carnitine shuttle strain IMX744 ($3.56 \pm 0.20 \mu\text{mol}\cdot(\text{mg protein})^{-1}\cdot\text{min}^{-1}$), while activity in reference strain IMX710 (*pda1Δ ach1Δ*) was below the detection limit ($< 0.01 \mu\text{mol}\cdot(\text{mg protein})^{-1}\cdot\text{min}^{-1}$). Without L-carnitine supplementation, strain IMX744 showed similar growth rates as the *pda1Δ ach1Δ* reference strain IMX710, irrespective of the nitrogen source (Table 4.5). However, when L-carnitine was added to the medium, the growth rate of IMX744 reached up to 79% of that of the *PDA1 ACH1* reference strain IMX585. These data show that in, the presence of L-carnitine, constitutive expression of the carnitine-shuttle genes indeed enables efficient transport of acetyl-units from the cytosol into the mitochondria in glucose-grown batch cultures.

4.3.5 A constitutively expressed carnitine shuttle does not affect respiro-fermentative metabolism in *PDA1 ACH1 S. cerevisiae*

S. cerevisiae is a Crabtree-positive yeast, using alcoholic fermentation as the predominant catabolic route in aerobic, glucose-grown batch cultures (55). To test whether an alternative entry into the TCA cycle via PDH bypass and carnitine shuttle might affect the distribution of glucose carbon over respiration and fermentation in aerobic, glucose-grown batch cultures of *S. cerevisiae*, we constructed the *PDA1 ACH1* reference strain IMX868, which constitutively expressed the carnitine-shuttle genes. Enzyme assays in glucose-grown batch cultures confirmed overexpression of the carnitine acetyltransferases, showing an activity of $3.01 \pm 0.03 \mu\text{mol}\cdot(\text{mg protein})^{-1}\cdot\text{min}^{-1}$, while activity in the reference strain IMX585 was below the detection limit ($< 0.01 \mu\text{mol}\cdot(\text{mg protein})^{-1}\cdot\text{min}^{-1}$). Strain IMX868 (*PDA1 ACH1 sga1Δ::[CARN]*) was grown in aerobic bioreactor batch cultures with glucose as the carbon source, in the presence and absence of L-carnitine (Figure 4.2). During growth on glucose, the strain showed similar growth rates ($0.39 \pm 0.00 \text{ h}^{-1}$) as the reference strain CEN.PK113-7D ($0.37 \pm 0.01 \text{ h}^{-1}$ (201)), when no L-carnitine was added. Upon L-carnitine supplementation, the growth

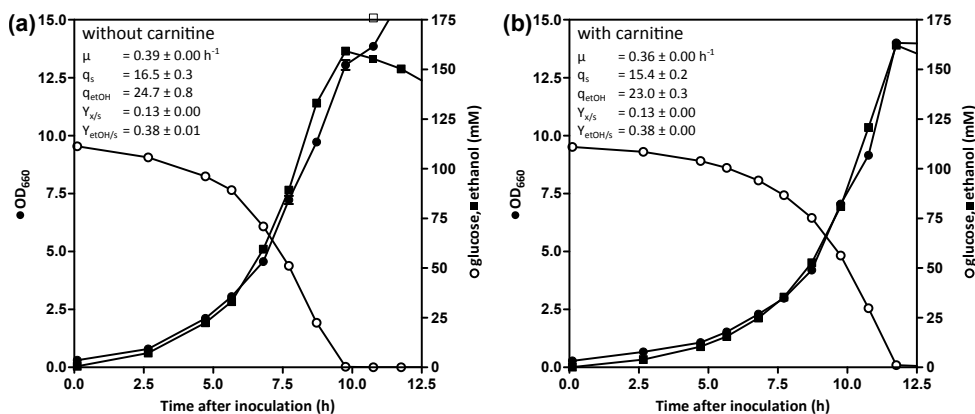


Figure 4.2. Impact of the constitutive expression of the carnitine shuttle on aerobic growth of *S. cerevisiae* on glucose in batch cultures. Growth of IMX868 (CARN) was analyzed in aerobic bioreactors on synthetic medium with an initial glucose concentration of 20 g·L⁻¹ without (a) or with 40 mg·L⁻¹ L-carnitine (b). Data shown in the graphs are from single batch experiments for each condition. Independent duplicate experiments for each condition gave essentially the same results. Biomass specific consumption (q_s) and production rates (q_{etOH}) are expressed in mmol·gDW⁻¹·h⁻¹, while yields are expressed in g·g⁻¹.

rate slightly decreased, to 0.36 ± 0.00 h⁻¹. Biomass and ethanol yields were highly similar in the absence and presence of L-carnitine, indicating that the presence of an active carnitine shuttle does not affect the balance between respiration and fermentation in aerobic batch cultures of *S. cerevisiae*.

4.4 DISCUSSION

Pyruvate and acetyl coenzyme A are key precursors for a wide variety of industrially relevant compounds produced by engineered *S. cerevisiae* strains (170, 186, 244, 280). Design and implementation of metabolic engineering strategies to improve fluxes towards these precursors not only requires knowledge of flux distribution in wild-type strains, but also on compensatory ‘back-up’ pathways that become active when the mechanisms that carry the majority of the flux in wild-type cells are inactivated by genetic modification or by changing process conditions.

In previous work, the PDH complex was shown to be the predominant link between glycolysis and TCA cycle in slow growing, glucose-limited aerobic chemostat cultures, in which sugar dissimilation is exclusively respiratory (245, 338). In aerobic, glucose-grown batch cultures *S. cerevisiae* employs alcoholic fermentation as the main dissimilatory pathway (55, 64, 239). In such cultures, the major role of the TCA cycle is not the dissimilation of pyruvate, but the provision of precursors for assimilation. The near-wild type growth rates of a *cit2Δ ach1Δ* strain and the impaired growth of a *pda1Δ* strain in glucose-grown cultures with urea as the nitrogen source show that the combination of mitochondrial pyruvate uptake via the recently discovered Mpc1/Mpc2 ‘MpcFerm’ mitochondrial carrier complex (12) and its conversion by the PDH complex to acetyl-CoA

is also the main entry into the TCA cycle during aerobic batch cultivation of *S. cerevisiae* on glucose (Table 4.2).

By growing *S. cerevisiae* on glutamate as the sole nitrogen source, we were able to dissect the role of the PDH complex in the biosynthesis of TCA cycle intermediates from its role in the direct provision of intramitochondrial acetyl-CoA. In glucose-grown batch cultures of *S. cerevisiae*, glucose catabolism is almost completely fermentative (64). Consequently, in glucose-urea medium, in which no direct precursors of TCA-cycle intermediates are available, the majority of the flux through the PDH complex will be directed towards the synthesis of TCA cycle-derived metabolic precursors. Under these conditions, cytosolic synthesis of citrate via Cit2 was shown as a key compensatory mechanism in the absence of a functional PDH complex, as evident from the very slow growth of the *pda1Δ cit2Δ* strain, which could be almost completely restored to wild-type levels when TCA-cycle intermediates were externally supplied by using glutamate instead of urea as the nitrogen source (Table 4.2). The lack of a marked phenotype of a *cit2Δ* strain in glucose-grown batch cultures indicates that Cit2 does not have a major role in fueling the TCA cycle in wild-type cells. However, its transcriptional regulation pattern (*CIT2* is transcribed in glucose-grown batch cultures but repressed by glutamate; (150)) suggests that under certain conditions Cit2 may contribute to synthesis of TCA-cycle intermediates and/or cytosolic acetyl-CoA homeostasis in the presence of a functional PDH complex. This is consistent with previous findings that *CIT2* expression is controlled by the retrograde regulation pathway, a communication pathway between the nucleus and mitochondria (42, 188, 193). As a result of retrograde regulation, functional expression of *CIT2* is up-regulated when respiratory capacity is reduced or absent, and when the TCA cycle is blocked (42, 188).

Cit2 is localised to the peroxisomes when proliferation of these organelles is induced by oleate (183). Its localisation under other growth conditions is ambiguous, with several subcellular fractionation studies indicating an at least partial cytosolic localization in glucose-grown cultures (66, 236, 251). A clear carbon-source-dependent localisation has previously been shown for the *MLS1*-encoded malate synthase, whose location is peroxisomal in oleate-induced cultures but cytosolic during growth on ethanol (176). Glucose-grown cultures of *S. cerevisiae* harbour only very few, small peroxisomes (310). Moreover, Acs2, the only active acetyl-CoA synthetase isoenzyme in the presence of excess glucose due to the glucose repression of *ACS1* and glucose catabolite inactivation of Acs1, is nucleocytosolic (13, 142). Since peroxisomal membranes are impermeable to acetyl-CoA (257), our results strongly indicate that, in *pda1Δ* strains in glucose-grown batch cultures, Cit2 is at least partially localised to the same compartment as Acs2. Although condition-dependent subcellular localization of Cit2 requires further study, the key role of Cit2 as a compensatory enzyme in *pda1Δ* mutants is fully consistent with a cytosolic localization in glucose-grown cultures.

Previous research on Ach1 mostly focused on its role during growth on ethanol and acetate, either as sole carbon sources or in their metabolism after the diauxic shift in glucose-grown cultures (28, 68, 80, 181, 225). Strains with *ACH1* deleted show impaired growth at high acetate concentrations, although growth on medium with ethanol is not affected (28, 80). Post-diauxic shift *ach1Δ* cultures show increased extracellular acetate accumulation and a reduced life span (68, 225). *ACH1* has been reported to be repressed

by glucose (181), but in case of the reference strain CEN.PK113-7D, high mRNA levels are found in cultures grown under conditions of glucose repression (157). Our growth experiments with glutamate as the nitrogen source indicated that Ach1 can replace the PDH complex in *pda1Δ* strains as the source of intramitochondrial acetyl-CoA for synthesis of arginine, leucine and lipoic acid (Table 4.2). The impact of the impaired mitochondrial acetyl-CoA synthesis in *pda1Δ ach1Δ* strains became apparent from a strongly reduced growth rate and a spectacularly high incidence of respiratory deficient cells in glucose-grown batch cultures (Table 4.3). A much less pronounced loss of respiratory deficiency was observed in previous experiments with *pda1Δ* strains (338), which can now be interpreted from a partial compensation by Ach1. The strong impact of the *pda1Δ ach1Δ* strains on respiratory competence resembles the phenotypes of strains impaired in mitochondrial fatty acid synthesis (109, 117, 314), which has been proposed to be essential for respiratory complex assembly (177) and requires mitochondrial acetyl-CoA. The frequent, irreversible loss of respiratory competence in these cells requires special measures in genetic modification and maintenance of *pda1Δ ach1Δ* strains. Use of non-fermentable carbon sources, as applied in this study, and/or inclusion of L-carnitine in growth media offer simple measures to minimize the frequency of respiratory-deficient mutants in stock cultures.

Glutamate also restores growth of *Kluyveromyces lactis pda1Δ* strains to near-wild type levels (345), suggesting that this yeast also harbours at least one compensatory pathway for synthesis of intramitochondrial acetyl-CoA. Indeed, the *K. lactis* genome harbours a gene with 82% sequence identity of its gene product with Ach1 (65). A recent study has demonstrated that, in addition to providing acetyl-CoA in the mitochondrial matrix, Ach1 can also play a role in another compensatory process. In pyruvate-decarboxylase-negative strains, where the PDH bypass cannot meet the cellular demand for cytosolic acetyl-CoA, Ach1 can generate acetate from mitochondrial acetyl-CoA. After its export to the cytosol and activation to acetyl-CoA, this enables growth of Pdc^- *S. cerevisiae* on glucose without addition of a C_2 source (44). These orthogonal roles suggest that Ach1 can play an important, flexible role in cytosolic and mitochondrial acetyl-CoA homeostasis. The ubiquitous presence of sequences homologous to *ACH1* in a large group of fungal genomes (28, 80, 336, 337), indicates that this role may be widespread among fungi.

An *S. cerevisiae* strain in which the PDH complex, Ach1 and Cit2 were all absent still showed a low, residual growth rate (Table 4.2). This observation indicates that *S. cerevisiae* harbours either another mechanism for intramitochondrial acetyl-CoA synthesis or a pathway that circumvents its necessity. One explanation could be a partial targeting of an acetyl-CoA synthetase isoenzyme to the mitochondrial matrix. Although most studies indicate an extramitochondrial localisation of Acs1 and Acs2 (129, 151, 159, 306), there are also reports that Acs1 is localised to the mitochondria (153, 174). However, deletion of the *ACS1* ORF in IMK641 (resulting in a *pda1Δ cit2Δ ach1Δ acs1Δ* genotype) did not result in a lower growth rate than already observed for the *pda1Δ cit2Δ ach1Δ* strain (data not shown). Based on enzymatic analysis, it was previously hypothesised that *S. cerevisiae* may harbour a 2-oxoacid dehydrogenase to catabolise branched-chain amino acids to mitochondrial acetyl-CoA (62). However, after this yeast was sequenced, it became clear that it does not contain the genes encoding the subunits for this complex

(98, 222). The residual growth rate of the *pda1Δ cit2Δ ach1Δ* strain illustrates that, even at the interface of the two most intensively studied pathways in central metabolism, our knowledge of pathway topology remains incomplete.

In contrast to the situation in *S. cerevisiae* (Table 4.2), L-carnitine addition restored growth of a *K. lactis pda1Δ* strain to near wild-type levels (345), suggesting that, in the latter yeast, the carnitine shuttle genes are not, or not as strongly, repressed by glucose as in the former. Indeed, under glucose-derepressed conditions in chemostat cultures, L-carnitine addition could restore respiratory growth of an *S. cerevisiae pda1Δ ach1Δ* strain in glucose-limited chemostats (Table 4.4). Constitutive expression of the genes involved in the carnitine shuttle strongly stimulated growth of a *pda1Δ ach1Δ* strain in the presence of L-carnitine (Table 4.5), indicating that there are no post-translational or allosteric regulation mechanisms that prevent this shuttle from operating in glucose-containing media. However, the incomplete (77%) recovery of the wild-growth rate may reflect a remaining limitation in this pathway in *S. cerevisiae*. This study demonstrates, for the first time, that the entire carnitine shuttle in this yeast can be functionally over-expressed. We therefore also investigated its impact in a ‘wild type’ *PDA1 ACH1 CIT2* reference strain (Figure 4.2). This experiment indicated that a mere facilitation of the entry of acetyl-CoA into the TCA cycle does not affect the balance between respiration and fermentation in aerobic, glucose-grown batch cultures of *S. cerevisiae*. Glucose repression of other key genes in respiratory glucose metabolism, e.g. those encoding TCA cycle and mitochondrial respiratory chain proteins, constrains the respiratory capacity under these conditions (77, 92). We anticipate that *S. cerevisiae* strains with a constitutively expressed carnitine shuttle will prove to be valuable tools for studies on metabolic engineering of *de novo* L-carnitine synthesis in this yeast (83) and on the requirements for *in vivo* reversibility of the mitochondrial carnitine shuttle (322, 330).

4.5 ACKNOWLEDGEMENTS

We thank Astrid van Uijen for help with initial growth studies, James Dykstra for constructing strain IMX744, Arthur Gorter de Vries for helping in constructing strain IMX868, Ioannis Papapetridis for constructing plasmid pUDR119 and Erik de Hulster for valuable technical assistance.

SUPPLEMENTARY MATERIALS

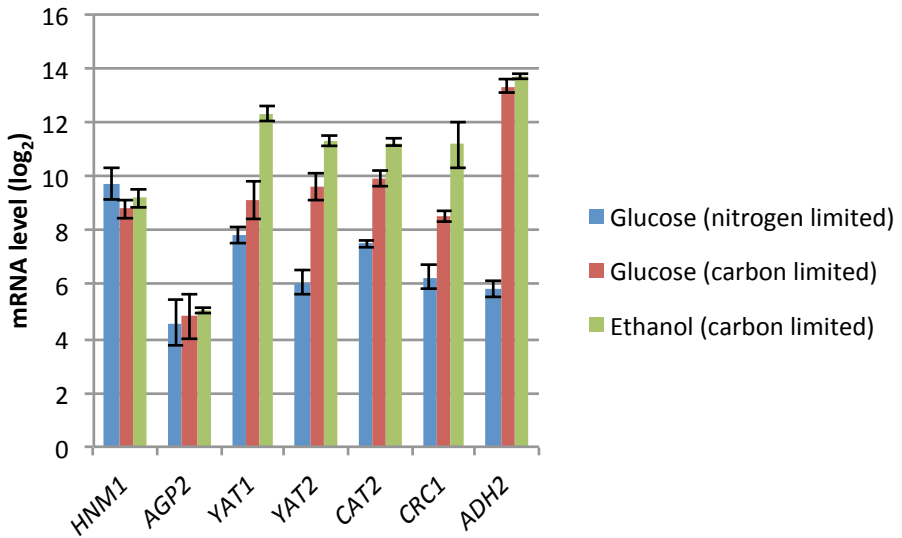


Figure S4.1. mRNA levels from genes involved in the carnitine shuttle, based on chemostat cultures with glucose or ethanol as a carbon source. During nitrogen-limited conditions, the high (residual) glucose levels cause glucose repression. *ADH2* is included for comparison with a typical glucose-repressible gene. Data are obtained from (157). The bars indicate log₂ of the mRNA levels during growth on glucose with nitrogen as the limiting element (blue), during growth with carbon as the limiting element with either glucose (red) or ethanol (green) as the substrate.

Table S4.1. Plasmids used in this study

Name	Relevant characteristics	Origin
pUG-natNT2	Template for natNT2 cassette	(164)
pUD301	pUC57 + <i>pTPI1-pdhA E. faecalis-tTEF1</i>	(167)
pUD302	pUC57 + <i>pTDH3-pdhB E. faecalis-tCYC1</i>	(167)
pUD303	pUC57 + <i>pADH1-aceF E. faecalis-tPGI1</i>	(167)
pUD304	pUC57 + <i>pTEF1-lpd E. faecalis-tADH1</i>	(167)
pUD305	pUC57 + <i>pPGK1-lplA E. faecalis-tPMA1</i>	(167)
pUD306	pUC57 + <i>pPGI1-lplA2 E. faecalis-tPYK1</i>	(167)
pMEL11	2μm ampR <i>amdSYM</i> gRNA- <i>CAN1.Y</i>	(200)
pROS13	2μm ampR <i>kanMX</i> gRNA- <i>CAN1.Y</i> gRNA- <i>ADE2.Y</i>	(200)
pUDE340	2μm ampR <i>kanMX</i> gRNA- <i>PDA1</i> gRNA- <i>ACH1</i>	This study
pUDR119	2μm ampR <i>amdSYM</i> gRNA- <i>SGA1</i>	This study
pUD366	pJET1.2 + <i>pTDH3-AGP2-tAGP2</i>	This study
pUD367	pJET1.2 + <i>pPGK1-HNM1-tHNM1</i>	This study
pUD368	pJET1.2 + <i>pADH1-YAT2-tYAT2</i>	This study
pUD369	pJET1.2 + <i>pPGI1-YAT1-tYAT1</i>	This study
pUD370	pJET1.2 + <i>pTPI1-CRC1-tCRC1</i>	This study
pUD371	pJET1.2 + <i>pTEF1-CAT2-tCAT2</i>	This study

Table S4.2. Primers used in this study.

Number	Name	Sequence 5' → 3'
PDA1 deletion		
9087	PDA1-S1B	CACAATTGGTCCGCGGGTTAGGAGCTGTTCTTCGC ACTCCCAGCTGAAGCTTCGTACGC
9088	PDA1-S2B	AGCTTTGACTTCAGCTTCAGTGGCAATACCTAGAT CAATCGCATAGGCCACTAGTGGATCTG
CIT2 deletion		
9089	CIT2-S1	ATGACAGTTCCTTATCTAAATTCAAACAGAAATGT TGCATCAGCTGAAGCTTCGTACGC
9090	CIT2-S2	CTATAGTTTGCTTTTCAATGTTTTTGACCAATTCCCT TGTATGCATAGGCCACTAGTGGATCTG
ACH1 deletion		
3636	ACH1KOf	GCGGCAAAACAAACAACACATTTCTTTTTTCTTT TTCACATATTGCACTAAAGAAGCTTCGTACGCTGC AGGTCGAC
3637	ACH1KOr	ATTTCTTTCTTTTTTTTGTTAAATACTCATCTCT CGGTTTGCGCACAAACACCGCATAGGCCACTAGTG GATCTG
Primers for CRISPR/Cas9 gene editing		
5792	pCAS9 fw	GTTTTAGAGCTAGAAATAGCAAGTTAAATAAG
5794	pCAS9 target pda1 fw	TGCGCATGTTTCGGCGTTCGAACTTCTCCGCAGT GAAAGATAAATGATCTACCGGGATCAGACATAGAA GTTTTAGAGCTAGAAATAGCAAGTTAAATAAGGC TAGTCCGTTATCAAC
5979	Primer_gRNA_426_fw	TATTGACGCCGGGCAAGAGC
5980	Primer_sRNA_426_rv	CGACCGAGTTGCTCTTG
6157	PDA1 repair fw	TGTTTATCTCTCTTCTGATTCTCCACCCCTTCCCT TACTCAACCGGGTAAATGTGCGCATCTTAATCGTAA GGAAAAATAAAAATAATAGTGCTGTGATCGCATGAT ATTCTTCCCTGGAAG
6158	PDA1 repair rv	CTTCCAGGGAAGAATATCATGCGATCAGCACTA TTATTTTATTTTTCCTTACGATTAAGATGCGACAT TTACCCGGTTGAGTAAGGAAGGGGTGGAGGAATCA GAAGAGAGATAAACA
6159	ACH1 gRNA	GTGCGCATGTTTCGGCGTTCGAACTTCTCCGCAG TGAAAGATAAATGATCCGAGGCAACGGCCATTAAA GGTTTTAGAGCTAGAAATAGCAAGTTAAATAAG
6160	ACH1 repair fw	GACAATAGCGGCAAAACAAACAACACATTTCTTTT TTTCTTTTTCACATATTGCACTAAATGTTTGTGCG CAAACCGAGAGATGAGTATTTAAAAAAAAGAA GGAAATGATATGATT
6161	ACH1 repair rv	AATCATATCATTTCTTTCTTTTTTTTTTAAATAC TCATCTCTCGGTTTGCGCACAAACATTTAGTGCAA TATGTGAAAAAGAAAAAGAAATGTGTTGTTTGT TTTGCCGCTATTGTC

Number	Name	Sequence 5' → 3'
7023	RV_sga1_gRNA	GTTGATAACGGACTAGCCTTATTTTAACTTGCTAT TTCTAGCTCTAAAACGAAGAATTCCAGTGGTCAAT GATCATTTATCTTTCACCTGCGGAGAAGTTTCGAAC GCCGAAACATGCGCA
Confirmation of <i>PDA1</i>, <i>CIT2</i> and <i>ACH1</i> deletion		
9091	K1-A	GGATGTATGGGCTAAATGTACG
9092	K2	GTTTCATTTGATGCTCGATGAG
9093	PDA1-A1	GCAACAGCAGCCACCTGC
9094	PDA1-A4	AAGAACCTCTACAGCAGAGG
9095	CIT2-A1	CATACGCGTATGCAACCGT
9096	CIT2-A4	AGTACGCTAGCCAAGGCAG
3146	ROSP031 DG PDA1 KO fw	ATCGCGCGTGTACATGTC
3147	ROSP032 DG PDA1 KO rv	GCGGCTATTTTCCGGTCTG
3770	ACH1kocheck2f	CGGGCTTACATTAGCACAC
3771	ACH1kocheck2r	GCAAGAAAAACAACGCATTGG
Construction of cassettes for constitutive expression of genes involved in the carnitine shuttle		
3051	ROSP015 TEF1 promoter rv	TTTGTAATTA AAACTTAGATTAGATTGC
3274	Fus Tag I-fw	TATTCACGTAGACGGATAGGTATAGC
3277	Fus Tag C rv	CTAGCGTGTCTCGCATAGTTCTTAGATTG
3283	Fus Tag C fw	ACGTCTCACGGATCGTATATGC
3285	Fus Tag J fw	GGCCGTCATATACGCGAAGATGTC
3289	Fus Tag F fw	CATACGTTGAAACTACGGCAAAGG
3354	D-fw	ACGCATCTACGACTGTGGGTC
3355	J-Re	CGACGAGATGCTCAGACTATGTG
3844	rev ldox	TGCCGAAC TTCCCTGTATG
4068	Nic1 amp Fwd	GCCTACGGT TCCGAAGTATGC
4187	FUS SGA1 -fw	TTACAATATAGTGATAATCGTGGACTAGAG
4224	SGA1 outside rv	TTGATGTAAATATCTAGGAAATACACTTG
4583	IlvC new tag fwd	ACGCATCTACGACTGTGGGTCC
5231	D-Tag Rev	AATCACTCTCCATACAGGG
5917	Primer_pPGK1_rv	TGTTTTATATTTGTTGTAAAAAGTAGATAATTACT TCC
6221	Sc_ADH1_P_FW	TGTATATGAGATAGTTGATTGTATGCTTGGTATAG
6374	TDH3_P_FW	TTTGTTTGTTTATGTGTGTTTATTCGAAACTAAG
6486	Sc_TPI1_P_RV	TTTTAGTTTATGTATGTGTTTTTTGTAGTTATAGA TTTAAGCAAG
6498	Sc_PGI_P_FW	TTTTAGGCTGGTATCTTGATTCTAAATCG
7334	AGP2 fw (ol TDH3)	GTTTTAAAACACCAAGAACTTAGTTTCGAATAAAC ACACATAAACAAACAAAATGACAAAGGAACGTATG ACCATC
7335	CAT2 fw ol pTEF1	CTTCTTGCTCATTAGAAAGAAAGCATAGCAATCTA ATCTAAGTTTTTAATTACAAAATGAGGATCTGTCAT TCGAGAAC

Number	Name	Sequence 5' → 3'
7336	CRC1 fw ol pTPI1	GTTTGTATTCTTTTCTTGCTTAAATCTATAACTAC AAAAAACACATACATAAACTAAAAATGTCTTCAGA CACTTCATTATCAG
7337	HNM1 fw ol pPGK1	CTCTTTTTTACAGATCATCAAGGAAGTAATTATCT ACTTTTTACAACAAATATAAAACAATGAGTATTCG GAATGATAATGCTTC
7338	pTDH3 fw ol tag I	TATTCACGTAGACGGATAGGTATAGCCAGACATCA GCAGCATACTTCGGGAACCGTAGGCATAAAAAACA CGCTTTTTTCAGTTTCG
7339	tAGP2 ol (pSGA1)	TTTACAATATAGTGATAATCGTGGACTAGAGCAAG ATTTCAAATAAGTAACAGCAGCAAAAAATGTAAACG TTTAGCATTTGATAG
7340	tCAT2 ol tSGA1	TATATTTGATGTAAATATCTAGGAAATACACTTGT GTATACTTCTCGCTTTTCTTTTATTTAATGATCAG TATGTATTCGTAAGCC
7341	tCRC1 rv ol tag F	CATACGTTGAACTACGGCAAAGGATTGGTCAGAT CGCTTCATACAGGGAAAGTTCGGCATTATACTGTA ATCAGCCACGTTG
7342	tHNM1 fw ol tag C	CTAGCGTGTCTCGCATAGTTCTTAGATTGTCGCT ACGGCATATACGATCCGTGAGACGTTTTAATCCCC TATATATCAAACGTGTAATAC
7343	tYAT1 rv ol tag F	TGCCGAACCTTCCCTGTATGAAGCGATCTGACCAA TCCTTTGCCGTAGTTTCAACGTATGGGTGTGTGGA GGGGTGAAAG
7344	tYAT2 rv ol tag C	ACGTCTCACGGATCGTATATGCCGTAGCGACAATC TAAGAACTATGCGAGGACACGCTAGGTCTACCTCT AATGCGCGATG
7345	YAT1 fw ol pPGI	GAATTTTAATACATATTCCTCTAGTCTTGCAAAAT CGATTTAGAATCAAGATACCAGCCTAAAAATGCCA AACTTAAAGAGACTACCC
7346	YAT2 fw ol pADH1	CTTTTTCTGCACAATATTTCAAGCTATACCAAGCA TACAATCAACTATCTCATATACAATGTCAAGCGGC AGTACTATTG
Confirmation of correct integration of genes involved in carnitine shuttle (IMX744)		
7486	AGP2_5	GGCTTACCACGTCCAACAAGATTC
4223	SGA1 outside fw	CTTGGCTCTGGATCCGTTATCTG
2916	I_FW (PDH construct ctrl)	GCAGGTATGCGATAGTTCTCTCAC
3362	Tag I forward (2)	CCAGGCAGGTTGCATCACTC
7705	1_YAT2_check	GCAGTCGTGTGGGTAGAAAG
7704	1_HNM1_check	CGGCCTCTGACGTTGAACTC
2669	m-PCR-HR2-RV	GCGCGTGGCTTCCTATAATC
3363	Tag K forward	AGTGTGTATGTACCTGTCTATTTACTG
7707	1_YAT1_check	CTGTTGTCCGGCTACGATTAC
7706	1_CRC1_check	GGTGTGGAGATGACTCATTC
7509	CAT2_1	TTCCGCCCAATAGTGTTC

Number	Name	Sequence 5' → 3'
2909	D_RV (PDH construct ctrl)	CCCGCTCACACTAACGTAGG
7479	Q_OutsideSGA_RV	GGACGTTCCGACATAGTATC
7514	CAT2_6	ATGGTGTCGATCGTCATTTC
7479	Q_OutsideSGA_RV	GGACGTTCCGACATAGTATC
4229	Sequence SGA1 2 rv	TGGTCGACAGATACAATCCTGG

Table S4.3. Primers and templates used to construct the cassettes with genes involved in the carnitine shuttle

Construct	Template(s)	Primers	Resulting fragment	Comment
I- <i>pTDH3</i> - <i>AGP2-tAGP2</i> (ol <i>pSGA1</i>)	pUD302 CEN.PK113-7D	6374, 7338 7339, 7334	I- <i>pTDH3</i> <i>AGP2-tAGP2</i> (ol <i>pSGA1</i> and <i>pTDH3</i>)	Fusion PCR
	<i>AGP2-tAGP2</i> (ol <i>pSGA1</i> and <i>pTDH3</i>) I- <i>pTDH3</i>	4187, 3274	I- <i>pTDH3-AGP2-tAGP2</i> (ol <i>pSGA1</i>)	
I- <i>pPGK1</i> - <i>HNMI-tHNMI-C</i>	pUD305 CEN.PK113-7D	5917, 4068 7342, 7337	I- <i>pPGK1</i> <i>HNMI-tHNMI-C</i> (ol <i>pPGK1</i>)	Fusion PCR
	<i>HNMI-tHNMI-C</i> (ol <i>pPGK1</i>) I- <i>pPGK1</i>	3277, 4068	I- <i>pPGK1</i> - <i>HNMI-tHNMI-C</i>	
J- <i>pADH1</i> - <i>YAT2-tYAT2-C</i>	pUD303 CEN.PK113-7D	6221, 3355 7344, 7346	J- <i>pADH1</i> <i>YAT2-tYAT2-C</i> (ol <i>pADH1</i>)	Fusion PCR
	<i>YAT2-tYAT2-C</i> (ol <i>pADH1</i>) J- <i>pADH1</i>	3355, 3283	J- <i>pADH1-YAT2-tYAT2-C</i>	
J- <i>pPGI1</i> - <i>YAT1-tYAT1-F</i>	pUD306 CEN.PK113-7D	6498, 3285 7343, 7345	J- <i>pPGI1</i> <i>YAT1-tYAT1-F</i> (ol <i>pPGI1</i>)	Fusion PCR
	<i>YAT1-tYAT1-F</i> (ol <i>pPGI1</i>) J- <i>pPGI1</i>	3844, 3285	J- <i>pPGI1-YAT1-tYAT1-F</i>	
D- <i>pTPI1</i> - <i>CRC1-tCRC1-F</i>	pUD301 CEN.PK113-7D	6486, 3354 7341, 7336	D- <i>pTPI1</i> <i>CRC1-tCRC1-F</i> (ol <i>pTPI1</i>)	Fusion PCR
	<i>CRC1-tCRC1-F</i> (ol <i>pTPI1</i>) <i>pTPI1-D</i>	3289, 4583	D- <i>pTPI1-CRC1-tCRC1-F</i>	
D- <i>pTEF1</i> - <i>CAT2-tCAT2</i> (ol <i>tSGA1</i>)	pUD304 CEN.PK113-7D	3051, 5231 7340, 7335	D- <i>pTEF1</i> <i>CAT2-tCAT2</i> (ol <i>tSGA1</i> and <i>pTEF1</i>)	Fusion PCR
	<i>CAT2-tCAT2</i> (ol <i>tSGA1</i> and <i>pTEF1</i>) D- <i>pTEF1</i>	4224, 5231	D- <i>pTEF1-CAT2-tCAT2</i> (ol <i>tSGA1</i>)	

REQUIREMENTS FOR CARNITINE-SHUTTLE-MEDIATED TRANSLOCATION OF MITOCHONDRIAL ACETYL MOIETIES TO THE YEAST CYTOSOL

CHAPTER

5

Harmen M. van Rossum, Barbara U. Kozak, Matthijs S. Niemeijer, James C. Dykstra, Marijke A.H. Luttik, Jean-Marc G. Daran, Antonius J.A. van Maris and Jack T. Pronk

Abstract

In many eukaryotes, the carnitine shuttle plays a key role in intracellular transport of acyl moieties. Fatty-acid grown *Saccharomyces cerevisiae* cells employ this shuttle to translocate acetyl units into their mitochondria. Mechanistically, the carnitine shuttle should be reversible, but previous studies indicate that carnitine-shuttle-mediated export of mitochondrial acetyl units to the yeast cytosol does not occur *in vivo*. This apparent unidirectionality was investigated by constitutively expressing genes encoding carnitine-shuttle-related proteins in an engineered *S. cerevisiae* strain, in which cytosolic acetyl coenzyme A (acetyl-CoA) synthesis could be switched off by omitting lipoic acid from growth media. Laboratory evolution of this strain yielded mutants whose growth on glucose, in the absence of lipoic acid, was L-carnitine dependent, indicating that *in vivo* export of mitochondrial acetyl units to the cytosol occurred via the carnitine shuttle. The mitochondrial pyruvate-dehydrogenase complex was identified as the predominant source of acetyl-CoA in the evolved strains. Whole-genome sequencing revealed mutations in genes involved in mitochondrial fatty-acid synthesis (*MCT1*), nuclear-mitochondrial communication (*RTG2*) and encoding a carnitine acetyl-transferase (*YAT2*). Introduction of these mutations into the non-evolved parental strain enabled L-carnitine-dependent growth on glucose. This study indicates intramitochondrial acetyl-CoA concentration and constitutive expression of carnitine-shuttle genes as key factors in enabling *in vivo* export of mitochondrial acetyl units via the carnitine shuttle.

Importance This study demonstrates, for the first time, that *Saccharomyces cerevisiae* can be engineered to employ the carnitine shuttle for export of acetyl moieties from the mitochondria and, thereby, to act as the sole source of cytosolic acetyl-CoA. Further optimization of this ATP-independent mechanism for cytosolic acetyl-CoA provision can contribute to efficient, yeast-based production of industrially relevant compounds derived from this precursor. The strains constructed in this study, whose growth on glucose depends on a functional carnitine shuttle, provide valuable models for further functional analysis and engineering of this shuttle in yeast and other eukaryotes.

5.1 INTRODUCTION

In eukaryotes, metabolic compartmentation necessitates mechanisms for translocation of metabolites between cellular compartments. Acetyl coenzyme A (acetyl-CoA) is an important precursor in cytosolic and mitochondrial biosynthetic pathways and, moreover, is involved in cellular regulation by acting as acetyl donor for acetylation of nuclear and cytosolic proteins (89, 219, 220, 238, 306). Eukaryotes have evolved several mechanisms for synthesis and intracellular transport of acetyl-CoA within and between cellular compartments. One of these, the carnitine shuttle, plays a key role in translocation of acetyl units between cellular compartments during growth of *Saccharomyces cerevisiae* on fatty acids (15, 86, 257).

In contrast to the situation in mammals, in which fatty-acid β -oxidation also occurs in mitochondria, this process is confined to peroxisomes in *S. cerevisiae* (118). Further metabolism of acetyl-CoA, the major product of fatty acid β -oxidation, requires transport of its acetyl moiety from peroxisomes to other cellular compartments (15). This transport is initiated by a peroxisomal carnitine acetyltransferase, which transfers the acetyl moiety of acetyl-CoA to L-carnitine, yielding acetyl-L-carnitine and coenzyme A. Acetyl-L-carnitine is then transported to other compartments, where carnitine acetyltransferases catalyze the reverse reaction, thereby regenerating acetyl-CoA and L-carnitine.

In *S. cerevisiae*, six proteins have been reported to contribute to the *in vivo* functionality of the carnitine shuttle. In contrast to many other eukaryotes, including mammals (319) and the yeast *Candida albicans* (302), *S. cerevisiae* lacks the genes required for L-carnitine biosynthesis (257, 305). As a consequence, operation of the carnitine shuttle in *S. cerevisiae* depends on import of exogenous L-carnitine via the Hnm1 plasma-membrane transporter (4), whose expression is regulated by the plasma-membrane protein Agp2 (4, 258). The three carnitine acetyltransferases in *S. cerevisiae* (15) have different subcellular localizations: Cat2 is active in the peroxisomal and mitochondrial matrices (69), Yat1 is localized to the outer mitochondrial membrane (271) and Yat2 has been reported to be cytosolic (129, 159, 305). The inner mitochondrial membrane contains an (acetyl)-carnitine translocase, Crc1 (84, 160, 233, 258), while export of acetyl-L-carnitine from peroxisomes has been proposed to occur via diffusion through channels in the peroxisomal membrane (103).

Catabolism of the acetyl-CoA generated during growth of *S. cerevisiae* on fatty acids involves the mitochondrial TCA cycle. Conversely, during growth on glucose, the mitochondria act as an important source of acetyl-CoA, with the pyruvate-dehydrogenase (PDH) complex catalyzing the predominant acetyl-CoA generating reaction (244, 318). The carnitine-acetyltransferase reaction is, in principle, mechanistically and thermodynamically reversible ($\Delta G_R^\circ = -1.1 \text{ kJ}\cdot\text{mol}^{-1}$ in the direction of acetyl-L-carnitine formation (79)). This observation suggests that the carnitine shuttle should not only be able to import acetyl units into the mitochondria, but also to export them from the mitochondrial matrix to the cytosol. Therefore, based on *in vitro* experiments, it was initially hypothesized that the carnitine shuttle was responsible for export of acetyl moieties from yeast mitochondria (160). Further studies, however, indicated the PDH bypass, which encompasses the concerted action of pyruvate decarboxylase, acetaldehyde dehydrogenase and acetyl-CoA synthetase (122), to be responsible for cytosolic acetyl-CoA provision in

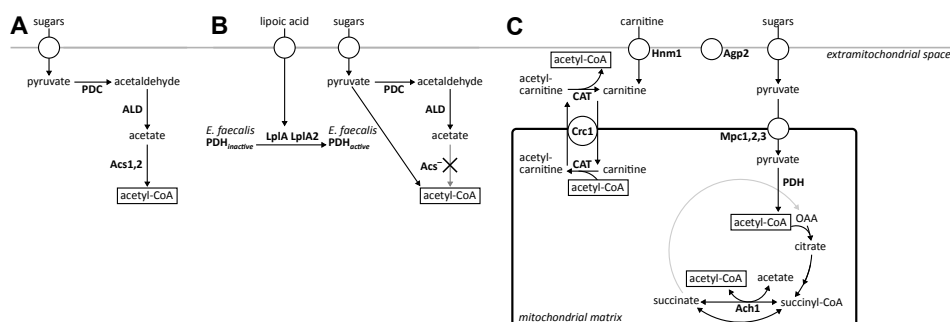


Figure 5.1. Cytosolic acetyl-CoA metabolism in (engineered) *Saccharomyces cerevisiae* strains. **A** In wild-type strains, cytosolic acetyl-CoA is produced via the PDH bypass, consisting of pyruvate carboxylase, acetaldehyde dehydrogenase and acetyl-CoA synthetase. **B** Replacing the native route of acetyl-CoA synthesis by the *Enterococcus faecalis* PDH complex requires the extracellular addition of lipoic acid for activation of the E2 subunit of the cytosolically expressed bacterial PDH complex. **C** In the evolved strains IMS0482 and IMS0483, extracellular L-carnitine is imported into the mitochondria via the Hnm1 transporter at the plasma membrane and the Crc1 transporter at the inner mitochondrial membrane. Pyruvate is imported into the mitochondria, following its oxidative decarboxylation by the native mitochondrial PDH complex. The acetyl moiety is then transferred to L-carnitine, followed by export of acetyl-L-carnitine to the cytosol. There, carnitine acetyltransferases move the acetyl moiety back to CoA, yielding cytosolic acetyl-CoA. Abbreviations: PDC, pyruvate decarboxylase; ALD, acetaldehyde dehydrogenase; Acs, Acs1, Acs2, acetyl-CoA synthetase; Agp2, regulator; CAT, carnitine acetyltransferase; Crc1, acetyl-carnitine translocase; Hnm1, carnitine transporter; LplA, LplA2, lipoylation proteins; Mpc1, Mpc2, Mpc3, mitochondrial pyruvate carrier; OAA, oxaloacetate; PDH, pyruvate dehydrogenase complex.

glucose-grown *S. cerevisiae* cultures (244) (Figure 5.1A). Several additional observations argue against an *in vivo* role of the carnitine shuttle in export of acetyl moieties from mitochondria to cytosol in glucose-grown cultures. In wild-type *S. cerevisiae*, transcription of genes involved in the carnitine shuttle is strongly glucose repressed (69, 151, 271), which precludes a significant contribution to cytosolic acetyl-CoA provision in glucose-grown batch cultures. Moreover, even in derepressed, glucose-limited chemostat cultures, supplementation of growth media with L-carnitine cannot complement the growth defect of strains lacking a functional PDH bypass, which is caused by an inability to synthesize cytosolic acetyl-CoA (203). Hence, based on currently available data, the carnitine shuttle of *S. cerevisiae* appears to operate unidirectionally (i.e. transporting acetyl moieties into the mitochondria) during growth on glucose.

The goal of the present study is to investigate the molecular basis for the apparent unidirectionality of the yeast carnitine shuttle. To this end, we studied growth on glucose of an *S. cerevisiae* strain in which the carnitine shuttle is constitutively expressed. We recently demonstrated that constitutive expression of the components of the carnitine shuttle enables efficient transport of acetyl moieties from cytosol to mitochondria in glucose-grown, L-carnitine-supplemented batch cultures (318). In the present study, overexpression of the carnitine-shuttle proteins was combined with replacement of the native *S. cerevisiae* pathway for cytosolic acetyl-CoA synthesis by a cytosolically expressed bacterial PDH complex (167). In the resulting strain, cytosolic acetyl-CoA synthesis could be switched off at will by omitting lipoic acid from growth media. After laboratory evolution, mutations required for L-carnitine-dependent growth in the absence

of lipoic acid were identified by whole-genome sequencing and functionally analyzed by their introduction in the non-evolved parental strain.

5.2 MATERIALS AND METHODS

5.2.1 Growth media

Yeast-extract/peptone (YP) medium contained 10 g·L⁻¹ Bacto yeast extract (BD, Franklin Lakes, NJ, USA) and 20 g·L⁻¹ Bacto peptone (BD) in demineralized water. Synthetic medium with ammonium as nitrogen source (SM-ammonium), was prepared according to Verduyn *et al.* (326). Synthetic medium with urea as nitrogen source (SM-urea) contained 38 mM urea (SM-urea) and 38 mM K₂SO₄ instead of (NH₄)₂SO₄. SM-ammonium was autoclaved at 121 °C for 20 min, SM-urea was sterilized using 0.2 µm bottle-top filters (Thermo Fisher Scientific, Waltham, MA, USA). Solid media were prepared by addition of 20 g·L⁻¹ agar (BD), prior to autoclaving at 121 °C for 20 min. Where indicated, urea was added after heat-sterilization of the solid media from a filter-sterilized 100-fold concentrated stock solution.

5

5.2.2 Strains, growth conditions and storage

All *S. cerevisiae* strains used in this study (Table 5.1) share the CEN.PK genetic background (71, 222). Shake-flask cultures in 500-mL flasks with 100 mL SM-urea and 20 g·L⁻¹ glucose were grown at 30 °C in an Innova incubator shaker (New Brunswick Scientific, Edison, NJ, USA) set at 200 rpm. Stock cultures were grown in YP medium with 20 g·L⁻¹ glucose. Where indicated, lipoic acid was added to sterile media to a concentration of 50 ng·L⁻¹. A 50 mg·L⁻¹ stock solution of lipoic acid was prepared by dissolving 5 g·L⁻¹ (±)-α-lipoic acid (Sigma-Aldrich, St. Louis, MO, USA) in ethanol and diluting the resulting solution 100 fold in sterile demineralized water. L-Carnitine (Sigma-Aldrich) was added to sterile media from a 40 g·L⁻¹ filter-sterilized stock solution at the concentration indicated. Frozen stock cultures of yeast strains were prepared by adding glycerol (-30% v/v) to exponentially growing shake-flask cultures and freezing 1-mL aliquots at -80 °C.

5.2.3 Plasmid construction

GuideRNA (gRNA) plasmids for CRISPR/Cas9-based genome editing (Table S5.1) were constructed as described previously (200). In short, double-gRNA cassettes were PCR-amplified using the primer(s) indicated in Tables S1 and S2. Plasmid backbones containing the desired marker gene were obtained by PCR with primer 6005, using the appropriate pROS plasmid (Table S5.1) as a template. The two fragments were then assembled into a plasmid with the Gibson Assembly kit (New England Biolabs, Ipswich, MA, USA) or NEBuilder HiFi DNA Assembly Cloning kit (New England Biolabs). Multi-copy plasmids carrying wild-type and mutated YAT2 variants were based on the pRS426 expression vector (48). *pADH1-YAT2-tYAT2* and *pADH1-YAT2^{C173G}-tYAT2* fragments were PCR amplified from strains IMX745 and IMS0482, respectively, using primers 8902 & 8903 and then inserted into the EcoRI-XhoI-linearized pRS426 backbone with the NEBuilder HiFi DNA Assembly Cloning kit. After transforming the resulting plasmids to *E. coli* and confirmation of their DNA sequences by Illumina sequencing, this yielded pUDE390 (2 µm ori *URA3 pADH1-YAT2-tYAT2*) and pUDE391 (2 µm ori *URA3 pADH1-YAT2^{C173G}-tYAT2*). A multi-copy plasmid carrying the *CAT2* gene under control of the *TDH3* promoter was similarly obtained by assembling a pRS426 backbone with a *CAT2* PCR fragment using Gibson Assembly. The *TDH3* promoter and *CYC1* terminator sequences were synthesized and assembled into the pRS426 vector by GenScript (Piscataway, NJ, USA). The resulting plasmid was linearized by PCR amplification using primers 3627

& 3921. The *CAT2* ORF was amplified via PCR from CEN.PK113-7D genomic DNA using primers 5948 & 5949. Gibson Assembly of the two fragments yielded pUDE336 (2 μ m ori *URA3 pTDH3-CAT2-His₆-tCYC1*).

5.2.4 Strain construction

S. cerevisiae strains were transformed according to Gietz and Woods (97) and transformants selected on solid YP medium with 20 g·L⁻¹ glucose. Appropriate antibiotics were added at the following concentrations: G418 (InvivoGen, San Diego, CA, USA), 200 mg·L⁻¹; hygromycin B (InvivoGen), 200 mg·L⁻¹; nourseothricin (Jena Bioscience, Jena, Germany), 100 mg·L⁻¹. Lipic acid was added as indicated above. Throughout the text we refer to chromosomally integrated gene clusters with four-capital acronyms surrounded by curly brackets (based on the common practice in set theory for indicating a collection of elements). A mutation in a gene that is part of the cluster is indicated within the curly brackets. For example, {CARN, *YAT2*^{C173G}} refers to the {CARN} set in which the *YAT2* gene carries a C173G nucleotide change.

Unless indicated otherwise, genetic engineering was done using CRISPR/Cas9 (200). The platform strain with constitutive expression of the genes involved in the carnitine shuttle (*HNM1*, *AGP2*, *CRC1*, *YAT1*, *YAT2* and *CAT2*) was constructed by modification of the previously constructed strain IMX719 (200), which had *ACS1* and *ACS2* replaced by the genes required for an active, lipoylated cytosolic *Enterococcus faecalis* PDH complex {PDHL}. Analogous to a previous description (318), the genes involved in the carnitine shuttle were placed under the control of strong constitutive promoters and integrated into the *SGA1* locus of strain IMX719, resulting in strain IMX745 (*acs1Δ acs2Δ::*{PDHL} *sga1Δ::*{CARN}) (Table 5.1). To remove the *E. faecalis* PDH genes {PDHL} or the set of carnitine shuttle expression cassettes {CARN} from strains IMS0482 and IMS0483, either plasmid pUDR072 (to remove {PDHL}) or pUDR073 (to remove {CARN}) was transformed together with a repair fragment obtained by annealing oligonucleotides 7349 & 7350 or oligonucleotides 8012 & 8013 (Table S5.2), respectively, resulting in strains IMW074 – IMW077. Deletion of *PDA1* and *ACH1* in strains IMS0482 and IMS0483 was done by transformation with pUDR047 (with oligonucleotides 6157 & 6158) and pUDR085 (with oligonucleotides 6160 & 6161), resulting in strains IMW078 – IMW082. To introduce the *MCT1*^{T641G} mutation, plasmid pUDR080 and a repair fragment obtained by annealing oligonucleotides 8417 & 8418 was transformed into strain IMX745 (Table 5.1), resulting in strain IMX847. Similarly, the *RTG2*^{G503T} mutation was introduced in strain IMX745 by transforming plasmid pUDR078 and oligonucleotides 8430 & 8431, resulting in strain IMX849. Double mutations *MCT1*^{T641G} *RTG2*^{G503T} were introduced in IMX745 using plasmid pUDR079 using oligonucleotides 8417 & 8418 and 8430 & 8431, resulting in strain IMX852. To selectively introduce the *YAT2*^{C173G} mutation in the *ADH1*-promoter-driven gene and not the *YAT2*-promoter driven gene (at chromosome V), the SNP was introduced in {CARN} via a two-step strategy. First, a synthetic CRISPR target site was introduced by transformation of strains IMX745, IMX847, IMX849 and IMX852 with plasmid pUDR073 and oligonucleotides 8621 & 8622, thereby removing part of the *ADH1* promoter and part of the *YAT2* ORF. Next, the fragment containing the *YAT2*^{C173G} mutation was PCR amplified from the IMS0482 genome using primers 8618 & 8619 and co-transformed with plasmid pUDR105, introducing the *YAT2*^{C173G} mutation and resulting in strains IMX907, IMX909, IMX911 and IMX913. In all these cases, after introduction of the desired mutations, the double gRNA plasmids were removed, followed by confirmation of the SNPs by Sanger sequencing (BaseClear BV, Leiden, The Netherlands) using the primers indicated in Table S5.2. The ORFs of *YAT2* (the copy present in {CARN}), *RTG2* and *MCT1* were deleted from the genome of, respectively, strains IMX852, IMX909 and IMX911 by transforming the following plasmids and repair fragments: strain IMX852, plasmid pUDR073 and oligonucleotides 8874 & 8875; strain IMX909, plasmid pUDR078 and oligonucleotides 8428 & 8429; and strain IMX911, plasmid

pUDR080 and oligonucleotides 8415 & 8416. After gene knockout was confirmed by diagnostic PCR (Table S5.2), the resulting strains were named IMX932 – IMX934, respectively.

The *pADH1-YAT2-tYAT2* variants were integrated in the *cas9*-bearing reference strain IMX585. *pADH1-YAT2-tYAT2* (wild-type) and *pADH1-YAT2^{C173G}-tYAT2* cassettes were amplified with PCR using primers 8647 & 8648 from genomic DNA of strains IMX745 and IMS0482, respectively. The resulting cassettes had overlaps with the promoter and terminator of *SGA1*, enabling integration into the *SGA1* locus. Cas9 was directed to the *SGA1* locus using the gRNA plasmid pUDR119 (Table S5.1), following integration of the cassette by *in vivo* homologous recombination. After confirmation of correct integration and sequence by PCR and Sanger sequencing, plasmid pUDR119 was removed as described earlier (200), resulting in strains IMX923 and IMX925, respectively. To get the multi-copy-based *YAT2* and *CAT2* expressing strains, plasmids pUDE336, pUDE390 and pUDE391 were transformed to CEN.PK113-5D, resulting in strains IME233, IME320 and IME321, respectively (Table 5.1).

Deletion of *CAT2* and *YAT1*, to get strain CEN.PK215-4A (*cat2Δ yat1Δ*), was carried out by transformation of a *kanMX* marker cassette, obtained by PCR using pUG6 as template (108) with the primers 9237 & 9238 for the *CAT2* deletion cassette and primers 9239 & 9240 for the *YAT1* deletion cassette. The amplified *kanMX* cassettes were used as selectable markers to replace the target genes in the prototrophic diploid strain CEN.PK122. Transformants were verified for correct gene replacement by diagnostic PCR (Table S5.2). After sporulation and tetrad dissection, the corresponding haploid deletion strains, CEN.PK194-2C (*MATa cat2Δ*) and CEN.PK196-2C (*MATa yat1Δ*), were obtained. To obtain a strain with both *CAT2* and *YAT1* deleted, strains CEN.PK194-2C and CEN.PK196-2C were crossed. After tetrad dissection, spores were subsequently analyzed by diagnostic PCR to confirm correct deletion of both genes, resulting in strain CEN.PK215-4A (*cat2Δ yat1Δ*) (Table 5.1).

5.2.5 Molecular biology techniques

PCR amplification with the Phusion® Hot Start II High Fidelity Polymerase (Thermo Fisher Scientific), was performed according to the manufacturer's instructions, using HPLC- or PAGE-purified oligonucleotide primers (Sigma-Aldrich). Diagnostic colony PCR was performed on randomly picked transformed colonies, using DreamTaq (Thermo Fisher Scientific) and desalted primers (Sigma-Aldrich). DNA fragments obtained by PCR were separated by gel electrophoresis on 1% (w/v) agarose gels (Thermo Fisher Scientific) in TAE buffer (Thermo Fisher Scientific). Alternatively, fragments were purified using the GenElute™ PCR Clean-Up Kit (Sigma-Aldrich). Plasmids were isolated from *E. coli* with Sigma GenElute Plasmid kit (Sigma-Aldrich) according to the supplier's manual. Yeast genomic DNA was isolated using a YeaStar Genomic DNA kit (Zymo Research) or using an SDS/LiAc-based lysis protocol (195). *E. coli* XL1-Blue (GE Healthcare Life Sciences, The Netherlands) was used for chemical transformation or for electroporation. Chemical transformation was done according to Inoue et al. (133). Electroporation was done in a 2 mm cuvette (165–2086, Bio-Rad, Hercules, CA, USA) using a Gene Pulser Xcell Electroporation System (Bio-Rad), following the manufacturer's protocol. Electrocompetent *E. coli* cells were prepared according to the same protocol, with the exception that, during preparation of competent cells, *E. coli* was grown in LB medium without sodium chloride.

5.2.6 Laboratory evolution

Strain IMX745 was inoculated in 500-mL shake flasks, containing 100 mL SM-urea with 20 g·L⁻¹ glucose and 400 mg·L⁻¹ L-carnitine. When stationary phase was reached, 1–3 mL of culture was transferred to a new shake flask. After 6–7 serial shake flask transfers, 8 individual cells were iso-

lated from each evolution experiment using a micromanipulator (Singer Instruments, Watchet, UK) and placed on SM-urea plates with 20 g·L⁻¹ glucose and 400 mg·L⁻¹ L-carnitine. For each evolution experiment, one colony was selected and restreaked once, yielding strains IMS0482 (evolution line 1) and IMS0483 (evolution line 2) (Table 5.1).

5.2.7 DNA sequencing and sequence analysis

After isolation of genomic DNA (164) of strains IMX745, IMS0482 and IMS0483, 350-bp insert libraries were constructed and paired-end sequenced (100 bp reads) with an Illumina HiSeq 2500 sequencer (Baseclear BV, Leiden, The Netherlands). At least 500 Mb of sequence data, corresponding to a ca. 40-fold coverage, was generated for each strain. Plasmids pUDE390 and pUDE391 were sequenced in-house using the Illumina MiSeq platform (San Diego, CA, USA). After quantification of plasmid DNA with the Qubit 2.0 fluorometer (Thermo Fisher Scientific), DNA libraries were prepared using the Nextera XT DNA kit (Illumina). 300 bp paired-end reads of plasmid DNA generated on the MiSeq platform were mapped to an *in silico*-generated plasmid sequence using the Burrows–Wheeler Alignment tool (184) and processed with Pilon (332). Sequence reads of genomic DNA were mapped onto the CEN.PK113-7D genome (222), supplemented with sequences containing the modified *SGA1*, *ACS2* and *CAN1* loci, using the Burrows–Wheeler Alignment tool (184). Data were further processed with Pilon (332) and sequence variations were extracted from the Pilon output file ‘changes’. Uniqueness of sequence differences in strains IMS0482 and IMS0483 were manually confirmed by comparison with strain IMX745 using the Integrative Genomics Viewer (311). Copy number variations in strains IMS0482 and IMS0483, relative to strain IMX745, were determined with the Poisson-mixture model based algorithm Magnolya (223). Raw sequencing data of strains IMX745, IMS0482 and IMS0483 are deposited at the NCBI Sequence Read Archive (www.ncbi.nlm.nih.gov/sra) under BioProject ID PRJNA313402.

5.2.8 Growth studies in shake flasks and using spot plate assays

For growth studies in shake flasks and using spot plates, strains were pre-grown in shake flasks with SM-urea and 20 g·L⁻¹ glucose with lipoic acid or L-carnitine, where appropriate. For growth studies in shake flasks, cells were washed twice with synthetic medium (326) and transferred to new shake flasks with SM-urea, 20 g·L⁻¹ glucose and 40 mg·L⁻¹ L-carnitine or 50 ng·L⁻¹ lipoic acid, where indicated. Growth rates were based on OD₆₆₀ measurements using a Libra S11 spectrophotometer (Biochrom, Cambridge, UK). Culture viability was estimated with the FungaLight AM-CFDA (acetoxymethyl ester 5-carboxyfluorescein diacetate)/propidium iodide yeast viability kit (Invitrogen, Carlsbad, CA) and a Cell Lab Quanta SC MPL flow cytometer (Beckman Coulter, Woerden, Netherlands) as described previously (16). For the preparation of spot plates, pre-cultures were washed once with synthetic medium and diluted in synthetic medium to an OD₆₆₀ of 0.273 (corresponding to 2·10⁶ cells·mL⁻¹). 5 µL samples of a dilution series, containing an estimated 2·10⁵, 2·10⁴ and 2·10³ cells per mL, were spotted on SM-urea agar plates with 20 g·L⁻¹ glucose and L-carnitine (400 mg·L⁻¹) or lipoic acid (50 ng·L⁻¹) as indicated.

5.2.9 Enzyme activity assays

Cell extracts were prepared as described before (318) from mid-exponentially growing cultures. The growth medium was SM-ammonium with either 20 g·L⁻¹ glucose or 2% (v/v) ethanol as carbon source and, where required, lipoic acid. Activities in cell extracts of carnitine-acetyltransferase activity (318) and glucose-6-phosphate dehydrogenase (241) (the latter activity was used to verify

the quality of cell extracts), were assayed spectrophotometrically as described previously (318). Protein concentrations in cell extracts were determined with the Lowry method (197).

5.3 RESULTS

5.3.1 Constitutive expression of carnitine-shuttle genes does not rescue growth on glucose of *acs1Δ acs2Δ S. cerevisiae*.

Interpretation of previous studies on the role of the carnitine shuttle in glucose-grown cultures of *S. cerevisiae* is complicated by the strong glucose repression of the structural genes encoding carnitine acetyltransferases and acetyl-carnitine translocase (69, 151, 157, 271). To re-examine whether the carnitine shuttle can translocate acetyl units from mitochondria to cytosol, a strain was constructed in which provision of cytosolic acetyl-CoA could be made strictly dependent on a constitutively expressed carnitine shuttle. Its construction (Figure 5.2A) started with a strain in which cytosolic acetyl-CoA metabolism had been modified by replacing the acetyl-CoA synthetase genes *ACS1* and *ACS2* by the 6-gene {PDHL} cluster ((200), Table 5.1), which enables functional expression in the yeast cytosol of the *E. faecalis* PDH complex (Figure 5.1B). This strain provided an experimental model in which cytosolic acetyl-CoA synthesis could be switched off at will by omitting lipoic acid from growth media. Functionality of alternative (introduced) routes to cytosolic acetyl-CoA could thus be tested by omitting lipoic acid and checking for growth. Expression cassettes were constructed in which the yeast carnitine-shuttle genes (*AGP2*, *CAT2*, *CRC1*, *HNMT1*, *YAT1* and *YAT2*) were controlled by strong, constitutive promoters. The resulting six DNA fragments were assembled and integrated as a single cluster ({CARN}; Figure 5.2B; Table 5.1) into the genome of the strain carrying the {PDHL} cluster. Consistent with an earlier study on cytosolic expression of the *E. faecalis* PDH complex in *S. cerevisiae* (167), growth of the resulting strain IMX745 (*acs1Δ acs2Δ::*{PDHL} *sga1Δ::*{CARN}) on glucose synthetic medium depended on addition of lipoic acid to the growth medium.

Table 5.1. *Saccharomyces cerevisiae* strains used in this study.

Name	Relevant genotype ^a	Parental strain(s)	Origin
CEN.PK113-7D	<i>MATa</i>		P. Kötter
IMX585	<i>MATa can1Δ::cas9-natNT2</i>	CEN.PK113-7D	(200)
IMX719	<i>MATa can1Δ::cas9-natNT2 acs1Δ acs2Δ::</i> {PDHL} ^b	IMX585	(200)
IMX868	<i>MATa can1Δ::cas9-natNT2 sga1Δ::</i> {CARN} ^c		(318)
IMX745	<i>MATa can1Δ::cas9-natNT2 acs1Δ acs2Δ::</i> {PDHL} <i>sga1Δ::</i> {CARN}	IMX719	This study
IMS0482	<i>MATa can1Δ::cas9-natNT2 acs1Δ acs2Δ::</i> {PDHL} <i>sga1Δ::</i> {CARN}	IMX745	This study
IMS0483	<i>MATa can1Δ::cas9-natNT2 acs1Δ acs2Δ::</i> {PDHL} <i>sga1Δ::</i> {CARN}	IMX745	This study

Name	Relevant genotype ^a	Parental strain(s)	Origin
IMW074	<i>MATa can1Δ::cas9-natNT2 acs1Δ acs2Δ::[PDHL] sga1Δ</i>	IMS0482	This study
IMW075	<i>MATa can1Δ::cas9-natNT2 acs1Δ acs2Δ sga1Δ::[CARN]</i>	IMS0482	This study
IMW076	<i>MATa can1Δ::cas9-natNT2 acs1Δ acs2Δ::[PDHL] sga1Δ</i>	IMS0483	This study
IMW077	<i>MATa can1Δ::cas9-natNT2 acs1Δ acs2Δ sga1Δ::[CARN]</i>	IMS0483	This study
IMW078	<i>MATa can1Δ::cas9-natNT2 acs1Δ acs2Δ::[PDHL] sga1Δ::[CARN] ach1Δ</i>	IMS0482	This study
IMW079	<i>MATa can1Δ::cas9-natNT2 acs1Δ acs2Δ::[PDHL] sga1Δ::[CARN] pda1Δ</i>	IMS0482	This study
IMW081	<i>MATa can1Δ::cas9-natNT2 acs1Δ acs2Δ::[PDHL] sga1Δ::[CARN] ach1Δ</i>	IMS0483	This study
IMW082	<i>MATa can1Δ::cas9-natNT2 acs1Δ acs2Δ::[PDHL] sga1Δ::[CARN] pda1Δ</i>	IMS0483	This study
IMX847	<i>MATa can1Δ::cas9-natNT2 acs1Δ acs2Δ::[PDHL] sga1Δ::[CARN] MCT1^{T641G}</i>	IMX745	This study
IMX849	<i>MATa can1Δ::cas9-natNT2 acs1Δ acs2Δ::[PDHL] sga1Δ::[CARN] RTG2^{G503T}</i>	IMX745	This study
IMX852	<i>MATa can1Δ::cas9-natNT2 acs1Δ acs2Δ::[PDHL] sga1Δ::[CARN] MCT1^{T641G} RTG2^{G503T}</i>	IMX745	This study
IMX907	<i>MATa can1Δ::cas9-natNT2 acs1Δ acs2Δ::[PDHL] sga1Δ::[CARN, pADH1-YAT2^{C173G}]</i>	IMX745	This study
IMX909	<i>MATa can1Δ::cas9-natNT2 acs1Δ acs2Δ::[PDHL] sga1Δ::[CARN, pADH1-YAT2^{C173G}] MCT1^{T641G}</i>	IMX847	This study
IMX911	<i>MATa can1Δ::cas9-natNT2 acs1Δ acs2Δ::[PDHL] sga1Δ::[CARN, pADH1-YAT2^{C173G}] RTG2^{G503T}</i>	IMX849	This study
IMX913	<i>MATa can1Δ::cas9-natNT2 acs1Δ acs2Δ::[PDHL] sga1Δ::[CARN, pADH1-YAT2^{C173G}] MCT1^{T641G} RTG2^{G503T}</i>	IMX852	This study
IMX932	<i>MATa can1Δ::cas9-natNT2 acs1Δ acs2Δ::[PDHL] sga1Δ::[CARN, yat2Δ] MCT1^{T641G} RTG2^{G503T}</i>	IMX852	This study
IMX933	<i>MATa can1Δ::cas9-natNT2 acs1Δ acs2Δ::[PDHL] sga1Δ::[CARN, pADH1-YAT2^{C173G}] MCT1^{T641G} rtg2Δ</i>	IMX909	This study
IMX934	<i>MATa can1Δ::cas9-natNT2 acs1Δ acs2Δ::[PDHL] sga1Δ::[CARN, pADH1-YAT2^{C173G}] mct1Δ RTG2^{G503T}</i>	IMX911	This study
IMX923	<i>MATa can1Δ::cas9-natNT2 sga1Δ::pADH1-YAT2-tYAT2</i>	IMX585	This study

Name	Relevant genotype ^a	Parental strain(s)	Origin
IMX925	<i>MATa can1Δ::cas9-natNT2</i> <i>sga1Δ::pADH1-YAT2^{C173G}-tYAT2</i>	IMX585	This study
CEN.PK122	<i>MATa/MATa</i>		P. Kötter
CEN.PK194-2C	<i>MATa cat2Δ::loxP-KanMX4-loxP</i>	CEN.PK122	This study
CEN.PK196-2C	<i>MATa yat1Δ::loxP-KanMX4-loxP</i>	CEN.PK122	This study
CEN.PK215-4A	<i>MATa cat2Δ::loxP-KanMX4-loxP</i> <i>yat1Δ::loxP-KanMX4-loxP</i>	CEN.PK194-2C × CEN.PK196-2C	This study
CEN.PK113-5D	<i>MATa ura3-52</i>		P. Kötter
IME140	<i>MATa ura3-52 p426GPD (2 μm ori URA3)</i>	CEN.PK113-5D	(166)
IME320	<i>MATa ura3-52 pUDE390 (2 μm ori URA3</i> <i>pADH1-YAT2-tYAT2)</i>	CEN.PK113-5D	This study
IME321	<i>MATa ura3-52 pUDE391 (2 μm ori URA3</i> <i>pADH1-YAT2^{C173G}-tYAT2)</i>	CEN.PK113-5D	This study
IME233	<i>MATa ura3-52 pUDE336 (2 μm ori URA3</i> <i>pTDH3-CAT2-His₆-tCYC1)</i>	CEN.PK113-5D	This study

^aThe *RTG2^{G503T}* mutation translates into a Rtg2^{W168L} protein, *MCT1^{T641G}* in Mct1^{L214W} and *YAT2^{C173G}* in Yat2^{P58R}
^b{PDHL}, *PDH E. faecalis*, *pADH1-aceF-tPGI1 pPGI1-lplA2-tPYK1 pPGK1-lplA-tPMA1*
pTDH3-pdhB-tCYC1 pTEF1-lpd-tADH1 pTPI1-pdhA-tTEF1
^c{CARN}, *pTDH3-AGP2-tAGP2 pPGK1-HNM1-tHNM1 pADH1-YAT2-tYAT2 pPGI1-YAT1-tYAT1*
pTPI1-CRC1-tCRC1 pTEF1-CAT2-tCAT2

Enzyme activities in cell extracts of strain IMX745 showed a carnitine acetyltransferase (CAT) activity of 3.2 ± 0.1 μmol·(mg protein)⁻¹·min⁻¹, while activities in extracts of the parental strain IMX719 (*acs1Δ acs2Δ::*{PDHL}) and of the reference strain IMX585 (*ACS1 ACS2*) were below the detection limit of the assay (< 0.01 μmol·(mg protein)⁻¹·min⁻¹). Growth of strain IMX745 was not observed when lipoic acid was replaced by L-carnitine or when both growth factors were omitted from the glucose synthetic medium (Figure 5.3). This result demonstrated that, even when constitutively expressed, the *S. cerevisiae* carnitine shuttle cannot export acetyl units from mitochondria at a rate that is sufficient to meet cytosolic acetyl-CoA requirements in an *acs1Δ acs2Δ* strain background.

5.3.2 Laboratory evolution yields mutants in which the carnitine shuttle provides cytosolic acetyl-CoA.

To investigate whether laboratory evolution can enable the carnitine shuttle to support export of acetyl units from the mitochondrial matrix, a laboratory evolution experiment was started with strain IMX745 (*Acs⁻* {PDHL} {CARN}) by starting two independent shake-flask cultures on synthetic medium with 20 g·L⁻¹ glucose and 400 mg·L⁻¹ L-carnitine (Figure 5.2C). Following two weeks of incubation, growth was observed in both shake flasks and after 6 to 7 subsequent transfers (corresponding to ca. 70 generations) single-cell lines were isolated from each experiment, resulting in strains IMS0482

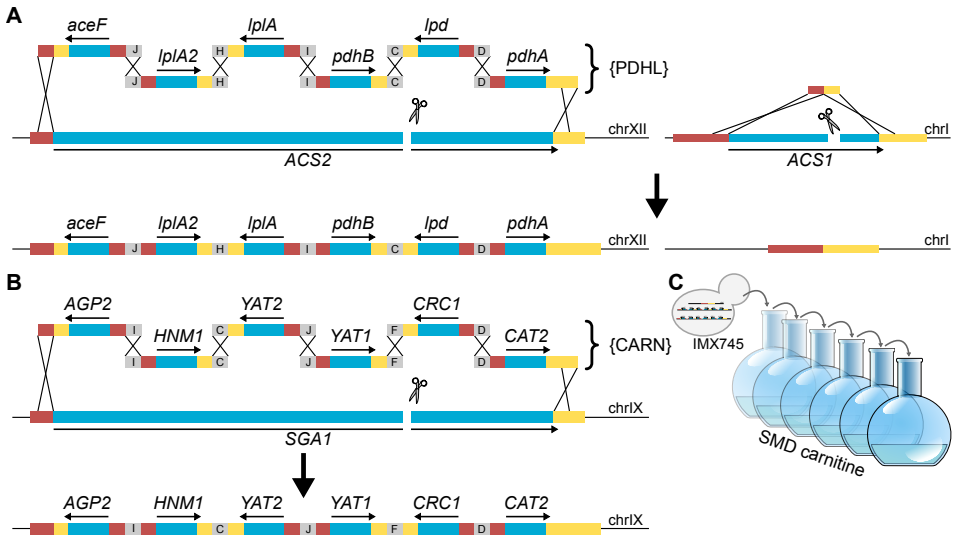


Figure 5.2. Construction of a lipinoic-acid-dependent, carnitine-shuttle-constitutive *S. cerevisiae* strain and its laboratory evolution for lipinoic-acid-independent, carnitine-dependent growth. **A** In a previous study (200), the {PDHL} cluster, consisting of 6 cassettes required for cytosolic expression of a functional *Enterococcus faecalis* pyruvate-dehydrogenase complex and flanked by 60 bp sequences was assembled *in vivo* via homologous recombination (indicated with black crosses) and introduced into ACS2 after introduction of a Cas9-induced double-strand break. ACS1 was removed using a 120 bp DNA repair fragment (figure adapted from (200)). **B** In this strain, the {CARN} cluster, consisting of 6 cassettes for constitutive expression of carnitine-shuttle genes, was similarly *in vivo* assembled and introduced into the SGA1 locus, resulting in strain IMX745 (*acs1Δ::*{PDHL} *sga1Δ::*{CARN}). Activity of the *E. faecalis* PDH in the yeast cytosol is lipinoic-acid dependent (167). **C** As strain IMX745 did not show L-carnitine-dependent growth when lipinoic acid was omitted from growth media, an evolution experiment was initiated using synthetic medium with 20 g·L⁻¹ glucose (SMD) and 400 mg·L⁻¹ L-carnitine.

and IMS0483. These evolved strains readily grew on glucose synthetic medium supplemented with either lipinoic acid or L-carnitine, but did not grow when both compounds were omitted from the medium (Figure 5.3). In shake-flask cultures on glucose synthetic medium, addition of L-carnitine supported specific growth rates of 0.14 h⁻¹ (IMS0482) and 0.10 h⁻¹ (IMS0483) (Table 5.2). When the synthetic gene cluster encoding the *E. faecalis* PDH complex {PDHL} was removed from the evolved strains, growth of the resulting strains on glucose could no longer be supported by lipinoic-acid addition and, instead, became uniquely dependent on L-carnitine (Figure 5.4). Conversely, deletion of the six carnitine-shuttle expression cassettes {CARN} from the evolved strains abolished their L-carnitine-dependent growth, leaving the strains uniquely dependent on lipinoic acid (Figure 5.4). Together, these results unequivocally show that, in the evolved strains, export of the acetyl moiety of mitochondrially produced acetyl-CoA via the constitutively expressed carnitine shuttle supported cytosolic acetyl-CoA provision (Figure 5.1C).

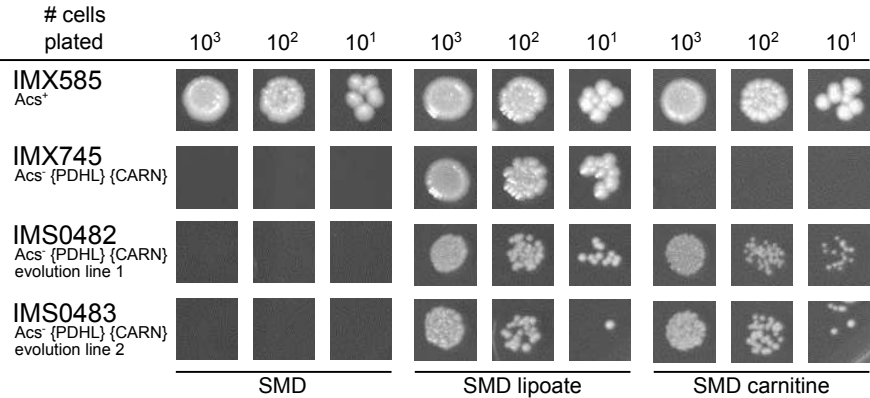


Figure 5.3. Growth on glucose of *S. cerevisiae* strains in the presence and absence of lipoleic acid and L-carnitine. *S. cerevisiae* strains were pre-grown in shake flasks on synthetic medium with 20 g·L⁻¹ glucose (strain IMX585), supplemented with lipoleic acid (strain IMX745) or L-carnitine (strains IMS0482 and IMS0483) and spotted on glucose synthetic medium plates without lipoleic acid or L-carnitine (left panel), with lipoleic acid (middle panel) and with L-carnitine (right panel). Plates were incubated for 100 h at 30 °C. Relevant strain descriptions are given in the figure.

Table 5.2. Specific growth rates of different *acs1Δ acs2Δ S. cerevisiae* strains on glucose in the presence of L-carnitine. *Acs*⁻ *S. cerevisiae* strains were grown on glucose synthetic medium lacking lipoleic acid, thereby blocking synthesis of cytosolic acetyl-CoA via heterologously expressed bacterial pyruvate dehydrogenase complex. Strains were grown in shake flasks with 20 g·L⁻¹ glucose; media were supplemented with 40 mg·L⁻¹ L-carnitine. Data represent averages of two independent experiments for each strain. With the exception of strain IMX909, which showed biphasic growth, the average deviation of the mean specific growth rate was ≤ 0.01 h⁻¹ in all experiments.

Strain	Short description ^a	Growth rate (h ⁻¹)
IMX745	Unevolved strain	no growth ^b
IMS0482	Evolution line 1	0.14
IMS0483	Evolution line 2	0.10
IMX909	Mct1 ^{L214W} Rtg2 ^{Yat2^{P58R}}	0.10 – 0.06 ^c
IMX913	Mct1 ^{L214W} Rtg2 ^{W168L} Yat2 ^{P58R}	0.14

^aAll strains harbour the {PDHL} and {CARN} gene sets. Composition of these gene sets is described in the Materials and methods section.

^bGrowth was only observed in the presence of lipoleic acid (0.29 h⁻¹).

^cShake-flask cultures of strain IMX909 showed decelerating growth rates from mid-exponential phase onwards.

5.3.3 The mitochondrial PDH complex is the predominant source of acetyl-CoA in evolved, L-carnitine-dependent *acs1Δ acs2Δ* strains.

In *S. cerevisiae*, mitochondrial acetyl-CoA can be generated by the native, mitochondrial PDH complex and by the mitochondrial succinyl-CoA:acetate CoA-transferase Ach1 (80,

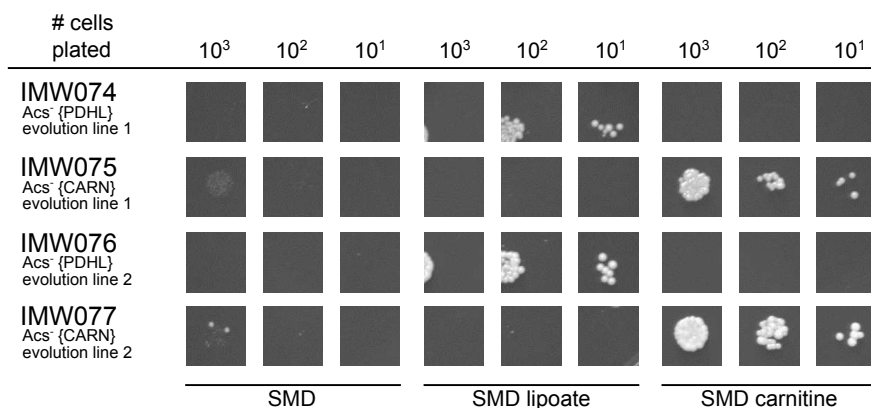


Figure 5.4. Growth on glucose of *S. cerevisiae* strains in the presence and absence of lipoic acid and L-carnitine. *S. cerevisiae* strains were pre-grown in shake flasks on synthetic medium with 20 g·L⁻¹ glucose, supplemented with lipoic acid (strains IMW074 and IMW076) or L-carnitine (strains IMW075 and IMW077) and spotted on glucose synthetic medium plates without lipoic acid or L-carnitine (left panel), with lipoic acid (middle panel) and with L-carnitine (right panel). Plates were incubated for 100 h at 30 °C. Relevant strain descriptions are given in the figure.

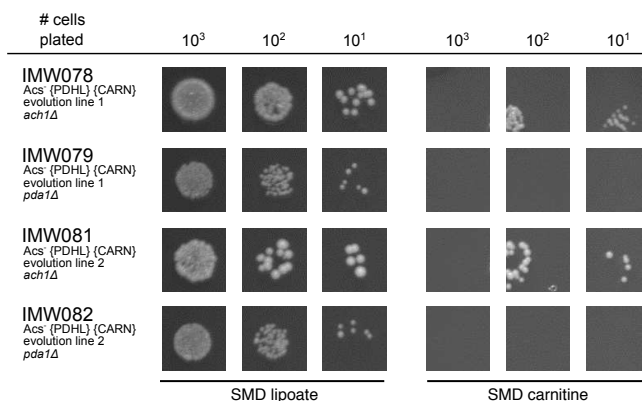


Figure 5.5. Growth on glucose of *S. cerevisiae* strains in the presence of lipoic acid or L-carnitine. *S. cerevisiae* strains were pre-grown in shake flasks on synthetic medium with 20 g·L⁻¹ glucose, supplemented with lipoic acid and spotted on glucose synthetic medium plates with lipoic acid (left panel) or with L-carnitine (right panel). Plates were incubated for 100 h at 30 °C. Relevant strain descriptions are given in the figure.

244, 318). To study which of these reactions provided mitochondrial acetyl-CoA in the evolved strains IMS0482 and IMS0483, the mitochondrial PDH complex was inactivated by deleting *PDA1* (245, 338) and Ach1 activity was abolished by disrupting *ACH1*. In both evolved strains, deletion of *PDA1* abolished L-carnitine-dependent growth on glucose, while *ACH1* disruption did not have a detectable impact on growth (Figure 5.5). These results demonstrate that, in glucose-grown batch cultures of the evolved strains, the *S. cerevisiae* PDH complex is the predominant source of mitochondrial acetyl-CoA and, via the constitutively expressed carnitine shuttle, of cytosolic acetyl-CoA.

5.3.4 Whole-genome sequencing and reverse engineering of evolved *L*-carnitine-dependent strains.

To identify the mutations that enabled *L*-carnitine-dependent growth of the evolved carnitine-dependent *acs1Δ acs2Δ* strains, the genomes of strains IMS0482 and IMS0483 (*Acs*[−] {PDHL} {CARN}, isolated from evolution lines 1 and 2, respectively) and of their parental strain IMX745 (*Acs*[−] {PDHL} {CARN}) were sequenced. Analysis of single-nucleotide changes and insertions/deletions (indels) in open-reading frames revealed only three mutations in strain IMS0482 (evolution line 1) and four in strain IMS0483 (evolution line 2), relative to the parental strain (Table 5.3). Analysis of copy number variations showed that strain IMS0482 carried a duplication of chromosome X (data not shown). Chromosome X did not carry either of the two synthetic gene clusters, nor any of three mutated genes. No copy-number variations relative to the parental strain were detected in strain IMS0483.

Both evolved strains carried mutations in *MCT1*, which is predicted to encode the mitochondrial malonyl-CoA:ACP transferase that catalyzes the second step of mitochondrial fatty-acid synthesis (159, 250, 273). In IMS0482, the *MCT1*^{T641G} mutation caused an amino-acid change from leucine to tryptophan at position 214 and in IMS0483 a *MCT1*^{C292T} mutation caused a premature stop codon at position 98. Strain IMS0482 carried an additional mutation in *RTG2*, which resulted in a W168L amino-acid change. *Rtg2* is involved in communication between mitochondria and nucleus and deletion of *RTG2* negatively affects activity of citrate synthase (oxaloacetate + acetyl-CoA + H₂O → citrate + CoA; (189, 283)). A third mutation in strain IMS0482 was found in the introduced expression cassette for *YAT2*, which has been reported to encode a cytosolic carnitine acetyltransferase (305) and caused a P58R amino-acid change in the evolved strain. In strain IMS0483, the abovementioned *MCT1*^{C292T} mutation was accompanied by single-nucleotide changes in the coding regions of *RPO21* and *STB2* and a deletion of either *HXT6* or *HXT7*. Since the protein products of these three genes did not show an obvious relation with mitochondrial metabolism (Table 5.3), further analysis was focused on the mutations found in strain IMS0482 which, moreover, exhibited the highest specific growth rate on glucose of the two evolved strains (Table 5.2).

5.3.5 Mutations in *MCT1*, *RTG1* and *YAT2* together enable in vivo reversal of the mitochondrial carnitine shuttle.

To investigate their biological relevance, the three mutations found in evolved strain IMS0482 were introduced individually and in different combinations into the non-evolved parental strain IMX745 (*Acs*[−] {PDHL} {CARN}). As expected, all resulting strains grew on synthetic medium with glucose and lipoic acid. However, on solid medium, only strains IMX909 (*Mct1*^{L214W} *Rtg2* *Yat2*^{P58R}) and IMX913 (*Mct1*^{L214W} *Rtg2*^{W168L} *Yat2*^{P58R}) showed *L*-carnitine-dependent growth (Figure 5.6), suggesting that both *Mct1*^{L214W} and *Yat2*^{P58R} were essential for the acquired phenotype. On spot plates, no clear impact of the mutation in *RTG2* was observed after 100 h of incubation (Figure 5.6). For a quantitative analysis of the impact of the *Rtg2*^{W168L} mutation on specific growth rates, strains

Table 5.3. Mutations in evolved *S. cerevisiae* strains with L-carnitine-dependent provision of cytosolic acetyl-CoA. Mutations in the open-reading frames of the laboratory-evolved strains IMS0482 and IMS0483 were identified by comparing whole genome sequence data to those of the unevolved parental strain IMX745. Descriptions of gene function were obtained from the *Saccharomyces* Genome Database website (45).

Gene	Nu- cleotide change	Amino acid change	Description
IMS0482			
<i>RTG2</i>	G503T	W168L	Sensor of mitochondrial dysfunction; regulates the subcellular location of Rtg1p and Rtg3p, transcriptional activators of the retrograde (RTG) and TOR pathways; Rtg2p is inhibited by the phosphorylated form of Mks1p
<i>MCT1</i>	T641G	L214W	Predicted malonyl-CoA:ACP transferase; putative component of a type-II mitochondrial fatty acid synthase that produces intermediates for phospholipid remodeling
<i>YAT2</i>	C173G	P58R	Carnitine acetyltransferase; has similarity to Yat1p, which is a carnitine acetyltransferase associated with the mitochondrial outer membrane
IMS0483			
<i>RPO21</i>	A2507G	Y836C	RNA polymerase II largest subunit B220; part of central core; phosphorylation of C-terminal heptapeptide repeat domain regulates association with transcription and splicing factors; similar to bacterial beta-prime
<i>HXT6</i> or <i>HXT7</i>	gene deletion		High-affinity glucose transporter; member of the major facilitator superfamily, nearly identical to Hxt7p, expressed at high basal levels relative to other HXTs, repression of expression by high glucose requires <i>SNF3</i> ;
<i>STB2</i>	C1073A	P358Q	Protein that interacts with Sin3p in a two-hybrid assay; part of a large protein complex with Sin3p and Stb1p; <i>STB2</i> has a paralog, <i>STB6</i> , that arose from the whole genome duplication
<i>MCT1</i>	C292T	Q98*	Predicted malonyl-CoA:ACP transferase; putative component of a type-II mitochondrial fatty acid synthase that produces intermediates for phospholipid remodeling

IMX909 (Mct1^{L214W} Rtg2^{P58R}) and IMX913 (Mct1^{L214W} Rtg2^{W168L} Yat2^{P58R}) were grown in shake-flask cultures on synthetic medium with glucose and L-carnitine (Table 5.2; Figure 5.7). Strain IMX909 showed decelerating exponential growth profile with growth rates of 0.10 h⁻¹ – 0.06 h⁻¹, while strain IMX913 exhibited monophasic exponential growth at a specific growth rate of 0.14 h⁻¹, which resembled the specific growth rate of evolved strain IMS0482 (Figure 5.7). This result showed that all three mutations in the laboratory-evolved strain IMS0482 contributed to its acquired phenotype. Exponentially growing cultures of the reverse engineered strain IMX913 on synthetic medium

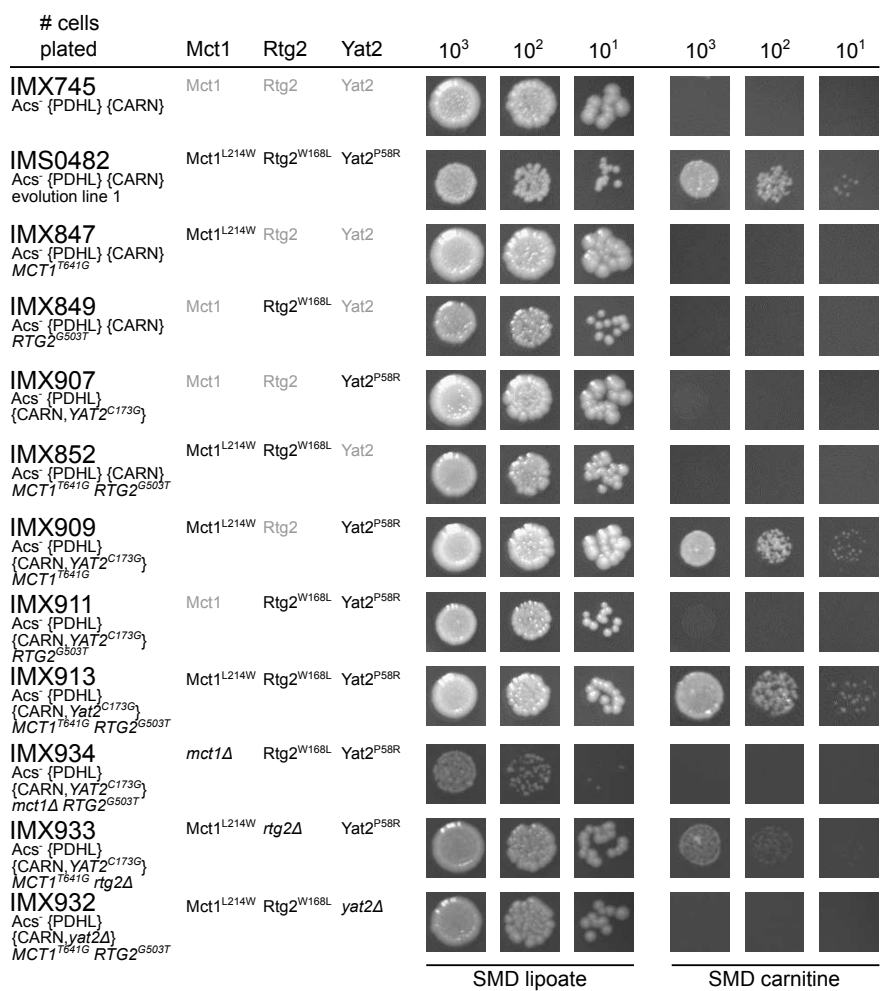


Figure 5.6. Growth on glucose of *S. cerevisiae* strains in the presence of lipoic acid or L-carnitine. *S. cerevisiae* strains were pre-grown in shake flasks on synthetic medium with 20 g.L⁻¹ glucose, supplemented with lipoic acid and spotted on glucose synthetic medium plates with lipoic acid (left panel) or with L-carnitine (right panel). Plates were incubated for 100 h at 30 °C. Relevant strain descriptions are given in the figure.

with glucose and L-carnitine exhibited a high viability (> 99 %), resembling that of the reference strain IMX585.

To investigate whether the mutations in *MCT1*, *RTG2* and *YAT2*, acquired by strain IMS0482 during laboratory evolution, might have caused a complete loss of function, three Acs⁻ {PDHL} {CARN} strains were constructed in which deletion of one of the three genes was combined with the acquired point mutations of the remaining two genes. The resulting three strains IMX932, IMX933 and IMX934 all showed growth after 100 h incubation on solid medium with glucose and lipoic acid (Figure 5.6). However, strains IMX934 (Acs⁻ {PDHL} {CARN, Yat2^{P58R}} *mct1*Δ *Rtg2*^{W168L}) and IMX932 (Acs⁻ {PDHL} {CARN, *yat2*Δ} *Mct1*^{L214W} *Rtg2*^{W168L}) were unable to grow on medium

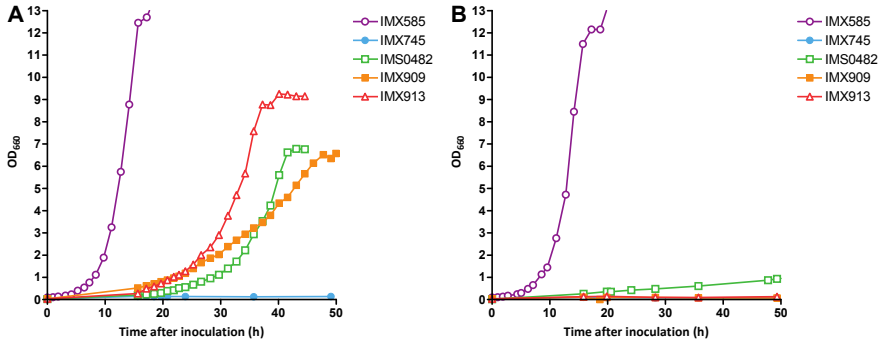


Figure 5.7. Growth curves of *S. cerevisiae* strains IMX585 (Acs^+ reference), IMX745 (Acs^- {PDHL} {CARN}), IMS0482 (Acs^- {PDHL} {CARN, evolution line 1}), IMX909 (Acs^- {PDHL} {CARN, $pADH1-YAT2^{C173G}$ } $MCT1^{T641G}$) and IMX913 (Acs^- {PDHL} {CARN, $pADH1-YAT2^{C173G}$ } $MCT1^{T641G}$ $RTG2^{G503T}$) on glucose synthetic medium with or without L-carnitine. All strains were pre-grown in liquid synthetic medium with 20 g·L⁻¹ glucose and lipoic acid, washed with synthetic medium and transferred to new shake flasks with synthetic medium, 20 g·L⁻¹ glucose. **A** Cultures supplemented with L-carnitine, **B** cultures without L-carnitine. The indicated averages and mean deviations are from single shake flask experiments that are quantitatively representatives of duplicate experiments.

5

with L-carnitine, while strain IMX933 (Acs^- {PDHL} {CARN, $Yat2^{P58R}$ } $Mct1^{L214W}$ $rtg2\Delta$) did show L-carnitine-dependent growth (Figure 5.6). This result indicated that the amino-acid changes in the $Mct1^{L214W}$ and $Yat2^{P58R}$ variants did not result in complete loss of function. Interestingly, the genetic context of the other evolved strain IMS0483, in which $MCT1$ contained a premature stop codon, did appear to enable carnitine-dependent growth in the absence of a functional $Mct1$ protein. The slightly lower L-carnitine-dependent growth of strain IMX933 (Acs^- {PDHL} {CARN, $Yat2^{P58R}$ } $Mct1^{L214W}$ $rtg2\Delta$) as compared to a congenic strain expressing the mutant $Rtg2^{W168L}$ variant, suggests that this amino acid change does not lead to a completely non-functional protein.

5.3.6 Enzyme assays do not confirm carnitine-acetyltransferase activity of *Yat2*.

The prior classification of *Yat2* as a cytosolic carnitine acetyltransferase was based on its homology with other carnitine-acetyltransferase genes and on a reported 50 % decrease of carnitine-acetyltransferase activity (not normalized for protein content) in cell extracts of ethanol-grown cultures of a $yat2\Delta$ strain (84, 129, 159, 305). To compare carnitine-acetyltransferase activities of *Yat2* and $Yat2^{P58R}$, $YAT2$ and $YAT2^{C173G}$ genes under control of the constitutive *ADH1* promoter were introduced in reference genetic backgrounds. Since the native *YAT1*, *YAT2* and *CAT2* carnitine acetyltransferases are repressed by glucose, enzyme assays on cell extracts of glucose-grown batch cultures should only reflect activity of these constitutively expressed *YAT2* genes. Surprisingly, no detectable ($< 0.01 \mu\text{mol} \cdot (\text{mg protein})^{-1} \cdot \text{min}^{-1}$) carnitine-acetyltransferase activity was found in such experiments with strains expressing the wild-type or evolved alleles of *YAT2* from single-copy or multi-copy, *pADH1*-controlled expression cassettes (Table 5.4). The same negative results were obtained with the carnitine-acetyltransferase assay pro-

Table 5.4. Specific carnitine-acetyltransferase activities in cell extracts of *S. cerevisiae* strains. Strains were grown in shake flasks containing synthetic medium with either 20 g·L⁻¹ glucose or 2% (v/v) ethanol as carbon source and harvested in mid-exponential phase. Carnitine-acetyltransferase activities in cell extracts were obtained from duplicate growth experiments and shown as average ± mean deviation. The detection limit of the enzyme assay was 0.01 μmol·(mg protein·min)⁻¹.

Strain	Short description	Carbon source medium	Carnitine-acetyltransferase activity (μmol·(mg protein) ⁻¹ ·min ⁻¹)
IMX585	reference strain	glucose	B.D.
IMX868	{CARN} ^a	glucose	2.69 ± 0.51
IMX923	<i>sga1Δ::pADH1-YAT2</i>	glucose	B.D.
IMX925	<i>sga1Δ::pADH1-YAT2^{C173G}</i>	glucose	B.D.
IME140	empty multi-copy plasmid	glucose	B.D.
IME320	multi-copy plasmid <i>pADH1-YAT2</i>	glucose	B.D.
IME321	multi-copy plasmid <i>pADH1-YAT2^{C173G}</i>	glucose	B.D.
IME233	multi-copy plasmid <i>pTDH3-CAT2</i>	glucose	4.24 ± 0.52
CEN.PK113-7D	<i>CAT2 YAT1 YAT2</i>	ethanol	1.75 ± 0.02
CEN.PK215-4A	<i>cat2Δ yat1Δ YAT2</i>	ethanol	B.D.
IMX745	{CARN}	glucose	3.19 ± 0.14
IMS0482	{CARN} evolution line 1	glucose	2.39 ± 0.05
IMX852	{CARN, <i>pADH1-YAT2</i> } <i>MCT1^{T641G} RTG2^{G503T}</i>	glucose	2.92 ± 0.73
IMX913	{CARN, <i>pADH1-YAT2^{C173G}</i> } <i>MCT1^{T641G} RTG2^{G503T}</i>	glucose	3.11 ± 0.71
IMX932	{CARN, <i>yat2Δ</i> } <i>MCT1^{T641G} RTG2^{G503T}</i>	glucose	2.82 ± 0.44

^aComposition of the {CARN} gene set is described in the Materials and methods section.

cedure described by Swiegers *et al.* (305). In contrast, strains IMX868 (*sga1Δ::*{CARN}) and IME233 (multi-copy plasmid with constitutively expressed *CAT2*) showed high activities (Table 5.4). To exclude the theoretical possibility that Yat2 is subject to glucose-catabolite inactivation, a *yat1Δ cat2Δ YAT2* strain (CEN.PK215-4A) was constructed and subsequently tested under glucose-derepressed, respiratory growth conditions. However, also in ethanol-grown cultures of this strain the Yat2-dependent carnitine-acetyltransferase activity remained below the detection limit. Under the same conditions, the reference strain CEN.PK113-7D showed a carnitine-acetyltransferase activity of 1.75 μmol·(mg protein)⁻¹·min⁻¹ (Table 5.4).

Possible explanations for our inability to detect Yat2-dependent carnitine-acetyltransferase activity include: (i) Yat2 is only active within a heteromeric complex with another carnitine acetyltransferase; (ii) Yat2 is a catalytically inactive regulator of other carnitine acetyltransferases, and (iii) assay conditions and/or Yat2 protein instability preclude accurate measurement of *in vitro* Yat2 carnitine-acetyltransferase activity. In the first two scenarios, the mutated form of Yat2 might still show a detectable impact on total carnitine-acetyltransferase activity. However, while enzyme assays on cell extracts of strains IMX745 ({PDHL} {CARN}), IMS0482 ({PDHL} {CARN} evolution line 1), IMX852 ({PDHL} {CARN, Yat2} *Mct1^{L214W} Rtg2^{W168L}*), IMX913 ({PDHL} {CARN,

Yat2^{P58R}}, Mct1^{L214W} Rtg2^{W168L}) and IMX932 ({PDHL} {CARN, yat2 Δ } Mct1^{L214W} Rtg2^{W168L}) all showed substantial carnitine-acetyltransferase activities, these did not show marked differences between the various strains (Table 5.4).

5.4 DISCUSSION

5.4.1 Requirements for reversal of the mitochondrial carnitine shuttle

To our knowledge, this study is the first to demonstrate that the carnitine shuttle can connect the mitochondrial acetyl-CoA pool to cytosolic, acetyl-CoA-consuming pathways in a eukaryote. Three requirements had to be met to enable export of acetyl units from mitochondria of glucose-grown *S. cerevisiae*. L-Carnitine, which cannot be synthesized by *S. cerevisiae* (257, 305), needed to be added to growth media. Furthermore, glucose repression of key genes encoding carnitine-shuttle proteins had to be circumvented, which in this study was done by expression from constitutive promoters. While these first two criteria also have to be met to enable the carnitine shuttle to effectively import acetyl units into mitochondria (15, 257, 305, 318), its operation in the reverse direction additionally required mutations in the yeast genome.

Single-amino-acid changes in three proteins (Mct1^{L214W}, Rtg2^{W168L} and Yat2^{P58R}) together enabled export of acetyl-units from mitochondria via a constitutively expressed carnitine shuttle. Mct1 is predicted to encode mitochondrial malonyl-CoA:ACP transferase (273), which is required for mitochondrial fatty-acid synthesis. This process uses mitochondrial acetyl-CoA as a precursor and might therefore compete for this substrate with the carnitine shuttle. Rather than acetyl-CoA itself, Mct1 uses malonyl-CoA, formed by the mitochondrial acetyl-CoA carboxylase Hfa1 (121), as a substrate. Inhibition of Hfa1 by malonyl-CoA, a property shared by several acetyl-CoA carboxylases (49, 148), could decrease its ability to compete for acetyl-CoA when Mct1 functions suboptimally. Rtg2, a sensor protein involved in the retrograde regulation pathway for nuclear-mitochondrial communication (189), was previously shown to affect levels of mitochondrial citrate synthase (283), which also uses mitochondrial acetyl-CoA as a substrate. We therefore propose that, in the evolved strains, mutations in *MCT1* and *RTG2* improved the driving force and/or kinetics of the export of acetyl units via the mitochondrial carnitine shuttle by negatively affecting pathways that compete for its substrate, intramitochondrial acetyl-CoA.

Mutations in mitochondrial lipid synthesis were previously shown to affect carnitine-shuttle activity in human cells. When mitochondrial β -oxidation of fatty acids in human cells is compromised, acyl-carnitines are exported from the mitochondria to the cytosol and can even be found in blood plasma (234, 330). Especially when yeast carnitine-shuttle genes can be functionally replaced by their human orthologs (132), the L-carnitine-dependent strains described in this study provide interesting platforms for studying the role of the carnitine shuttle in healthy and diseased human cells. Many eukaryotes use a citrate-oxaloacetate shuttle, consisting of mitochondrial citrate synthase, a mitochondrial citrate transporter and cytosolic ATP-dependent citrate lyase, for export of acetyl units from their mitochondria (20, 26, 131). Conversion of mitochondrial

acetyl-CoA to acetate, followed by its export and cytosolic ATP-dependent activation to acetyl-CoA, occurs in *Trypanosoma brucei* (253). The latter mechanism also supports slow growth of pyruvate-decarboxylase-negative *S. cerevisiae* mutants, which cannot use the PDH bypass for cytosolic acetyl-CoA synthesis (44). The ATP requirement of these naturally occurring acetyl-CoA shuttles is consistent with our hypothesis that *in vivo* concentrations of acetyl-CoA in cytosol and mitochondria of wild-type yeast cells do not allow outward translocation of acetyl units via the energy-independent carnitine shuttle. Quantification of trade-offs between ATP-efficiency and *in vivo* kinetics of cytosolic acetyl-CoA provision via different pathways requires analysis of mitochondrial and cytosolic acetyl-CoA pools in wild-type and engineered strains. Such studies will, however, have to await development of techniques for accurate measurement of acetyl-CoA concentrations in different cellular compartments.

YAT2, the third gene in which a point mutation stimulated carnitine-dependent growth of *acs1Δ acs2Δ* strains, was reported to encode a carnitine acetyltransferase (305). Yat2 shows substantial sequence identity with the two other yeast carnitine-acetyltransferases (28% and 22% amino acid sequence identity with Yat1 and Cat2, respectively (337)). However, Yat2 is substantially longer than Yat1 and Cat2, by 236 and 253 amino acids, respectively and its 169 amino-acid C-terminal sequence is only conserved in some closely related orthologs within the Saccharomycetaceae (127). The mutation in YAT2 is intriguing because Cat2 (active in the mitochondrial and peroxisomal matrices) and Yat1 (active in the cytosol) should in theory suffice to form a functional mitochondrial carnitine shuttle. Prompted by its essential role in reversal of the mitochondrial carnitine shuttle in evolved strain IMS0482, we sought to compare enzyme kinetics of wild-type Yat2 and Yat2^{P58R}. Our inability to detect activity of either Yat2 isoform in cell extracts does not rule out that these proteins are carnitine acetyltransferases. Combined with the impact of a mutation in YAT2 on *in vivo* carnitine-shuttle activity, this result underlines the need for further biochemical characterization of Yat2.

5.4.2 (Energetic) implications of the carnitine shuttle in cytosolic acetyl-CoA provision for biotechnological applications.

In the native *S. cerevisiae* pathway for cytosolic acetyl-CoA synthesis, cytosolic acetate is activated by the Acs1 and/or Acs2 acetyl-CoA synthetases (14, 142, 244, 306). This activation involves hydrolysis of ATP to AMP and pyrophosphate which, when pyrophosphate is subsequently hydrolyzed to inorganic phosphate, is equivalent to the hydrolysis of 2 moles of ATP to ADP and inorganic phosphate. Cytosolic acetyl-CoA is an important precursor for many industrially relevant compounds and much effort has been invested in metabolic engineering of alternative, more ATP-efficient pathways for cytosolic acetyl-CoA supply into *S. cerevisiae*. Examples of such strategies include cytosolic expression of heterologous phosphoketolase and phosphotransacetylase, acetylating acetaldehyde dehydrogenase, pyruvate-formate lyase and a heterologous pyruvate-dehydrogenase complex (166, 167, 291). The present study demonstrates that reversal of the mitochondrial carnitine shuttle can directly link acetyl-CoA synthesis via the mitochondrial PDH complex, the predominant source of acetyl-CoA in aerobic, glucose-grown *S. cerevisiae* cul-

tures (245), to provision of cytosolic acetyl-CoA. The low specific growth rates of the evolved and reverse engineered L-carnitine-dependent strains indicate that this novel strategy for engineering cytosolic acetyl-CoA provision in *S. cerevisiae* requires optimization before industrial implementation can be considered. Progress in this direction would provide a strong incentive to engineer a complete L-carnitine biosynthesis pathway in *S. cerevisiae*. Despite recent advances (83), synthesis of the key precursor trimethyl-lysine in *S. cerevisiae* remains an important metabolic engineering challenge.

Export of acetyl units from mitochondria via the carnitine shuttle may also be relevant for eukaryotic cell factories other than *S. cerevisiae*. Oleaginous eukaryotes such as the yeast *Yarrowia lipolytica* employ the mitochondrial PDH complex and a citrate-oxaloacetate shuttle to provide cytosolic acetyl-CoA for lipid synthesis (20, 192). The citrate-oxaloacetate shuttle requires 1 ATP for each molecule of mitochondrial pyruvate converted into cytosolic acetyl-CoA. Eliminating this ATP requirement could further improve the ATP-efficiency of lipid synthesis and, consequently, the lipid yield in oleaginous eukaryotes.

5.5 OUTLOOK

5

By demonstrating *in vivo* reversibility of mitochondrial carnitine shuttle, a ubiquitous mechanism in eukaryotes, this study provides new leads for investigating and understanding the role of this shuttle in yeast and other eukaryotes. The ‘switchable’ L-carnitine-dependent yeast strains described here provide valuable experimental platforms for functional analysis of the native yeast carnitine shuttle, for heterologous complementation studies on carnitine-shuttle components from other eukaryotes and for engineering of a complete L-carnitine biosynthesis pathway into *S. cerevisiae* (83). After further optimization of the kinetics, the ‘reverse’ mitochondrial carnitine shuttle offers a potential new strategy for energetically efficient synthesis of cytosolic acetyl-CoA as a precursor for a wide range of biotechnologically relevant compounds by eukaryotic cell factories.

5.6 ACKNOWLEDGEMENTS

We thank Peter Kötter, Annabel Giezekamp, Marlous van Dijk, Henri Duine, Ioannis Pappetridis and Xavier Hakkaart for help in strain construction and growth studies. Pilar de la Torre and Melanie Wijsman are gratefully acknowledged for sequencing plasmids pUDE320 and pUDE321. Marcel van den Broek and Thomas Abeel are thanked for their help with sequence analysis. The authors declare no conflicts of interest related to the results described in this study.

SUPPLEMENTARY MATERIALS

Table S5.1. GuideRNA plasmids used in this study. For amplification of the double guideRNA cassette, a pROS plasmid (200) was used as a template with the primer(s) as indicated.

Plasmid	Target(s)	Target sequence(s)	Template backbone	Relevant primer(s)
pUDR047	<i>PDA1</i>	TACCGGGATCAGACATAGAATGG	pROS12	5794
pUDR072	<i>LplA1</i>	AGAAACGATTTGTTGATTGACGG	pROS13	8016
pUDR073	<i>pADH1-YAT2</i> ^a	ATCTCATATACAATGTCAAGCGG	pROS13	8014
pUDR078	<i>RTG2</i>	GCGGTAGTACTCAGTTATCATGG	pROS13	8427
pUDR079	<i>RTG2</i> , <i>MCT1</i>	GCGGTAGTACTCAGTTATCATGG TAAGAACAGAATTGAACCTAAGG	pROS13	8427, 8413
pUDR080	<i>MCT1</i>	TAAGAACAGAATTGAACCTAAGG	pROS13	8413
pUDR085	<i>ACH1</i>	CGAGGCAACGGCCATTAAAGAGG	pROS13	6159
pUDR105	Synthetic CRISPR site	TGTAGAATTCACCTAGACGTGG	pROS12	8558
pUDR119 ^b	<i>SGA1</i>	ATTGACCACTGGAATTCTTCCGG	pROS11	

^aTarget sequence is at the junction of *ADH1* promoter and *YAT2* ORF

^bConstructed earlier, see (318)

Table S5.2. Primers used in this study.

Number	Name	Sequence 5' → 3'
Primers for guideRNA cassette construction		
6005	p426 CRISP rv	GATCATTTATCTTTCACTGCGGAGAAG
5794	pCAS9 target <i>pda1</i> fw	TGCGCATGTTTCGGCGTTTCGAAACTTCTCCGCAGT GAAAGATAAAATGATCTACCGGGATCAGACATAGAA GTTTTAGAGCTAGAAATAGCAAGTTAAAATAAGGC TAGTCCGTTATCAAC
6159	<i>ACH1</i> gRNA	GTGCGCATGTTTCGGCGTTCGAAACTTCTCCGCAG TGAAAGATAAAATGATCCGAGGCAACGGCCATTAAA GGTTTTAGAGCTAGAAATAGCAAGTTAAAATAAG
8016	<i>LplA1</i> target_RNA FW	TGCGCATGTTTCGGCGTTCGAAACTTCTCCGCAGT GAAAGATAAAATGATCAGAAACGATTTGTTGATTGA GTTTTAGAGCTAGAAATAGCAAGTTAAAATAAG
8014	pADH1-YAT2 target_RNA FW	TGCGCATGTTTCGGCGTTCGAAACTTCTCCGCAGT GAAAGATAAAATGATCATCTCATATACAATGTCAAG GTTTTAGAGCTAGAAATAGCAAGTTAAAATAAG
8427	<i>RTG2</i> _targetRNA FW RsaI	TGCGCATGTTTCGGCGTTCGAAACTTCTCCGCAGT GAAAGATAAAATGATCGCGGTAGTACTCAGTTATCA GTTTTAGAGCTAGAAATAGCAAGTTAAAATAAG
8413	<i>MCT1</i> _targetRNA- L214W FW EcoRI	TGCGCATGTTTCGGCGTTCGAAACTTCTCCGCAGT GAAAGATAAAATGATCTAAGAACAGAATTGAACCTA GTTTTAGAGCTAGAAATAGCAAGTTAAAATAAG
8558	CRISPR target gRNA	TGCGCATGTTTCGGCGTTCGAAACTTCTCCGCAGT GAAAGATAAAATGATCTGTAGAATTCACCTAGACG GTTTTAGAGCTAGAAATAGCAAGTTAAAATAAG

Number	Name	Sequence 5' → 3'
CRISPR <i>acs2Δ</i> locus		
7349	ACS2_repair oligo rv	AAAATAGAAAACAGAAAAGGAGCGAAATTTTATCT CATTACGAAATTTTCTCATTTAAGATTTTATTAT TGTATTGATTACTTTCCTGTATTCTGTTTGTGTA TAACAATCACTAACC
7350	ACS2_repair oligo fw	GGTTAGTGATTGTTATACACAAACAGAATACAGGA AAGTAAATCAATACAATAAAAAATCTTAAATGAG AAAAATTTTCGTAATGAGATAAAATTTTCGCTCCTTT TCTGTTTTCTATTTT
CRISPR <i>sga1Δ</i> locus		
8012	SGA1_repair oligo fw	ATTTACAATATAGTGATAATCGTGGACTAGAGCAA GATTTCAAATAAGTAACAGCAGCAAAACAAAAAAA ATAAAAGAAAAGCGAGAAGTATACACAAGTGTATT TCCTAGATATTTACA
8013	SGA1_repair oligo rv	TGTAAATATCTAGGAAATACACTTGTGTATACTTC TCGCTTTTCTTTATTTTTTTTTTGTTTGCTGCTGT TACTTATTTGAAATCTTGCTCTAGTCCACGATTAT CACTATATTGTAAAT
CRISPR <i>MCT1</i>^{T641G} mutation and <i>MCT1</i> deletion		
8417	MCT1_repair oligo L214W fw	GTAAAGCAATGTGTAGTCACCGGTCTGGTTGATGA TTTAGAGTCCTTAAGAACAGAATGGAACCTAAGGT TCCCGCGTTTAAGAATTACAGAATTAACCTAACCCA TACAACATCCCTTC
8418	MCT1_repair oligo L214W rv	GAAGGGGATGTGTATGGGTTAGTTAATTCTGTAA TTCTTAAACGCGGGAACCTTAGGTTCCATTCTGTT CTTAAGGACTCTAAATCATCAACCAGACCGGTGAC TACACATTGCTTTAC
8415	MCT1_repair oligo fw	AGGGTAGTAACAAAGCGTTTTGCACTTTTCTGATC GTGGTACACATATATAAGCGTTTGTGAAAGAGATC AAAACGCGAACTCTCTCCACTCCCAGTCTGTGCT TCTACGCATTCAATG
8416	MCT1_repair oligo rv	CAATGAATGCGTAGAAGCACAGACTGGGAGTGGAG AGAGTTCGCAGTTTTGATCTCTTTCACAAACGCTT ATATATGTGTACCACGATCAGAAAAGTGCAAAACG CTTGTTACTACCCT
CRISPR <i>RTG2</i>^{G503T} mutation and <i>RTG2</i> deletion		
8430	RTG2_repair oligo W168L fw	CATTTAATACAGTAAGAGGTCTATATCTAGATGTG GCAGGCGGTAGTACTCAGTTATCATTGGTAATAAG CTCGCACGGAGAAGTCAAGCAATCCAGCAAACCTG TATCTTTGCCATATG
8431	RTG2_repair oligo W168L rv	CATATGGCAAAGATACAGGTTTGCTGGATTGCTTG ACTTCTCCGTGCGAGCTTATTACCAATGATAACTG AGTACTACCGCTGCCACATCTAGATATAGACCTC TTACTGTATTAAATG

Number	Name	Sequence 5' → 3'
8428	RTG2_repair oligo fw	ACTCTTGGAAGTGCCTTTACTAAGGATTGTTTTG AACGAAAAGTGTAGGCGTGCCACAAAGACATCTAG TCTTTAAATACTTGAACAATAAATACGAAATCCTT ATATAAGCATCTTTT
8429	RTG2_repair oligo rv	AAAAGATGCTTATATAAGGATTTTCGTATTTATTGT TCAAGTATTTAAAGACTAGATGCTTTGTGGCACG CCTACACTTTTCGTTCAAAACAATCCTTAGTAAAG GACACTCCAAGAGT
CRISPR <i>pADH1-yat2(-11,174)::CRISPRR</i> site incorporation and <i>YAT2</i> deletion		
8621	YAT2 repair oligo CRISPRR fw	GTTTCTTTTCTGCACAATATTTCAGCTATACCA AGCATACAATCAACTAGTAGAATTTACCTAGACG TGGGAACAAATTGAGAAGCTGTCATCCATAATAAG AGATTTTGAAGAG
8622	YAT2 repair oligo CRISPRR rv	CTCTTCAAAATCTCTTATTATGGATGACAGCTTCT CAATTTGTTCCCACGTCTAGGTGAAATTCTACTAG TTGATTGTATGCTTGGTATAGCTTGAAATATTGTG CAGAAAAAGAAAC
8874	pADH1-YAT2 repair oligo fw	TTTCTTCCTTGTTTCTTTTCTGCACAATATTTC AGCTATACCAAGCATACAATCAACTGAACGCTCTT TGTTTATCTATTTTATTACTAGCATTATGCGTAAGC TTGGCGTGATGTGAT
8875	pADH1-YAT2 repair oligo rv	ATCACATCACGCCAAGCTTACGCATAATGCTAGTA ATAAATAGATAAACAAAGAGCGTTCAGTTGATTGT ATGCTTGGTATAGCTTGAAATATTGTGCAGAAAAA GAAACAAGGAAGAAA
CRISPR <i>PDA1</i> deletion		
6157	PDA1 repair fw	TGTTTATCTCTCTTCTGATTTCCTCCACCCCTTCCT TACTCAACCGGTAATGTGCGATCTTAATCGTAA GGAAAAATAAAATAATAGTGCTGTGATCGCATGAT ATTCTTCCCTGGAAG
6158	PDA1 repair rv	CTTCCAGGGAAGAATATCATGCGATCACAGCACTA TTATTTTATTTTTCCTTACGATTAAGATGCGACAT TTACCCGGTTGAGTAAGGAAGGGTGAGGAATCA GAAGAGAGATAAACA
CRISPR <i>ACH1</i> deletion		
6160	ACH1 repair fw	GACAATAGCGGCAAAACAAACAACACATTTCTTTT TTTCTTTTTCACATATTGCACTAAATGTTTGTGCG CAAACCGAGAGATGAGTATTTAAAAAAGAAA GGAAATGATATGATT
6161	ACH1 repair rv	AATCATATCATTTCTTTCTTTTAAAAATAC TCATCTCTCGGTTTGCGCACAACATTTAGTGCAA TATGTGAAAAAGAAAAAGAAATGTGTTGTTGT TTTGCCGCTATTGTC
Marker cassette <i>CAT2</i> deletion		
9237	CAT2-S1	ATGAGGATCTGTCATTTCGAGAACTCTCTCAAACCT AAAGGCAGCTGAAGCTTCGTACGC

Number	Name	Sequence 5' → 3'
9238	CAT2-S2	ATTGATATGCAGCCACTCGTTATTCAACATGTATG CCAGTGCATAGGCCACTAGTGGATCTG
Marker cassette <i>YAT1</i> deletion		
9239	YAT1-S1	ATGCCAACTTAAAGAGACTACCCATCCCGCCACT GCAGGCAGCTGAAGCTTCGTACGC
9240	YAT1-S2	GTAATCGTAGCCGACAACAGGTATTCATGTCTT CTGATGCATAGGCCACTAGTGGATCTG
Primers for amplification of the <i>YAT2</i>^{C173G} mutation		
8618	pADH1 fw	CCTCGTCATTGTTCTCGTTC
8619	YAT2 rv	GTTTAGATTGCAGCTTCTCAC
Primers for amplification of the <i>pADH1-YAT2-tYAT2</i> cassettes		
8647	tag C fw ol pSGA1	TTTACAATATAGTGATAATCGTGGAAGTAGAGCAAG ATTTCAAATAAGTAACAGCAGCAAAACGTCTCACG GATCGTATATGC
8648	tag J rv (ol tSGA1)	TATATTTGATGTAAATATCTAGGAAATACACTTGT GTATACTTCTCGCTTTTCTTTTATTCGACGAGATG CTCAGACTATG
8902	tag J fw (ol pRS426)	CTATAGGGCGAATTGGGTACCGGGCCCCCCCCGAC GAGATGCTCAGACTATG
8903	tag C rv (ol pRS426)	GAAGTAGTGGATCCCCGGGCTGCAGGAATTACGT CTCACGGATCGTATATG
Primers for amplification of <i>CAT2</i> ORF and pRS426-pTDH3...tCYC1 plasmid		
3627	pTDH3 rv	TTGTTTGTATTATGTGTGTTTATTCGAAAC
3921	tCYC1 fw (smaller)	CAGGCCCTTTTCCTTGG
5948	pRS426-CAT2 fw	TTTAAAACACCAAGAAGCTTAGTTTCGAATAAACAC ACATAAACAAACAAATGAGGATCTGTCATTTCGAG AAC
5949	pRS426-CAT2 rv	TAAGCGTGACATAACTAATTACATGATATCGACAA AGGAAAAGGGGCTGTCACTGATGGTGGTATGAT GTAACTTTGCTTTTCGTTTATTCTCATTTTC
Confirmation of <i>PDA1</i> deletion		
3146	ROSP031 DG PDA1 KO fw	ATCGCGCGTGATCATGTC
3147	ROSP032 DG PDA1 KO rv	GCGGCTATTTTCCGGTCTG
Confirmation of <i>ACH1</i> deletion		
3770	ACH1kocheck2f	CGGGCTTACATTAGCACAC
3771	ACH1kocheck2r	GCAAGAAAAACAACGCATTGG
Confirmation of <i>sga1Δ</i> locus		
4223	SGA1 outside fw	CTTGGCTCTGGATCCGTTATCTG
4229	Sequence SGA1 2 rv	TGGTCGACAGATACAATCCTGG
Confirmation of <i>acs2Δ</i> locus		
2618	acs2 Ctrl Fw	TACCCTATCCCGGGCGAAGAAC
2619	acs2 KO Ctrl Rv	CCGATATTCGGTAGCCGATTCC
Confirmation of <i>cat2Δ</i> and <i>yat1Δ</i> loci		
9091	K1-A	GGATGTATGGGCTAAATGTACG
9092	K2	GTTTCATTGATGCTCGATGAG

Number	Name	Sequence 5' → 3'
9265	CAT2-A1	TTCACCTCTTCTCAACGCTG
9266	CAT2-A4	CAGGCGTACCACGAGATAG
9267	YAT1-A1	ACGATTACATACAAGATGAACG
9268	YAT1-A4	TTCGTTTAGATCAAGATGGATG
Confirmation of SNPs		
8423	MCT1_dg fw-2	GAGTCAGAACGGCAAGGAATC
8426	MCT1_dg rv-3	CTCCATCAACGTGTGAGTTC
8507	RTG1 inside DG fw	ACAGAAGCCACGCGAGATG
8508	RTG1 inside DG rv	AGAAGCAGATGTCCCATACC
706	5Padh1-3	GTCGTTGTTCCAGAGCTGATGAG
7497	YAT2_3	AAAGCGTCATCTGCGAGAACC



- (1) Abbott DA, Knijnenburg TA, De Poorter LM, Reinders MJ, Pronk JT and Van Maris AJA (2007) Generic and specific transcriptional responses to different weak organic acids in anaerobic chemostat cultures of *Saccharomyces cerevisiae*. *FEMS Yeast Res.* **7**:819–833.
- (2) Alberti S, Gitler AD and Lindquist S (2007) A suite of Gateway cloning vectors for high-throughput genetic analysis in *Saccharomyces cerevisiae*. *Yeast* **24**:913–919.
- (3) Annaluru N, Muller H, Mitchell LA, Ramalingam S, Stracquadanio G, Richardson SM, Dymond JS, Kuang Z, Scheifele LZ, Cooper EM, Cai Y, Zeller K, Agmon N and Han JS (2014) Total synthesis of a functional designer eukaryotic chromosome. *Science* **344**:55–58.
- (4) Aouida M, Rubio-Teixeira M, Rubio Teixeira M, Thevelein JM, Poulin R and Ramotar D (2013) Agp2, a member of the yeast amino acid permease family, positively regulates polyamine transport at the transcriptional level. *PLoS One* **8**:e65717.
- (5) Aranda A and Del Olmo ML (2004) Exposure of *Saccharomyces cerevisiae* to acetaldehyde induces sulfur amino acid metabolism and polyamine transporter genes, which depend on Met4p and Haa1p transcription factors, respectively. *Appl. Environ. Microbiol.* **70**:1913–1922.
- (6) Avalos JL, Fink GR and Stephanopoulos G (2013) Compartmentalization of metabolic pathways in yeast mitochondria improves the production of branched-chain alcohols. *Nat. Biotechnol.* **31**:335–41.
- (7) Bakker BM, Overkamp KM, Van Maris AJA, Kötter P, Luttik MAH, Van Dijken JP and Pronk JT (2001) Stoichiometry and compartmentation of NADH metabolism in *Saccharomyces cerevisiae*. *FEMS Microbiol. Rev.* **25**:15–37.
- (8) Bao Z, Xiao H, Liang J, Zhang L, Xiong X, Sun N, Si T and Zhao H (2014) Homology-Integrated CRISPR-Cas (HI-CRISPR) system for one-step multigene disruption in *Saccharomyces cerevisiae*. *ACS Synth. Biol.* **4**:585–94.
- (9) Barrangou R, Fremaux C, Deveau H, Richards M, Boyaval P, Moineau S, Romero Da and Horvath P (2007) CRISPR provides acquired resistance against viruses in prokaryotes. *Science* **315**:1709–12.
- (10) Beekwilder J, Van Rossum HM, Koopman F, Sonntag F, Buchhaupt M, Schrader J, Hall RD, Bosch D, Pronk JT, Van Maris AJA and Daran JM (2014) Polycistronic expression of a β -carotene biosynthetic pathway in *Saccharomyces cerevisiae* coupled to β -ionone production. *J. Biotechnol.* **192 Pt B**:383–92.
- (11) Bekers KM, Heijnen JJ and Van Gulik WM (2015) Determination of the *in vivo* NAD:NADH ratio in *Saccharomyces cerevisiae* under anaerobic conditions, using alcohol dehydrogenase as sensor reaction. *Yeast* **32**:541–557.
- (12) Bender T, Pena G and Martinou JC (2015) Regulation of mitochondrial pyruvate uptake by alternative pyruvate carrier complexes. *EMBO J.* **34**:911–924.
- (13) Van den Berg MA, De Jong-Gubbels P, Kortland CJ, Van Dijken JP, Pronk JT and Steensma HY (1996) The two acetyl-coenzyme A synthetases of *Saccharomyces*

- cerevisiae* differ with respect to kinetic properties and transcriptional regulation. *J. Biol. Chem.* **271**:28953–28959.
- (14) Van den Berg MA and Steensma HY (1995) ACS2, a *Saccharomyces cerevisiae* gene encoding acetyl-coenzyme A synthetase, essential for growth on glucose. *FEBS J.* **231**:704–13.
- (15) Bieber LL (1988) Carnitine. *Annu. Rev. Biochem.* **57**:261–83.
- (16) Boender LG, Almering MJ, Dijk M, Van Maris AJA, De Winde JH, Pronk JT and Daran-Lapujade P (2011) Extreme calorie restriction and energy source starvation in *Saccharomyces cerevisiae* represent distinct physiological states. *Biochim. Biophys. Acta* **1813**:2133–2144.
- (17) Boer VM, De Winde JH, Pronk JT and Piper MD (2003) The genome-wide transcriptional responses of *Saccharomyces cerevisiae* grown on glucose in aerobic chemostat cultures limited for carbon, nitrogen, phosphorus, or sulfur. *J. Biol. Chem.* **278**:3265–3274.
- (18) Bogorad IW, Lin TS and Liao JC (2013) Synthetic non-oxidative glycolysis enables complete carbon conservation. *Nature* **502**:693–7.
- (19) Botstein D and Fink GR (2011) Yeast: An experimental organism for 21st Century biology. *Genetics* **189**:695–704.
- (20) Boulton CA and Ratledge C (1981) Correlation of lipid accumulation in yeasts with possession of ATP:citrate lyase. *J. Gen. Microbiol.* **127**:169–176.
- (21) Braglia P, Percudani R and Dieci G (2005) Sequence context effects on oligo(dT) termination signal recognition by *Saccharomyces cerevisiae* RNA polymerase III. *J. Biol. Chem.* **280**:19551–62.
- (22) Branduardi P, Longo V, Berterame NM, Rossi G and Porro D (2013) A novel pathway to produce butanol and isobutanol in *Saccharomyces cerevisiae*. *Biotechnol. Biofuels* **6**:68.
- (23) Bricker DK, Taylor EB, Schell JC, Orsak T, Boutron A, Chen YC, Cox JE, Cardon CM, Van Vranken JG, Dephore N, Redin C, Boudina S, Gygi SP, Brivet M, Thummel CS and Rutter J (2012) A mitochondrial pyruvate carrier required for pyruvate uptake in yeast, *Drosophila* and humans. *Science* **337**:96–100.
- (24) Brody S, Oh C, Hoja U and Schweizer E (1997) Mitochondrial acyl carrier protein is involved in lipoic acid synthesis in *Saccharomyces cerevisiae*. *FEBS Lett.* **408**:217–220.
- (25) Brouns SJJ, Jore MM, Lundgren M, Westra ER, Slikhuis RJH, Snijders APL, Dickman MJ, Makarova KS, Koonin EV and Van der Oost J (2008) Small CRISPR RNAs guide antiviral defense in prokaryotes. *Science* **321**:960–4.
- (26) Brunengraber H and Lowenstein JM (1973) Effect of (–)-hydroxycitrate on ethanol metabolism. *FEBS Lett.* **36**:130–2.
- (27) Buchanan BB and Arnon DI (1990) A reverse KREBS cycle in photosynthesis: Consensus at last. *Photosynth. Res.* **24**:47–53.
- (28) Buu LM, Chen YC and Lee FJS (2003) Functional characterization and localization of acetyl-CoA hydrolase, Ach1p, in *Saccharomyces cerevisiae*. *J. Biol. Chem.* **278**:17203–9.

- (29) Cai L, Sutter BM, Li B and Tu BP (2011) Acetyl-CoA induces cell growth and proliferation by promoting the acetylation of histones at growth genes. *Mol. Cell* **42**:426–437.
- (30) Canelas AB, Van Gulik WM and Heijnen JJ (2008a) Determination of the cytosolic free NAD/NADH ratio in *Saccharomyces cerevisiae* under steady-state and highly dynamic conditions. *Biotechnol. Bioeng.* **100**:734–743.
- (31) Canelas AB, Ras C, Ten Pierick A, Van Dam JC, Heijnen JJ and Van Gulik WM (2008b) Leakage-free rapid quenching technique for yeast metabolomics. *Metabolomics* **4**:226–239.
- (32) Carlson R, Fell D and Sreenc F (2002) Metabolic pathway analysis of a recombinant yeast for rational strain development. *Biotechnol. Bioeng.* **79**:121–134.
- (33) Carroll D (2011) Genome engineering with zinc-finger nucleases. *Genetics* **188**:773–82.
- (34) Casini A, MacDonald JT, De Jonghe J, Christodoulou G, Freemont PS, Baldwin GS and Ellis T (2014) One-pot DNA construction for synthetic biology: The Modular Overlap-Directed Assembly with Linkers (MODAL) strategy. *Nucleic Acids Res.* **42**:e7.
- (35) Caspeta L, Chen Y, Ghiaci P, Feizi A, Buskov S, Hallström BM, Petranovic D and Nielsen J (2014) Altered sterol composition renders yeast thermotolerant. *Science* **346**:75–78.
- (36) Caspi R, Altman T, Billington R, Dreher K, Foerster H, Fulcher CA, Holland TA, Keseler IM, Kothari A, Kubo A, Krummenacker M, Latendresse M, Mueller LA, Ong Q, Paley S, Subhraveti P, Weaver DS, Weerasinghe D, Zhang P and Karp PD (2014) The MetaCyc database of metabolic pathways and enzymes and the BioCyc collection of Pathway/Genome Databases. *Nucleic Acids Res.* **42**:D459–71.
- (37) Caštegna A, Scarcia P, Agrimi G, Palmieri L, Rottensteiner H, Spera I, Germinario L and Palmieri F (2010) Identification and functional characterization of a novel mitochondrial carrier for citrate and oxoglutarate in *Saccharomyces cerevisiae*. *J. Biol. Chem.* **285**:17359–70.
- (38) Chakrabarti A, Miskovic L, Soh KC and Hatzimanikatis V (2013) Towards kinetic modeling of genome-scale metabolic networks without sacrificing stoichiometric, thermodynamic and physiological constraints. *Biotechnol. J.* **8**:1043–1057.
- (39) Chang A, Schomburg I, Placzek S, Jeske L, Ulbrich M, Xiao M, Sensen CW and Schomburg D (2014) BRENDA in 2015: Exciting developments in its 25th year of existence. *Nucleic Acids Res.* **43**:D439–D446.
- (40) Chantrenne H and Lipmann F (1950) Coenzyme A dependence and acetyl donor function of the pyruvate-formate exchange system. *J. Biol. Chem.* **187**:757–767.
- (41) Chee MK and Haase SB (2012) New and redesigned pRS Plasmid shuttle vectors for genetic manipulation of *Saccharomyces cerevisiae*. *G3* **2**:515–26.
- (42) Chelstowska A and Butow RA (1995) RTG genes in yeast that function in communication between mitochondria and the nucleus are also required for expression of genes encoding peroxisomal proteins. *J. Biol. Chem.* **270**:18141–18146.
- (43) Chen Y, Daviet L, Schalk M, Siewers V and Nielsen J (2013) Establishing a platform cell factory through engineering of yeast acetyl-CoA metabolism. *Metab. Eng.* **15**:48–54.

- (44) Chen Y, Zhang Y, Siewers V and Nielsen J (2015) Ach1 is involved in shuttling mitochondrial acetyl units for cytosolic C2 provision in *Saccharomyces cerevisiae* lacking pyruvate decarboxylase. *FEMS Yeast Res.* **15**:fov015.
- (45) Cherry JM, Hong EL, Amundsen C, Balakrishnan R, Binkley G, Chan ET, Christie KR, Costanzo MC, Dwight SS, Engel SR, Fisk DG, Hirschman JE, Hitz BC, Karra K, Krieger CJ, Miyasato SR, Nash RS, Park J, Skrzypek MS, Simison M, Weng S and Wong ED (2012) *Saccharomyces* Genome Database: The genomics resource of budding yeast. *Nucleic Acids Res.* **40**:700–705.
- (46) Choi JW and Da Silva NA (2014) Improving polyketide and fatty acid synthesis by engineering of the yeast acetyl-CoA carboxylase. *J. Biotechnol.* **187**:56–59.
- (47) Christian M, Cermak T, Doyle EL, Schmidt C, Zhang F, Hummel A, Bogdanove AJ and Voytas DF (2010) Targeting DNA double-strand breaks with TAL effector nucleases. *Genetics* **186**:757–61.
- (48) Christianson TW, Sikorski RS, Dante M, Shero JH and Hieter P (1992) Multifunctional yeast high-copy-number shuttle vectors. *Gene* **110**:119–122.
- (49) Chuakrut S, Arai H, Ishii M and Igarashi Y (2003) Characterization of a bifunctional archaeal acyl coenzyme A carboxylase. *J. Bacteriol.* **185**:938–947.
- (50) Cipollina C, Ten Pierick A, Canelas AB, Seifar RM, Van Maris AJ, Van Dam JC and Heijnen JJ (2009) A comprehensive method for the quantification of the non-oxidative pentose phosphate pathway intermediates in *Saccharomyces cerevisiae* by GC-IDMS. *J. Chromatogr. B* **877**:3231–3236.
- (51) Cronan JE, Zhao X and Jiang Y (2005) Function, attachment and synthesis of lipoic acid in *Escherichia coli*. *Adv. Microb. Physiol.* **50**:103–46.
- (52) Cueto-Rojas HF, Van Maris AJA, Wahl SA and Heijnen JJ (2015) Thermodynamics-based design of microbial cell factories for anaerobic product formation. *Trends Biotechnol.* **33**:534–546.
- (53) Van Dam JC, Eman MR, Frank J, Lange HC, Van Dedem GWK and Heijnen JJ (2002) Analysis of glycolytic intermediates in *Saccharomyces cerevisiae* using anion exchange chromatography and electrospray ionization with tandem mass spectrometric detection. *Anal. Chim. Acta* **460**:209–218.
- (54) Dandekar T, Schuster S, Snel B, Huynen M and Bork P (1999) Pathway alignment: Application to the comparative analysis of glycolytic enzymes. *Biochem. J.* **343 Pt 1**:115–24.
- (55) De Deken RH (1966) The Crabtree effect: A regulatory system in yeast. *J. Gen. Microbiol.* **44**:149–156.
- (56) Delneri D, Tomlin GC, Wixon JL, Hutter A, Sefton M, Louis EJ and Oliver SG (2000) Exploring redundancy in the yeast genome: An improved strategy for use of the cre-loxP system. *Gene* **252**:127–35.
- (57) DeLoache WC, Russ ZN, Narcross L, Gonzales AM, Martin VJJ and Dueber JE (2015) An enzyme-coupled biosensor enables (S)-reticuline production in yeast from glucose. *Nat. Chem. Biol.* **11**:465–471.
- (58) Deltcheva E, Chylinski K, Sharma CM, Gonzales K, Chao Y, Pirzada ZA, Eckert MR, Vogel J and Charpentier E (2011) CRISPR RNA maturation by trans-encoded small RNA and host factor RNase III. *Nature* **471**:602–7.

- (59) Dhaoui M, Auchere F, Blaiseau PL, Lesuisse E, Landoulsi A, Camadro JM, Haguenaue-Tsapis R and Belgareh-Touze N (2011) Gex1 is a yeast glutathione exchanger that interferes with pH and redox homeostasis. *Mol. Biol. Cell* **22**:2054–2067.
- (60) DiCarlo JE, Conley AJ, Penttilä M, Jäntti J, Wang HH and Church GM (2013a) Yeast oligo-mediated genome engineering (YOGI). *ACS Synth. Biol.* **2**:741–9.
- (61) DiCarlo JE, Norville JE, Mali P, Rios X, Aach J and Church GM (2013b) Genome engineering in *Saccharomyces cerevisiae* using CRISPR-Cas systems. *Nucleic Acids Res.* **41**:4336–43.
- (62) Dickinson JR and Dawes IW (1992) The catabolism of branched-chain amino acids occurs via 2-oxoacid dehydrogenase in *Saccharomyces cerevisiae*. *J. Gen. Microbiol.* **138**:2029–33.
- (63) Van Dijken JP, Bauer J, Brambilla L, Duboc P, Francois JM, Gancedo C, Giuseppin MLF, Heijnen JJ, Hoare M, Lange HC, Madden EA, Niederberger P, Nielsen J, Parrou JL, Petit T, Porro D, Reuss M, Van Riel N, Rizzi M, Steensma HY, Verrips CT, Vindeløv J and Pronk JT (2000) An interlaboratory comparison of physiological and genetic properties of four *Saccharomyces cerevisiae* strains. *Enzyme Microb. Technol.* **26**:706–714.
- (64) Van Dijken JP, Weuſthuis RA and Pronk JT (1993) Kinetics of growth and sugar consumption in yeasts. *Antonie van Leeuwenhoek* **63**:343–352.
- (65) Dujon B, Sherman D, Fischer G, Durrens P, Casaregola S, Lafontaine I, De Montigny J, Marck C, Neuvégliſe C, Talla E, Goffard N, Frangeul L, Aigle M, Anthouard V, Babour A, Barbe V, Barnay S, Blanchin S, Beckerich JM, Beyne E, Bleykaſten C, Boisramé A, Boyer J, Cattolico L, Confanioleri F, De Daruvar A, Despons L, Fabre E, Fairhead C, Ferry-Dumazet H, Groppi A, Hantraye F, Hennequin C, Jauniaux N, Joyet P, Kachouri R, Kerreſt A, Koszul R, Lemaire M, Lesur I, Ma L, Muller H, Nicaud JM, Nikolski M, Oztas S, Ozier-Kalogeropoulos O, Pellenz S, Potier S, Richard GF, Straub ML, Suleau A, Swennen D, Tekaia F, Wésolowski-Louvel M, Weſthof E, Wirth B, Zeniou-Meyer M, Zivanovic I, Bolotin-Fukuhara M, Thierry A, Bouchier C, Caudron B, Scarpelli C, Gaillardin C, Weissenbach J, Wincker P and Souciet JL (2004) Genome evolution in yeasts. *Nature* **430**:35–44.
- (66) Duntze W, Neumann D, Gancedo JM, Atzpodien W and Holzer H (1969) Studies on the regulation and localization of the glyoxylate cycle enzymes in *Saccharomyces cerevisiae*. *FEBS J.* **10**:83–89.
- (67) Dyer JM, Chapital DC, Kuan JW, Mullen RT and Pepperman AB (2002) Metabolic engineering of *Saccharomyces cerevisiae* for production of novel lipid compounds. *Appl. Microbiol. Biotechnol.* **59**:224–230.
- (68) Eisenberg T, Schroeder S, Andryushkova A, Pendl T, Küttner V, Bhukel A, Mariño G, Pietrocola F, Harger A, Zimmermann A, Mouſtafa T, Sprenger A, Jany E, Büttner S, Carmona-Gutierrez D, Ruckenstein C, Ring J, Reichelt W, Schimmel K, Leeb T, Moser C, Schatz S, Kamolz LP, Magnes C, Sinner F, Sedej S, Fröhlich KU, Juhasz G, Pieber TR, Dengjel J, Sigriſt SJ, Kroemer G and Madeo F (2014) Nucleocytosolic depletion of the energy metabolite acetyl-coenzyme A stimulates autophagy and prolongs lifespan. *Cell Metab.* **19**:431–44.

- (69) Elgersma Y, Van Roermund CW, Wanders RJ and Tabak HF (1995) Peroxisomal and mitochondrial carnitine acetyltransferases of *Saccharomyces cerevisiae* are encoded by a single gene. *EMBO J.* **14**:3472–3479.
- (70) Emanuelsson O, Brunak S, Von Heijne G and Nielsen H (2007) Locating proteins in the cell using TargetP, SignalP and related tools. *Nat. Protoc.* **2**:953–971.
- (71) Entian KD and Kötter P (2007) Yeast genetic strain and plasmid collections. *Methods in Microbiology* **36**:629–666.
- (72) Evans CT and Ratledge C (1984) Induction of xylulose-5-phosphate phosphoketolase in a variety of yeasts grown on D-xylulose: The key to efficient xylose metabolism. *Arch. Microbiol.* **148**:48–52.
- (73) Falcon AA, Chen S, Wood MS and Aris JP (2010) Acetyl-coenzyme A synthetase 2 is a nuclear protein required for replicative longevity in *Saccharomyces cerevisiae*. *Mol. Cell. Biochem.* **333**:99–108.
- (74) Farhi M, Marhevka E, Masci T, Marcos E, Eyal Y, Ovadis M, Abeliovich H and Vainstein A (2011) Harnessing yeast subcellular compartments for the production of plant terpenoids. *Metab. Eng.* **13**:474–481.
- (75) Fast D (1973) Sporulation synchrony of *Saccharomyces cerevisiae* grown in various carbon sources. *J. Bacteriol.* **116**:925–930.
- (76) Fatland BL, Ke J, Anderson MD, Mentzen WI, Cui LW, Allred CC, Johnston JL, Nikolau BJ and Wurtele ES (2002) Molecular characterization of a heteromeric ATP-citrate lyase that generates cytosolic acetyl-coenzyme A in *Arabidopsis*. *Plant Physiol.* **130**:740–56.
- (77) Fendt SM and Sauer U (2010) Transcriptional regulation of respiration in yeast metabolizing differently repressive carbon substrates. *BMC Syst. Biol.* **4**:12.
- (78) Feng Z, Zhang B, Ding W, Liu X, Yang DL, Wei P, Cao F, Zhu S, Zhang F, Mao Y and Zhu JK (2013) Efficient genome editing in plants using a CRISPR/Cas system. *Cell Res.* **23**:1229–32.
- (79) Flamholz A, Noor E, Bar-Even A and Milo R (2012) eQuilibrator—the biochemical thermodynamics calculator. *Nucleic Acids Res.* **40**:D770–D775.
- (80) Fleck CB and Brock M (2009) Re-characterisation of *Saccharomyces cerevisiae* Ach1p: Fungal CoA-transferases are involved in acetic acid detoxification. *Fungal Genet. Biol.* **46**:473–485.
- (81) Flikweert MT, De Swaaf M, Van Dijken JP and Pronk JT (1999) Growth requirements of pyruvate-decarboxylase-negative *Saccharomyces cerevisiae*. *FEMS Microbiol. Lett.* **174**:73–79.
- (82) Flikweert MT, Van der Zanden L, Janssen WM, Steensma HY, Van Dijken JP and Pronk JT (1996) Pyruvate decarboxylase: An indispensable enzyme for growth of *Saccharomyces cerevisiae* on glucose. *Yeast* **12**:247–57.
- (83) Franken J, Burger A, Swiegers JH and Bauer FF (2015) Reconstruction of the carnitine biosynthesis pathway from *Neurospora crassa* in the yeast *Saccharomyces cerevisiae*. *Appl. Microbiol. Biotechnol.* **99**:6377–89.
- (84) Franken J, Kroppenstedt S, Swiegers JH and Bauer FF (2008) Carnitine and carnitine acetyltransferases in the yeast *Saccharomyces cerevisiae*: A role for carnitine in stress protection. *Curr. Genet.* **53**:347–60.

- (85) Fritz IB, Schultz SK, Srere PA, Fritz B and Schultz K (1963) Properties of partially purified carnitine acetyltransferase. *J. Biol. Chem.* **238**:2509–2517.
- (86) Fukui S and Tanaka A (1979) Yeast peroxisomes. *Trends Biochem. Sci.* **4**:246–249.
- (87) Gailiusis J, Rinne RW and Benedict CR (1964) Pyruvate-oxaloacetate exchange reaction in baker's yeast. *Biochim. Biophys. Acta* **92**:595–601.
- (88) Galdieri L and Vancura A (2012) Acetyl-CoA carboxylase regulates global histone acetylation. *J. Biol. Chem.* **287**:23865–23876.
- (89) Galdieri L, Zhang T, Rogerson D, Lleshi R and Vancura A (2014) Protein acetylation and acetyl coenzyme A metabolism in budding yeast. *Eukaryot. Cell* **13**:1472–1483.
- (90) Gancedo C (1971) Inactivation of fructose-1,6-diphosphatase by glucose in yeast. *J. Bacteriol.* **107**:401–5.
- (91) Gancedo JM and Gancedo C (1971) Fructose-1,6-diphosphatase, phosphofructokinase and glucose-6-phosphate dehydrogenase from fermenting and non fermenting yeasts. *Arch. Microbiol.* **138**:132–138.
- (92) Gancedo JM (1998) Yeast carbon catabolite repression. *Microbiol. Mol. Biol. Rev.* **62**:334–361.
- (93) Gao Y and Zhao Y (2014) Self-processing of ribozyme-flanked RNAs into guide RNAs *in vitro* and *in vivo* for CRISPR-mediated genome editing. *J. Integr. Plant Biol.* **56**:343–9.
- (94) Gardner TS, Hawkins KM, Meadows AL, Tsong AE and Tsegaye Y (2013) *Production of acetyl-coenzyme A derived isoprenoids* (Patent no. WO2013071172A1).
- (95) Geertman JM, Van Dijken JP and Pronk JT (2006) Engineering NADH metabolism in *Saccharomyces cerevisiae*: Formate as an electron donor for glycerol production by anaerobic, glucose-limited chemostat cultures. *FEMS Yeast Res.* **6**:1193–1203.
- (96) Gibson DG, Benders Ga, Andrews-Pfannkoch C, Denisova Ea, Baden-Tillson H, Zaveri J, Stockwell TB, Brownley A, Thomas DW, Algire Ma, Merryman C, Young L, Noskov VN, Glass JI, Venter JC, Hutchison Ca and Smith HO (2008) Complete chemical synthesis, assembly, and cloning of a *Mycoplasma genitalium* genome. *Science* **319**:1215–20.
- (97) Gietz RD and Woods RA (2002) Transformation of yeast by lithium acetate/single-stranded carrier DNA/polyethylene glycol method. *Methods Enzymol.* **350**:87–96.
- (98) Goffeau A, Barrell BG, Bussey H, Davis RW, Dujon B, Feldmann H, Galibert F, Hoheisel JD, Jacq C, Johnston M, Louis EJ, Mewes HW, Murakami Y, Philippsen P, Tettelin H and Oliver SG (1996) Life with 6000 genes. *Science* **274**:546, 563–7.
- (99) González F, Zhu Z, Shi ZD, Lelli K, Verma N, Li QV and Huangfu D (2014) An iCRISPR platform for rapid, multiplexable, and inducible genome editing in human pluripotent stem cells. *Cell Stem Cell* **15**:215–226.
- (100) González-Ramos D, Van den Broek M, Van Maris AJA, Pronk JT and Daran JMG (2013) Genome-scale analyses of butanol tolerance in *Saccharomyces cerevisiae* reveal an essential role of protein degradation. *Biotechnol. Biofuels* **6**:48.
- (101) Gratz SJ, Cummings AM, Nguyen JN, Hamm DC, Donohue LK, Harrison MM, Wildonger J and O'Connor-Giles KM (2013) Genome engineering of *Drosophila* with the CRISPR RNA-guided Cas9 nuclease. *Genetics* **194**:1029–35.

- (102) Grote A, Hiller K, Scheer M, Munch R, Nortemann B, Hempel DC and Jahn D (2005) JCat: A novel tool to adapt codon usage of a target gene to its potential expression host. *Nucleic Acids Res.* **33**:W526–W531.
- (103) Grunau S, Mindthoff S, Rottensteiner H, Sormunen RT, Hiltunen JK, Erdmann R and Antonenkov VD (2009) Channel-forming activities of peroxisomal membrane proteins from the yeast *Saccharomyces cerevisiae*. *FEBS J.* **276**:1698–1708.
- (104) Guadalupe Medina V, Almering MJ, Van Maris AJA and Pronk JT (2010) Elimination of glycerol production in anaerobic cultures of a *Saccharomyces cerevisiae* strain engineered to use acetic acid as an electron acceptor. *Appl. Environ. Microbiol.* **76**:190–195.
- (105) Guadalupe-Medina V, Wisselink HW, Luttik MA, De Hulster E, Daran JM, Pronk JT and Van Maris AJA (2013) Carbon dioxide fixation by Calvin-Cycle enzymes improves ethanol yield in yeast. *Biotechnol. Biofuels* **6**:125.
- (106) Guan KL and Xiong Y (2011) Regulation of intermediary metabolism by protein acetylation. *Trends Biochem. Sci.* **36**:108–116.
- (107) Gueldener U, Heinisch J, Koehler GJ, Voss D and Hegemann JH (2002) A second set of *loxP* marker cassettes for Cre-mediated multiple gene knockouts in budding yeast. *Nucleic Acids Res.* **30**:e23.
- (108) Güldener U, Heck S, Fielder T, Beinhauer J and Hegemann JH (1996) A new efficient gene disruption cassette for repeated use in budding yeast. *Nucleic Acids Res.* **24**:2519–24.
- (109) Harington A, Herbert CJ, Tung B, Getz GS and Slonimski PP (1993) Identification of a new nuclear gene (*CEM1*) encoding a protein homologous to a β -keto-acyl synthase which is essential for mitochondrial respiration in *Saccharomyces cerevisiae*. *Mol. Microbiol.* **9**:545–555.
- (110) Hawkins KM, Mahatdejkul-Meadows TT, Meadows AL, Pickens LB, Tai A and Tsong AE (2014) *Use of phosphoketolase and phosphotransacetylase for production of acetyl-coenzyme A derived compounds* (Patent no. WO2014144135A3).
- (111) Heath EC, Hurwitz J, Horecker BL and Ginsburg A (1958) Pentose fermentation by *Lactobacillus plantarum*. I. The cleavage of xylulose 5-phosphate by phosphoketolase. *J. Biol. Chem.* **231**:1009–1029.
- (112) Hegemann JH and Heick SB (2011) Delete and repeat: A comprehensive toolkit for sequential gene knockout in the budding yeast *Saccharomyces cerevisiae*. *Methods Mol. Biol.* **765**:189–206.
- (113) Heijnen JJ, Van Loosdrecht MCM and Tijhuis L (1992) A black box mathematical model to calculate auto- and heterotrophic biomass yields based on Gibbs energy dissipation. *Biotechnol. Bioeng.* **40**:1139–1154.
- (114) Henriksen P, Wagner SA, Weinert BT, Sharma S, Bacinskaja G, Rehman M, Juffer AH, Walther TC, Lisby M and Choudhary C (2012) Proteome-wide analysis of lysine acetylation suggests its broad regulatory scope in *Saccharomyces cerevisiae*. *Mol. Cell. Proteomics* **11**:1510–1522.
- (115) Henry CS, Broadbelt LJ and Hatzimanikatis V (2007) Thermodynamics-based metabolic flux analysis. *Biophys. J.* **92**:1792–1805.

- (116) Herzig S, Raemy E, Montessuit S, Veuthey JL, Zamboni N, Westermann B, Kunji ERS and Martinou JC (2012) Identification and functional expression of the mitochondrial pyruvate carrier. *Science* **337**:93–6.
- (117) Hiltunen JK, Okubo F, Kursu VAS, Autio KJ and Kašaniotis AJ (2005) Mitochondrial fatty acid synthesis and maintenance of respiratory competent mitochondria in yeast. *Biochem. Soc. Trans.* **33**:1162–5.
- (118) Hiltunen JK, Mursula AM, Rottensteiner H, Wierenga RK, Kašaniotis AJ and Gurvitz A (2003) The biochemistry of peroxisomal β -oxidation in the yeast *Saccharomyces cerevisiae*. *FEMS Microbiol. Rev.* **27**:35–64.
- (119) Van Hoek P, Van Dijken J P and Pronk JT (2000) Regulation of fermentative capacity and levels of glycolytic enzymes in chemostat cultures of *Saccharomyces cerevisiae*. *Enzyme Microb. Technol.* **26**:724–736.
- (120) Hoelsch K, Sührer I, Heusel M and Weuster-Botz D (2013) Engineering of formate dehydrogenase: Synergistic effect of mutations affecting cofactor specificity and chemical stability. *Appl. Microbiol. Biotechnol.* **97**:2473–2481.
- (121) Hoja U, Marthol S, Hofmann J, Stegner S, Schulz R, Meier S, Greiner E and Schweizer E (2004) *HFA1* encoding an organelle-specific acetyl-CoA carboxylase controls mitochondrial fatty acid synthesis in *Saccharomyces cerevisiae*. *J. Biol. Chem.* **279**:21779–86.
- (122) Holzer H and Goedde HW (1957) [Two ways from pyruvate to acetyl-coenzyme A in yeast]. *Biochem. Z.* **329**:175–91.
- (123) Hong KK and Nielsen J (2012) Metabolic engineering of *Saccharomyces cerevisiae*: A key cell factory platform for future biorefineries. *Cell. Mol. Life Sci.* **69**:2671–2690.
- (124) Hong KK, Vongsangnak W, Vemuri GN and Nielsen J (2011) Unravelling evolutionary strategies of yeast for improving galactose utilization through integrated systems level analysis. *Proc. Natl. Acad. Sci. U. S. A.* **108**:12179–84.
- (125) Hsu PD, Lander ES and Zhang F (2014) Development and applications of CRISPR-Cas9 for genome engineering. *Cell* **157**:1262–1278.
- (126) Hsu PD, Scott DA, Weinstein JA, Ran FA, Konermann S, Agarwala V, Li Y, Fine EJ, Wu X, Shalem O, Cradick TJ, Marraffini LA, Bao G and Zhang F (2013) DNA targeting specificity of RNA-guided Cas9 nucleases. *Nat. Biotechnol.* **31**:827–32.
- (127) Huerta-Cepas J, Szklarczyk D, Forslund K, Cook H, Heller D, Walter MC, Rattei T, Mende DR, Sunagawa S, Kuhn M, Jensen LJ, Von Mering C and Bork P (2015) eggNOG 4.5: A hierarchical orthology framework with improved functional annotations for eukaryotic, prokaryotic and viral sequences. *Nucleic Acids Res.* **3**:3–10.
- (128) Hughes NJ, Clayton CL, Chalk PA and Kelly DJ (1998) *Helicobacter pylori* *porCDAB* and *oorDABC* genes encode distinct pyruvate:flavodoxin and 2-oxoglutarate:acceptor oxidoreductases which mediate electron transport to NADP. *J. Bacteriol.* **180**:1119–1128.
- (129) Huh WK, Falvo JV, Gerke LC, Carroll AS, Howson RW, Weissman JS and O'Shea EK (2003) Global analysis of protein localization in budding yeast. *Nature* **425**:686–91.

- (130) Hwang WY, Fu Y, Reyon D, Maeder ML, Tsai SQ, Sander JD, Peterson RT, Yeh JRJ and Joung JK (2013) Efficient genome editing in zebrafish using a CRISPR-Cas system. *Nat. Biotechnol.* **31**:227–9.
- (131) Hynes MJ and Murray SL (2010) ATP-citrate lyase is required for production of cytosolic acetyl coenzyme A and development in *Aspergillus nidulans*. *Eukaryot. Cell* **9**:1039–48.
- (132) IJlst L, Van Roermund CW, Iacobazzi V, Oostheim W, Ruiter JP, Williams JC, Palmieri F and Wanders RJ (2001) Functional analysis of mutant human carnitine acylcarnitine translocases in yeast. *Biochem. Biophys. Res. Commun.* **280**:700–706.
- (133) Inoue H, Nojima H and Okayama H (1990) High efficiency transformation of *Escherichia coli* with plasmids. *Gene* **96**:23–8.
- (134) Inui H, Miyatake K, Nakano Y and Kitaoka S (1984a) Fatty acid synthesis in mitochondria of *Euglena gracilis*. *FEBS J.* **142**:121–126.
- (135) Inui H, Miyatake K and Nakano Y (1984b) Occurrence of oxygen-sensitive, NADP⁺-dependent pyruvate dehydrogenase in mitochondria of *Euglena gracilis*. *J. Biochem.* **96**:931–934.
- (136) Inui H, Yamaji R, Saidoh H, Nakano Y and Kitaoka S (1991) Pyruvate:NADP⁺ oxidoreductase from *Euglena gracilis*: Limited proteolysis of the enzyme with trypsin. *Arch. Biochem. Biophys.* **286**:270–276.
- (137) Jacobs JZ, Ciccaglione KM, Tournier V and Zaratiegui M (2014) Implementation of the CRISPR-Cas9 system in fission yeast. *Nat. Commun.* **5**:5344.
- (138) Jauniaux Jc, Urrestarazu LA and Wlame Jm (1978) Arginine metabolism in *Saccharomyces cerevisiae*: Subcellular localization of the enzymes. *J. Bacteriol.* **133**:1096–1107.
- (139) De Jong BW, Shi S, Siewers V and Nielsen J (2014) Improved production of fatty acid ethyl esters in *Saccharomyces cerevisiae* through up-regulation of the ethanol degradation pathway and expression of the heterologous phosphoketolase pathway. *Microb. Cell Fact.* **13**:39.
- (140) De Jonge LP, Buijs NA, Ten Pierick A, Deshmukh A, Zhao Z, Kiel JA, Heijnen JJ and Van Gulik WM (2011) Scale-down of penicillin production in *Penicillium chrysogenum*. *Biotechnol. J.* **6**:944–958.
- (141) De Jong-Gubbels P, Van den Berg MA, Steensma HY, Van Dijken JP and Pronk JT (1997a) The *Saccharomyces cerevisiae* acetyl-coenzyme A synthetase encoded by the *ACS1* gene, but not the *ACS2*-encoded enzyme, is subject to glucose catabolite inactivation. *FEMS Microbiol. Lett.* **153**:75–81.
- (142) De Jong-Gubbels P, Van den Berg MA, Steensma HY, Van Dijken JP and Pronk JT (1997b) The *Saccharomyces cerevisiae* acetyl-coenzyme A synthetase encoded by the *ACS1* gene, but not the *ACS2*-encoded enzyme, is subject to glucose catabolite inactivation. *FEMS Microbiol. Lett.* **153**:75–81.
- (143) Jung WS, Yoo YJ, Park JW, Park SR, Han AR, Ban YH, Kim EJ, Kim E and Yoon YJ (2011) A combined approach of classical mutagenesis and rational metabolic engineering improves rapamycin biosynthesis and provides insights into methylmalonyl-CoA precursor supply pathway in *Streptomyces hygroscopicus* ATCC 29253. *Appl. Microbiol. Biotechnol.* **91**:1389–97.

- (144) Von Kamp A and Schuster S (2006) Metatool 5.0: Fast and flexible elementary modes analysis. *Bioinformatics* **22**:1930–1931.
- (145) Kandler O (1983) Carbohydrate metabolism in lactic acid bacteria. *Antonie van Leeuwenhoek* **49**:209–224.
- (146) Kanehisa M, Goto S, Sato Y, Kawashima M, Furumichi M and Tanabe M (2014) Data, information, knowledge and principle: Back to metabolism in KEGG. *Nucleic Acids Res.* **42**:199–205.
- (147) Kaplan RS, Mayor JA, Gremse DA and Wood DO (1995) High level expression and characterization of the mitochondrial citrate transport protein from the yeast *Saccharomyces cerevisiae*. *J. Biol. Chem.* **270**:4108–14.
- (148) Kaushik VK, Kavana M, Volz JM, Weldon SC, Hanrahan S, Xu J, Caplan SL and Hubbard BK (2009) Characterization of recombinant human acetyl-CoA carboxylase-2 steady-state kinetics. *Biochim. Biophys. Acta* **1794**:961–967.
- (149) Khan A and Kolattukudy PE (1973) A microsomal fatty acid synthetase coupled to acyl-CoA reductase in *Euglena gracilis*. *Arch. Biochem. Biophys.* **158**:411–420.
- (150) Kim KS, Rosenkrantz MS and Guarente L (1986) *Saccharomyces cerevisiae* contains two functional citrate synthase genes. *Mol. Cell. Biol.* **6**:1936–42.
- (151) Kispal G, Cseko J, Alkonyi I and Sandor A (1991) Isolation and characterization of carnitine acetyltransferase from *S. cerevisiae*. *Biochim. Biophys. Acta* **1085**:217–22.
- (152) Kispal G, Evans CT, Malloy C and Srere PA (1989) Metabolic studies on citrate synthase mutants of yeast. A change in phenotype following transformation with an inactive enzyme. *J. Biol. Chem.* **264**:11204–10.
- (153) Klein HP and Jahnke L (1979) Effects of aeration on formation and localization of the acetyl coenzyme A synthetases of *Saccharomyces cerevisiae*. *J. Bacteriol.* **137**:179–84.
- (154) Knappe J, Blaschkowski HP, Gröbner P and Schmitt T (1974) Pyruvate formate-lyase of *Escherichia coli*: The acetyl-enzyme intermediate. *Eur. J. Biochem.* **50**:253–63.
- (155) Knappe J, Schacht J, Mockel W, Hopner T, Vetter H. J and Edenharder R (1969) Pyruvate formate-lyase reaction in *Escherichia coli*. The enzymatic system converting an inactive form of the lyase into the catalytically active enzyme. *Eur. J. Biochem.* **11**:316–327.
- (156) Knijnenburg TA, De Winde JH, Daran JM, Daran-Lapujade P, Pronk JT, Reinders MJ and Wessels LF (2007) Exploiting combinatorial cultivation conditions to infer transcriptional regulation. *BMC Genomics* **8**:25.
- (157) Knijnenburg TA, Daran JMG, Van den Broek MA, Daran-Lapujade PAS, De Winde JH, Pronk JT, Reinders MJT and Wessels LFA (2009) Combinatorial effects of environmental parameters on transcriptional regulation in *Saccharomyces cerevisiae*: A quantitative analysis of a compendium of chemostat-based transcriptome data. *BMC genomics* **10**:53.
- (158) Kocharin K, Siewers V and Nielsen J (2013) Improved polyhydroxybutyrate production by *Saccharomyces cerevisiae* through the use of the phosphoketolase pathway. *Biotechnol. Bioeng.* **110**:2216–24.

- (159) Koh JLY, Chong YT, Friesen H, Moses A, Boone C, Andrews BJ and Moffat J (2015) CYCLoPs: A comprehensive database constructed from automated analysis of protein abundance and subcellular localization patterns in *Saccharomyces cerevisiae*. *G3* **5**:1223–1232.
- (160) Kohlhaw GB and Tan-Wilson A (1977) Carnitine acetyltransferase: Candidate for the transfer of acetyl groups through the mitochondrial membrane of yeast. *J. Bacteriol.* **129**:1159–61.
- (161) Koike M, Reed LJ and Carroll WR (1963) α -Keto acid dehydrogenation complexes. IV. Resolution and reconstitution of the *Escherichia coli* pyruvate dehydrogenation complex. *J. Biol. Chem.* **238**:30–9.
- (162) De Kok S, Yilmaz D, Suij E, Pronk JT, Daran JM and Van Maris AJ (2011) Increasing free-energy (ATP) conservation in maltose-grown *Saccharomyces cerevisiae* by expression of a heterologous maltose phosphorylase. *Metab. Eng.* **13**:518–526.
- (163) De Kok S, Kozak BU, Pronk JT and Van Maris AJA (2012a) Energy coupling in *Saccharomyces cerevisiae*: Selected opportunities for metabolic engineering. *FEMS Yeast Res.* **12**:387–397.
- (164) De Kok S, Nijkamp JF, Oud B, Roque FC, Ridder D, Daran JM, Pronk JT and Maris AJA (2012b) Laboratory evolution of new lactate transporter genes in a *jen1* Δ mutant of *Saccharomyces cerevisiae* and their identification as *ADY2* alleles by whole-genome resequencing and transcriptome analysis. *FEMS Yeast Res.* **12**:359–374.
- (165) Koopman F, Beekwilder J, Crimi B, Van Houwelingen A, Hall RD, Bosch D, Van Maris AJ, Pronk JT and Daran JM (2012) *De novo* production of the flavonoid naringenin in engineered *Saccharomyces cerevisiae*. *Microb. Cell Fact.* **11**:155.
- (166) Kozak BU, Van Rossum HM, Benjamin KR, Wu L, Daran JMG, Pronk JT and Van Maris AJA (2014a) Replacement of the *Saccharomyces cerevisiae* acetyl-CoA synthetases by alternative pathways for cytosolic acetyl-CoA synthesis. *Metab. Eng.* **21**:46–59.
- (167) Kozak BU, Van Rossum HM, Luttik MAH, Akeroyd M, Benjamin KR, Wu L, De Vries S, Daran JM, Pronk JT and Van Maris AJA (2014b) Engineering acetyl coenzyme A supply: Functional expression of a bacterial pyruvate dehydrogenase complex in the cytosol of *Saccharomyces cerevisiae*. *mBio* **5**:e01696–14.
- (168) Kozak BU, Van Rossum HM, Niemeijer MS, Van Dijk M, Benjamin K, Wu L, Daran JMG, Pronk JT and Van Maris AJA (2016) Replacement of the initial steps of ethanol metabolism in *Saccharomyces cerevisiae* by ATP-independent acetylating acetaldehyde dehydrogenase. *Metab. Eng.*
- (169) Krivoruchko A, Serrano-Amatriain C, Chen Y, Siewers V and Nielsen J (2013) Improving biobutanol production in engineered *Saccharomyces cerevisiae* by manipulation of acetyl-CoA metabolism. *J. Ind. Microbiol. Biotechnol.* **40**:1051–1056.
- (170) Krivoruchko A, Zhang Y, Siewers V, Chen Y and Nielsen J (2015) Microbial acetyl-CoA metabolism and metabolic engineering. *Metab. Eng.* **28**:28–42.
- (171) Kuipers NGA, Chroumpi S, Vos T, Solis-Escalante D, Bosman L, Pronk JT, Daran JM and Daran-Lapujade P (2013a) One-step assembly and targeted integration of multigene constructs assisted by the I-SceI meganuclease in *Saccharomyces cerevisiae*. *FEMS Yeast Res.* **13**:769–81.

- (172) Kuijpers NGA, Solis-Escalante D, Bosman L, Van den Broek M, Pronk JT, Daran JM and Daran-Lapujade P (2013b) A versatile, efficient strategy for assembly of multi-fragment expression vectors in *Saccharomyces cerevisiae* using 60 bp synthetic recombination sequences. *Microb. Cell Fact.* **12**:47.
- (173) Kulzer R, Pils T, Kappl R, Huttermann J and Knappe J (1998) Reconstitution and characterization of the polynuclear iron-sulfur cluster in pyruvate formate-lyase-activating enzyme. Molecular properties of the holoenzyme form. *J. Biol. Chem.* **273**:4897–4903.
- (174) Kumar A, Agarwal S, Heyman JA, Matson S, Heidtman M, Piccirillo S, Uman-sky L, Drawid A, Jansen R, Liu Y, Cheung Kh, Miller P, Gerstein M, Roeder GS and Snyder M (2002) Subcellular localization of the yeast proteome. *Genes Dev.* **16**:707–19.
- (175) Kunes S, Botstein D and Fox SM (1985) Transformation of yeast with linearized plasmid DNA. Formation of inverted dimers and recombinant plasmid products. *J. Mol. Biol.* **184**:375–387.
- (176) Kunze M, Kragler F, Binder M, Hartig A and Gurvitz A (2002) Targeting of malate synthase 1 to the peroxisomes of *Saccharomyces cerevisiae* cells depends on growth on oleic acid medium. *FEBS J.* **269**:915–22.
- (177) Kursu VAS, Pietikäinen LP, Fontanesi F, Aaltonen MJ, Suomi F, Raghavan Nair R, Schonauer MS, Dieckmann CL, Barrientos A, Hiltunen JK and Kašaniotis AJ (2013) Defects in mitochondrial fatty acid synthesis result in failure of multiple aspects of mitochondrial biogenesis in *Saccharomyces cerevisiae*. *Mol. Microbiol.* **90**:824–840.
- (178) Lange HC, Eman M, Van Zuijlen G, Visser D, Van Dam JC, Frank J, De Mattos MJT and Heijnen JJ (2001) Improved rapid sampling for *in vivo* kinetics of intracellular metabolites in *Saccharomyces cerevisiae*. *Biotechnol. Bioeng.* **75**:406–415.
- (179) Langmead B, Trapnell C, Pop M and Salzberg SL (2009) Ultrafast and memory-efficient alignment of short DNA sequences to the human genome. *Genome Biol.* **10**:R25.
- (180) Leaf TA, Peterson MS, Stoup SK, Somers D and Srien F (1996) *Saccharomyces cerevisiae* expressing bacterial polyhydroxybutyrate synthase produces poly-3-hydroxybutyrate. *Microbiology* **142**:1169–80.
- (181) Lee FJS, Lin LW and Smith JA (1990) A glucose-repressible gene encodes acetyl-CoA hydrolase from *Saccharomyces cerevisiae*. *J. Biol. Chem.* **265**:7413–7418.
- (182) Lesage G, Shapiro J, Specht CA, Sdicu AM, Menard P, Hussein S, Tong AH, Boone C and Bussey H (2005) An interactional network of genes involved in chitin synthesis in *Saccharomyces cerevisiae*. *BMC Genet.* **6**:8.
- (183) Lewin AS, Hines V and Small GM (1990) Citrate synthase encoded by the *CIT2* gene of *Saccharomyces cerevisiae* is peroxisomal. *Mol. Cell. Biol.* **10**:1399–405.
- (184) Li H and Durbin R (2009) Fast and accurate short read alignment with Burrows-Wheeler transform. *Bioinformatics* **25**:1754–1760.
- (185) Lian J, Si T, Nair NU and Zhao H (2014) Design and construction of acetyl-CoA overproducing *Saccharomyces cerevisiae* strains. *Metab. Eng.* **24**:139–49.

- (186) Lian J and Zhao H (2015a) Recent advances in biosynthesis of fatty acids derived products in *Saccharomyces cerevisiae* via enhanced supply of precursor metabolites. *J. Ind. Microbiol. Biotechnol.* **42**:437–451.
- (187) — (2015b) Reversal of the β -oxidation cycle in *Saccharomyces cerevisiae* for production of fuels and chemicals. *ACS Synth. Biol.* **4**:332–341.
- (188) Liao XS, Small WC, Srere PA and Butow RA (1991) Intramitochondrial functions regulate nonmitochondrial citrate synthase (*CIT2*) expression in *Saccharomyces cerevisiae*. *Mol. Cell. Biol.* **11**:38–46.
- (189) Liao X and Butow RA (1993) *RTG1* and *RTG2*: Two yeast genes required for a novel path of communication from mitochondria to the nucleus. *Cell* **72**:61–71.
- (190) Lin Y, Cradick TJ, Brown MT, Deshmukh H, Ranjan P, Sarode N, Wile BM, Vertino PM, Stewart FJ and Bao G (2014) CRISPR/Cas9 systems have off-target activity with insertions or deletions between target DNA and guide RNA sequences. *Nucleic Acids Res.* **42**:7473–85.
- (191) Lipmann F (1940) A phosphorylated oxidation product of pyruvic acid. *J. Biol. Chem.* **134**:463–464.
- (192) Liu XY, Chi ZM, Liu GL, Madzak C and Chi ZM (2013) Both decrease in *ACL1* gene expression and increase in *ICL1* gene expression in marine-derived yeast *Yarrowia lipolytica* expressing *INU1* gene enhance citric acid production from inulin. *Mar. Biotechnol.* **15**:26–36.
- (193) Liu Z and Butow RA (1999) A transcriptional switch in the expression of yeast tricarboxylic acid cycle genes in response to a reduction or loss of respiratory function. *Mol. Cell. Biol.* **19**:6720–6728.
- (194) Ljungdahl L and Wood HG (1969) Total synthesis of acetate from CO₂ by heterotrophic bacteria. *Annu. Rev. Microbiol.* **23**:515–538.
- (195) Lööke M, Krištjuhan K and Krištjuhan A (2011) Extraction of genomic DNA from yeasts for PCR-based applications. *Biotechniques* **50**:325–8.
- (196) Lorenz R, Bernhart SH, Höner Zu Siederdisen C, Tafer H, Flamm C, Stadler PF and Hofacker IL (2011) ViennaRNA Package 2.0. *Algorithms Mol. Biol.* **6**:26.
- (197) Lowry OH, Rosebrough NJ, Farr AL and Randall RJ (1951) Protein measurement with the Folin phenol reagent. *J. Biol. Chem.* **193**:265–275.
- (198) Lynd LR, Wyman CE and Gerngross TU (1999) Biocommodity engineering. *Biotechnol. Progr.* **15**:777–793.
- (199) Mainguet SE, Gronenberg LS, Wong SS and Liao JC (2013) A reverse glyoxylate shunt to build a non-native route from C₄ to C₂ in *Escherichia coli*. *Metab. Eng.* **19**:116–127.
- (200) Mans R, Van Rossum HM, Wijsman M, Backx A, Kuijpers NGA, Van den Broek M, Daran-Lapujade P, Pronk JT, Van Maris AJA and Daran JMG (2015) CRISPR/Cas9: A molecular Swiss army knife for simultaneous introduction of multiple genetic modifications in *Saccharomyces cerevisiae*. *FEMS Yeast Res.* **15**:fov004.
- (201) Van Maris AJA, Bakker BM, Brandt M, Boorsma A, Teixeira De Mattos MJ, Grivell LA, Pronk JT and Blom J (2001) Modulating the distribution of fluxes among respiration and fermentation by overexpression of *HAP4* in *Saccharomyces cerevisiae*. *FEMS Yeast Res.* **1**:139–149.

- (202) Van Maris AJA, Geertman JMA, Vermeulen A, Groothuizen MK, Winkler AA, Piper MDW, Van Dijken JP and Pronk JT (2004a) Directed evolution of pyruvate decarboxylase-negative *Saccharomyces cerevisiae*, yielding a C₂-independent, glucose-tolerant, and pyruvate-hyperproducing yeast. *Appl. Environ. Microbiol.* **70**:159–66.
- (203) Van Maris AJA, Luttik MAH, Winkler AA, Van Dijken JP and Pronk JT (2003) Overproduction of threonine aldolase circumvents the biosynthetic role of pyruvate decarboxylase in glucose-limited chemostat cultures of *Saccharomyces cerevisiae*. *Appl. Environ. Microbiol.* **69**:2094–2099.
- (204) Van Maris AJA, Winkler AA, Porro D, Van Dijken JP and Pronk JT (2004b) Homofermentative lactate production cannot sustain anaerobic growth of engineered *Saccharomyces cerevisiae*: Possible consequence of energy-dependent lactate export. *Appl. Environ. Microbiol.* **70**:2898–2905.
- (205) Marraffini LA and Sontheimer EJ (2008) CRISPR interference limits horizontal gene transfer in staphylococci by targeting DNA. *Science* **322**:1843–1845.
- (206) Mascal M (2012) Chemicals from biobutanol: Technologies and markets. *Biofuels, Bioprod. Biorefin.* **6**:483–493.
- (207) Mashego MR, Van Gulik WM, Vinke JL and Heijnen JJ (2003) Critical evaluation of sampling techniques for residual glucose determination in carbon-limited chemostat culture of *Saccharomyces cerevisiae*. *Biotechnol. Bioeng.* **83**:395–399.
- (208) Matsufuji Y, Yamamoto K, Yamauchi K, Mitsunaga T, Hayakawa T and Nakagawa T (2013) Novel physiological roles for glutathione in sequestering acetaldehyde to confer acetaldehyde tolerance in *Saccharomyces cerevisiae*. *Appl. Microbiol. Biotechnol.* **97**:297–303.
- (209) Max B, Salgado JM, Rodríguez N, Cortés S, Converti A and Domínguez JM (2010) Biotechnological production of citric acid. *Braz. J. Microbiol.* **41**:862–75.
- (210) McIver L, Leadbeater C, Campopiano DJ, Baxter RL, Daff SN, Chapman SK and Munro AW (1998) Characterisation of flavodoxin NADP⁺ oxidoreductase and flavodoxin; key components of electron transfer in *Escherichia coli*. *FEBS J.* **257**:577–585.
- (211) Melnikov S, Ben-Shem A, Garreau de Loubresse N, Jenner L, Yusupova G and Yusupov M (2012) One core, two shells: Bacterial and eukaryotic ribosomes. *Nat. Struct. Mol. Biol.* **19**:560–567.
- (212) Miller C, Fosmer A, Rush B, McMullin T, Beacom D and Suominen P (2011a) Industrial production of lactic acid. *Comprehensive Biotechnology*:179–188.
- (213) Miller JC, Tan S, Qiao G, Barlow Ka, Wang J, Xia DF, Meng X, Paschon DE, Leung E, Hinkley SJ, Dulay GP, Hua KL, Ankoudinova I, Cošt GJ, Urnov FD, Zhang HS, Holmes MC, Zhang L, Gregory PD and Rebar EJ (2011b) A TALE nuclease architecture for efficient genome editing. *Nat. Biotechnol.* **29**:143–8.
- (214) Mumberg D, Muller R and Funk M (1995) Yeast vectors for the controlled expression of heterologous proteins in different genetic backgrounds. *Gene* **156**:119–122.
- (215) Mussolino C, Morbitzer R, Lütge F, Dannemann N, Lahaye T and Cathomen T (2011) A novel TALE nuclease scaffold enables high genome editing activity in combination with low toxicity. *Nucleic Acids Res.* **39**:9283–93.

- (216) Nagarajan L and Storms RK (1997) Molecular characterization of GCV3, the *Saccharomyces cerevisiae* gene coding for the glycine cleavage system hydrogen carrier protein. *J. Biol. Chem.* **272**:4444–4450.
- (217) Navarro-Avino JP, Prasad R, Miralles VJ, Benito RM and Serrano R (1999) A proposal for nomenclature of aldehyde dehydrogenases in *Saccharomyces cerevisiae* and characterization of the stress-inducible *ALD2* and *ALD3* genes. *Yeast* **15**:829–842.
- (218) Navas MA and Gancedo JM (1996) The regulatory characteristics of yeast fructose-1,6-bisphosphatase confer only a small selective advantage. *J. Bacteriol.* **178**:1809–1812.
- (219) Nielsen J (2014) Synthetic biology for engineering acetyl coenzyme A metabolism in yeast. *mBio* **5**:e02153.
- (220) Nielsen J, Larsson C, Van Maris A and Pronk J (2013) Metabolic engineering of yeast for production of fuels and chemicals. *Curr. Opin. Biotechnol.* **24**:398–404.
- (221) Nielsen J, Siewers V, Kirvoruchko A, Zhang Y, Zhou Y, Buds NAA and Dai Z (2015) *Engineering of acetyl-CoA metabolism in yeast* (Patent no. WO2015057154 A3).
- (222) Nijkamp JF, Van den Broek M, Datema E, De Kok S, Bosman L, Luttik MA, Daran-Lapujade P, Vongsangnak W, Nielsen J, Heijne WH, Klaassen P, Paddon CJ, Platt D, Kotter P, Van Ham RC, Reinders MJ, Pronk JT, De Ridder D and Daran JM (2012a) *De novo* sequencing, assembly and analysis of the genome of the laboratory strain *Saccharomyces cerevisiae* CEN.PK113-7D, a model for modern industrial biotechnology. *Microb. Cell Fact.* **11**:36.
- (223) Nijkamp JF, Van Den Broek MA, Geertman JMA, Reinders MJT, Daran JMG and De Ridder D (2012b) *De novo* detection of copy number variation by co-assembly. *Bioinformatics* **28**:3195–3202.
- (224) Noor E, Haraldsdóttir HS, Milo R and Fleming RMT (2013) Consistent estimation of Gibbs energy using component contributions. *PLoS Comput. Biol.* **9**:e1003098.
- (225) Orlandi I, Casatta N and Vai M (2012) Lack of Ach1 CoA-transferase triggers apoptosis and decreases chronological lifespan in yeast. *Front. Oncol.* **2**:67.
- (226) Orr-Weaver TL, Szołtak JW and Rothstein RJ (1983) Genetic applications of yeast transformation with linear and gapped plasmids. *Methods Enzymol.* **101**:228–45.
- (227) Orr-Weaver TL and Szołtak JW (1983) Yeast recombination: The association between double-strand gap repair and crossing-over. *Proc. Natl. Acad. Sci. U. S. A.* **80**:4417–4421.
- (228) Oud B, Flores CL, Gancedo C, Zhang X, Trueheart J, Daran JM, Pronk JT and Van Maris AJA (2012) An internal deletion in *MTH1* enables growth on glucose of pyruvate-decarboxylase negative, non-fermentative *Saccharomyces cerevisiae*. *Microb. Cell Fact.* **11**:131.
- (229) Oud B, Guadalupe-Medina V, Nijkamp JF, De Ridder D, Pronk JT, Van Maris AJA and Daran JM (2013) Genome duplication and mutations in *ACE2* cause multicellular, fast-sedimenting phenotypes in evolved *Saccharomyces cerevisiae*. *Proc. Natl. Acad. Sci. U. S. A.* **110**:E4223–31.
- (230) Oura E (1972) “The effect of aeration on the growth energetics and biochemical composition of baker’s yeast.” PhD Thesis.

- (231) Overkamp KM, Kotter P, Van der Hoek R, Schoondermark-Stolk S, Luttik MA, Van Dijken JP and Pronk JT (2002) Functional analysis of structural genes for NAD(+)-dependent formate dehydrogenase in *Saccharomyces cerevisiae*. *Yeast* **19**:509–520.
- (232) Paddon CJ, Westfall PJ, Pitera DJ, Benjamin K, Fisher K, McPhee D, Leavell MD, Tai A, Main A, Eng D, Polichuk DR, Teoh KH, Reed DW, Treynor T, Lenihan J, Fleck M, Bajad S, Dang G, Dengrove D, Diola D, Dorin G, Ellens KW, Fickes S, Galazzo J, Gaucher SP, Geistlinger T, Henry R, Hepp M, Horning T, Iqbal T, Jiang H, Kizer L, Lieu B, Melis D, Moss N, Regentin R, Secrest S, Tsuruta H, Vazquez R, Westblade LF, Xu L, Yu M, Zhang Y, Zhao L, Lievense J, Covello PS, Keasling JD, Reiling KK, Renninger NS and Newman JD (2013) High-level semi-synthetic production of the potent antimalarial artemisinin. *Nature* **496**:528–32.
- (233) Palmieri L, Lasorsa FM, Iacobazzi V, Runswick MJ, Palmieri F and Walker JE (1999) Identification of the mitochondrial carnitine carrier in *Saccharomyces cerevisiae*. *FEBS Lett.* **462**:472–6.
- (234) Pasquali M, Monsen G, Richardson L, Alston M and Longo N (2006) Biochemical findings in common inborn errors of metabolism. *Am. J. Med. Genet.* **142C**:64–76.
- (235) Pel HJ, De Winde JH, Archer DB, Dyer PS, Hofmann G, Schaap PJ, Turner G, De Vries RP, Albang R, Albermann K, Andersen MR, Bendtsen JD, Benen JA, Van den Berg M, Breestraat S, Caddick MX, Contreras R, Cornell M, Coutinho PM, Danchin EGJ, Debets AJM, Dekker P, Van Dijk PWM, Van Dijk A, Dijkhuizen L, Driessen AJM, D'Enfert C, Geysens S, Goosen C, Groot GSP, De Groot PWJ, Guillemette T, Henrissat B, Herweijer M, Van den Hombergh JPTW, Van den Hondel CAMJJ, Van der Heijden RTJM, Van der Kaaij RM, Klis FM, Kools HJ, Kubicek CP, Van Kuyk PA, Lauber J, Lu X, Van der Maarel MJEC, Meulenberg R, Menke H, Mortimer MA, Nielsen J, Oliver SG, Olsthoorn M, Pal K, Van Peij NNME, Ram AFJ, Rinas U, Roubos JA, Sagt CMJ, Schmoll M, Sun J, Ussery D, Varga J, Vervecken W, Van de Vondervoort PJJ, Wedler H, Wösten HAB, Zeng AP, Van Ooyen AJJ, Visser J and Stam H (2007) Genome sequencing and analysis of the versatile cell factory *Aspergillus niger* CBS 513.88. *Nat. Biotechnol.* **25**:221–231.
- (236) Perlman PS and Mahler HR (1970) Intracellular localization of enzymes in yeast. *Arch. Biochem. Biophys.* **136**:245–59.
- (237) Piper MD, Daran-Lapujade P, Bro C, Regenber B, Knudsen S, Nielsen J and Pronk JT (2002) Reproducibility of oligonucleotide microarray transcriptome analyses. An interlaboratory comparison using chemostat cultures of *Saccharomyces cerevisiae*. *J. Biol. Chem.* **277**:37001–37008.
- (238) Pokholok DK, Harbison CT, Levine S, Cole M, Hannett NM, Lee TI, Bell GW, Walker K, Rolfe PA, Herbolzheimer E, Zeitlinger J, Lewitter F, Gifford DK and Young RA (2005) Genome-wide map of nucleosome acetylation and methylation in yeast. *Cell* **122**:517–27.
- (239) Polakis ES and Bartley W (1965) Changes in the enzyme activities of *Saccharomyces cerevisiae* during aerobic growth on different carbon sources. *Biochem. J.* **97**:284–297.

- (240) Porro D, Brambilla L, Ranzi BM, Martegani E and Alberghina L (1995) Development of metabolically engineered *Saccharomyces cerevisiae* cells for the production of lactic acid. *Biotechnol. Progr.* **11**:294–298.
- (241) Postma E, Verduyn C, Scheffers WA and Van Dijken JP (1989) Enzymic analysis of the crabtree effect in glucose-limited chemostat cultures of *Saccharomyces cerevisiae*. *Appl. Environ. Microbiol.* **55**:468–477.
- (242) Powlowski J, Sahlman L and Shingler V (1993) Purification and properties of the physically associated *meta*-cleavage pathway enzymes 4-hydroxy-2-ketovalerate aldolase and aldehyde dehydrogenase (acylating) from *Pseudomonas* sp. strain CF600. *J. Bacteriol.* **175**:377–385.
- (243) Pronk JT, Van Maris AJ and Guadalupe Medina V (2011) *Fermentative glycerol - free ethanol production* (Patent no. EP2456851 A1).
- (244) Pronk JT, Steensma HY and Van Dijken JP (1996) Pyruvate metabolism in *Saccharomyces cerevisiae*. *Yeast* **12**:1607–1633.
- (245) Pronk JT, Wenzel TJ, Luttik MA, Klaassen CC, Scheffers WA, Steensma HY and Van Dijken JP (1994) Energetic aspects of glucose metabolism in a pyruvate-dehydrogenase-negative mutant of *Saccharomyces cerevisiae*. *Microbiology* **140**:601–610.
- (246) Pronk JT (2002) Auxotrophic yeast strains in fundamental and applied research. *Appl. Environ. Microbiol.* **68**:2095–2010.
- (247) Przybyla-Zawislak B, Dennis RA, Zakharkin SO and McCammon MT (1998) Genes of succinyl-CoA ligase from *Saccharomyces cerevisiae*. *Eur. J. Biochem.* **258**:736–743.
- (248) Ragsdale SW (2003) Pyruvate ferredoxin oxidoreductase and its radical intermediate. *Chem. Rev.* **103**:2333–2346.
- (249) Ratledge C and Holdsworth J (1985) Properties of a pentulose-5-phosphate phosphoketolase from yeasts grown on xylose. *Appl. Microbiol. Biotechnol.* **22**:217–221.
- (250) Reinders J, Zahedi RP, Pfanner N, Meisinger C and Sickmann A (2006) Toward the complete yeast mitochondrial proteome: Multidimensional separation techniques for mitochondrial proteomics. *J. Proteome Res.* **5**:1543–54.
- (251) Rickey TM and Lewin AS (1986) Extramitochondrial citrate synthase activity in bakers' yeast. *Mol. Cell. Biol.* **6**:488–93.
- (252) Riddles PW, Blakeley RL and Zerner B (1983) Reassessment of Ellman's reagent. *Methods Enzymol.* **91**:49–60.
- (253) Rivière L, Moreau P, Allmann S, Hahn M, Biran M, Plazolles N, Franconi JM, Boshart M and Bringaud F (2009) Acetate produced in the mitochondrion is the essential precursor for lipid biosynthesis in procyclic trypanosomes. *Proc. Natl. Acad. Sci. U.S.A.* **106**:12694–12699.
- (254) Ro DK, Paradise EM, Ouellet M, Fisher KJ, Newman KL, Ndungu JM, Ho KA, Eachus RA, Ham TS, Kirby J, Chang MCY, Withers ST, Shiba Y, Sarpong R and Keasling JD (2006) Production of the antimalarial drug precursor artemisinic acid in engineered yeast. *Nature* **440**:940–3.
- (255) Roberts RJ (2005) How restriction enzymes became the workhorses of molecular biology. *Proc. Natl. Acad. Sci. U. S. A.* **102**:5905–8.

- (256) Rodriguez S, Denby CM, Van Vu T, Baidoo EEK, Wang G and Keasling JD (2016) ATP citrate lyase mediated cytosolic acetyl-CoA biosynthesis increases mevalonate production in *Saccharomyces cerevisiae*. *Microb. Cell. Fact.* **15**:48.
- (257) Van Roermund CW, Elgersma Y, Singh N, Wanders RJ and Tabak HF (1995) The membrane of peroxisomes in *Saccharomyces cerevisiae* is impermeable to NAD(H) and acetyl-CoA under *in vivo* conditions. *EMBO J.* **14**:3480–6.
- (258) Van Roermund CW, Hettema EH, Van den Berg M, Tabak HF and Wanders RJ (1999) Molecular characterization of carnitine-dependent transport of acetyl-CoA from peroxisomes to mitochondria in *Saccharomyces cerevisiae* and identification of a plasma membrane carnitine transporter, Agp2p. *EMBO J.* **18**:5843–52.
- (259) Van Rossum HM, Kozak BU, Niemeijer MS, Dykstra JC, Luttik MAH, Daran JMG, Pronk JT and Van Maris AJA (2016) Requirements for carnitine-shuttle-mediated translocation of mitochondrial acetyl moieties to the yeast cytosol. *Accepted manuscript*.
- (260) Rotte C, Stejskal F, Zhu G, Keithly JS and Martin W (2001) Pyruvate:NADP⁺ oxidoreductase from the mitochondrion of *Euglena gracilis* and from the apicomplexan *Cryptosporidium parvum*: A biochemical relic linking pyruvate metabolism in mitochondriate and amitochondriate protists. *Mol. Biol. Evol.* **18**:710–20.
- (261) Rude MA and Schirmer A (2009) New microbial fuels: A biotech perspective. *Curr. Opin. Microbiol.* **12**:274–281.
- (262) Rudolph FB, Purich DL and Fromm HJ (1968) Coenzyme A-linked aldehyde dehydrogenase from *Escherichia coli*. I. Partial purification, properties, and kinetic studies of the enzyme. *J. Biol. Chem.* **243**:5539–5545.
- (263) Ruijter GJG, Panneman H, Xu DB and Visser J (2000) Properties of *Aspergillus niger* citrate synthase and effects of *citA* overexpression on citric acid production. *FEMS Microbiol. Lett.* **184**:35–40.
- (264) Ruiz-Amil M, De Torrontegui G, Palacián E, Catalina L and Losada M (1965) Properties and function of yeast pyruvate carboxylase. *J. Biol. Chem.* **240**:3485–3492.
- (265) Ryan OW, Skerker JM, Maurer MJ, Li X, Tsai JC, Poddar S, Lee ME, DeLoache W, Dueber JE, Arkin AP and Cate JHD (2014) Selection of chromosomal DNA libraries using a multiplex CRISPR system. *eLife*:e03703.
- (266) Salusjarvi L, Kauništo S, Holmström S, Vehkomäki ML, Koivuranta K, Pitkanen JP and Ruohonen L (2013) Overexpression of NADH-dependent fumarate reductase improves D-xylose fermentation in recombinant *Saccharomyces cerevisiae*. *J. Ind. Microbiol. Biotechnol.* **40**:1383–1392.
- (267) Sánchez BJ and Nielsen J (2015) Genome scale models of yeast: Towards standardized evaluation and consistent omic integration. *Integr. Biol.* **7**:846–858.
- (268) Sanchez LB (1998) Aldehyde dehydrogenase (CoA-acetylating) and the mechanism of ethanol formation in the amitochondriate protist, *Giardia lamblia*. *Arch. Biochem. Biophys.* **354**:57–64.
- (269) Sandoval CM, Ayson M, Moss N, Lieu B, Jackson P, Gaucher SP, Horning T, Dahl RH, Denery JR, Abbott DA and Meadows AL (2014) Use of pantothenate as a

- metabolic switch increases the genetic stability of farnesene producing *Saccharomyces cerevisiae*. *Metab. Eng.* **25**:1–12.
- (270) Sawers RG (1994) The hydrogenases and formate dehydrogenases of *Escherichia coli*. *Antonie van Leeuwenhoek* **66**:57–88.
- (271) Schmalix W and Bandlow W (1993) The ethanol-inducible *YAT1* gene from yeast encodes a presumptive mitochondrial outer carnitine acetyltransferase. *J. Biol. Chem.* **268**:27428–39.
- (272) Schmidt M, Schaumberg JZ, Steen CM and Boyer MP (2010) Boric acid disturbs cell wall synthesis in *Saccharomyces cerevisiae*. *Int. J. Microbiol.* **2010**:930465.
- (273) Schneider R, Brors B, Bürger F, Camrath S and Weiss H (1997) Two genes of the putative mitochondrial fatty acid synthase in the genome of *Saccharomyces cerevisiae*. *Curr. Genet.* **32**:384–388.
- (274) Schramm M, Klybas V and Racker E (1958) Phosphorolytic cleavage of fructose-6-phosphate by fructose-6-phosphate phosphoketolase from *Acetobacter xylinum*. *J. Biol. Chem.* **233**:1283–1288.
- (275) Schramm M and Racker E (1957) Formation of erythrose-4-phosphate and acetyl phosphate by a phosphorolytic cleavage of fructose-6-phosphate. *Nature* **179**:1349–1350.
- (276) Schuchmann K and Müller V (2014) Autotrophy at the thermodynamic limit of life: A model for energy conservation in acetogenic bacteria. *Nat. Rev. Microbiol.* **12**:809–821.
- (277) Serov AE, Popova AS, Fedorchuk VV and Tishkov VI (2002) Engineering of coenzyme specificity of formate dehydrogenase from *Saccharomyces cerevisiae*. *Biochem. J.* **367**:841–7.
- (278) Shannon KW and Rabinowitz JC (1988) Isolation and characterization of the *Saccharomyces cerevisiae* *MIS1* gene encoding mitochondrial C1-tetrahydrofolate synthase. *J. Biol. Chem.* **263**:7717–7725.
- (279) Shao Z, Zhao H and Zhao H (2009) DNA assembler, an *in vivo* genetic method for rapid construction of biochemical pathways. *Nucleic Acids Res.* **37**:e16.
- (280) Sheng J and Feng X (2015) Metabolic engineering of yeast to produce fatty acid-derived biofuels: Bottlenecks and solutions. *Front. Microbiol.* **6**:1–11.
- (281) Shiba Y, Paradise EM, Kirby J, Ro DK and Keasling JD (2007) Engineering of the pyruvate dehydrogenase bypass in *Saccharomyces cerevisiae* for high-level production of isoprenoids. *Metab. Eng.* **9**:160–168.
- (282) Siewers V (2014) An overview on selection marker genes for transformation of *Saccharomyces cerevisiae*. *Methods Mol. Biol.* **1152**:3–15.
- (283) Small WC, Brodeur RD, Sandor A, Fedorova N, Li G, Butow RA and Srere PA (1995) Enzymatic and metabolic studies on retrograde regulation mutants of yeast. *Biochemistry* **34**:5569–5576.
- (284) Smith LT and Kaplan NO (1980) Purification, properties, and kinetic mechanism of coenzyme A-linked aldehyde dehydrogenase from *Clostridium kluyveri*. *Arch. Biochem. Biophys.* **203**:663–675.
- (285) Snoep JL, De Graef MR, Westphal AH, De Kok A, Teixeira de Mattos MJ and Neijssel OM (1993) Differences in sensitivity to NADH of purified pyruvate dehydrogenase complexes of *Enterococcus faecalis*, *Lactococcus lactis*, *Azotobacter*

- vinelandii* and *Escherichia coli*: Implications for their activity *in vivo*. *FEMS Microbiol. Lett.* **114**:279–283.
- (286) Snoep JL, Westphal AH, Benen JAE, Teixeira de Mattos MJ, Neijssel OM and Kok A (1992) Isolation and characterisation of the pyruvate dehydrogenase complex of anaerobically grown *Enterococcus faecalis* NCTC 775. *Eur. J. Biochem.* **203**:245–250.
- (287) Soh KC, Miskovic L and Hatzimanikatis V (2012) From network models to network responses: Integration of thermodynamic and kinetic properties of yeast genome-scale metabolic networks. *FEMS Yeast Res.* **12**:129–143.
- (288) Solis-Escalante D, Kuijpers NG, Bongaerts N, Bolat I, Bosman L, Pronk JT, Daran JM and Daran-Lapujade P (2013) *amdSYM*, a new dominant recyclable marker cassette for *Saccharomyces cerevisiae*. *FEMS Yeast Res.* **13**:126–139.
- (289) Solis-Escalante D, Van den Broek M, Kuijpers NGA, Pronk JT, Boles E, Daran JMG and Daran-Lapujade P (2014a) The genome sequence of the popular hexose transport deficient *Saccharomyces cerevisiae* strain EBY.VW4000 reveals *LoxP*/Cre-induced translocations and gene loss. *FEMS Yeast Res.*(in press).
- (290) Solis-Escalante D, Kuijpers NGA, Van der Linden FH, Pronk JT, Daran JM and Daran-Lapujade P (2014b) Efficient simultaneous excision of multiple selectable marker cassettes using I-SceI-induced double-strand DNA breaks in *Saccharomyces cerevisiae*. *FEMS Yeast Res.* **14**:741–754.
- (291) Sonderegger M, Schumperli M and Sauer U (2004) Metabolic engineering of a phosphoketolase pathway for pentose catabolism in *Saccharomyces cerevisiae*. *Appl. Environ. Microbiol.* **70**:2892–2897.
- (292) Spange S, Wagner T, Heinzl T and Kramer OH (2009) Acetylation of non-histone proteins modulates cellular signalling at multiple levels. *Int. J. Biochem. Cell Biol.* **41**:185–198.
- (293) Staben C and Rabinowitz JC (1986) Nucleotide sequence of the *Saccharomyces cerevisiae* *ADE3* gene encoding C1-tetrahydrofolate synthase. *J. Biol. Chem.* **261**:4629–4637.
- (294) Stadtman ER (1952) The purification and properties of phosphotransacetylase. *J. Biol. Chem.* **196**:527–534.
- (295) Stairs CW, Roger AJ and Hampl V (2011) Eukaryotic pyruvate formate lyase and its activating enzyme were acquired laterally from a firmicute. *Mol. Biol. Evol.* **28**:2087–2099.
- (296) Stanley GA, Douglas NG, Every EJ, Tzanatos T and Pamment NB (1993) Inhibition and stimulation of yeast growth by acetaldehyde. *Biotechnol. Lett.* **15**:1199–1204.
- (297) Stanley GA and Pamment NB (1993) Transport and intracellular accumulation of acetaldehyde in *Saccharomyces cerevisiae*. *Biotechnol. Bioeng.* **42**:24–29.
- (298) Starheim KK, Gevaert K and Arnesen T (2012) Protein N-terminal acetyltransferases: When the start matters. *Trends Biochem. Sci.* **37**:152–161.
- (299) Steen EJ, Chan R, Prasad N, Myers S, Petzold CJ, Redding A, Ouellet M and Keasling JD (2008) Metabolic engineering of *Saccharomyces cerevisiae* for the production of *n*-butanol. *Microb. Cell Fact.* **7**:36.

- (300) Storici F, Coglievina M and Bruschi CV (1999) A 2- μ m DNA-based marker recycling system for multiple gene disruption in the yeast *Saccharomyces cerevisiae*. *Yeast* **15**:271–83.
- (301) Storici F, Lewis LK and Resnick MA (2001) *In vivo* site-directed mutagenesis using oligonucleotides. *Nat. Biotechnol.* **19**:773–6.
- (302) Strijbis K, Van Roermund CWT, Hardy GP, Van den Burg J, Bloem K, De Haan J, Van Vlies N, Wanders RJA, Vaz FM and Dištel B (2009) Identification and characterization of a complete carnitine biosynthesis pathway in *Candida albicans*. *FASEB J.* **23**:2349–2359.
- (303) Sutendra G, Kinnaird A, Dromparis P, Paulin R, Stenson TH, Haromy A, Hashimoto K, Zhang N, Flaim E and Michelakis ED (2014) A nuclear pyruvate dehydrogenase complex is important for the generation of acetyl-CoA and histone acetylation. *Cell* **158**:84–97.
- (304) Swidah R, Wang H, Reid PJ, Ahmed HZ, Pisanelli AM, Persaud KC, Grant CM and Ashe MP (2015) Butanol production in *S. cerevisiae* via a synthetic ABE pathway is enhanced by specific metabolic engineering and butanol resistance. *Biotechnol. Biofuels* **8**:97.
- (305) Swiegers JH, Dippenaar N, Pretorius IS and Bauer FF (2001) Carnitine-dependent metabolic activities in *Saccharomyces cerevisiae*: Three carnitine acetyltransferases are essential in a carnitine-dependent strain. *Yeast* **18**:585–95.
- (306) Takahashi H, McCaffery JM, Irizarry RA and Boeke JD (2006) Nucleocytosolic acetyl-coenzyme A synthetase is required for histone acetylation and global transcription. *Mol. Cell* **23**:207–217.
- (307) Tang X, Feng H and Chen WN (2013) Metabolic engineering for enhanced fatty acids synthesis in *Saccharomyces cerevisiae*. *Metab. Eng.* **16**:95–102.
- (308) Tehlivets O, Scheuringer K and Kohlwein SD (2007) Fatty acid synthesis and elongation in yeast. *Biochim. Biophys. Acta* **1771**:255–70.
- (309) Terentiev Y, Pico AH, Böer E, Wartmann T, Klabunde J, Breuer U, Babel W, Suckow M, Gellissen G and Kunze G (2004) A wide-range integrative yeast expression vector system based on *Arxula adeninivorans*-derived elements. *J. Ind. Microbiol. Biotechnol.* **31**:223–8.
- (310) Thieringer R, Shio H, Han YS, Cohen G and Lazarow PB (1991) Peroxisomes in *Saccharomyces cerevisiae*: Immunofluorescence analysis and import of catalase A into isolated peroxisomes. *Mol. Cell. Biol.* **11**:510–522.
- (311) Thorvaldsdóttir H, Robinson JT and Mesirov JP (2013) Integrative Genomics Viewer (IGV): High-performance genomics data visualization and exploration. *Briefings Bioinf.* **14**:178–192.
- (312) Thykaer J and Nielsen J (2007) Evidence, through C13-labelling analysis, of phosphoketolase activity in fungi. *Process Biochem.* **42**:1050–1055.
- (313) Tittmann K, Wille G, Golbik R, Weidner A, Ghisla S and Hübner G (2005) Radical phosphate transfer mechanism for the thiamin diphosphate- and FAD-dependent pyruvate oxidase from *Lactobacillus plantarum*. Kinetic coupling of intercofactor electron transfer with phosphate transfer to acetyl-thiamin diphosphate via a transient FAD semiquinone/hydroxyethyl-ThDP radical pair. *Biochemistry* **44**:13291–13303.

- (314) Torkko JM, Koivuranta KT, Miinalainen IJ, Yagi AI, Schmitz W, Kašaniotis AJ, Airenne TT, Gurvitz A and Hiltunen KJ (2001) *Candida tropicalis* Etr1p and *Saccharomyces cerevisiae* Ybr026p (Mrf1'p), 2-enoyl thioester reductases essential for mitochondrial respiratory competence. *Mol. Cell. Biol.* **21**:6243–53.
- (315) Tucci S, Vacula R, Krajcovic J, Proksch P and Martin W (2010) Variability of wax ester fermentation in natural and bleached *Euglena gracilis* strains in response to oxygen and the elongase inhibitor flufenacet. *J. Eukaryot. Microbiol.* **57**:63–69.
- (316) Tusher VG, Tibshirani R and Chu G (2001) Significance analysis of microarrays applied to the ionizing radiation response. *Proc. Natl. Acad. Sci. U. S. A.* **98**:5116–5121.
- (317) Urnov FD, Rebar EJ, Holmes MC, Zhang HS and Gregory PD (2010) Genome editing with engineered zinc finger nucleases. *Nat. Rev. Genet.* **11**:636–46.
- (318) Van Rossum HM, Kozak BU, Niemeijer MS, Duine HJ, Luttik MA, Kötter P, Daran JMG, Van Maris AJA and Pronk JT (2016) Alternative reactions at the interface of glycolysis and citric acid cycle in *Saccharomyces cerevisiae*. *FEMS Yeast Res.* **16**:fow017.
- (319) Vax FM and Wanders RJA (2002) Carnitine biosynthesis in mammals. *Biochem. J.* **361**:417.
- (320) Veen M and Lang C (2004) Production of lipid compounds in the yeast *Saccharomyces cerevisiae*. *Appl. Microbiol. Biotechnol.* **63**:635–646.
- (321) Vélot C, Lebreton S, Morgunov I, Usher KC and Srere PA (1999) Metabolic effects of mislocalized mitochondrial and peroxisomal citrate synthases in yeast *Saccharomyces cerevisiae*. *Biochemistry* **38**:16195–204.
- (322) Ventura FV, Ijlšt L, Ruiter J, Ofman R, Cošta CG, Jakobs C, Duran M, De Almeida IT, Bieber LL and Wanders RJA (1998) Carnitine palmitoyltransferase II specificity towards β -oxidation intermediates: Evidence for a reverse carnitine cycle in mitochondria. *Eur. J. Biochem.* **253**:614–618.
- (323) Verduyn C (1991) Physiology of yeasts in relation to biomass yields. *Antonie van Leeuwenhoek* **60**:325–353.
- (324) Verduyn C, Poštma E, Scheffers WA and Van Dijken JP (1990a) Energetics of *Saccharomyces cerevisiae* in anaerobic glucose-limited chemostat cultures. *J. Gen. Microbiol.* **136**:405–412.
- (325) — (1990b) Physiology of *Saccharomyces cerevisiae* in anaerobic glucose-limited chemostat cultures. *J. Gen. Microbiol.* **136**:395–403.
- (326) — (1992) Effect of benzoic acid on metabolic fluxes in yeasts: A continuous-culture study on the regulation of respiration and alcoholic fermentation. *Yeast* **8**:501–517.
- (327) Verduyn C, Stouthamer AH, Scheffers WA and Van Dijken JP (1991) A theoretical evaluation of growth yields of yeasts. *Antonie van Leeuwenhoek* **59**:49–63.
- (328) Verduyn C, Zomerdijk TPL, Van Dijken JP and Scheffers WA (1984) Continuous measurement of ethanol-production by aerobic yeast suspensions with an enzyme electrode. *Appl. Microbiol. Biotechnol.* **19**:181–185.
- (329) Verwaal R, Wang J, Meijnen JP, Visser H, Sandmann G, Van den Berg JA and Van Ooyen AJJ (2007) High-level production of β -carotene in *Saccharomyces cerevisiae*

- by successive transformation with carotenogenic genes from *Xanthophyllomyces dendrorhous*. *Appl. Environ. Microbiol.* **73**:4342–4350.
- (330) Violante S, IJlst L, Te Brinke H, De Almeida IT, Wanders RJA, Ventura FV and Houten SM (2013) Carnitine palmitoyltransferase 2 and carnitine/acylcarnitine translocase are involved in the mitochondrial synthesis and export of acylcarnitines. *FASEB J.* **27**:2039–2044.
- (331) Waks Z and Silver PA (2009) Engineering a synthetic dual-organism system for hydrogen production. *Appl. Environ. Microbiol.* **75**:1867–1875.
- (332) Walker BJ, Abeel T, Shea T, Priest M, Abouelliel A, Sakthikumar S, Cuomo Ca, Zeng Q, Wortman J, Young SK and Earl AM (2014) Pilon: An integrated tool for comprehensive microbial variant detection and genome assembly improvement. *PLoS One* **9**:e112963.
- (333) Wang H, Yang H, Shivalila CS, Dawlaty MM, Cheng AW, Zhang F and Jaenisch R (2013) One-step generation of mice carrying mutations in multiple genes by CRISPR/Cas-mediated genome engineering. *Cell* **153**:910–8.
- (334) Wang Q and Wang L (2008) New methods enabling efficient incorporation of unnatural amino acids in yeast. *J. Am. Chem. Soc.* **130**:6066–7.
- (335) Wang X, Mann CJ, Bai Y, Ni L and Weiner H (1998) Molecular cloning, characterization, and potential roles of cytosolic and mitochondrial aldehyde dehydrogenases in ethanol metabolism in *Saccharomyces cerevisiae*. *J. Bacteriol.* **180**:822–830.
- (336) Wapinski I (2009) *Fungal Orthogroups Repository*. [Online]. Available from: <http://www.broadinstitute.org/regev/orthogroups/>.
- (337) Wapinski I, Pfeffer A, Friedman N and Regev A (2007) Automatic genome-wide reconstruction of phylogenetic gene trees. *Bioinformatics* **23**:549–558.
- (338) Wenzel TJ, Van den Berg MA, Visser W, Van den Berg JA and Steensma HY (1992) Characterization of *Saccharomyces cerevisiae* mutants lacking the E1 alpha subunit of the pyruvate dehydrogenase complex. *FEBS J.* **209**:697–705.
- (339) Weuſthuis RA, Lamot I, Van der Ooſt J and Sanders JPM (2011) Microbial production of bulk chemicals: Development of anaerobic processes. *Trends Biotechnol.* **29**:153–158.
- (340) Wiczorke R, Krampe S, Weierſtall T, Freidel K, Hollenberg CP and Boles E (1999) Concurrent knock-out of at leaſt 20 transporter genes is required to block uptake of hexoses in *Saccharomyces cerevisiae*. *FEBS Lett.* **464**:123–128.
- (341) Wu L, Mashego MR, Van Dam JC, Proell AM, Vinke JL, Ras C, Van Winden WA, Van Gulik WM and Heijnen JJ (2005) Quantitative analysis of the microbial metabolome by isotope dilution mass spectrometry using uniformly ¹³C-labeled cell extracts as internal ſtandards. *Anal. Biochem.* **336**:164–171.
- (342) Yamashita I and Fukui S (1985) Transcriptional control of the sporulation-specific glucoamylase gene in the yeast *Saccharomyces cerevisiae*. *Mol. Cell. Biol.* **5**:3069–3073.
- (343) Yan D, Wang C, Zhou J, Liu Y, Yang M and Xing J (2014) Conſtruction of reductive pathway in *Saccharomyces cerevisiae* for effective succinic acid fermentation at low pH value. *Bioresour. Technol.* **156**:232–239.
- (344) Yon J and Fried M (1989) Precise gene fusion by PCR. *Nucleic Acids Res.* **17**:4895.

- (345) Zeeman AM, Luttik MAH, Pronk JT, Van Dijken JP and Steensma HY (1999) Impaired growth on glucose of a pyruvate dehydrogenase-negative mutant of *Kluyveromyces lactis* is due to a limitation in mitochondrial acetyl-coenzyme A uptake. *FEMS Microbiol. Lett.* **177**:23–28.
- (346) Zelle RM, De Hulster E, Van Winden WA, De Waard P, Dijkema C, Winkler AA, Geertman JMA, Van Dijken JP, Pronk JT and Van Maris AJA (2008) Malic acid production by *Saccharomyces cerevisiae*: Engineering of pyruvate carboxylation, oxaloacetate reduction, and malate export. *Appl. Environ. Microbiol.* **74**:2766–2777.
- (347) Zhang F (2014) *CRISPR-Cas systems and methods for altering expression of gene products* (Patent no. US8697359 B1).
- (348) Zhang G, Kong II, Kim H, Liu J, Cate JHD and Jin YS (2014) Construction of a quadruple auxotrophic mutant of an industrial polyploidy *Saccharomyces cerevisiae* using RNA-guided Cas9 nuclease. *Appl. Environ. Microbiol.* **80**:7694–7701.
- (349) Zhang J, Pierick At, Van Rossum HM, Seifar RM, Ras C, Daran JM, Heijnen JJ and Wahl AS (2015a) Determination of the cytosolic NADPH/NADP ratio in *Saccharomyces cerevisiae* using shikimate dehydrogenase as sensor reaction. *Sci. Rep.* **5**:12846.
- (350) Zhang Y, Dai Z, Krivoruchko A, Chen Y, Siewers V and Nielsen J (2015b) Functional pyruvate formate lyase pathway expressed with two different electron donors in *Saccharomyces cerevisiae* at aerobic growth. *FEMS Yeast Res.* **15**:fov024.
- (351) Zhou ZH, McCarthy DB, O'Connor CM, Reed LJ and Stoops JK (2001) The remarkable structural and functional organization of the eukaryotic pyruvate dehydrogenase complexes. *Proc. Natl. Acad. Sci. U.S.A.* **98**:14802–14807.



ACKNOWLEDGMENTS

During the four years leading up to the very last ‘dot’ of this thesis, many people have contributed to my PhD project, both knowingly and unknowingly. Here, I would like to thank everyone who played a role, even though I realise this does not reflect the tremendous contribution they have had.

Even before my PhD studies, many people stimulated my scientific interests and creativity. I would like to especially thank my inspiring supervisors from the University of Utrecht, Gert Folkers (BSc project) and Berend Snel (MSc project), who both have played a key role in preparing me for my PhD project.

During my PhD studies, I got superb guidance from my supervisors Ton (co-promoter), Jack (promoter) and Jean-Marc. Many thanks for a fantastic time and learning experience! Ton – you are an involved and educating supervisor, your constructive criticism (‘streng doch rechtvaardig’ ;-)) was invaluable for shaping my scientific skills. Many thanks for making me enthusiastic for (quantitative) physiology and metabolic engineering. Of course, I also greatly enjoyed our trips in the USA and Canada! Jack – thank you for your contagious enthusiasm, your Socrates-like style of educating, your scientific and personal involvement both in good and bad times, the meetings and conversations we had (scheduled and unscheduled) and your ‘good’ sense of humour, which were crucial for my great time at IMB! Jean-Marc – at the start of my PhD more than later on, I frequently asked you for advice on molecular biology strategies; I greatly appreciated that you were often directly available to help me out! You always generated a bunch of (wild) ideas and after making a selection or combination, this often resulted in achieving the desired goal.

Many thanks to the external parties DSM and Amyris that contributed to this project through the BE-Basic platform. Special thanks to Kirsten Benjamin (Amyris) and Liang Wu (DSM) for many interesting and constructive discussions and a fruitful collaboration. I am also grateful for the FES subsidy from the Dutch Ministry of Economic Affairs, Agriculture and Innovation (EL&I).

Furthermore, I would like to thank my ‘acetyl-ColleAgues’ Barbara, Nakul and Matthijs. Barbara – although we had our differences, I want to thank you for the things I learned from you, the laughs at our weekly meetings and of course the great beers ;-)! Nakul – thanks for helping me out with the fermentations (Chapter 3). All-rounder Matthijs – thank you for helping me with various things: fermentations, growth studies, enzymatic assays, molecular biology, etc. etc. Of course, next to that I also greatly enjoyed our chats, beers and night experiments (including the nice fireplace and movies ;-)! Robert – I immensely appreciated the weekly, energetic meetings, our ((semi-)scientific) discussions, your (weird) humour about even the smallest things and of course a beneficial collaboration that, among other things, culminated in a nice paper and workshop. Thanks! Maarten – it was always enlightening to discuss our mutual results on a regular basis, your frequent visits to .220 were adding to the awesomeness of office .220 ;-)!

This thesis would not have been possible without the outstanding technical and moral support of my dear colleagues Erik, Marcel, Marijke, Marinka and Pilar. Thanks for taking all the time and huge effort!! Other people that also contributed to my chapters in thought, word and deed are greatly acknowledged: Annabel, Antoon, Arthur, Arthur, Astrid, Feibai, Ioannis, Lot, Marlous, Melanie, Niels, Peter Kötter, Reza, Thomas, Tim, Viktor Boer and Xavier.

Lesley – thank you for demonstrating to me how to use Anthonie-van-Leeuwenhoek microscopes and for having the patience to take some beautiful microscopic pictures of CEN.PK113-7D that feature in this thesis.

I also thank the students I had the privilege to supervise: Rudy, Hilde, Linda, Henri, Pieter, Annie, Inge and James. Thanks for a wonderful time, but also for contributing to the (hidden) work behind this PhD thesis.

Special thanks to the lads and ladies from the workshop and MSD kitchen: Arno, Marko, Marcel, Astrid, Apilena and Jannie, thanks for your essential contribution! The occasional inspiring walk, talk or lunch in the botanical garden was made possible by a hard working team. Thanks a lot! Many thanks also to everyone that helped running the facilities, in particular Erwin, Jos, Kees, Robert, Sjaak and Tracey. The team of the Coop supermarket – thanks for advancing my skills in patience.

I thank all my colleagues from office room .220: Angel, Eline, Jules, Laura, Luka, Marit, Mark, Matthijs and Nuria. Thanks for all the (scientific) discussions, stories, coping with my peculiarities (sometimes under protest) and an awesome atmosphere!

My paranymphs Robert and Matthijs, thank you for organising everything related to my defense and for standing by my side! The members of the PhD committee are thanked for making time available to join the committee and defense, for reading my thesis and for additional preparations.

I did my PhD project with an immense amount of joy. This was mainly because of the great atmosphere that radiated from my well-appreciated IMB colleagues: Alex, Alexey, Angel, Anja, Arthur, Barbara, Barbara, Bart, Benjamin, Beth, Bianca, Corinna, Dani, Daniel, Dick, Eline, Emilio, Erik, Francine, Frank, Gabriele, Gijs, Hannes, Ioannis, Irina, Ishwar, Jack, Jasmine, Jasper, Jean-Marc, Jules, Jurgen, Kerstin, Laura, Lex, Lizanne, Luka, Maarten, Marcel, Marijke, Marinka, Marit, Mark, Marlous, Matthias, Matthijs, Melanie, Nakul, Nick, Nick, Niels, Nuria, Pascale, Pilar, Reno, Robert, Roberto, Ruben, Sofia, Stefan, Susan, Thomas, Tim, Tim, Ton, Victor, Wesley, Wouter, Xavier and Yuching. Thanks for everything!

Vaccaeanen, Epifanen, neighbors en andere vrienden, familie en schoonfamilie – fijn dat ik jullie regelmatig als klankbord kon gebruiken!

Pa en ma – jullie hebben mij van jongs af aan enorm gestimuleerd in mijn wetenschappelijke en technische nieuwsgierigheid. Ontzettend bedankt! Eveneens wil ik mijn broers en zus bedanken in hun bijdrage aan mijn persoonlijke en wetenschappelijke eigenschappen die onontbeerlijk was in mijn ontwikkeling tot wetenschapper. Ook Oma Log – het is altijd heerlijk met je over van alles en nog wat (inclusief mijn gijsjes) te praten!

Hanneke – onmetelijk veel dank voor al je steun door dik en dun! Met jou durf ik elk avontuur aan!



CURRICULUM VITAE

Harmen van Rossum was born on November 13, 1986 in Dirksland, The Netherlands. After following pre-university education (VWO) at the CSG Prins Maurits school in Middelharnis and graduating in 2005, he enrolled in the BSc Chemistry programme at the University of Utrecht. Harmen performed his BSc research project at the Utrecht NMR-spectroscopy group, under the supervision of dr. Gert Folkers. In this project, he optimised and used a high-throughput GST pull-down technique for quantification of protein-protein binding. During his subsequent MSc study in Molecular and Cellular Life Sciences, also at the University of Utrecht, he investigated evolution of protein complexes at the Utrecht Bioinformatics group, under supervision of prof. dr. Berend Snel. In a second internship at the Industrial Microbiology group (Delft University of Technology), supervised by dr. Frank Koopman, Harmen worked on polycistronic expression in *Saccharomyces cerevisiae*. After he graduated his MSc studies with honours in 2011, Harmen started a PhD project at the Delft Industrial Microbiology group, supervised by prof. dr. Jack Pronk (promoter) and dr. ir. Ton van Maris (co-promoter). This project, the results of which are described in this thesis, focused on analysis and engineering of acetyl-CoA metabolism in *S. cerevisiae*. After his PhD project, Harmen joined the team of Zymergen (Emeryville, California, USA) as an industrial postdoctoral scientist.

PUBLICATIONS

- (1) Van Rossum HM, Kozak BU, Pronk JT and Van Maris AJA (2016a) Engineering cytosolic acetyl-coenzyme A supply in *Saccharomyces cerevisiae*: Pathway stoichiometry, free-energy conservation and redox-cofactor balancing. *Metab. Eng.* **36**:99–115.
- (2) Mans R¹, Van Rossum HM¹, Wijsman M, Backx A, Kuijpers NGA, Van den Broek M, Daran-Lapujade P, Pronk JT, Van Maris AJA and Daran JMG (2015) CRISPR/-Cas9: A molecular Swiss army knife for simultaneous introduction of multiple genetic modifications in *Saccharomyces cerevisiae*. *FEMS Yeast Res.* **15**:fov004.
- (3) Kozak BU¹, Van Rossum HM¹, Benjamin KR, Wu L, Daran JMG, Pronk JT and Van Maris AJA (2014) Replacement of the *Saccharomyces cerevisiae* acetyl-CoA synthetases by alternative pathways for cytosolic acetyl-CoA synthesis. *Metab. Eng.* **21**:46–59.
- (4) Van Rossum HM, Kozak BU, Niemeijer MS, Duine HJ, Luttik MAH, Kötter P, Daran JMG, Van Maris AJA and Pronk JT (2016b) Alternative reactions at the interface of glycolysis and citric acid cycle in *Saccharomyces cerevisiae*. *FEMS Yeast Res.* **16**:fow017.
- (5) Van Rossum HM, Kozak BU, Niemeijer MS, Dykstra JC, Luttik MAH, Daran JMG, Pronk JT and Van Maris AJA (2016c) Requirements for carnitine-shuttle-mediated translocation of mitochondrial acetyl moieties to the yeast cytosol. *Accepted manuscript*.
- (6) Kozak BU, Van Rossum HM, Niemeijer MS, Van Dijk M, Benjamin K, Wu L, Daran JMG, Pronk JT and Van Maris AJA (2016) Replacement of the initial steps of ethanol metabolism in *Saccharomyces cerevisiae* by ATP-independent acetylating acetaldehyde dehydrogenase. *FEMS Yeast Res.* **16**:fow006.
- (7) Kozak BU, Van Rossum HM, Luttik MAH, Akeroyd M, Benjamin KR, Wu L, De Vries S, Daran JM, Pronk JT and Van Maris AJA (2014) Engineering acetyl coenzyme A supply: Functional expression of a bacterial pyruvate dehydrogenase complex in the cytosol of *Saccharomyces cerevisiae*. *mBio* **5**:e01696–14.
- (8) Beekwilder J, Van Rossum HM, Koopman F, Sonntag F, Buchhaupt M, Schrader J, Hall RD, Bosch D, Pronk JT, Van Maris AJA and Daran JM (2014) Polycistronic expression of a β -carotene biosynthetic pathway in *Saccharomyces cerevisiae* coupled to β -ionone production. *J. Biotechnol.* **192**:382–392.
- (9) Zhang J, Ten Pierick A, Van Rossum HM, Seifar MR, Ras C, Daran JM, Heijnen JJ and Wahl AS (2015) Determination of the cytosolic NADPH/NADP Ratio in *Saccharomyces cerevisiae* using shikimate dehydrogenase as sensor reaction. *Sci. Rep.* **5**:12846.